Biosynthesis of indoles and global metabolomic, proteomic responses of *Rubrivivax benzoatilyticus* JA2 to aniline stress

Thesis submitted to the University of Hyderabad for the award of

Doctor of Philosophy

By

Mujahid Mohammed

(Regd. No. 06LPPH05)

Department of Plant Sciences

School of Life Sciences

University of Hyderabad

Hyderabad - 500 046

INDIA

October 2012

University of Hyderabad
(A central university established in 1974 by Act of Parliament)
HYDERABAD-500046

DECLARATION

I **Mujahid Mohammed**, hereby declare that this thesis entitled **"Biosynthesis of indoles and global metabolomic, proteomic responses of *Rubrivivax benzoatilyticus* JA2 to aniline stress"** submitted by me under the guidance and supervision of **Prof. Ch.V. Ramana** is an original and independent research work. I also declare that it has not been submitted previously in part or in full to this University or any other University or Institution for the award of any degree or diploma.

Mujahid Mohammed
(Research scholar)

Supervisor
Prof. Ch.V. Ramana

University of Hyderabad
(A central university established in 1974 by Act of Parliament)
HYDERABAD-500046

CERTIFICATE

This is to certify that this thesis entitled **"Biosynthesis of indoles and global metabolomic, proteomic responses of *Rubrivivax benzoatilyticus* JA2 to aniline stress"** is a record of bonafide work done by **Mr. Mujahid Mohammed**, a research scholar for Ph.D. programme in Department of Plant Sciences, School of Life Sciences, University of Hyderabad, under my guidance and supervision.

Prof. Ch. V. Ramana
Supervisor

HEAD
Department of Plant Sciences

DEAN
School of Life Sciences

Acknowledgements

I extend my gratitude to my supervisor Dr. Ch. V. Ramana for his constant guidance and support throughout my doctoral research.

I thank the present and former Heads of the Department of Plant Sciences, Prof. A. R. Reddy, Prof. Appa Rao Podile for the departmental facilities.

I thank Prof. M. Ramanadham, Dean, School of Life Sciences, and former Dean, Prof. A. S. Raghavendra, for allowing me to use the general facilities of the school.

I thank my Doctoral Committee members Prof. S. Dayananda and Prof. Appa Rao Podile for their valuable suggestions.

I thank Dr. Ch. Sasikala, JNTU for extending her lab facilities.

I would like to thank Prof. Appa Rao Podile and Dr. J. S. S. Prakash for extending their lab facilities.

I am grateful to all my teachers, who are instrumental in shaping up my life.

I am thankful to all my teachers at School of Life Sciences who taught me the ABCs of biology.

I thank all the faculty members of School of Life Sciences.

I would like to thank all my present and former lab mates for their help and cooperation throughout my research.

I thank all the research scholars of School of Life Sciences for their cooperation.

I thank all my friends at University of Hyderabad for making my stay in campus delightful.

I thank all the members of "just for fun" cricket team for making my Sundays more joyful.

The help and cooperation of the non-teaching staff is highly acknowledged.

I acknowledge the CSIR and DST for financial aid. DST-FIST, UGC-SAP, DBT-CREEB are acknowledged for school and departmental facilities.

I am extremely grateful to my parents, my brothers and family members for their unwavering love, support and patience throughout my life.

Above the all, I vow my thanks to Almighty, for providing me everything.

I sincerely apologies to all whom I may have hurt.

Finally I thank one and all for their support.

Mujahid Mohammed….

Dedicated

to my

Parents and Teachers

Table of contents

Abstract

Aniline is an aromatic amine widely used in various industrial applications and owing to its extensive usage it is continuously released into the environment. Aniline is a recalcitrant, persistent pollutant and is toxic to the life forms hence its fate in the environment is of serious concern. Few bacteria utilize aniline as a sole source of carbon or nitrogen for their growth, others transform aniline into nontoxic/less toxic forms. In an earlier study biotransformation of aniline to indole esters was reported in a photosynthetic bacterium *Rhodobacter sphaeroides* OU5 which was fumarate dependent, however, biosynthesis of indoles from aniline was not investigated. In addition, studies were also not extended in understanding bacterial tolerance and cellular response to aniline. Deciphering of these processes enhances the current knowledge of aniline metabolism and possible survival mechanisms to aniline stress by bacteria which helps in developing effective bioremediation methods. The present work aims at elucidation of indoles biosynthesis from aniline and deciphering the metabolic/molecular responses of *Rubrivivax benzoatilyticus* JA2 to aniline stress by metabolomic and proteomic approaches.

Tryptophan, indole 3-acetic acid (IAA) and indole 3-aldehyde were identified as major indole metabolites from aniline exposed cultures of *R. benzoatilyticus* JA2 and indoles production was observed only in aniline exposed cultures. Stable isotope precursor feeding experiments revealed that aniline was not a precursor of indoles biosynthesis. Fumarate enhanced the production of indoles and stable isotope feeding revealed that fumarate as precursor of indoles. Inhibition of indoles production by glyphosate indicates indoles biosynthesis occurs *via* shikimate pathway. Anthranilate synthase, tryptophan synthase proteins, involved in tryptophan biosynthesis were up-regulated to aniline stress and this was corroborated with up-regulation of anthranilate synthase gene in aniline exposed cells. Anthranilate synthase and tryptophan catabolizing enzyme activities were high in aniline exposed cells correlating well with tryptophan, indoles accumulation. These results indicate that aniline triggers indoles biosynthesis *via* shikimate pathway and IAA biosynthesis was tryptophan dependent in *R. benzoatilyticus* JA2.

GC-MS based metabolic profiling followed by multivariate statistical analysis of fingerprints (endometabolomes) revealed marked variation in metabolisms of aniline exposed and unexposed cells. Sixty metabolites were identified by GC-MS analysis of aniline exposed and unexposed fingerprints. Functional annotation of differential regulated metabolites revealed modulation of amino acid, carbohydrate, fatty acid, nitrogen, nucleic acid, co-factor-vitamin, TCA, butanoate, tryptophan and lipid metabolisms to aniline stress. Further, aniline stress induced polyhydroxybutyrates (PHBs) accumulation and this was supported by up-regulation of phasin proteins involved in PHBs synthesis. Extracellular polymeric substance (EPS) formation was observed in aniline exposed cells and EPS was a hetero-polymer of carbohydrate, proteins and nucleic acids. Aniline exposed cells accumulated more saturated fatty acids in membranes compared to control indicating membrane adaption to aniline stress.

Global proteomic analysis of aniline exposed and unexposed cells by isobaric tags relative and absolute quantitation (iTRAQ) revealed a total of 750 proteins, of which 114 proteins were differentially regulated. Proteins related to membrane transport, folding sorting and degradation, transcription, translation and stress, amino acid, cofactor-vitamin, central carbon metabolism were highly differential regulated to aniline stress. Proteins related to energy, signal transduction and biosynthesis of secondary metabolites were up-regulated while replication-repair, lipid and entire TCA cycle metabolism were down regulated to aniline stress. Gluconeogenesis, pentose phosphate pathway, and tryptophan biosynthesis related proteins were up-regulated corroborating well with the accumulation of EPS and indoles. Proteome analysis of aniline exposed cells revealed up-regulation of RND (resistance nodulation cell division) efflux pumps which play an important role in toxic compound extrusion. Proteome analysis also revealed up-regulation of heat shock protein network involved in protein quality control under stress. Integrated metabolic and proteomic analysis of strain JA2 revealed a global metabolic shift, re-adjustment and plausible multiple survival/tolerance mechanisms of *R. benzoatilyticus* JA2 to aniline stress.

LIST OF ABBREVIATIONS

µg	Microgram
µl	Microliter
µs	Microsecond
2D LC-MS	Two dimensional liquid chromatography
ACN	Acetonitrile
APB	Anoxygenic photosynthetic bacteria
APS	Ammonium persulfate
ATCC	American Type Culture Collection
BSTFA	N,O-bis(trimethylsilyl)trifluoroacetamide
CFU	Colony forming unit
CID	Collision induced dissociation
CLSM	Confocal laser scanning microscopy
CP/TOSS	Cross polarization/total sideband suppression
DAHP	3-deoxy-D-arabinoheptulosonate 7-phosphate
DCM	Dichloromethane
DEPC	Diethyl pyrocarbonate
DMSO	Dimethyl sulfoxide
DTT	Dithiothreitol
EDTA	Ethylenediaminetetraacetic acid
EDX	Energy dispersive X-ray
EPS	Extracellular polymeric substance
ESI	Electrospray ionization
FAME	Fatty acid methyl esters
FDA	Fluorescein diacetate
FTIR	Fourier transformation infra-red
g	force of gravity
GC-MS	Gas chromatography mass spectrometry
GRAVY	Grand average of hydropathy

h	Hour
HEPES	4-(2-hydroxyethyl)-1-piperazineethanesulfonic acid
HOAc	Acetic acid
HPLC	High performance liquid chromatography
IAA	Indole-3-acetic acid
IAld	Indole-3-aldehyde
IAM	Indole-3-acetamide
IAN	Indole-3-acetonitrile
IC50	Half maximal inhibitory concentration
iTRAQ	Isobaric tag for relative and absolute quantitation
JCM	Japan Collection of Microorganisms
KEGG	Kyoto encyclopedia of genes and genomes
LC-MS	Liquid chromatography and mass spectrometry
m/z	Mass-to-charge ratio
MeOH	Methanol
mg	Milligram
MIC	Minimum inhibitory concentration
min	Minutes
ml	milliliter
MS	Mass spectrometry
MS/MS	Tandem mass spectrometry
MudPIT	Multidimensional protein identification technology
NIST	National institute of standards and technology
nm	Nanometer
NMR	Nuclear magnitic resonance
PAGE	Polyacrylamide gel electrophoresis
PCA	Principal component analysis
PDA	Photodiode array
PEP	Phosphoenolpyruvate
PHAs	Polyhydroxyalkanoates
PHBs	Polyhydroxybutyrates

Phe	Phenylalanine
PLP	Pyridoxal-phosphate
PLS-DA	Partial least squares discriminant analysis
PMSF	Phenyl methyl sulfonyl fluoride
PPM	Parts per million
qRT-PCR	Quantitative real time polymerase chain reaction
QTOF	Quadrupole time-of-flight
RND	Resistance nodulation cell division
s	Seconds
SCX	Strong cation exchange
SDS	Sodium dodecyl sulfate
SEM	Scanning electron microscopy
TCEP	Tris (2-Carboxyethyl) phosphine
TE	Tris EDTA
TEMED	N,N,N′,N′-Tetramethylethane-1,2-diamine
TFA	Trifluoroacetic acid
TMCS	Trimethylchlorosilane
Tris	Tris (hydroxymethyl) aminomethane
TRITC	Tetramethylrhodamine iso-thiocyanate
Trp	Tryptophan
Tyr	Tyrosine
v/v	volume per volume
VIP	Variable importance in projection
w/v	weight per volume

INTRODUCTION

1.0 Introduction

Bacteria are widely distributed in the environment and occupy diverse habitats. They are constantly exposed to ever changing environmental conditions and thus adopted various mechanisms for survival. Some bacteria live under certain extreme conditions such as high temperatures (thermal vents, hot springs), low temperatures (icy lakes of Antarctica), high saline, alkaline, and acidic conditions. Bacteria senses different environmental stressors and bring necessary adaptations to survive. Owing to their unique adaptation capabilities bacteria thrive in some of the most hostile and inhospitable environments. Since from the industrial revolution diverse array of anthropogenic chemicals are produced and their usage in various applications immensely increased. Many of these chemicals are constantly released in to the environment and they are recalcitrant, persistent, alien (xenobiotic) and toxic to life forms. High concentration of these xenobiotics created extreme conditions (xenobiotic stress) and bacteria particularly adopted different kinds of mechanisms to combat the stress. Organic solvents/aromatic compounds are one among the xenobiotics used in various applications.

1.1 Organic solvents and their usage

Organic solvents are liquids used to dissolve solutes and they are hydrophilic or hydrophobic in nature. Organic solvents are aliphatic (ethyl acetate, hexane, carbon tetrachloride) or aromatic (xylene, benzene, toluene, aniline) in origin with various chemical substitutions. Organic solvents arose in the latter half of the 19^{th} century from the coal-tar industry and these are volatile. They are used in organic synthesis as an active substance, in dry-cleaning, preparation of dyes, paints, detergents, adhesives, and perfumery. Organic solvents are extensively used in formulation of herbicides, pesticides, drugs and in extraction of compounds. The pharmaceutical industry is one of the largest consumers of organic solvents per amount of the final product synthesised (Grodowska and Parczewski, 2010).

1.2 Organic solvent toxicity towards bacteria

Toxicity of an organic solvent is evaluated by its log P_{ow} (the logarithm of the partitioning coefficient of a solvent in a defined octanol-water mixture (log P_{ow}). Generally solvents with a log P_{ow} below 5.0 are considered as extremely toxic to microorganisms (Ramos *et al*., 2002). Toxicity of solvents is due to their accumulation in

cytoplasmic membranes and disruption of the membrane integrity (Ramos *et al*., 2002). Organic solvents disrupts the protein-protein, protein-lipid interactions and there by impairing vital functions of the membranes such as energy transduction, transport of nutrients and signal transduction. Impaired membranes lead to leakage of ions, metabolites, dissipation of the pH, proton motive force, and loss of osmotic balance ultimately leads to the cell death (Ramos *et al*., 2002). Some of these toxic chemicals may interfere with cellular metabolism and inhibit the growth of the organism (Fernandes *et al*., 2003). Among the solvents, aryl (aromatic) solvents are highly toxic as they readily disrupt the membranes (Sikkema *et al*., 1995) and bacteria adopted different tolerance mechanisms to overcome the deleterious effects of toxic compounds.

1.3 Aryl solvents tolerance in bacteria

Some bacteria use aromatic compounds as a sole source of carbon or energy for their growth. Bacteria capable of degrading wide array of aromatic compounds have been isolated and their degradation pathways under aerobic (Habe and Omori, 2003) as well as anaerobic conditions were well studied (Carmona *et al*., 2009). However, all the bacteria cannot degrade these aromatic compounds yet some of them tolerate high concentrations of xenobiotics (Ramos *et al*., 2002). Moreover, utilization of solvents as carbon source and tolerance are considered as an independent events (Udaondo *et al*., 2012). Both degraders and non-degraders are exposed to these xenobiotics and bacteria adopt various tolerance mechanisms to thrive under xenobiotic stress (Ramos *et al*., 2002; Udaondo *et al*., 2012). Some of the common solvent/xenobiotic tolerance mechanisms adopted by bacteria are focused here.

1.3.1 Membrane adaptions to toxic compounds

Among various solvent tolerance mechanisms of bacteria membrane adaptations are one. Cell membrane is a barrier between extracellular and intracellular environment and performs many vital functions. Aromatic compounds interacts with membrane, alter the membrane organization and fluidity finally leading to the cell death (Ramos *et al*., 1997). Bacteria employ appropriate response mechanisms to diminish the adverse effects of xenobiotics. Primarily, bacteria re-adjust the membrane fluidity by altering the composition of the lipid bilayer. Bacteria respond to aromatic compound by increasing *trans* to *cis* unsaturated fatty acid ratio and this is catalysed by *cis-trans* isomerase (Ramos *et al*., 2002). Isomerization lead to decrease in membrane fluidity (regidification), prevents

the entry of solvent molecules and there by enhances the solvent tolerance (Segura *et al*., 2012). *Cis-trans* isomerization is the short term response observed in many Gram-stained negative bacteria to aryl solvents (Loffler *et al*., 2010). Some bacteria alter the saturated to unsaturated fatty acid ratio as a long term response, more saturated fatty acids enable the denser packing of membrane and contribute to the solvent tolerance (Dunlop, 2011; Segura *et al*., 2012). Changes in the phospholipid head groups have also been reported to involve in tolerance but it is not well studied (Ramos *et al*., 1997; Segura *et al*., 2012). Change in outer membrane lipopolysaccharides was also observed in some solvent tolerating bacteria (Baumgarten *et al*., 2012b). Formation of membrane vesicles was reported as an active mechanism of solvent tolerance in *Pseudomonas putida* DOT-T1E to chlorophenols (Baumgarten *et al*., 2012b) and toluene (Baumgarten *et al*., 2012a).

1.3.2 Efflux pumps and toxic compounds extrusion

Extrusion of toxic compounds from the cytoplasm to external medium is major cell protective mechanism against deleterious compounds (Dunlop, 2011; Segura *et al*., 2012). Efflux pumps are membrane transporters which recognise and exports toxic substances from the cell by using proton motive force. Efflux pumps are divided into RND (Resistance nodulation cell division) family, small multidrug resistance family, major facilitator super family (MFS) and ATP binding cassette family (ABC) (Aeschlimann, 2003; Fernandes *et al*., 2003). RND family efflux pumps are considered as most efficient system of toxic compound tolerance in Gram-negative bacteria (Segura *et al*., 2012). RND efflux system is multicomponent complex made of three proteins extending from inner membrane to outer membrane. Up-regulation of proteins/genes related to RND efflux system were observed in toluene, xylene exposed *Pseudomonas* sp and implicated in tolerance to solvent (Dominguez-Cuevas *et al*., 2006; Wijte *et al*., 2010). Up regulation of RND efflux pumps upon toxic compounds exposure and their direct role in tolerance is reported in Gram-stained negative bacteria (Aeschlimann, 2003; Fernandes *et al*., 2003). Apart from RND efflux pumps members of ABC family transporters were also implicated in toxic compounds tolerance (Fernandes *et al*., 2003).

1.3.3 Chaperones and stress tolerance

Heat shock proteins are involved in the synthesis, transport, folding and degradation of proteins. Under stress, proteins tend to aggregate and denatured/aggregated proteins hamper the growth. Heat shock proteins prevent aggregation, refold the misfolded

proteins or degrade denatured proteins and thus helps in quality control of proteins (Dunlop, 2011). Heat shock proteins are mainly chaperones, co-chaperones and proteases. Up regulation of heat shock proteins to solvent (toxic compound) stress was reported in many bacteria (Segura *et al*., 2012). Proteins/genes related to heat response such as GroEl, GroES, DnaK, DnaJ and other heat shock proteins were overexpressed in toluene, xylene, ethanol and butanol stress (Wijte *et al*., 2010; Dunlop, 2011). Overexpression of GroESL improved solvent tolerance in *Corynebacterium acetobutylicum* (Tomas *et al*., 2003). Overexpression of heat shock proteins in *Lactobacillus plantarum* (Desmond *et al*., 2004*)* and *E. coli* enhanced the solvent tolerance (Reyes *et al*., 2011). Accumulation of heat shock proteins in *Pseudomonas putida* R2 lead to enhanced tolerance to toluene (Kobayashi *et al*., 2010). Numerous evidences suggest the role of heat shock proteins in stress tolerance hence they are considered as good engineering targets for improving tolerance to toxic compounds (Dunlop, 2011).

1.3.4 Extracellular polymeric substance (EPS)

Extracellular polymeric substance is a biopolymer of microbial origin in which microorganisms are embedded. EPS is a heterogeneous mixture of carbohydrates, proteins, nucleic acids, lipids and humic substances (Flemming *et al*., 2007). EPS acts as an extracellular matrix in biofilm and more than 90% of the dry weight of biofilm is EPS, which gives structural integrity and strength to the biofilm (Halan *et al*., 2011). Diverse environmental cues induce EPS formation, in natural habitats many bacteria produce EPS and thrive as biofilms/microbial flocks/ aggregates (Halan *et al*., 2012). EPS plays vital role in nutrients sorption, adherence, prevents dehydration of biofilms and protection from stress (Flemming *et al*., 2007). Biofilm associated cells exhibit unique gene expression, metabolic adaptations and physiological heterogeneity which enables them to thrive under the adverse conditions (Booth *et al*., 2011; Shimada *et al*., 2012).

Matrix entrapped cells or biofilms are more resistant to environmental stresses (anti-microbial substances, heavy metals, toxic chemicals and organic acids) compared to their free living (planktonic) counterparts (Halan *et al*., 2011; Halan *et al*., 2012; Shimada *et a*l., 2012). Heavy metals (Cd, Cu, Pb, Zn, Al, Cr), and toxic chemicals (glutaraldehyde, phenol) stimulated EPS formation in sulphate-reducing bacteria (Fang *et al*., 2002). Increased resistance of *Lactobacillus plantarum* JCM1149 to acid, ethanol stress was attributed to EPS secretion and three dimensional structure of biofilm (Kubota *et al*.,

2008). EPS also enhances surface hydrophobicity of bacterial cells and confers resistance to toxic chemicals such as benzylkonium (quaternary ammonium salts) (Campanac *et al*., 2002). Styrene induced EPS formation was reported in *Pseudomonas putida* and EPS forming cells were more resistant to styrene compared to free living (Halan *et al*., 2011).

1.3.5 Polyhydroxyalkanoates (PHAs)

Polyhydroxyalkanoates (PHAs) are intracellular storage compounds of carbon and energy that are produced by many bacteria (Quillaguaman *et al*., 2010). PHAs are endo-biopolymers and chemically these are polyesters of hydroxyalkanoic acids (Gorenflo *et al*., 1999). PHAs form water insoluble inclusion bodies in the cytoplasm known as PHA granules. PHA inclusions are composed of hydroxyalkanoic acid polymer and catalytic, non-catalytic proteins on its surface (Sudesh *et al*., 2000). PHA synthase, depolymerizing proteins are catalytic ones which are involved in synthesis and degradation of PHAs. Phasins are non-catalytic proteins involved in PHA granule formation and regulation (York *et al*., 2001; Galan *et al*., 2012). Predominant forms of PHAs are 3-hydroxybutyrate (3HB) homopolymers or copolymer of 3HB and 3-hydroxyvelarates (Sudesh *et al*., 2000). Based on degree of polymerization PHAs are divided into short chain, medium chain and long chain PHAs. Multiple pathways provide monomers for PHAs biosynthesis in bacteria including fatty acid biosynthesis/degradation and other pathways (Sudesh *et al*., 2000).

Wide varieties of environmental and endogenous signals induce PHA biosynthesis in bacteria such as, nutrient limitations, desiccation, nitrogen/carbon ratio, toxic chemical stress and sporulation (Gorenflo *et al*., 1999). PHAs enhance the survival of bacteria under environmental stress (Susana castro *et al*., 2010). PHAs biosynthesis and accumulation was implicated in tolerance of *Pseudomonas aeruginosa* PAO1 to temperature stress (Pham *et al*., 2004). Disruption of PHAs biosynthesis reduced the survival ability of *Aeromonas hydrophila* 4AK4 under stress conditions (Zhao *et al*., 2007). *Aromatoleum aromaticum* EbN1 accumulates PHB during growth in the presence of toluene and ethylbenzene (Trautwein *et al*. 2008). PHA content correlated positively with increased survival rates of *Pseudomonas* sp after exposure to adverse conditions such as salinity, thermal, oxidative stress, UV irradiation, desiccation, and osmotic pressure (Susana castro *et al*., 2010). Based on current knowledge of the various solvent tolerance mechanisms adopted by bacteria a model was constructed which illustrates major solvent tolerance mechanisms (Fig. 1).

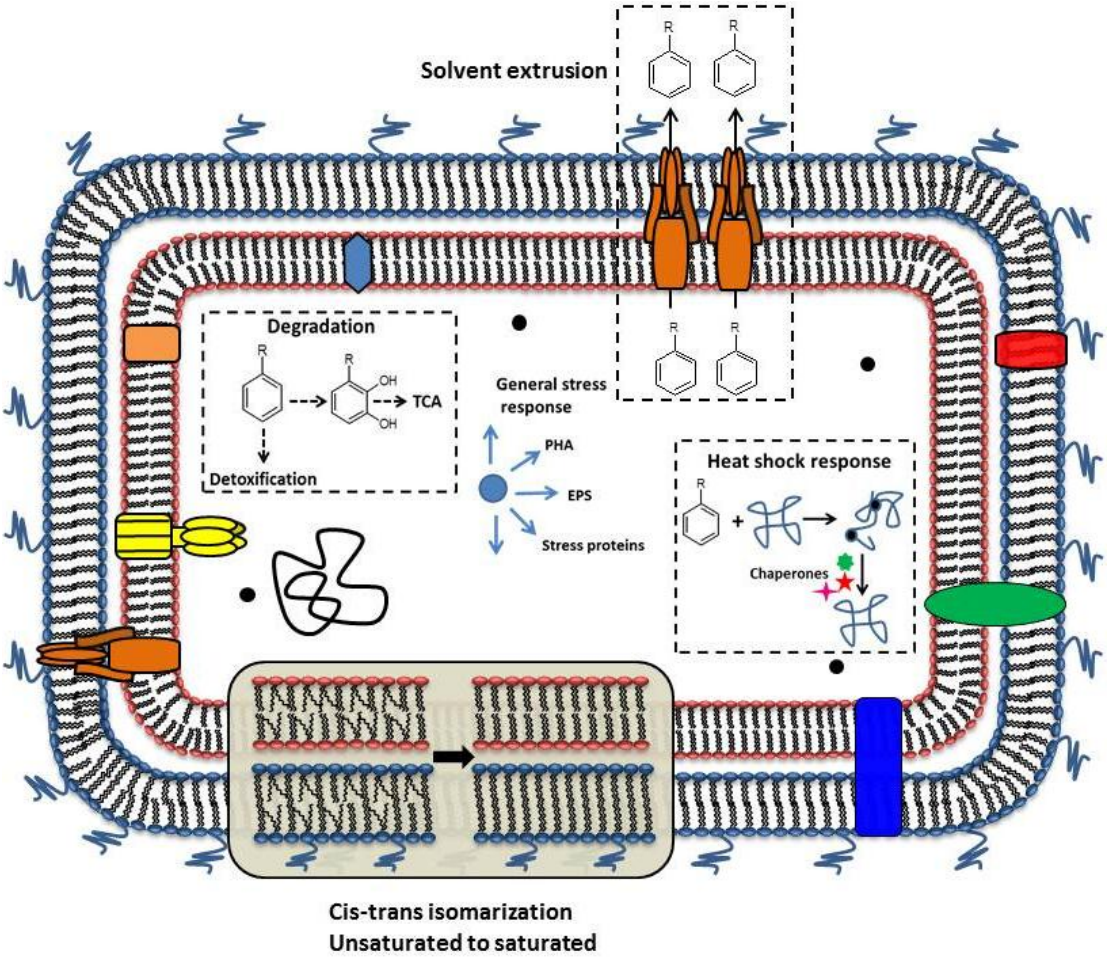

Fig. 1. Schematic representation of the major mechanisms involved in the solvent tolerance of bacteria (Dunlop, 2011; Ramos *et al*., 2002; Segura *et al*., 2012;)

1.4 Metabolic responses of bacteria to stress

Stress induces multiple responses in bacteria and one among them are metabolic responses which are not studied well until recently. Bacteria adapt to the changing environmental conditions/stress by remodelling the molecular and metabolic processes (Kotte *et al*., 2010). Metabolites are end products of gene expression and metabolic profiling offers unique snapshot of physiological status of cell at functional level (Tremaroli *et al*., 2009; Tang, 2011). Understanding the metabolism provides more comprehensive insights on re-adjustments to stress at the systems level (Jozefczuk *et al*., 2010). Qualitative and quantitative studies of intracellular (endometabolome) or an extracellular (exometabolome) small molecules is known as metabolic profiling (Dettmer *et al*., 2007). Metabolic profiling of *E. coli* revealed global metabolic responses and metabolic adaptations to the heat stress mainly *via* suppressing the energy associated metabolism, reducing the nucleotide biosynthesis, altering the amino acid metabolism and promoting osmotic regulation (Ye *et al*., 2012b). Global metabolic shift towards gluconeogenesis and stress resistance pathways (osmo-regulators) were linked to the multicellular behaviour of *Salmonella typhimurium* ATCC14028 upon nutritional stress (White *et al*., 2010).

Metabolic and transcriptomic profiling of *E. coli* MG1655 revealed conserved, specific responses to four different stress conditions and all the stress conditions had similar global impact on metabolism, largely on energy conservation mechanism (Jozefczuk *et al*., 2010). *Pseudomonas fluorescens* ATCC13525 reprogrammed its metabolic network to nitrosative (Nitric oxide) stress and the study revealed role of metabolism in adaptation to nitrosative stress (Auger *et al*., 2011). Nitrosative stress impaired the TCA cycle, electron transport chain and bacteria overcome this by generating ATP by substrate level phosphorylation to survive under stress. Resistance mechanisms of *Pseudomonas pseudoalcaligenes* KF707 to toxic metalloid tellurium were deciphered by NMR based metabolomics, phenotypic microarray techniques and studies revealed extensive reconfiguration of metabolism, role of oxidative stress responses in tellurium tolerance (Tremaroli *et al*., 2009). Metabolic response of *Pseudomonas* sp. HF-1 to nicotine stress was unravelled by NMR based metabolomic approach, which revealed enhanced nucleotide biosynthesis, decreased glucose catabolism, elevated succinate accumulation and severe disturbance in osmoregulation (Ye *et al*., 2012a). GC-MS based metabolic profiling of *Lactococcus lactis subsp. cremoris* MG1363 under changing

temperature, aeration revealed changes of amino acids and fermentation products (Azizan *et al*., 2012). NMR based metabolic profiling revealed metabolic adaptations of *Pseudomonas aeruginosa* during cystic fibrosis chronic lung infection mainly *via* altering the amino acid metabolism and evolving amino acid uptake (Behrends *et al*., 2012). Metabolic responses and their possible role in adaptation to biotic (host-pathogen, inter-intra species interaction) and abiotic stress were recently been illustrated in bacteria. One such metabolic response to the changing environmental conditions is aromatic metabolites (indole derivatives) synthesis which play vital role in adaptation and interaction with other species in some bacteria (Kuczynska-Wisnik *et al*., 2010; Lee and Lee, 2010).

1.5 Aromatic amino acid biosynthesis and its regulation

Aromatic metabolites are major group of small molecules of all living cell and they participate in different cellular processes. Aromatic metabolites are largely biosynthesised *via* shikimate pathway which operate in bacteria, fungi and plants but absent in higher animals. Shikimate pathway leads to the formation of all three aromatic amino acids, quinones, folic acid, essential cofactors and secondary metabolites (Webby *et al*., 2010; Maeda and Dudareva, 2012). Shikimate pathway starts with the condensation of erythrose-4-phospphate and phosphoenolpyruvate forming 3-Deoxy-D-arabino-heptulosonate7-phosphate (DAHP) and is catalysed by DAHP synthase. Series of enzymatic reactions convert DAHP to chorismate, a universal precursor from which shikimate pathway branches off into biosynthesis of phenylalanine, tyrosine and tryptophan (Fig. 2). Bacteria regulates carbon flux into shikimate pathway both at transcriptional and post-translation levels (Maeda and Dudareva, 2012). Formation of DAHP is a first committed, rate limiting step in shikimate pathway and several bacteria have two or more isoforms of DAHP synthases (Maeda and Dudareva, 2012). This enzyme is feedback inhibited either by Phe, Try or Trp and thus regulates carbon flux into shikimate pathway (Maeda and Dudareva, 2012). DAHP synthase, shikimate kinase and entire tryptophan biosynthetic pathway genes are transcriptionally regulated by repressors (TyrR and TrpR) (Panina *et al*., 2003). Chorismate mutase, anthranilate synthase are feedback inhibited by end products of pathway Phe/Tyr and Trp, respectively (Fig. 2) (Panina *et al*., 2001).

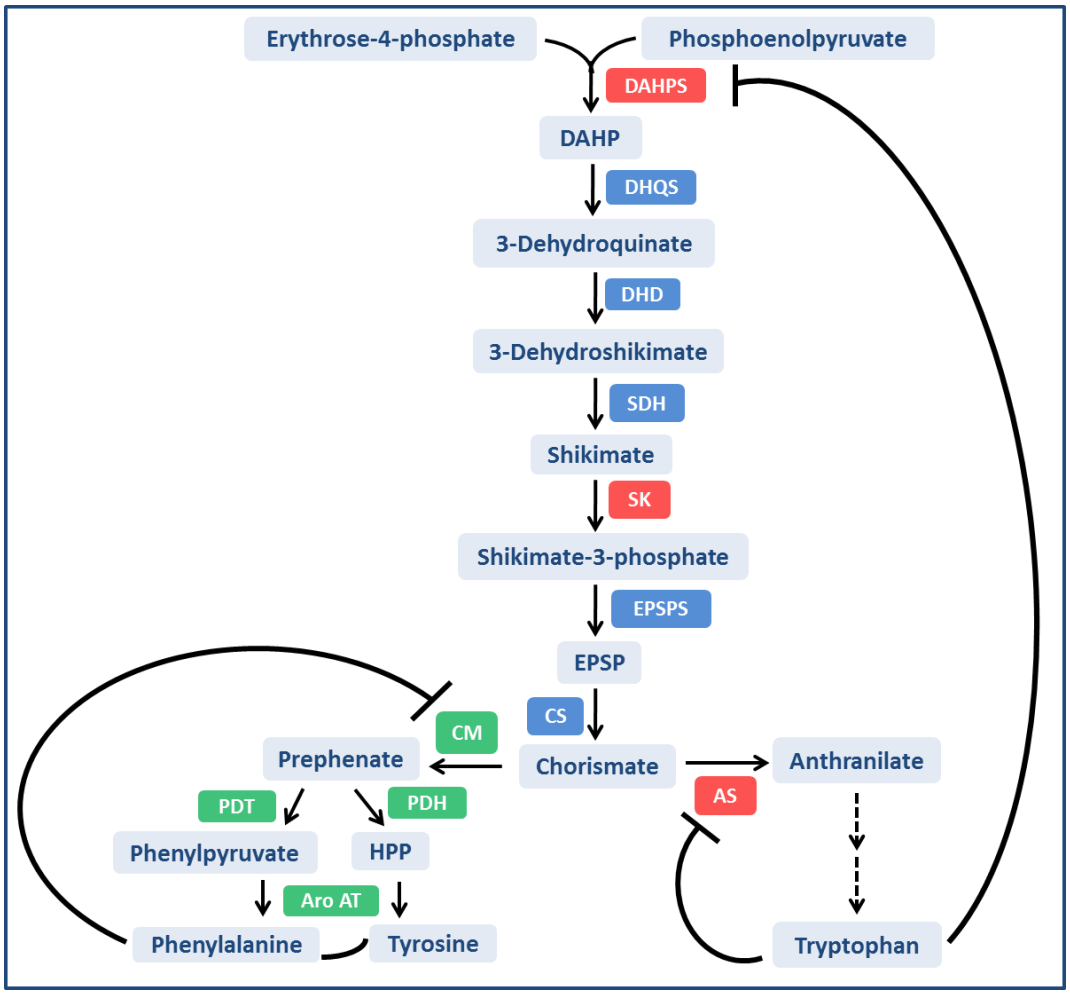

Fig. 2. Aromatic amino acid biosynthesis and its regulation in bacteria (Maeda and Dudareva, 2012)**.**

Solid lines (bold) indicate allosteric feedback inhibition by end products and dashed arrows indicate multiple steps in pathway. Enzymes shaded in red indicate their transcriptional regulation.

DAHP, 3-deoxy-D-arabino-heptulosonate 7-phosphate; DAHPS, 3-deoxy-D-arabino-heptulosonate 7-phosphate synthase; DHQS, 3-dehydroquinate synthase; DHD, 3-dehydroquinate dehydratase; SDH, shikimate dehydrogenase; SK, shikimate kinase; EPSPS, 5-enolpyruvylshikimate 3-phosphate; EPSPS, 5-enolpyruvylshikimate 3-phosphatesynthase; CS, chorismate synthase; CM, chorismate mutase; AS, anthranilate synthase; PDT, prephenate dehydratase; PDH, prephenate dehydrogenase; Aro AT, aromatic aminotransferase.

1.6 Tryptophan biosynthesis and its regulation in bacteria

Among aromatic metabolites tryptophan or its derivatives are implicated in various physiological functions of bacteria (Lee and Lee, 2010), organization and regulation of tryptophan biosynthesis in bacteria vary greatly (Xie *et a*l., 2003). Tryptophan is an aromatic amino acid, it is a substrate for protein synthesis and precursor for many secondary metabolites (Merino *et al*., 2008). Tryptophan biosynthesis starts from conversion of chorismate to anthranilate and this is the first committed, rate limiting step of tryptophan biosynthesis. Anthranilate synthase (TrpE) catalyses the conversion of chorismate to anthranilate followed by series of 5 different catalytic reactions leads to the formation of tryptophan (Fig. 3A). Tryptophan biosynthetic pathway is universal pathway for its biosynthesis and genes, enzymes of tryptophan pathway are evolutionarily conserved (Yanofsky, 2007). Tryptophan biosynthesis is one of the most biochemically expensive, complex process which requires products of four other pathways and their co-ordinate regulation for efficient tryptophan biosynthesis (Yanofsky, 2007).

Organization of tryptophan biosynthetic genes varies greatly in bacteria wherein, bacteria may have whole pathway operon or split (dispersed) operons or genes scattered (gene scrambling) in genome (Merino *et al*., 2008). Tryptophan biosynthesis is stringently regulated at transcriptional, post-translational levels in bacteria and regulatory mechanisms vary greatly (Xie *et al*., 2003; Merino *et al*., 2008). In post-translational level of regulation, anthranilate synthase is feedback regulated by pathway end product tryptophan. Transcriptional regulation involves active repressor mediated transcription termination and attenuation mechanisms. Active repressor transcription termination mechanism was well studied in *E. coli* and in Gammaproteobacteria in which tryptophan biosynthesis genes organised into a single transcriptional unit and expression of these genes regulated by a repressor TrpR (Fig. 3B) (Merino *et al*., 2008). Attenuation mechanism involves pre-mature transcription termination and different groups of bacteria employ different attenuation mechanisms (Xie *et al*., 2003; Merino *et al*., 2008). One such attenuation mechanism is well characterised in *E. coli* and in this transcription is regulated by sensing tryptophan charged tRNA (tRNA ^{trp}) (Fig. 3B). Organization of tryptophan genes and their regulation is largely governed by selective pressure under which bacteria thrive and thus their regulatory mechanisms vary greatly and these are not yet completely understood (Xie *et al*., 2003; Merino *et al*., 2008). Tryptophan or its derivatives are biosynthesised by bacteria at various physiological/developmental stages and one such metabolite is IAA (Merino *et al*., 2008; Spaepen *et al*., 2007).

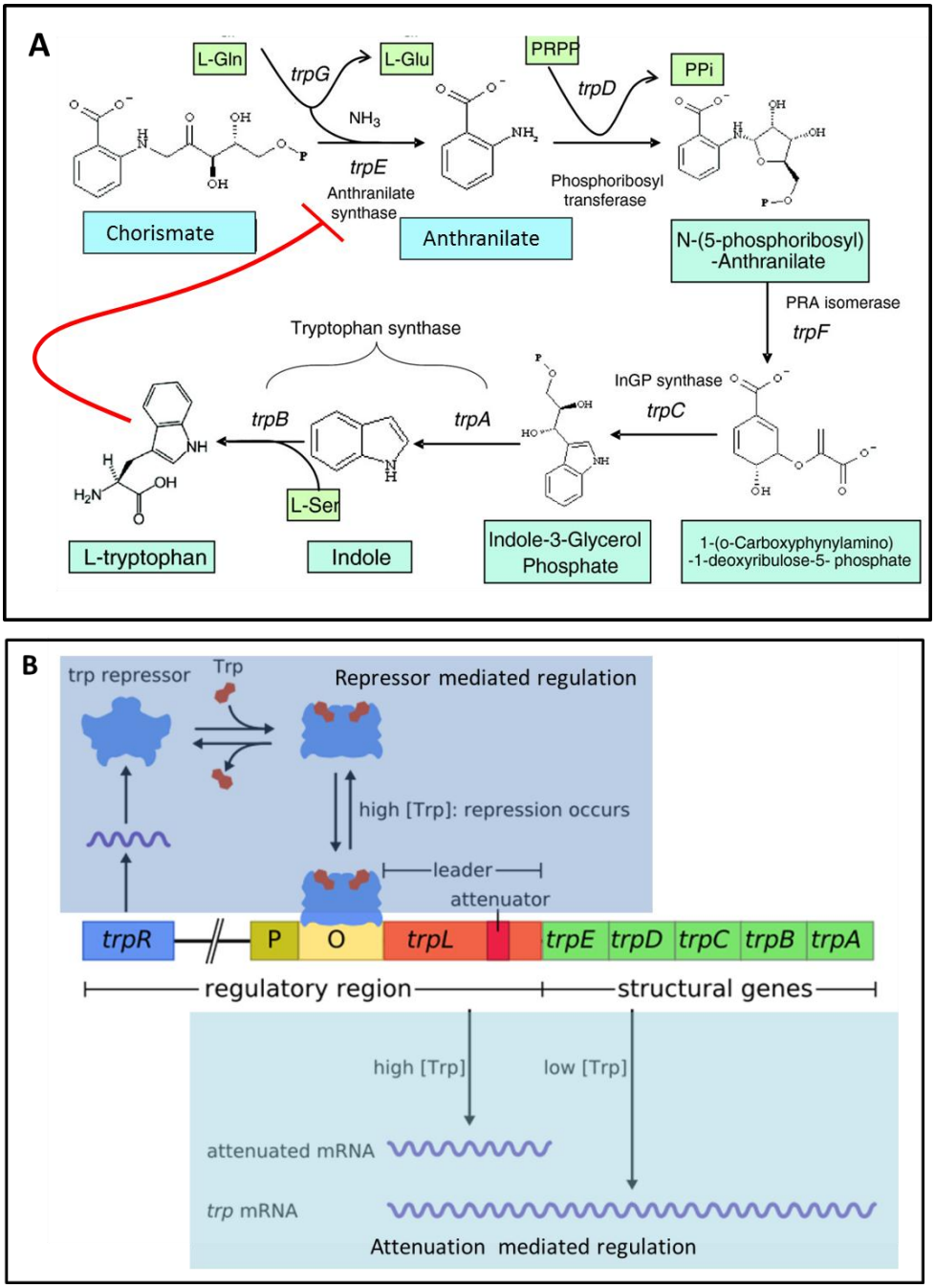

Fig. 3. Tryptophan biosynthesis (A) and its regulation (B) in gammaproteobacteria

PRP, phosphoribosyl pyrophosphate; PPi, pyrophosphate; PRA, phosphoribosylamine; Trp, tryptophan; Gln, Glu, Ser, three latter code for amino acid. Solid line in red indicate feedback inhibition by tryptophan.

1.7 Indole-3-acetic acid biosynthesis in bacteria

Indole-3-acetic acid (IAA) is one of the indole molecules produced by both plants, bacteria and performs diverse physiological functions (Bianco *et al*., 2006; Spaepen *et al*., 2007). Diverse group of bacteria produce IAA and many of the rhizospheric bacteria are capable of IAA production (Spaepen *et al*., 2007). IAA is biosynthesised *via* multiple pathways and redundancy of IAA biosynthesis is wide spread among the bacteria (Spaepen *et al*., 2007). IAA biosynthesis is largely tryptophan dependent where tryptophan acts as precursor while tryptophan independent pathway was observed only in *Azospirillum brasilense* SpF49 (Spaepen *et al*., 2007). However, enzymes or genes responsible for the tryptophan independent pathway are yet to be identified in bacteria and plants (Spaepen *et al*., 2007). At least four different tryptophan dependent IAA biosynthetic pathways were reported from diverse group of bacteria mainly, Indole-3-pyruvate, indole-3-acetamide, indole-3-acetonitrile and tryptamine pathways (Spaepen *et al*., 2007). Indole-3-pyruvate pathway was considered as a major pathway of IAA biosynthesis in bacteria, all the tryptophan dependent pathways of IAA biosynthesis and their corresponding enzymes, genes are well characterised in bacteria (Spaepen *et al*., 2007). Schematic representation of IAA biosynthesis in bacteria is illustrated in figure 4.

1.8 Physiological role of indoles in bacteria

Indole nucleus occurs in many naturally occurring metabolites such alkaloids, pigments, phytohormones, neurotransmitters and indole scaffold considered as "privileged structure" (de Sa Alves *et al*., 2009). Although many bacteria produce indolic compounds but their biological role was not discovered until recently (Spaepen *et al*., 2007; Lee and Lee, 2010). Bacteria use signalling molecules to coordinate their behaviour under certain conditions to survive and one such signalling molecule is indole (Lee *et al*., 2007a; Lee and Lee, 2010). Many Gram-positive and Gram-negative bacteria produce indole from tryptophan. As an intercellular signal molecule, indole controls diverse aspects of bacterial physiology, such as spore formation, plasmid stability, drug resistance, biofilm formation, and virulence (Lee and Lee, 2010). Enterohemorrhagic *E. coli* K12 biofilms were inhibited by 7-hydroxyindole while it stimulated biofilm formation in *Pseudomonas aeruginosa* PAO1 and 7-hydroxyindole was considered as interspecies signal (Lee *et al*., 2007b).

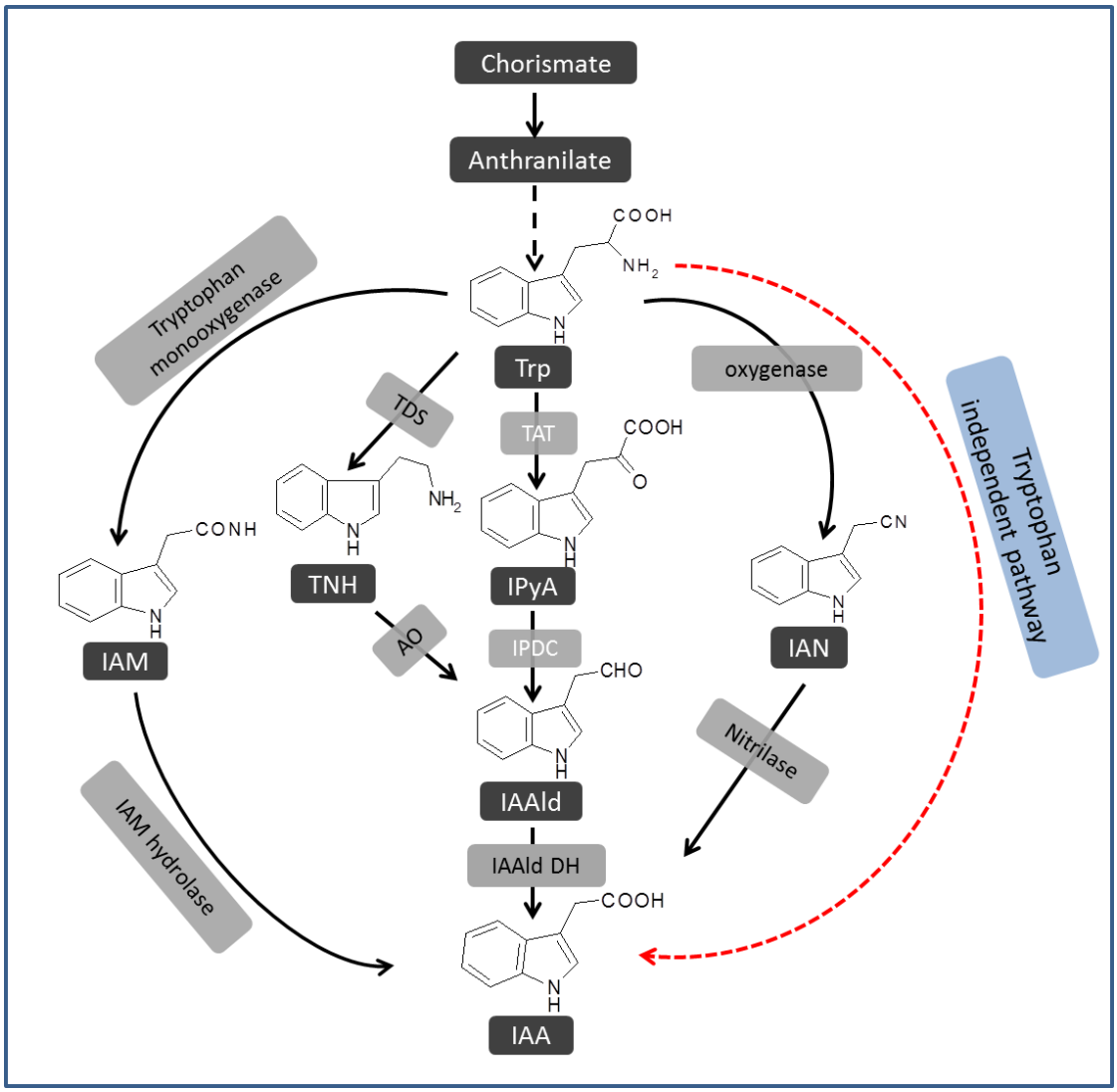

Fig. 4. Indole-3-acetic acid (IAA) biosynthesis in bacteria.

Black dotted arrow indicate multiple steps in pathway; red dotted arrow indicate pathway without enzymatic confirmation

Trp, tryptophan; TAT, tryptophan aminotransferase; TDS, tryptophan decarboxylase; TNH, tryptamine; IPyA, indole-3-pyruvic acid; IPDC, indole pyruvate decarboxylase; IAM, indole -3-acetamide; IAN, indole -3-acetonitrile; IAAld, indole -3-acetaldehyde; IAAldDH, indole -3-acetaldehyde dehydrogenase; AO, amino-oxidase.

Indole imparts population wide antibiotic resistance by turning on drug efflux pumps and oxidative protective mechanisms in *E. coli* MG1655 (Lee *et al*., 2010). Apart from indole, other indolic compounds such as IAA acts as signaling molecule in *Agrobacterium tumefaciens* C58 and inactivates virulence (*Vir)* genes expression (Liu and Nester, 2006). Indole-3-acetic acid also regulates virulence factors of *Erwinia chrysanthemi* 3937 and is implicated in plant-microbe interactions (Spaepen *et al*., 2007). IAA increased tolerance of *E. coli* K-12 to several stress conditions (heat and cold shock, UV-irradiation, osmotic and acid shock and oxidative stress) and to different toxic compounds (antibiotics, detergents and dyes) (Bianco *et al*., 2006; Hirakawa *et al*., 2010). Bacterial indole and its derivatives attenuates the virulence of fungal pathogen *Candida albicans* and indoles are considered as cross kingdom signaling molecules in microbial interactions (Oh *et al*., 2012). Indole and 3-indolylacetonitrile inhibit spore maturation in *Paenibacillus alvei* (Kim *et al*., 2011), decreases biofilm formation in *E. coli* O157:H7 and virulence in *Pseudomonas aeruginosa* PAO1 (Lee *et al*., 2011). Increasing evidences suggest that indole molecules modulate gene expression under stress and act as signalling molecules of microbial interactions (Fig. 5) (Bianco et al., 2006; Hirakawa et al., 2010; Lee and Lee, 2010).

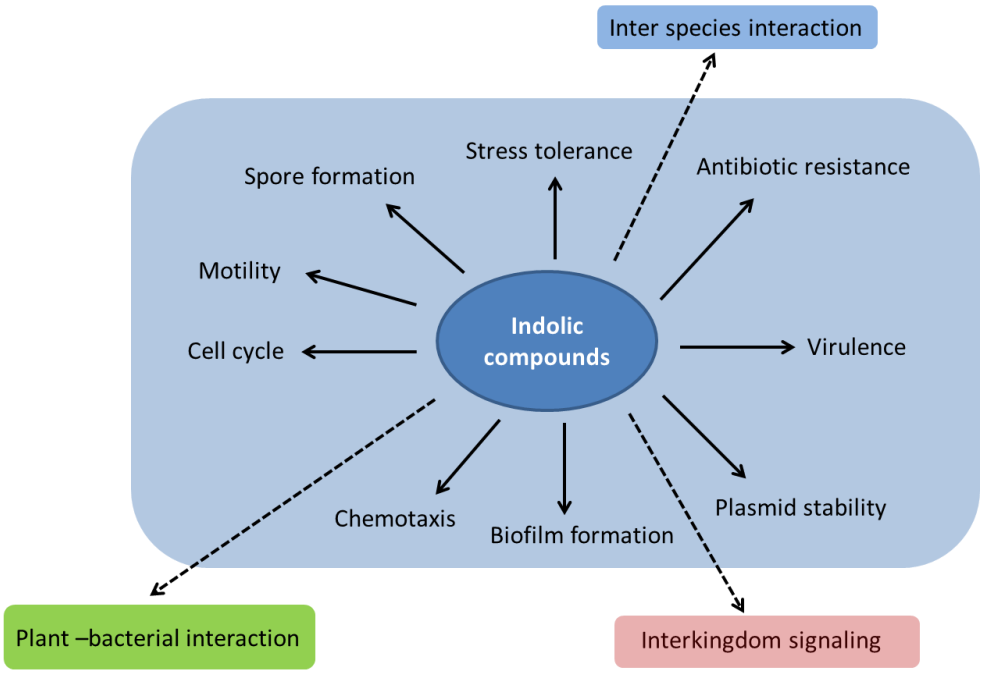

Fig. 5. Schematic representation of physiological role of indolic compounds in bacteria (Lee and Lee, 2010; Spaepen *et al*., 2007; Lee *et al*., 2011). Solid arrows indicate intracellular functions and dotted arrows indicate extracellular function.

1.9 Aniline and aniline derivatives in the environment

Many aromatic pollutants are released into the environment and aniline is one among them. Aniline and its derivatives are primary aromatic amines widely used in manufacturing of plastics, dyes, pesticides, herbicides, paints, rubber additives, polyurethanes, pharmaceuticals and as solvent in organic synthesis (Liang *et al*., 2005). They are also formed by microbial transformation of nitro aromatic compounds and aniline based herbicides (Vangnai and Petchkroh, 2007). Owing to their extensive usage large quantities of anilines are released into the environment by industrial effluents and their direct application to the soil (Liang et al., 2005). They are widely distributed and frequently found in both terrestrial and aquatic environments. Anilines are accumulated in sediments, sludge and agricultural soil (Vangnai and Petchkroh, 2007). In soil, anilines bound to soil organic matter by adsorption and remains persistent (Konopka *et al*., 1989). Aniline is considered as one of the priority pollutant by US Environmental Protection Agency (Federal Register, 1979) due to its recalcitrant properties (EEC, 1976; Federal Register, 1979).

1.10 Aniline toxicity in microorganisms

Aniline and its derivatives being aromatic amines, they are mutagenic and their carcinogenicity is reported in animals and bacteria (Scribner *et al*., 1979). Toxic effect of aniline derivatives on acetoclastic methanogenic bacteria revealed inhibition of methanogenic activity (Donlon *et al*., 1995). Aniline in yeast generates free radicals resulting in oxidative stress leading to lethality (Brennan and Schiestl, 1997). Toxic effect of anilines on some algae and *Vibrio fischeri*, a luminescent bacterium was due to their hydrophobicity (Aruoja *et al*., 2011). Toxic effect of anilines was well studied in animal models (Jones and Fox, 2003; Fan *et al*., 2011) however, a detailed study on the mechanism of toxicity is scarce in microorganisms.

1.11 Aniline metabolism in bacteria

Metabolism of aniline and its derivatives by soil microorganisms was considered to be an effective measure for bioremediation (Konopka *et al*., 1989). Many aniline degrading bacteria were isolated from agriculture soils or industrial areas (Liang *et al*., 2005; Vangnai and Petchkroh, 2007)). Species of *Alcaligenes, Acinitobacter, Pseudomonas, Rhodococcus, Frateuria, Moraxella, Nocardia, and Delftia* are able to degrade aniline or its derivatives (Liang *et al*., 2005). Bacteria utilize aniline as carbon and

nitrogen sources or carbon source. Aerobic and anaerobic metabolism of aniline by bacteria was reported and bacterial strain HY99 degrades aniline by both metabolisms (Kahng *et al*., 2000). Aniline degrading genes are located on chromosome or plasmid of bacteria (Liang *et al*., 2005). Biotransformation of anilines to acetanilides, formanilide was wide spread among eukaryotes and prokaryotes (Suzuki *et al*., 2007).

1.11.1 Biotransformation of aniline

Biotransformation of aniline is one of the methods of aniline detoxification (Fig. 6A) (Pluvinage *et al*., 2007; Suzuki *et al*., 2007). Aniline and its derivatives are transformed to less toxic acetanilides by arylamine N-acetyltransfarase (NAT). Many bacteria reported to have NAT activity (Delomenie *et al*., 2001) NAT detoxifies xenobiotics by transferring acetyl group from acetylCoA to nitrogen atom of arylamine (Suzuki *et al*., 2007). Aniline is transformed to formanilide by N-formylation and hydroxylation of aniline leads to the formation of aminophenol in some bacteria (Cerniglia *et al*., 1981). Biotransformation of aniline to indole derivatives speculated in *Desulfovibrio* strains (Drzyzga *et al*., 1996) and *Rhodobacter sphaeroides* OU5 (Shanker *et al*., 2006).

1.11.2 Anaerobic biodegradation

Anaerobic metabolism of aniline occurs by reductive deamination of aniline (Schnell *et al*., 1989). Anaerobic degradation of aniline starts by carboxylation of aniline to 4-aminobenzoate which is then activated by 4-aminobenzoyl- CoA- synthetase to 4-aminobenzoyl-CoA. Reductive deamination of 4-aminobenzoyl-CoA leads to formation of benzoyl-CoA and this enters into general benzoyl-CoA degradation pathway to form three molecules of acetyl CoA. Benzoyl-CoA is a central intermediate in the anaerobic degradations of many aromatic hydrocarbons (Fig. 6B) (Carmona *et al*., 2009).

1.11.3 Aerobic biodegradation of aniline

Bacteria utilize aniline as sole source of carbon and nitrogen or as carbon source. Many bacteria capable of degrading aniline under aerobic conditions via oxidative deamination were isolated (Boon *et al*., 2001). Aerobic degradation starts with the conversion of aniline to catechol by aniline dioxygenase (Fig. 7). Catechol can undergo *meta* cleavage by catechol 2,3-dioxygenase to form hydroxymucanic semialdehyde finally to acetylCoA (Liang *et al*., 2005). Catechol enters *ortho* cleavage by catechol 1,2-dioxygenase leading to the formation of *cis,cis* mucanoic acid, finally to succinate and

acetylCoA (Kim *et al*., 2002). Ortho cleavage (β-ketoadipate) pathway of aniline degradation is predominant in bacteria and only 8% of aniline-assimilating bacteria metabolize aniline through the *meta* cleavage pathway (Murakami *et al*., 1998). The β-ketoadipate pathway genes (cat genes) are widely distributed in soil bacteria involved in degradation of various aromatic compounds (Kim *et al*., 2002).

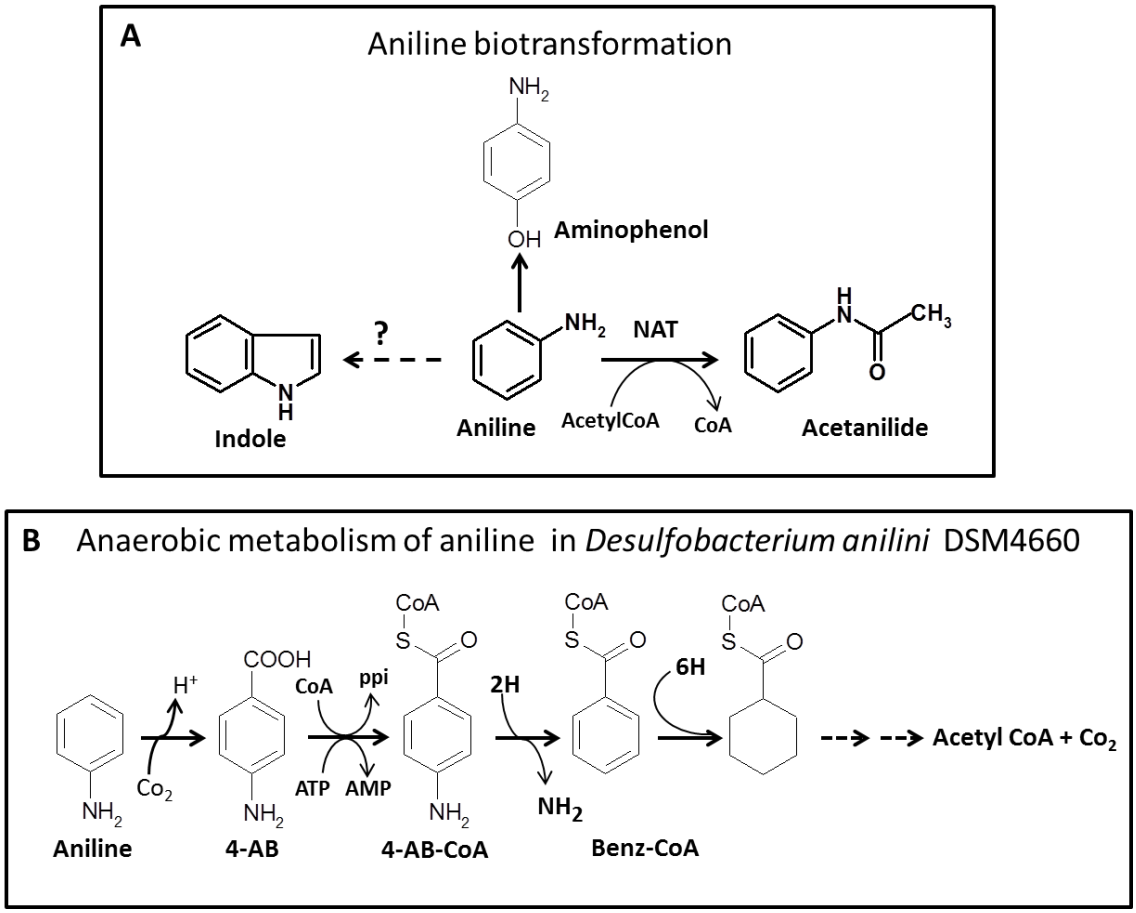

Fig. 6. Bacterial transformation (A) and anaerobic metabolism (B) of aniline.

NAT, N-acetyltransferase; 4-AB, 4-aminobenzoate; 4-AB-CoA, 4-aminobenzoyl CoA; Benz-CoA; benzoylCoA; ?, pathway not confirmed. Dashed arrows indicate multiple reactions.

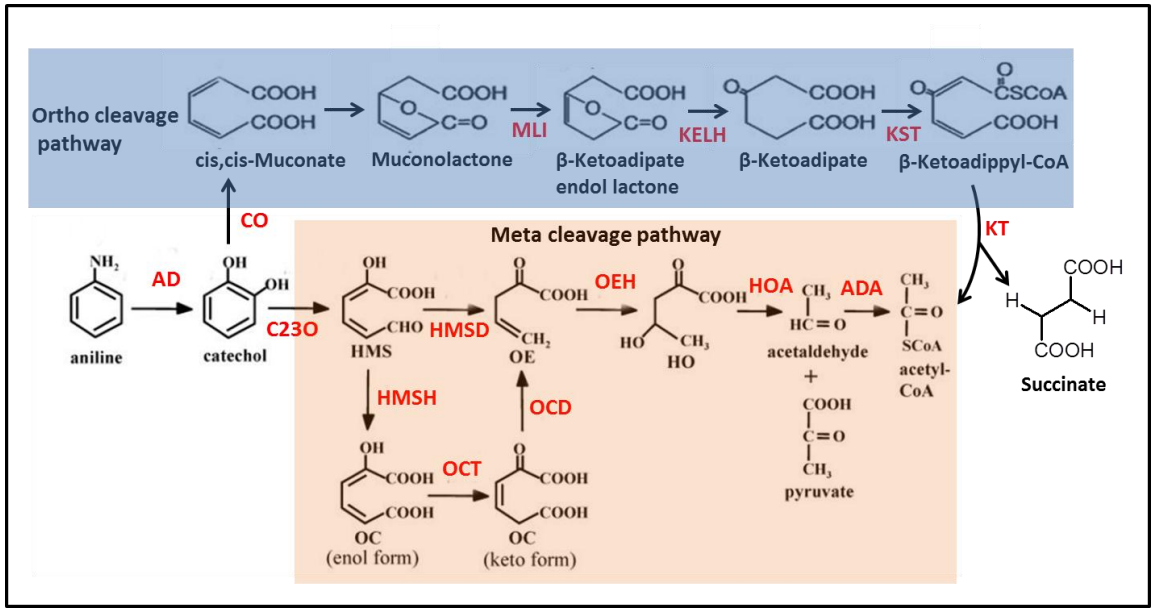

Fig. 7. Aerobic metabolism of aniline in bacteria (Murakami *et al.*, 1998; Liang *et al.*, 2005).

CO, catechol oxygenase; MLI, muconolactone isomerase; KELH, β-ketoadipate enol lactone hydrolase; KST, β-ketoadipate:succinyl-CoA transferase; KT, β-ketoadipate-CoA thiolase.

AD, aniline dioxygenase; C23O, catechol 2,3-dioxygenase; HMS, 2-hydroxymuconic semialdehyde; HMSD, 2-hydroxymuconic semialdehyde dehydrogenase; HMSH, 2-hydroxymuconic semialdehyde hydrolase; OE, 2-oxopent-4-dienoate; OEH, 2-oxopent-4-dienoate hydratase; OC, 4-oxalocrotonate; OCD, 4-oxalocrotonate decarboxylase; OCT, 4-oxalocrotonate tautomerase; HO, 4-hydroxy-2-oxovalerate; HOA, 4-hydroxy-2-oxovalerate aldolase; ADA, acetaldehyde dehydrogenase.

1.12 Definition of the problem

Diverse group of bacteria degrade or transform aromatic compounds to thrive under xenobiotic stress and one such group of bacteria are anoxygenic photosynthetic bacteria (APB) (Carmona *et al*., 2009). APB are unique physiological group of bacteria widely distributed in the environment occupying different habitats and they thrive in both oxic/anoxic zones (Larimer *et al*., 2004; Steunou *et al*., 2004). APB are metabolically versatile bacteria, capable of growing under different growth modes (Steunou *et al*., 2004; Glaeser and Klug, 2005). APB utilize wide array of organic compounds for their growth as sole source of carbon or nitrogen. Although a few APB are capable of degrading aromatic compounds for their growth, they also have remarkable ability to transform aromatic compounds (Sasikala and Ramana, 1998). APB transforms phenylalanine or tyrosine to phenol terpenoids (Kumavath et al., 2010a) and tryptophan/anthranilate to novel indoles (Sunayana et al., 2005; Kumavath et al., 2010b).

Biotransformation of aniline to indole esters by a photosynthetic bacterium *Rhodobacter sphearoides* OU5 was reported and the process was dependent on fumarate, TCA cycle intermediates (Shanker *et al*., 2006). However, biosynthetic pathway of indoles in aniline exposed cells and the role of fumarate in indoles biosynthesis was not investigated. On the other hand aniline degradation/transformation was well studied but bacterial cellular responses and their tolerance mechanisms to aniline stress were not studied so far. Deciphering of these processes enhances the current knowledge of aniline metabolism and reveals possible survival mechanisms of bacteria to aniline stress, which may help in developing effective bioremediation methods. The present work aims at elucidation of indoles biosynthesis from aniline and deciphering the metabolic/molecular responses of *Rubrivivax benzoatilyticus* JA2 to aniline stress by metabolomic and proteomic approaches.

1.13 Objectives of the study

- **Elucidation of biosynthetic pathway of indoles in aniline exposed cultures of *Rubrivivax benzoatilyticus* JA2**
- **Deciphering the metabolomic and proteomic responses of *Rubrivivax benzoatilyticus* JA2 to aniline stress**

MATERIALS AND METHODS

2.0 Materials and methods

2.1 Materials, chemicals and devices

2.1.1 Glassware

All the glassware used in the present study including test tubes, pipettes, measuring cylinders, culturing flasks, reagent bottles, petriplates, screw cap test tubes were of Borosil or Duran brand.

2.1.2 *Deionized water*

Deionized water obtained from deionizer plant (ion exchange India Ltd. Model-CA 20/U) was routinely used for rinsing of glassware and for media preparation. Distilled water and double distilled water was used for preparation of stock solutions and chemical analysis.

Milli-Q water was used for HPLC analysis.

2.1.3 Chemicals

All the chemicals used in this study are analytical grade from Sigma-Aldrich, Alfa Acer, Lancaster, Qualigens, Merck, Himedia, Cambridge Isotope Laboratories, Fluka, Supelco and Bio Rad.

2.1.4 Filtration devices

Filter papers, membrane filters and filtration units used in this study were from Millipore, PALL Life sciences or from Whattman.

2.1.5 Determination of pH

pH was determined using a digital pH meter (Digisun electronics, India model DI-707) and pH meter was often calibrated with standard buffer solutions.

2.1.6 Buffers and standard solutions

Deionised and sterile water (Milli-Q) was used for buffers preparation. Buffers were prepared according to standard protocols and pH was adjusted at room temperature unless otherwise stated.

2.1.6.1 General buffers

Phosphate buffer; 50 mM potassium phosphate, pH range 5.5, 6.5, 7.5.

Borate buffer; 50 mM borate, pH 10.

Tris buffer; 100 mM Tris/HCl pH 7.8

2.1.6.2 Buffers used in proteome analysis

Proteome extraction buffer*;* 50 mM HEPES-KOH, pH 7.5; 0.1% SDS (w/v), 0.1% Tritan-X-100 (w/v).

Re-suspension buffer; 50 mM Tris, pH 8.0; 100 mM NaCl, 1 mM EDTA.

2D Nano LC-ESI-MS/MS; Buffer A (98% H2O, 2% ACN, 0.2% formic acid, and 0.005% TFA (v/v),

Buffer B (100% ACN, 0.2% formic acid, and 0.005% TFA(v/v),

Buffer C (5% ACN, 0.2% formic acid(v/v), and 0.5 M ammonium acetate.

2.1.6.3 RNA isolation buffers

TE buffer; 10 mM Tris.HCl, 1 mM EDTA, pH 8.0.

2.1.6.4 SDS-PAGE buffers and solutions

Stacking gel; 5% polyacrylamide (30/0.8 acrylamide/bisacrylamide (w/w)); 125 mM Tris/HCl, pH 6.8; 0.1% (w/v) SDS; 0.015% (v/v) TEMED; 0.05% (w/v) APS.

Separating gel; 12.5% polyacrylamide (30/0.8 acrylamide/bisacrylamide (w/w)); 375 mM Tris/HCl, pH 8.8; 0.1% (w/v) SDS; 0.015% (v/v) TEMED; 0.05% (w/v) APS.

Running buffer; 25 mM Tris/HCl, pH 8.3; 0.192 M glycine; 0.1% (w/v) SDS.

Sample/loading buffer (5x concentrated); 50 mM Tris/HCl, pH 6.8; 100 mM DTT; 2% (w/v) SDS; 0.1% bromophenol blue; 10% glycerol.

Fixation/staining solution; 0.1% (w/v) Coomassie brilliant blue R-250 dissolved in 45/45/10 Methanol/H_2O dest /acetic acid (v/v/v).

Destaining solution; 12.5/77.5/10 isopropanol/H_2O dest /acetic acid (v/v/v).

2.1.6.5 Standard stock solutions

100 mM of tryptophan and anthranilate stock solutions were prepared in distilled water, filter sterilised and stored at 4°C for one month. Aniline (250 mM), fumarate 6% (w/v, pH 7) stocks were prepared, sterilised by autoclaving. Aniline stock was stored in dark at room temperature.

2.1.7 Dyes for confocal microscopy

1 mg.ml^{-1} (w/v) stock solutions of nile red, fluorescein diacetate (FDA), tetramethyl rhodamine isothiocyanate (TRITC), acridine orange were prepared in DMSO (dimethyl sufoxide) and calcofluor white (1 mg.ml^{-1}), aniline blue (1 mg.ml^{-1}) solutions were

prepared in sterile Mill-Q water. SYTOX Green (5 mM) in DMSO solution was from Invitrogen. All dyes were stored in dark at -20°C.

2.1.8 Sterilization

Sterilization of the culture media and glassware was done by autoclaving at 15 lbs, 120°C for 15 min. Thermolabile stock solutions were filter sterilised by 0.22 µm membrane filter (Millipore).

2.1.9 Media preparation

2.1.9.1 Malate mineral medium (components g.l^{-1})

KH_2PO_4 -0.5, $MgSO_4$.7 H_2O -0.2, NaCl-0.4, NH_4Cl -0.37,$CaCl_2$.2H_2O-0.05, Malate-3.0, yeast extract-0.2, ferric citrate 0.1% (w/v) 5 ml.l^{-1}, Trace elements SL_7 1 ml. (SL_7 (mg.ml^{-1}): HCl (25% v/v) 1 ml^{-1}; $ZnCl_2$-7; $MnCl_2$.4H_2O-100; H_3BO_3-60; $CoCl_2$.6H_2O-200; $CuCl_2$.H_2O-20; $NiCl_2$.6$H_2$0-20; $NaMoO_4$.6H_2O-40). Malate (22 mM) was used as carbon, electron donor and ammonium chloride (7 mM) as nitrogen source. Ingredients were dissolved in distilled water, pH was adjusted to 6.8 with 5N NaOH. Malate was replaced with other carbon sources whenever required (22 mM).

2.1.9.2 Nutrient Agar (ingredients g.l^{-1})

NaCl – 5, Peptone -10, yeast -3.5 and agar-20, pH 7.0.

2.2. Organism and growth conditions

2.2.1. Organism

Rubrivivax benzoatilyticus JA2^T (=ATCC BAA-35^T=JCM 13220^T=MTCC 7087^T) was used for all the experiments.

2.2.2 Photoheterotrophic (Anaerobic) and aerobic growth

Rubrivivax benzoatilyticus JA2 (=ATCCBAA-35) was grown photoheterotrophically (anaerobic, 30 ±2°C; light 2,400 lux) on malate minimal medium supplemented with malate (22 mM) as carbon source and ammonium chloride (7 mM) as nitrogen source in fully filled screw cap test tubes (10x100 mm)/reagent bottles (250 ml) at pH 6.8. Culture was grown aerobically on mineral medium in 250 ml conical flasks at 150 rpm and at 30°C. When aniline was used as sole source of carbon or nitrogen, malate or ammonium chloride was replaced with aniline (1or10 mM).

2.2.3 Maintenance of stock culture

Stock cultures of *R. benzoatilyticus* JA2 was maintained as agar stabs. Stabs were prepared by using 2% (w/v) agar in malate mineral medium, filled to the ¾ volume of 5 ml capacity screw cap test tubes. Pure culture of *R. benzoatilyticus* JA2 was stabbed into the solidified mineral medium and the culture tubes were illuminated (2,400 lux) and incubated at 30 ±2°C. After 2-3 days of growth, the stab cultures were preserved under refrigeration at 4°C for further use. *R. benzoatilyticus* JA2 culture was grown under photoheterotrophic conditions to reach the OD_{660nm} 0.25 and this culture (10%) was used as inoculum for all the experiments.

2.2.4 Purity of the cultures

Culture purity was monitored by streaking on nutrient agar plates and incubating aerobically at 30 ±2°C. Purity of the culture was routinely checked before and after the experiment.

2.2.5 Growth and biomass

Growth was measured turbidometrically (OD_{660nm}) and the biomass as dry weight. Dry weight was calculated by empirical formula generated from plot of $OD_{660\ nm}$ against dry weight. $0.1(OD_{660\ nm}) = 0.15$ mg.dry wt.ml^{-1}.

2.2.6 Minimum inhibitory (MIC) and inhibitory concentration 50 (IC50)

Minimum inhibitory and IC50 concentrations of the compounds were determined by growing *R. benzoatilyticus* JA2 on photoheterotrophic medium with malate as carbon source along with different concentrations (1-30 mM) of test compounds (solvents). Culture was grown under photoheterotrophic conditions (anaerobic, 30°C, 2400 lux) and growth was measured at $OD_{660\ nm}$. MIC and IC50 values were determined from the plot of growth against concentration of the compound.

2.2.7 Bacterial viability

Viability of the culture was determined by standard plate count method. Cultures were serial diluted in sterile 0.9% NaCl (w/v) and appropriate dilutions were spread (150 µl) onto nutrient agar plate, incubated at 30°C for 3-4 days. Colony forming units were counted using empirical formula

CFU/ml = No of colonies x dilution / volume plated x 1 ml

2.2.8 Resting cell assay

Rubrivivax benzoatilyticus JA2 was grown on malate (22 mM) minimal medium under photoheterotrophic conditions for 48 h. After 48 h of the growth, cells were harvested by centrifugation (10,000 x g, 4°C for 10 min) in sterile Okridge tubes (tarson). Supernatant was discarded, pellet was washed in mineral medium (devoid of carbon and nitrogen sources) and finally cells were suspended in the same media.

2.2.9 Aniline exposure

Rubrivivax benzoatilyticus JA2 was grown photoheterotrophically on malate mineral medium for 48 h (0.4 $OD_{660\ nm}$) and then culture was exposed to 25 mM aniline, 13 mM of fumarate. Aniline exposed culture was incubated under photoheterotrophic conditions for 48 h or to a desired time period. Control culture was exposed to fumarate (13 mM) alone**.**

2.2.10 Tryptophan/ anthranilate feeding

Rubrivivax benzoatilyticus JA2 was grown on malate mineral medium under photoheterotrophic conditions for 48 h (0.4 $OD_{660\ nm}$) and then culture was supplemented with 1mM of anthranilate or 1 mM of tryptophan, culture was incubated under photoheterotrophic conditions for 48 h or to desired time period.

2.2.11 Glyphosate treatment

To evaluate the effect of glyphosate on growth of *R. benzoatilyticus* JA2, different concentrations (1-10 mM) of glyphosate was added to malate mineral medium and inoculated with culture. Growth restoration experiments were done by adding 200 µM of aromatic amino acids or its precursors along with glyphosate (1 mM) to medium and inoculated with culture. Growth was measured at 660 nm over a period of time. To monitor the effect of glyphosate on indoles production different concentrations (0-2 mM) of the glyphosate was added to culture during aniline (25 mM) or anthranilate (1 mM) exposure.

2.2.12 pH shift assay

Rubrivivax benzoatilyticus JA2 was grown photoheterotrophically on malate/glucose mineral medium for 48 h (0.4 $OD_{660\ nm}$) and the cells were harvested by centrifugation (10,000 x g, 4°C for 10 min) in sterile Okridge tubes (tarson). Supernatant was discarded; cell pellet was washed in buffer and finally suspended in buffers of

different pH ranges (4.5-10). Malate/glucose grown cultures were exposed to aniline as described in 2.2.9 and to change the pH of the culture sterile 5N HCl or NaOH was used and culture pH was monitored by pH strips.

2.3 Extraction of metabolites

2.3.1 Extraction of indoles

Control or aniline exposed culture of *Rubrivivax benzoatilyticus* JA2 as described in section 2.2.9 was used for extraction of indoles. After 48 h of aniline exposure, cells were harvested by centrifugation (10,000 x g, 10 min, 4°C) and the supernatant was collected and concentrated to dryness under vacuum in rotary flash evaporator (Heidolph, Germany) at 45°C. After complete dryness, the brown residue was fractionated according to the protocol used by Powell (1964).

Dried residue was dissolved in 10 ml of 10N NaOH and fractioned into organic, aqueous phase by adding equal volume of dichloromethane (DCM). pH of aqueous, organic phase was adjusted to 3. Aqueous phase was fractionated into acidic (organic) and water soluble (aqueous) fractions with equal volume of DCM. Similarly, organic phase was partitioned to neutral (organic) and basic (aqueous) fractions. Fractions were evaporated to dryness using flash evaporator, redissolved in HPLC grade methanol (1 ml), filtered (0.22 µm membrane) and used for HPLC and mass analysis.

2.3.2 Extraction of indoles from tryptophan fed cultures

Rubrivivax benzoatilyticus JA2 was grown under photoheterotrophic conditions for 48 h, induced with tryptophan (1 mM) and incubated for 48 h. After 48 h of incubation, cells were harvested by centrifugation (10,000 x g, 4°C,10 min). Cell pellet was discarded, culture supernatant was acidified to pH 2.5 with 5N HCl and the metabolites were extracted thrice with equal volumes of ethyl acetate. The ethyl acetate layers were pooled and evaporated to dryness under vacuum in rotary flash evaporator (Heidolph, Germany) at 45°C. After complete dryness, the brown residue was dissolved in HPLC grade methanol (1 ml), filtered (0.22 µm membrane) and used for HPLC and mass spectral analysis.

2.3.3 Isolation of extracellular polymeric substance (EPS)

EPS was isolated according to Cao *et al* (2011) with slight modifications. Briefly, aniline exposed cells of *R. benzoatilyticus* JA2 as described in section 2.2.9 were used for

EPS isolation. After 48 h of exposure to aniline, cells were harvested by centrifugation (4°C, 10,000 x g for 10 min) and the cell pellet was suspended in 5 ml of 0.9% NaCl (w/v) incubated for 30 min at 4°C. Cells were centrifuged and the supernatant was collected, process was repeated three times. Supernatants were combined, filtered through 0.22 µm membrane filter (PVDF Millipore) and chilled isopropanol was added to the filtrate in 3:1 ratio, EPS was precipitated overnight at -20°C. Precipitated EPS was concentrated by centrifugation (10,000 x g, 10 min), lyophilised and stored at -20°C till usage. Purified EPS was used for NMR, EDAX, FTIR and GC-MS analysis.

2.3.4 Extraction of polyhydroxyalkanoates (PHAs)

Aniline exposed or control cells of *R. benzoatilyticus* JA2 as described in section 2.2.9 were used for PHAs extraction. Aniline exposed (after 48 h of aniline exposure) or control cells were harvested by centrifugation (10,000 x g for 10 min, 4°C) and the cell pellet was washed twice with distilled water. Finally cell pellet was re-suspended in distilled water and freeze dried (Labcanco USA). Freeze dried biomass (300 mg) was suspended in 30 ml of chloroform and incubated overnight in rotary shaker (120 rpm) at 30°C, obtained suspension was filtered through Whatman No1 paper to remove cell debris and filtrate was subjected to precipitation overnight -20°C in 10 volumes of ethanol. Finally obtained precipitate was concentrated by centrifugation (15,000 x g for 20 min) and dissolved in 5 ml of acetone. PHAs were purified by adding 20 ml of 70% ethanol (v/v), methanol in 1:1 ratio to PHAs suspended in acetone. Finally pure PHAs were obtained by centrifugation (15,000 x g for 20 min), purified PHAs were air dried, sealed stored at -20°C.

2.3.5 Extraction of intracellular metabolites (endometabolome)

Aniline exposed or control cells of *R. benzoatilyticus* JA2 as described in section 2.2.9 were used for extraction of intracellular metabolites. Aniline exposed (after 48 h of aniline exposure) and control cells were harvested by centrifugation (10,000 x g, 10 min, 4 °C) and cell pellet was washed with cold Mill-Q water, rapidly quenched in liquid nitrogen, and the cell pellet was lyophilized for 10 h. Intracellular metabolites were extracted from lyophilized sample by methanol/chloroform method (Gromova and Roby, 2010). Nine millilitre of methanol:chloroform:water (3:1:1 v/v/v) mixture was added to 300 mg of lyophilized cell pellet vertexed and sonicated for 15 sec, 7 times (8cyle, 50% power, 4°C) with time interval of 1 min. Chloroform (1.5 ml) and 3 ml of water was

added to sonicated sample, vertexed and centrifuged (12,000 x g, 4°C, 10 mins). Finally polar phase which contains hydrophilic metabolites was collected, methanol was evaporated from sample and lyophilized, stored at -20°C till further analysis by GC-MS.

2.4 Analytical methods

2.4.1 High Performance Liquid Chromatography (HPLC)

HPLC analysis was done according to Graham (1991) with slight modifications. Reverse phase HPLC analysis was performed on Shimadzu Prominence (LC- 20AT) system equipped with binary pump Photodiode array detector and Phenomenex C-18 column (Luna, 5µm, 250 x 4.6 mm). Gradient method was employed for separation of metabolites with 30 min run time. 1% Acetic acid in water (v/v) and acetonitrile (100%) were used as mobile phase. Gradient program; linear gradient of 0-55% acetonitrile for 25 min followed by step increase to 100% acetonitrile, held for 3 min and finally return to 1% acetic acid wash. Flow rate was 1.5 $ml.min^{-1}$; injection volume was 20 µl and the metabolites were detected at 230, 280 and 350 nm. Metabolites were identified by comparing the retention time (R_t) and co-eluting with authentic standards. UV spectra were recorded by photodiode array detector and metabolites were quantified with reference to the peak areas of known concentrations of authentic standards. Aniline, fumarate, tryptophan, indole-3-acetic acid, indole-3-aldehyde, anthranilate, and indole-3-acetamid were quantified by HPLC with reference to the peak areas of known concentrations of authentic standards.

2.4.2 Liquid chromatography tandem mass spectrometry (LC- MS/MS-QTOF)

Mass analysis was performed on microQTOF (Brukars deltanoics) mass spectrometer coupled to HPLC (Agilent 1200 series) equipped with UV-VIS detector and auotosampler. Metabolites were separated on reverse phase column; C-18, 5µm, 150 x 4.6 mm (Water's) or C-18, 5µm, 250 x 4.6 mm (Phenomenex). Separation of metabolites were carried as described in HPLC conditions except the flow rate was 0.8 $ml.min^{-1}$ and detection was done at 280 nm, with a post column split effluent was introduced into electro spray ionization (ESI) ion source (80 ºC, Cone voltage 15-25V). ESI was performed in positive and a negative mode to detect molecular ion masses, fragmentation was obtained by collision energy of 5-20 eV depending upon the nature of the molecule and helium as collision gas. Mass spectra were recorded from 50-1000 Da. Metabolites

were identified by matching the spectra with authentic standards and against database (*www.massbank.jp*).

2.4.3 Gas chromatography mass spectrometry (GC-MS) of EPS

Purified EPS as described in section 2.3.3 was used for GC-MS analysis and 10 mg of lyophilsed EPS was hydrolysed (120°C in pressure chamber) with 2N TFA (Trifluoroacetic acid) for 4 h. TFA was evaporated from the sample by rotary flash evaporator, the residue was dissolved in 0.5 ml Milli-Q water and finally lyophlised. Lyphilised sample was dissolved in 20 µl of pyridine and derivatized with 40 µl of BSTFA+TMCS (99:1 Sigma Aldrich) incubated at 70 $^{\circ}$C for 1h under dark. Derivatised sample was immediately analysed by GC-MS.

GC-MS analysis was performed on Pegasus HT TOF-MS (Leco, USA) system equipped with Agilent series (7890) gas chromatography. 1 µl of derivatized EPS sample was injected into HP-5 column (30 m, internal diameter 0.32 mm, thickness 0.25 µm), with helium as carrier gas at a constant flow of 1.2 ml.min^{-1} in splitless mode. Initial oven temperature was held at 65°C for 2 min, ramped to 150°C by 6°C min^{-1} and held for 5 min. Finally temperature was ramped to 300°C by 6°C min^{-1} and isocratic hold for 15 min (300°C). Inlet temperature 280°C, transfer line temperature 225°C, source temperature 235°C and ionization energy -70 eV. Mass spectra were recorded at 50-900 *m/z* with 10 spectra /sec.

Chromatograms were processed using Leco ChromaTOF software (version 4.21) A reference chromatogram was defined that had a maximum of detected peaks over a signal/noise ratio of 10 and used for automated peak identification based on mass spectral comparison to a standard NIST (National Institute of Standards and technology) 98 library, mass spectral libraries of Golm Metabolome Database and some authentic standards run under same conditions. Mass spectral matching was manually supervised and matches accepted with similarity of match >750 (with maximum match equal to 1000).

2.4.4 GC-MS analysis of the endometabolome

Intracellular metabolites extracted from control and aniline exposed cells as described in section 2.3.5 were used for analysis. Metabolites were derivatized according to Jozefczuk *et al* (2010). Samples were first derivatized to protect carbonyl moieties through methoxyamination by adding 20 µl of 40 mg.ml^{-1} methoxyamine hydrochloride

(Sigma-Aldrich) in pyridine (Sigma-Aldrich) and incubated at 30°C for 90 min, followed by derivatization of acidic proton by adding 40 µl of BSTFA (N,O-Bis(trimethylsilyl)trifluoroacetamide) and TMCS (99:1) and incubated at 37°C for 30 min. GC-MS analysis was performed on Pegasus HT TOF-MS (Leco, USA) system equipped with Agilent series (7890) gas chromatography. 1 µl of derivatized sample was injected into HP-5 column (30 m, internal diameter 0.32 mm, thickness 0.25 µm), with helium as carrier gas at a constant flow of 1.2 $ml.min^{-1}$ in splitless mode. Initial oven temperature was held at 80°C for 2 min, ramped to 180°C by 3°C min^{-1} held for 1 min finally ramped to 310°C by 4°C min^{-1} and isocratic hold for 3 min (310°C). Inlet temperature 250°C, transfer line temperature 225°C, source temperature 230°C and ionization energy -70 eV. Mass spectra were recorded at 40-1000 *m/z* with 3 spectra /sec.

Chromatograms were processed using Leco ChromaTOF software (version 4.21) A reference chromatogram was defined that had a maximum of detected peaks over a signal/noise ratio of 10 and this was used for automated peak identification. Metabolites were identified based on mass spectral comparison to standard NIST 98 library, mass spectral libraries of Golm Metabolome database (www.*gmd.mpimp-golm.mpg.de*) and some authentic standards run under same conditions. Mass spectral matching was manually supervised and matches accepted with thresholds of match >750 (with maximum match equal to 1000).

2.4.5 Solid state C-13 NMR

Purified EPS sample as described in section 2.3.3 was used for solid state NMR analysis. Solid state ^{13}C-NMR spectra were recorded at room temperature on Avance III Bruker 500 MHz NMR at ^{13}C frequency of 100.62 MHz, ^{1}H 400 MHz, equipped with 5 mm double resonance probe head. Eighty milligrams of freeze dried EPS sample was packed into zirconia rotor. ^{13}C cross polarization/total sideband suppression (CP/TOSS) experiment was run at spinning speed of 7 kHz, 1H 90° pulse length was 2.83 µs and the ^{13}C 180° pulse length was 6.52 µs. The contact time was 2000 µs, acquisition time of 33 ms, the recycle delay was 8 s with total 11000 scans. Chemical shifts were referenced to $CDCl_3$ (77.4 ppm).

2.4.6 ^{1}H and ^{13}C NMR analysis

Purified PHAs as described in section 2.3.3 were used for NMR analysis and PHAs were dissolved in $CDCl_3$. ^{1}H NMR (proton magnetic resonance) and ^{13}C NMR spectra

were recorded on Bruker Avance 400 MHz spectrometer (Bruker Co., Billerica, MA) with a 5 mm inverse probe. Spectra were obtained in $CDCl_3$ unless otherwise mentioned, with TMS (delta = 0 ppm) as internal standard.

2.4.7 FTIR analysis

Purified EPS or PHAs samples were used for FTIR analysis and spectra were obtained on JASCO 5300 FTIR spectrometer equipped with laser detector (Jasco, Japan). Sample was mixed, ground with KBr to form discs. Spectra were recorded in transmittance mode at wave number range of 4000 to 500 cm^{-1}, resolution of 4 cm^{-1} and 30 scans per sample.

2.4.8 FAME analysis

Fatty acids of the samples were identified by FAME analysis done by Royal Life Science Pvt Ltd. Fatty acids were saponified, methylated, and extracted by using the protocol of the Sherlock microbial identification system (MIDI Inc.). FAME were analysed by gas chromatography.

2.4.9 Energy dispersive X-ray analysis (EDX)

Purified EPS as described in section 2.3.3 was used for EDX analysis. EDX was done on SEM (Philips XL30 series) coupled with EDX (EDAX PV9800). Freeze dried EPS was mounted on a stub and coated with gold. A spot size of 500 nm was used to record spectra with 100s counting time and voltage of 30Kv. Atom percentage was calculated from the spectrum by software and at least 3 different locations were analysed per sample.

2.5 Microscopic techniques

2.5.1 Confocal laser scanning microscopy

Purified EPS as described in section 2.3.3 or aniline exposed cells as described in section 2.2.9 were used in confocal microscopy. EPS or cells were stained with calcofluor white, aniline blue (β polysachharides), nile red (lipids), SYTOX Green (nucleic acids) and rhodamine isothiosynite (proteins, amino groups). 5 µl of each dye (1 $mg.ml^{-1}$) was added to EPS/cells, after 20 min incubation in the dark excess of the dye was washed with sterile Mill-Q water. Sometimes cells were also stained with fluorescein diacetate (FDA) in a similar way. Stained samples were mounted on to glass slide and visualised by confocal laser microscopy.

Confocal laser microscopic analysis of samples was performed on Zeiss Observer LSM 710 confocal microscope equipped with blue, green and red lasers. Images were taken by 10x and 40x objectives. Probes were visualised at their respective excitation and emission wave lengths. Calcofluor white ($_{Ex}$400/$_{Em}$480 nm), Nile Red ($_{Ex}$552/$_{Em}$636 nm), SYTOX green ($_{Ex}$504/ $_{Em}$523 nm), tetramehtyl rhodamine isothiosynite ($_{Ex}$ 547/$_{Em}$572nm) and FDA ($_{Ex}$ 490/$_{Em}$514nm). Five random places were visualised for one sample.

2.5.2 Scanning electron microscopy (SEM)

Control or aniline exposed (25 mM) cells as described in section 2.2.9 were used for SEM analysis. Scanning electron microscopy was done according to Priester *et al* (2007) with slight modifications. Cells were harvested by centrifugation (4°C, 10,000 x g, 6 min) and supernatant was discarded, pellet was suspended in 0.1 M phosphate buffer saline (PBS, pH 7.2). Phosphate buffer saline suspended cells were centrifuged, PBS was discarded and the cells were pre-fixed in mixture of glutaraldehyde (2.4% final concentration), ruthenium red (0.01%) and incubated for 30 min. After pre-fixation cells were removed by centrifugation (4°C, 10,000 x g, 6 min) and suspended in 2.4% glutaraldehyde and 0.01% ruthenium red for overnight fixation at 4°C. Cells were removed by centrifugation (4°C, 10,000 x g, 6 min) from fixation solution, washed with PBS three time and finally cell pellet obtained was post-fixed in 1% osmium tetroxide solution for 2 h at 4 °C. After post-fixation cells were harvested by centrifugation (4°C, 10,000 x g, 6 min) and washed with PBS for three times and the cells were dehydrated by series of ethanolic washes starting form 20%, 30%, 50%, 70%, 90% and 100% ethanol. Finally cells were washed with 100% ethanol twice, incubated for 20 min. After dehydration cells were mounted on glass pieces (0.5x0.5 cm) and dried by critical point dryer using standard protocol, dried samples were fixed to SEM stubs and coated with gold. The specimens were examined by using SEM (Philips XL30 series) at different magnification ranges.

2.6 Biochemical methods

2.6.1 Spectrophotometric assays

2.6.1.1 Estimation of total indoles

Total indoles were measured by Salper's method (Gordon and Paleg, 1957). One millilitre of culture supernatant was mixed with 1 ml of ethyl acetate and to this 2 ml of freshly prepared Salper's reagent [1ml of 0.5 M $FeCl_3$ in 50 ml of 35% (v/v) perchloric

acid] was added and the absorbance was read at 535 nm against reagent blank. Indole was used as standard.

2.6.1.2 Total sugars

Total sugars were measured by phenol-sulphuric acid method (Jiao *et al*., 2010). 50 µl of the sample was mixed with 125 µl of the concentrated H_2SO_4 followed by 25 µl of the 10% phenol (w/v) and incubated at 100°C water bath for 10 min. Sample were cooled and absorbance was read at 490 nm. Glucose was used as standard.

2.6.1.3 DNA estimation from EPS

DNA was measured by diphenylamine method (Burton, 1956) with slight modifications. 0.5 ml of the sample was mixed with 0.5 ml of water to this 2 ml of the diphenylamine reagent [5 g of diphenylamine dissolved in 500 ml glacial acetic acid and 13.75 ml concentrated H_2SO_4, Stored in brown bottle stable for six months at 2°C] was added. Samples were incubated in boiling water bath for 10 min, cooled and absorbance was read at 600 nm. Genomic DNA of *R. benzoatilyticus* JA2 was used as standard.

2.6.1.4 Total Protein

Protein content was measured by Bradford's method (Bradford, 1976) which involves the binding of Coomassie brilliant blue G-250 to proteins. Dissolve 100 mg of G-250 in 100 ml of absolute/distilled ethanol/methanol and kept on a shaker for ~ 60 min. Hundred millilitre of 88% O-phosphoric acid was added, mixed well, volume made up to 500 ml with distilled water. Filtered through Whattman No.1, diluted 1:1 with water and the absorption was read at 550 nm against water blank (OD ~ 1.1), reagent was stored in 4°C. Twenty microliter of the sample was mixed with 180 µl of the water and to this 800 µl of the Bradford's reagent was added, incubated for 5 min and absorbance was read at 595 nm against reagent blank. Bovine serum albumin (BSA) was used as standard.

2.6.2 Enzyme assays

2.6.2.1 Preparation of cell free extracts

Control or aniline exposed cells of *R. benzoatilyticus* JA2 as described in section 2.2.9 were used for preparation of cell free extracts. Cells of *R. benzoatilyticus* JA2 were harvested by centrifugation (4°C, 10,000 x g, 10 min), cell pellet was washed with Tris-HCl buffer 50 mM, pH 7.8, 50 µM PMSF (phenylmethylsulfonyl fluoride) was added and

finally suspended in 4 ml of same buffer. Cells were lysed by sonication with MS-70 probe (Bandelin, Germany make, model-UW 2070) at 45% power, 4°C, 7 cycles of 1 min duration and 5 min gap between each cycle. After sonication, lysate was centrifuged (20,000 x g, 20 min, 4°C) clear supernatant obtained was used as source of enzyme.

2.6.2.2 Tryptophan 2-monooxygenase activity

Tryptophan 2- monooxygenase enzyme activity was carried out in a final volume of 0.7 ml Tris buffer (50 mM, pH 7.8) containing 0.5 mM of L-tryptophan and appropriate amount of cell free extract (300 µl). Reaction was incubated at 37°C for 20 min and then reaction was stopped by adding 100 µl of 5N HCl. Pre-denatured enzyme was taken as blank. Reaction mixture was centrifuged (4°C for 10 min at 10,000 x g) and the supernatant was collected and extracted twice with ethyl acetate. The ethyl acetate layers were pooled, evaporated to dryness under vacuum, dissolved in 50 µl of methanol and product (indole-3-acetamide) was analysed by HPLC as described in 2.4.1. One unit (U) of enzyme activity was defined as the amount of enzyme required for the formation of 1 nmole of product. Specific activity was expressed as unit activity per mg protein

2.6.2.3 Tryptophan aminotransferase activity

Tryptophan aminotransferase enzyme activity was carried out in a final volume of 3 ml containing tryptophan 1 mM, α-ketogluatrate 1 mM, 50 µM of PLP (pyridoxal-5'-phosphate) as cofactor and 1.5 ml of cell free extract. Reaction was incubated for 20 min at 37°C then reaction was stopped by 300 µl of 5N HCl. Reaction mixture was centrifuged (4°C for 10 min at 10,000 g) and the supernatant was collected and extracted twice with ethyl acetate. The ethyl acetate layer was pooled, evaporated to dryness under vacuum, dissolved in 100 µl methanol and product IAA (indolepyruvate is unstable readily converts into IAA) was analysed by HPLC as described in 2.4.1. One unit (U) of enzyme activity was defined as the amount of enzyme required for the formation of 1 µmole of product. Specific activity was expressed as unit activity per mg protein.

2.6.2.4 Tryptophanase activity

Tryptophanase enzyme activity was carried out in a final volume of 3 ml; tryptophan 1 mM, 50 µM of PLP as cofactor and 1.5 ml of cell free extract. Reaction was incubated for 20 min at 37°C then reaction was stopped by 300 µl of 5N HCl. Product (indole) was extracted into ethyl acetate from reaction supernatant, evaporated, dissolved

in 100 µl of methanol and analysed by HPLC as described in 2.4.1. One unit (U) of enzyme activity was defined as the amount of enzyme required for the formation of 1 nmole of product. Specific activity was expressed as unit activity per mg protein e unit.

2.6.2.5 Anthranilate synthase

Anthranilate synthase enzyme reaction mixture contained 1 mM chorismate, 1 mM gluatamine, 50 µM $MgCl_2$ and cell free extract (1.5ml) in a final volume of 3 ml and the reaction was stopped after 1h of incubation at 37°C by 5N HCl (300 µl). Reaction mixture was centrifuged and product (anthranilate) was extracted by ethyl acetate from reaction supernatants. Ethyl acetate was concentrated and dissolved in methanol and analysed by HPLC as described in 2.4.1 except for detection of anthranilate at 325 nm. One unit (U) of enzyme activity was defined as the amount of enzyme required for the formation of 1 µmole of product. Specific activity was expressed as unit activity per mg protein.

2.7 Metabolomic mehtods

2.7.1 Stable isotope labeled aniline and fumarate feeding

Rubrivivax benzoatilyticus JA2 was grown photoheterotrophically for 48 h (0.4 OD_{660nm}) then culture was fed with deuterium labeled aniline (aniline-d_5) or deuterium labelled fumarate (fumarate-d_4), control culture was fed with unlabelled aniline or unlabeled fumarate and incubated for 48 h. Cells were harvested and the supernatant was extracted for indoles as described in 2.3.1, indolic fractions were analysed by LC-MS/MS as described in section 2.4.1.

2.7.2 Stable isotope labeled tryptophan feeding

Rubrivivax benzoatilyticus JA2 was grown photoheterotrophically for 48 h (0.4 $OD_{660\ nm}$) and fed with either deuterium labaled tryptophan (tryptophan-d_5) or unlabelled tryptophan (0.5 mM). Culture was allowed to grow for 48 h and cells were harvested, supernatant was fractionated for indoles as described in 2.3.2, indolic extracts were analysed by LC-MS/MS as described in section 2.4.1.

2.7.3 GC-MS data processing and statistical analysis

Data obtained from GC-MS analysis of endometabolome as described in section 2.4.4 was used for processing and subjected to statistical analysis. Relative metabolite abundances were calculated from peak areas of identified metabolites obtained from GC-

MS analysis. Peak areas were normalised to dry weight of the sample and more than 50% of missing values excluded from the data. Data was log transformed and subjected to quantile normalization using MetaboAnalyst and normalised data was used for multivariate statistical analysis. Principal component analysis (PCA), partial least-squares discrimination analysis (PLS-DA) and hierarchical clustering analysis (HCA) was performed using MetaboAnalyst (*www.metaboanalyst.ca/MetaboAnalyst*). HCA was done using Pearson correlation as distance matrix. Data was subjected to *t* test analysis to identify metabolites significantly regulated between control and aniline exposed cells. Metabolites having fold change >2 and *p* value <0.05 were considered as statistically significant, finally significant metabolites were annotated to metabolic pathways according to KEGG (*Kyoto Encyclopedia of Genes and Genomes, www.genome.jp/kegg*) database to identify metabolic pathways influenced by aniline stress.

2.8 Proteomic methods

2.8.1 Isolation of R. benzoatilyticus JA2 *proteome*

Aniline exposed and control cells as described in section 2.2.9 were used for proteome analysis. Experimental design contained three independent experiments, each with three biological replicates and to minimize the biological variations all three biological replicates of an individual experiment were pooled together.

Aniline exposed and control cells were harvested by centrifugation (4°C, 10,000 x g, 10 min) and the cell pellet was suspended in 50 mM HEPES-KOH buffer pH 7.5 and washed twice with the same buffer. Finally cells were re-suspended in 3 ml of the HEPES-KOH buffer containing 0.1% SDS (w/v) and 0.1% triton-X-100(v/v) and sonicated (MS 70 probe, 45% power, 7cycle, 4°C) to lyse the cells. Lysate was incubated for 30 min at 4 °C and centrifuged (4°C, 20,000 x g for 30 min) and the clear supernatant was taken as soluble proteome. Total proteins were precipitated by six volumes pre-chilled acetone at -20°C (1: 6) overnight and precipitated proteins were centrifuged (4°C, 10,000 x g for 15 min), washed with 100% acetone twice, after acetone was decanted and protein was lyophilized and stored at -20°C till analysis.

2.8.2 Isobaric tags relative and absolute quantitation (iTRAQ) labelling of proteome

Isobaric tags relative and absolute quantitation analysis was outsourced from California University, USA and they have adopted following protocol. One hundred fifty

micrograms of each sample was re-suspended in TNE buffer [50 mM Tris pH 8.0, 100 mM NaCl, 1 mM EDTA]. RapiGest SF reagent (Waters) was added to the mix to a final concentration of 0.1%, samples were then heated for 5 min at 95°C. Proteins were reduced with 1 mM Tris-(2-carboxyethyl) phosphine (TCEP) for 30 min at 37°C (Pierce Chemical) and carboxymethylated with 0.5 mg/ml of iodoacetamide for 30 min at 37°C. Iodoacetamide was then neutralized with an additional 1 mM TCEP. Proteins were digested with trypsin overnight at 37°C. trypsin ratio 1:100 (trypsin: protein). Samples were then treated with 50 mM HCl at 37°C for 1 hour followed by centrifuge at maximum speed for 30 min at 4°C to degrade and remove the RapiGest. The soluble fraction was then removed to a new tube and pH of the solution was adjusted to 3.0 using NH_4OH. The peptides were then extracted and desalted using Aspire RP30 Desalting Tips (Thermo Scientific). Peptides were re-quantified using bicinchonic acid assay. 100 µg of each sample was labeled with a unique iTRAQ tag (114, 115, 116, and 117) as described in the manufacturer's protocol (ABSCIEX). Control sample was labeled with 114 and three aniline exposed samples with 115,116 and 117, respectively. The 4 samples were then combined and dried down to remove ethanol using a speed-vac. The samples were re-suspended in 100 µl of Buffer A (98% H2O, 2% ACN, 0.2% formic acid, and 0.005% TFA) 5 µl sample was used for the MudPIT (multidimensional protein identification technique) analysis (Link et al 1999).

2.8.3 Two dimensional Nano LC-ESI-MS/MS analysis (MudPIT)

iTRAQ labelled peptide mixture was analysed on a QSTAR-Elite hybrid mass spectrometer (AB/MDS Sciex) interfaced to the nano-flow HPLC. Peptides were separated using nano-flow high pressure liquid chromatography (HPLC) coupled with tandem mass spectroscopy (LC-MS/MS) using nano-spray ionization source. Strong cation exchange (SCX) fractionation was carried on BioX-SCX (5 µm particle size, 0.5 mm inner diameter x 15 mm. LC Packings P/N 161395) trap column. Sample was loaded onto the SCX column and eluted with 7.5 µl/min flow rate for 10 min using gradient of buffer A and buffer C (5% ACN, 0.2% formic acid, and 0.5 M ammonium acetate) The SCX salt steps(first dimension) used for separation were 5%, 7.5%, 10%, 12.5%, 15%, 20%, 25%, 30%, 40%, 50%, 75% and 100% .

In second dimension (reverse phase) peptides were eluted from the ZorbaxTM C18 column (100 x 0.18 mm, 5-µm, Agilent Technologies, Santa Clara, CA) into the mass spectrometer using a linear gradient of 5–80% Buffer B (100% ACN, 0.2% formic acid,

and 0.005% TFA) and Buffer A (98% H2O, 2% ACN, 0.2% formic acid, and 0.005% TFA) over 60 min at 400 nl/min flow rate. LC-MS/MS data was acquired in a data-dependent fashion by selecting the 6 most intense peaks with charge state of plus 2 to 4 that exceeds 35 counts, with exclusion of former target ions set to "60 seconds" and the mass tolerance for exclusion set to 100 ppm. Time-of-flight MS were acquired at m/z 400 to 2000 Da for 0.75 sec with 12 time bins to sum. MS/MS data were acquired from m/z 50 to 2,000 Da by using "enhance all" and 24 time bins to sum, dynamic background subtract, automatic collision energy, and automatic MS/MS accumulation with the fragment intensity multiplier set to 6 and maximum accumulation set to 2 s before returning to the survey scan. Data obtained form this was used for identification and quantification of proteins.

2.8.4 Mass spectral data analysis, protein identification and quantification

Data was combined into a single search for identification and quantification using ProteinPilot 2.0 (Life Technologies Inc, Carlsbad, CA). The Paragon algorithm in the ProteinPilot software was used for the peptide identification and further processed by Pro Group algorithm where isoform-specific quantification was adopted to trace the differences between expressions of various isoforms. The defined parameters were as follows: (i) Sample type, iTRAQ 4-plex (Peptide Labeled); (ii) Cysteine alkylation, IAM; (iii) Digestion, Trypsin; (iv) Instrument, QSTAR Elite ESI; (v) Special factors, None; (vi) Species, *Rubrivivax benzoatilyticus* JA2; (vii) Specify Processing, Quantitate, Bias correction (viii) ID Focus, Biological modifications; (ix) Database, NCBI protein sequence of *R. benzoatilyticus* JA2; (x) Search effort, thorough. For iTRAQ quantification, the peptide for quantification was automatically selected by Pro Group algorithm with the criterion that the peptide identified with good confidence and not shared with another protein, identified with higher confidence to calculate the reporter peak area, error factor (EF) and *p*-value. Proteins met the criteria that; Unused prot score >2(confidence level 99%), with two unique peptide, *p*-value <0.05, EF <2, fold change of <0.8 (down regulated) and > 1.2 (up-regulated) were considered for further analysis. Proteins were functionally categorised according to KEGG (*Kyoto Encyclopedia of Genes and Genomes, www.genome.jp/kegg/*) database. *In silico* analysis of proteins by using ExPASy tools (*www*.expasy.org).

2.9 Real time PCR technique

2.9.1 Softwares and oligonucleotides

Sigma Plot 9, Origin, Excel 2010, Excel stat, ProteinPilot 2, MestReNova, MetaboAnalyst

Primers used in real time PCR were

***Gene Name* (Accession number)**		***Sequence***
Phospho-2-dehydro-3-deoxyheptonate aldolase (gi|332525529)	FP	5'-AGTACCTGGCCGACCTCAT-3'
	RP	5'-CGTCGGTGCCGTTCTTGAA-3'
Phospho-2-dehydro-3-deoxyheptonate aldolase (gi|332525163)	FP	5'-ATGTTGCCGTCGGTGCCG-3'
	RP	5'-GTGATCTCGCCGCAGTACA-3'
Chorismate mutase (gi|332527557)	FP	5'-GTTCTTCACCGACAGCACG-3'
	RP	5'-CGAGTTCGGCCTGCACGT-3'
Anthranilate synthase (gi|332524751)	FP	5'-TGGCCGATGACGACCTGC-3'
	RP	5'-GCTGCGTTATTCGGTCACC-3'
Tryptophan synthase_beta (gi|332524263)	FP	5'-CCGTTGTCGTCCTGCAGC-3'
	RP	5'-GCAGCAACGCGATGGGCA-3'
16s rRNA (gi|343201659)	FP	5'ACCTGAAGAATAAGCACCGG3'
	RP	5'-AATGCAGTTCCCAGGTAAGC-3'
Chorismate synthase (gi|332526664)	FP	5'-CAAGTGGCTGAAGGAACGC-3'
	RP	5'-GTGTTGGCGGCGAAGAAGT-3'

2.9.2 RNA isolation

For RNA isolation all the plastic ware was treated with 0.1% (v/v) DEPC (Diethylpyrocarbonate) overnight, dried and autoclaved. *Rubrivivax benzoatilyticus* JA2 culture was grown photoheterotrophically and exposed to aniline as described in 2.2.9, 2.5 ml culture (0.45 OD $_{660\ nm}$) was harvested at 20 min, 60 min and 140 min after the aniline exposure and flash frozen in liquid nitrogen, stored at -80°C. RNA was isolated by RNase mini kit (Qiagen) according to manufacturer's instructions before RNA isolation cells were treated with lysozyme (30mg.ml^{-1} in Tris.HCl buffer pH 7.0) for 5 min. On column DNase treatment was done with DSNase I (Qiagen) according to manufacturer's instructions. Isolated RNA was stored at -80°C for further analysis. RNA integrity was analysed on Bioanalyser 2100 and quantity by nanodrop

2.9.3 cDNA synthesis and qRT-PCR analysis

DNase treated RNA (925 ng) was reverse transcribed to make 37 ng.µl of cDNA using the Affinity Script QPCR cDNA synthesis kit (Agilent - Lot# 6077352) according to manufacturer's protocol. Real time PCR was performed by using Brilliant II SYBR Green qPCR Master mix (Lot # 1105284). Each sample was run in duplicates for each gene using 37 ng input per reaction and PCR conditions are as follows; initial denaturation at 95°C for 10 min followed by 40 cycles of 95°C for 30 s, 58°C for 1min, 72°C for 1 min. A melt curve was also performed after the assay to check for specificity of the reaction. Real time PCR was performed on Stratagene Mx3005P (Agilent technologies) platform. The relative expression levels of the genes were determined after normalizing with 16s rRNA as the reference gene by using Delta Ct method.

RESULTS

3.0 Results

3.1 Aniline induced indoles biosynthesis and its regulation

3.1.1 Effect of aniline and its derivatives on biomass, viability and on indoles production

Biomass yields of *R. benzoatilyticus* JA2 were 0.5-0.6 mg.dry wt ml^{-1} in the presence of 4-bromoaniline and 3-aminobenzoate under photoheterotrophic conditions while in the presence of other aniline derivatives, biomass yields were 0.8-1.2 mg.dry wt. ml^{-1} (Table.1). Indoles production was observed only in the presence of aniline (0.15 mM) and 2-aminobenzoate (0.3 mM) among all aniline derivatives tested. Photoheterotrophic growth of *R. benzoatilyticus* JA2 was not observed when aniline derivatives were used as sole source of carbon or nitrogen. However, aniline (0.3 mM), 2-amnobenzoate (0.8 mM) and 4-bromoanilines (0.1 mM) loss was observed. More than 80% of cells were viable when *R. benzoatilyticus* JA2 was grown in presence of aniline derivatives (Table. 1).

3.1.2 Production of indoles by aniline exposed cultures of *R. benzoatilyticus* JA2

Production of indoles (0.34-0.4 mM) was observed in aniline exposed culture supernatants of *R. benzoatilyticus* JA2 while no detectable amounts of indoles were observed in unexposed cultures. Production of indoles (0.21 mM) was observed within 12 h of aniline exposure with simultaneous utilization of fumarate (7.8 mM). Indoles production was high (0.4 mM) at 60 h while at the same time 90% of the (11.5 mM) fumarate was utilized (Fig. 8). 0.35 mM of aniline was utilized with near stoichiometric yields of 0.4 mM indoles.

3.1.3 Extraction and identification of indolic fractions

Culture supernatant of *R. benzoatilyticus* JA2 was dried under vacuum and fractionated as illustrated in figure 9 to identify indolic fractions. Acidic and neutral fractions were positive for indole's test by Salper's reagent while water soluble and basic fractions were negative (Flow chart. 1).

Table.1. Effect of aniline and its derivatives on biomass, viability and indole production.

Aniline and its derivatives (10 mM)	Biomass yield (mg dry wt.ml^{-1})	Utilization (mM)	Indoles production (mM)	Viability (%)
Aniline	1.0	0.3	0.15	82
2-Aminobenzoate	0.9	0.8	0.3	96
3-Aminobenzoate	0.6	Un	-	87
Sulphanilate	1.2	Un	-	98
4-Nitroaniline	0.9	0.04	-	95
4-Bromoaniline	0.5	0.1	-	86
4-Aminophenol	0.8	Un	-	Nc
1,2-Phenyldiamine	0.9	Un	-	95
2,6-Dichloroaniline	0.9	Un	-	90
3,5-Dimethylaniline	0.9	0.1	-	96
Control (without anilines)	1.0	NA	-	100

Un, unutilized; Nc, no visible colonies formed; NA, Not applicable.

Malate grown mid log phase culture (0.25 OD $_{660nm}$) of *R. benzoatilyticus* JA2 was used as inoculum (10%) for experiment. Culture was grown on malate medium photoheterotrophically for 48 h and culture was exposed to aniline/aniline derivatives (10 mM), fumarate (13 mM) incubated for 48 h. Culture supernatant after 48 h of incubation was analysed for indoles production, anilines utilization and viability by plate count method.

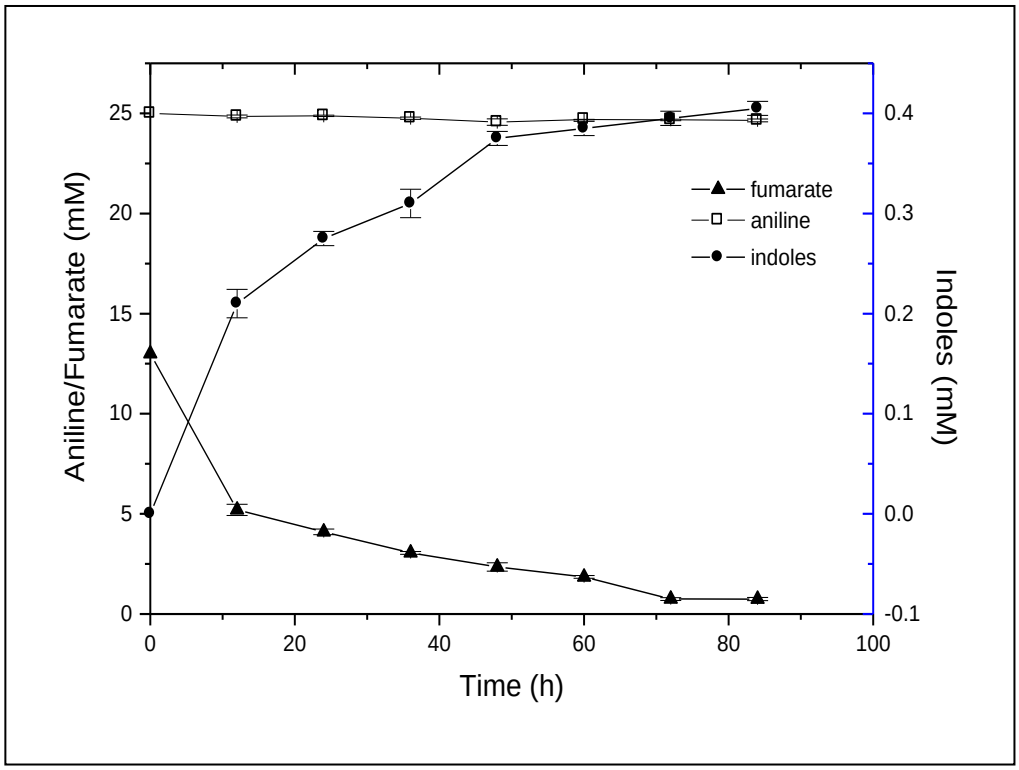

Fig. 8. Utilization of aniline, fumarate and production of indoles by *R. benzoatilyticus* JA2.

Malate grown mid log phase culture (0.25 OD_{660nm}) of *R. benzoatilyticus* JA2 was used as inoculum (10%) and the culture was grown on malate medium for 48 h photoheterotrophically then exposed to aniline (25 mM) and fumarate (13 mM). Samples were drawn at regular intervals for analysis.

Data represents mean ± standard deviation of three independent experiments done in duplicates.

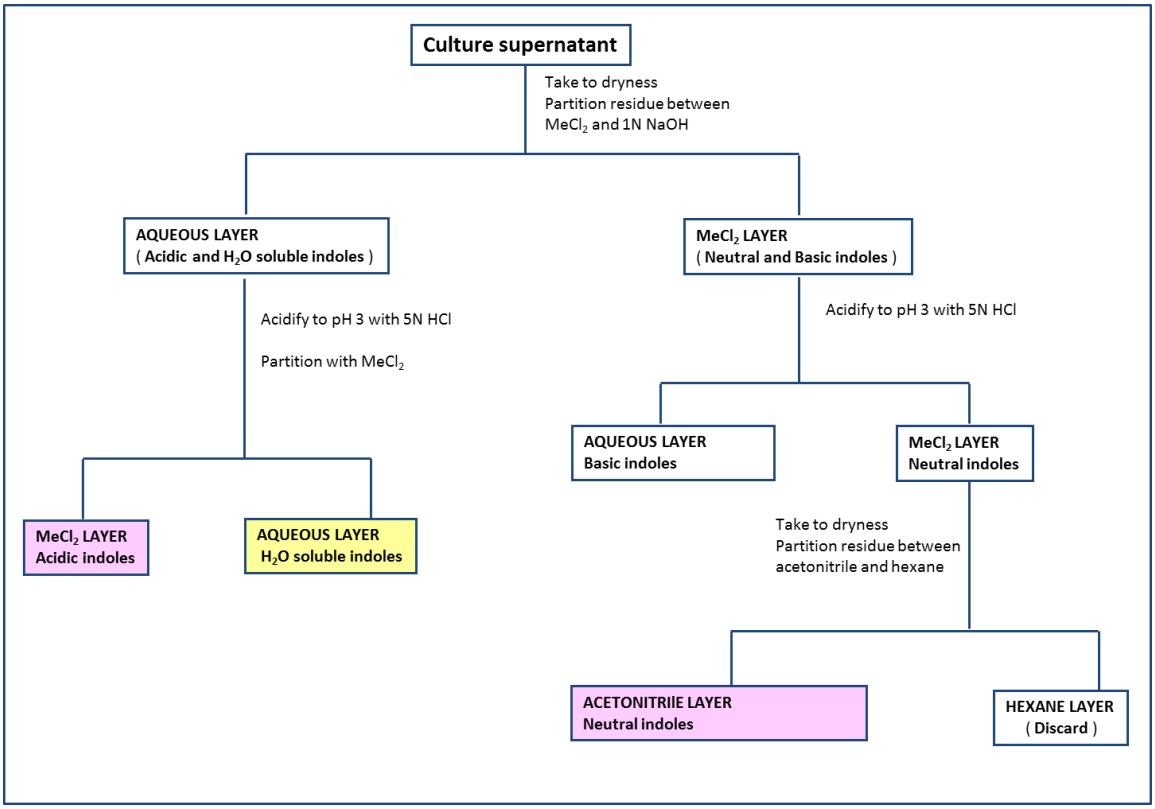

Flow chart. 1. Flow chart of extraction and identification of indolic fractions from culture supernatants of *R. benzoatilyticus* JA2.

Culture and growth conditions were similar as described under Fig. 8, and supernatant was collected and subjected to fractionation. Fractions which were positive for indole derivatives were shaded in pink and yellow. $MeCl_2$, Dichloromethane.

3.1.4 HPLC and LCMS metabolite profiling of indolic fractions

High performance liquid chromatography (HPLC) and liquid chromatography mass spectrometric (LCMS) analysis of indolic fractions was performed to identify indole metabolites. HPLC analysis of the aqueous fraction indicated a major metabolite with retention time (R_t) of 9.45 min (Fig. 9A) and co-eluted with authentic tryptophan standard. LCMS analysis of this metabolite (R_t 9.45 min) indicated a molecular ion mass of 205$[M+H]^+$ with fragmentation of 205$[M+H]^+$, 188$[M-NH_3]^+$, 146, 118 (Fig. 9B) which was well in accordance with the authentic mass spectrum of the tryptophan. Based on R_t, mass spectrum and co-elution with the authentic tryptophan, metabolite (R_t 9.45 min) was identified as tryptophan.

HPLC analysis of acidic fraction detected a major metabolite of R_t 19.1 min (Fig. 10A) and this was co-eluted with the authentic indole-3-acetic acid (IAA). Further, mass analysis of this metabolite detected a molecular ion mass of 176$[M+H]^+$, fragmentation of 176$[M+H]^+$, 130$[M-COOH]^+$, 103 (Fig. 10B) and the mass spectrum of metabolite was identical to that of authentic mass spectrum of the IAA. Based on R_t, mass spectrum and co-elution with authentic IAA the metabolite of acidic fraction (R_t 19.1 min) was identified as IAA. HPLC analysis of neutral fraction detected a major metabolite with R_t of 18.5 min (Fig. 11A) and its mass analysis detected a molecular ion mass of 146$[M+H]^+$ with fragmentation of 118$[M-CHO]^+$ (Fig. 11B). Neutral fraction metabolite (R_t18.5 min) was co-eluted with the authentic indole-3-aldehyde (IAld) and mass spectrum of metabolite was well in accordance with the mass spectrum of authentic IAld, based on this metabolite was identified as indole-3-aldehyde. Tryptophan, IAA and IAld were identified as major metabolites from aniline exposed cultures supernatants of *R. benzoatilyticus* JA2.

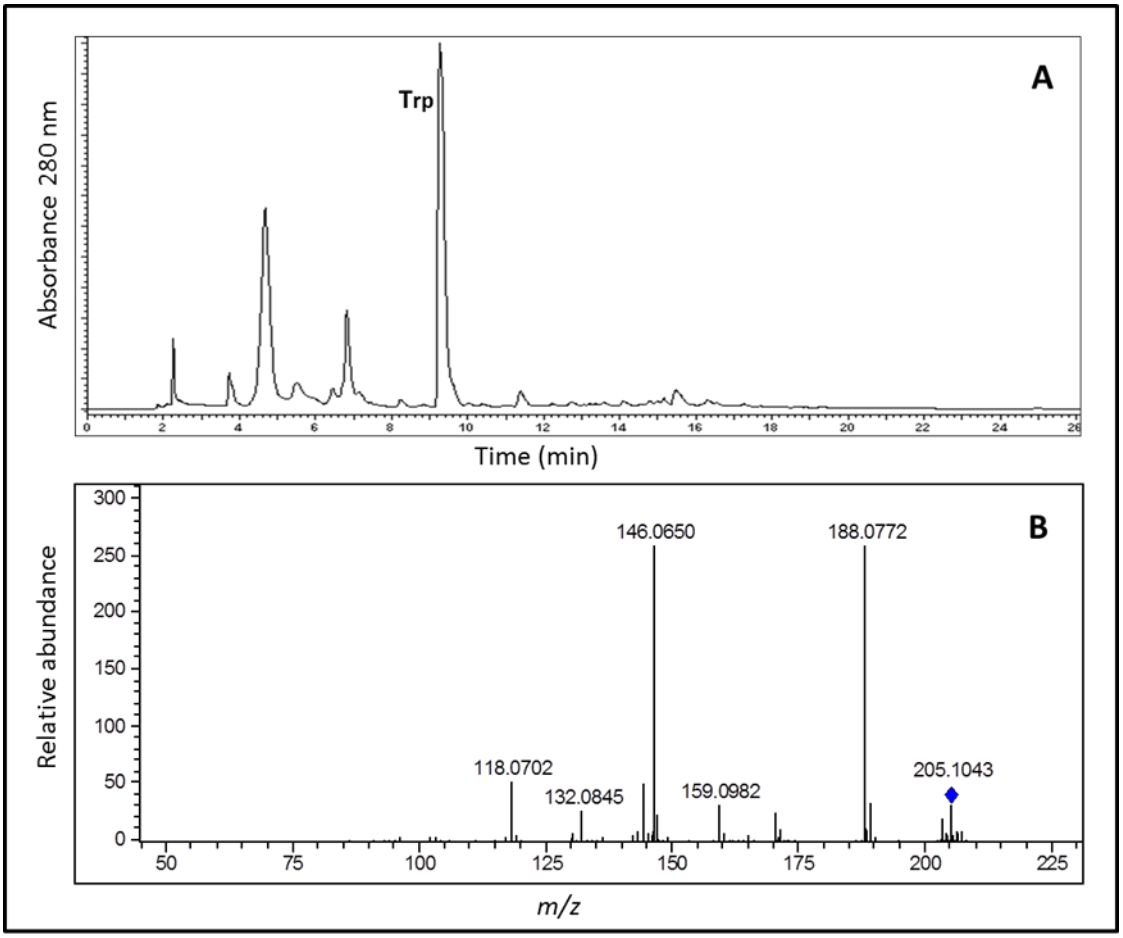

Fig. 9. HPLC and LCMS profiling of aqueous fraction obtained from culture supernatants of *R. benzoatilyticus* JA2 exposed to aniline

HPLC chromatogram showing Trp as major metabolite having a R_t of 9.45 min (**A**) and mass spectrum of Trp (**B**).

Experimental conditions were similar as described under Fig. 8 except for culture supernatant was collected after 48 h of aniline exposure, fractionated and subjected to HPLC and mass analysis. Trp, tryptophan**;** R_t, retention time.

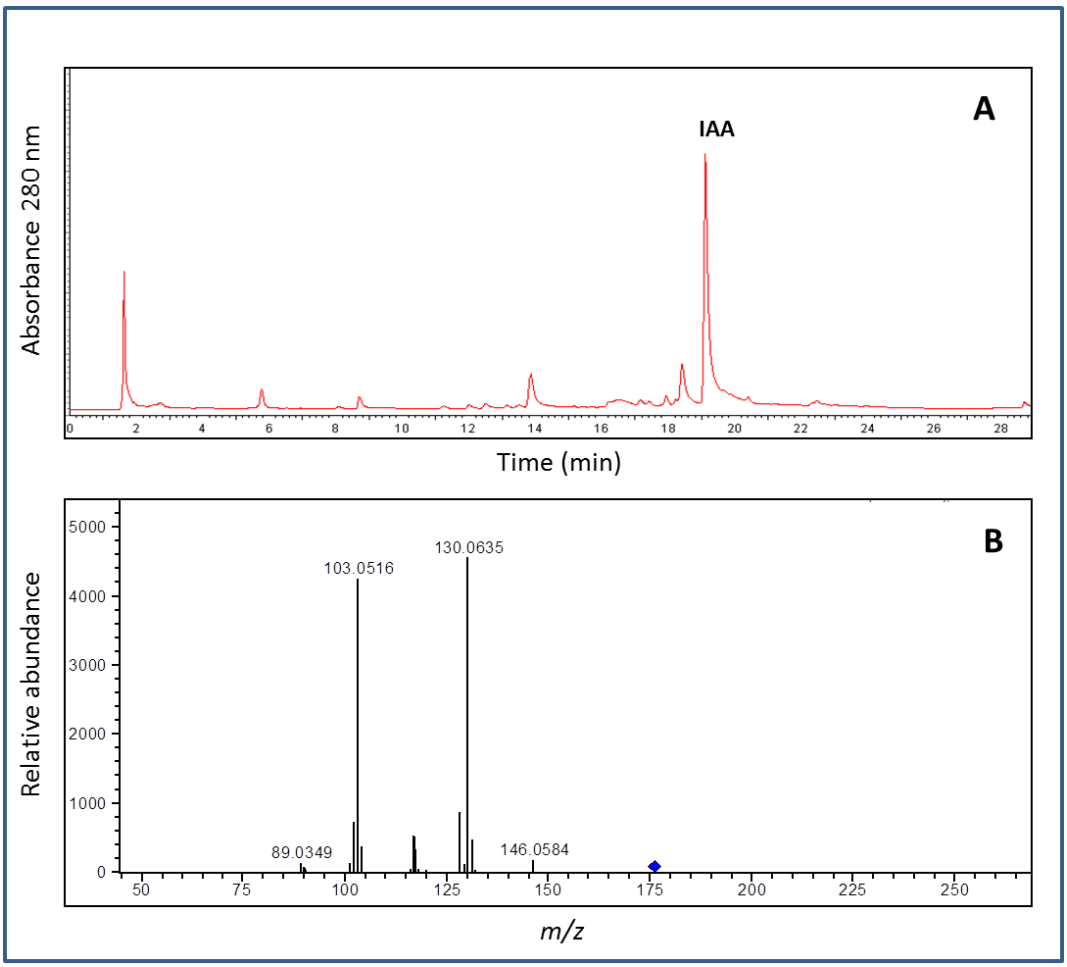

Fig. 10. HPLC and LCMS profiling of acidic fraction obtained from the culture supernatants of aniline exposed *R. benzoatilyticus* JA2.

HPLC chromatogram of acidic fraction showing IAA having a R_t 19.1 min (**A**) and corresponding mass spectrum of IAA (**B**).

Experimental conditions were similar as described under Fig. 9. IAA, indole-3-acetic acid; R_t, retention time.

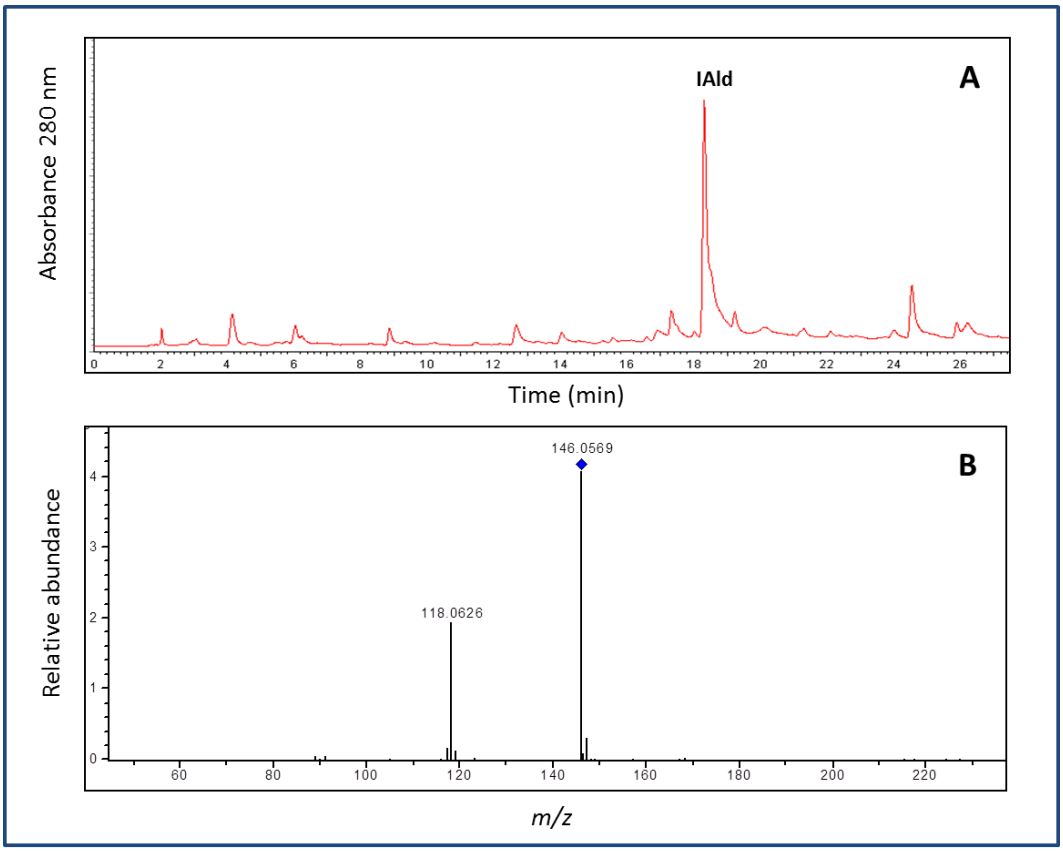

Fig. 11. **HPLC and LCMS profiling of neutral fraction obtained from the culture supernatants of aniline exposed *R. benzoatilyticus* JA2.**

HPLC chromatogram showing IAld having a R_t of 18.57 min (**A**) and corresponding mass spectrum of IAld (**B**).

Experimental conditions were similar as described under Fig. 9.

IAld, indole-3-aldehyde; R_t, retention time.

3.1.5 Time series analysis of the tryptophan, indole-3-acetic acid and indole-3-aldehyde

Aniline exposed (25 mM) culture supernatants of *R. benzoatilyticus* JA2 were analysed by HPLC to quantify indole metabolites over a period of time. Tryptophan production was observed within 3 h of aniline exposure and production was high (1048 µg.250 ml^{-1}) at 48 h (Fig. 12A) while at 0 h no tryptophan was observed. Indole-3-acetic acid and IAld levels were low (IAA 15 µg.250 ml^{-1}; IAld 7 µg.250 ml^{-1}) at 0 h and their levels increased at 3 h (Fig. 12B). High concentrations of IAA (76 µg.250 ml^{-1}) and IAld (39 µg.250 ml^{-1}) were observed at 48 h of aniline exposure. Study state levels of tryptophan, IAA and IAld increased with time upon aniline exposure of *R. benzoatilyticus* JA2.

3.1.6 Quantitative metabolic profiling of tryptophan, indole-3-acetic acid and indole-3-aldehyde

Aniline exposed (25 mM) and unexposed culture supernatants of *R. benzoatilyticus* JA2 were analysed by HPLC to quantify the tryptophan, IAA and IAld levels. High performance liquid chromatography analysis of the aniline exposed aqueous fraction detected a peak corresponds to tryptophan (R_t 9.45 min; Fig. 13B) and no such detectable peak was observed in unexposed aqueous fractions (Fig. 13A). Aniline exposed culture of *R. benzoatilyticus* JA2 accumulated 700-950 µg.250 ml^{-1} of tryptophan and no detectable amount of tryptophan was found in unexposed culture (Fig. 13C). High levels of IAA (55 µg.250ml^{-1}) and IAld (80 µg.250ml^{-1}) accumulation was observed in aniline exposed cultures compared to those of unexposed (IAA 1.2 µg.250ml^{-1}; IAld 1.6 µg.250ml^{-1}) (Fig. 13D). Production of tryptophan and accumulation of IAA, IAld was observed only in aniline exposed cultures.

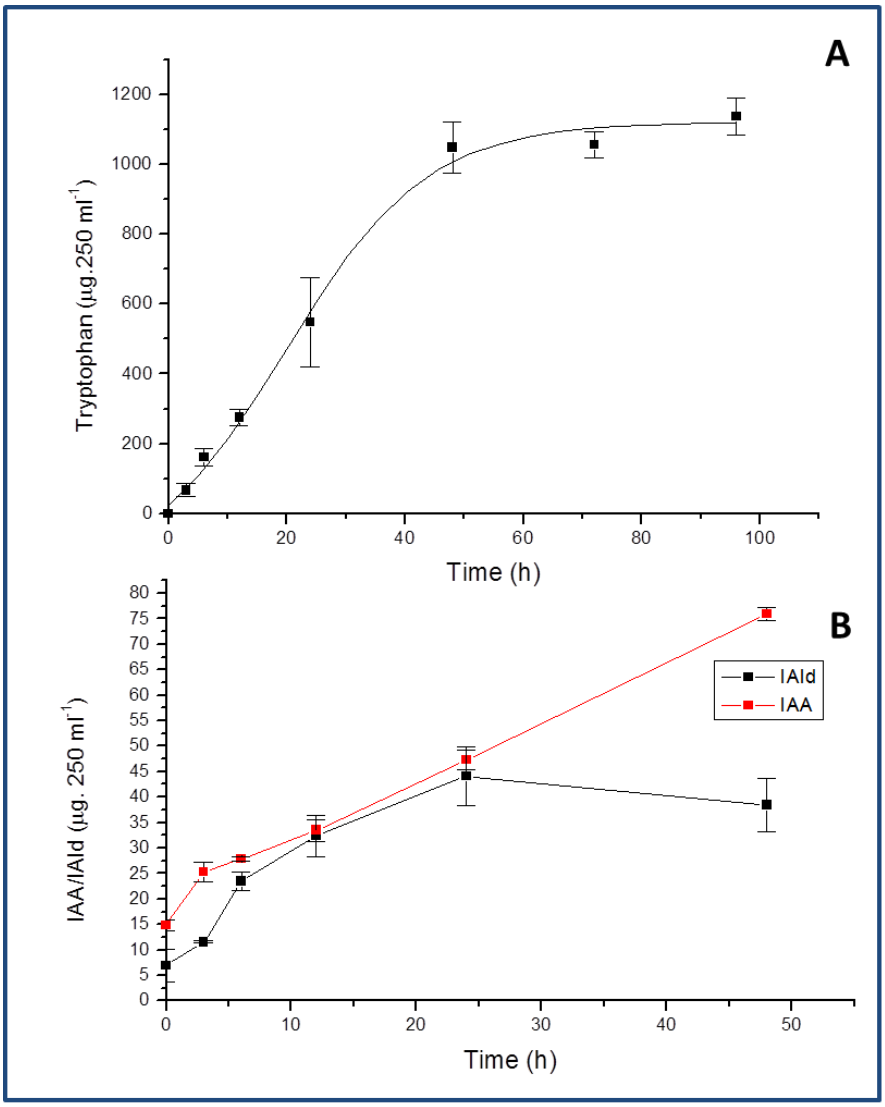

Fig. 12. Kinetics of Trp, IAA and IAld production by *R. benzoatilyticus* JA2 exposed to aniline.

Production of Trp (**A**), production of IAA and IAld (**B**).

Experimental conditions were similar as described under Fig. 9, except for samples were drawn at regular intervals for analysis. Metabolites were quantitated by HPLC analysis.

Data expressed as mean ± standard deviation of three independent experiments. Trp, tryptophan; IAA, indole-3-acetic acid; IAld, indole-3-aldehyde.

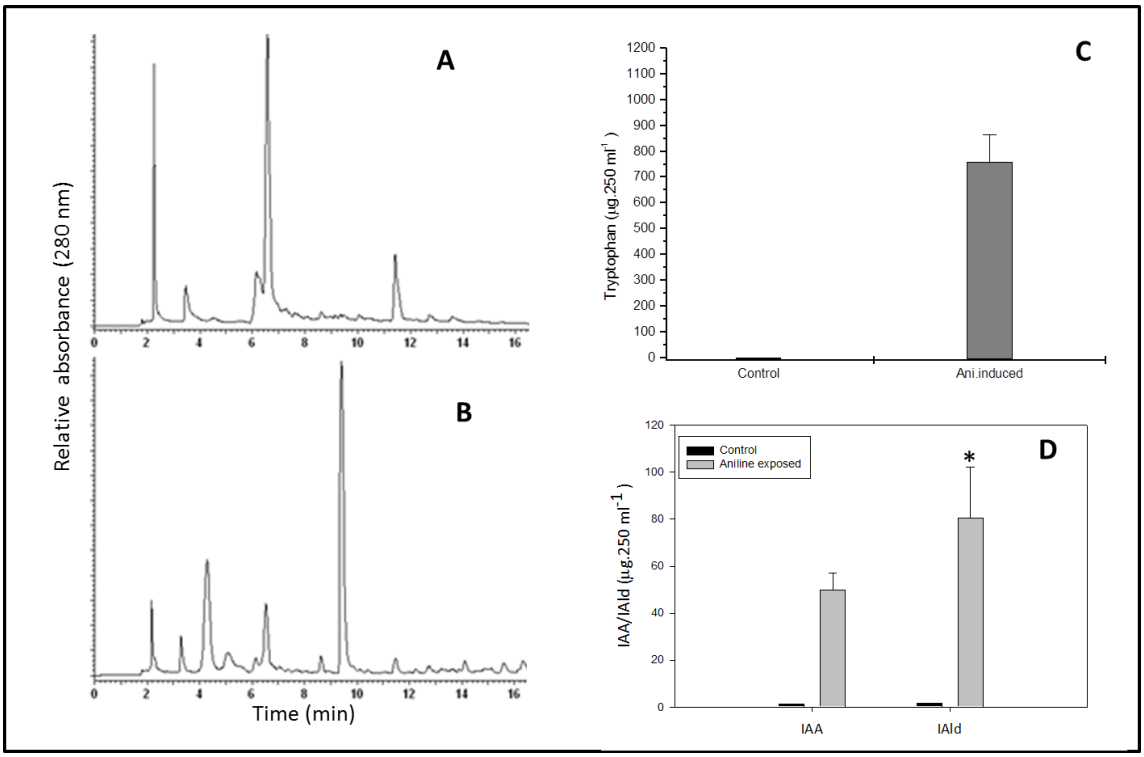

Fig. 13. Quantitative metabolic profiling of Trp, IAA and IAld in *R. benzoatilyticus* JA2.

HPLC chromatogram of aqueous fraction from control cultures (**A**), from aniline exposed cultures of *R. benzoatilyticus* JA2 (**B**). Peak at R_t 9.4 min indicate Trp.

Quantification of Trp (**C**) and quantification of IAA, IAld from control and aniline exposed cultures (**D**).

Experimental conditions were similar as described under Fig.12.

Data represents mean ± standard deviation of three independent experiments done in duplicates. * *p* value <0.05 obtained from Student's *t*-test.

3.1.7 Inhibition of growth and indoles production by glyphosate

3.1.7.1 Effect of glyphosate on growth of R. benzoatilyticus JA2

Photoheterotrophic growth of *R. benzoatilyticus* JA2 was inhibited by an aromatic amino acid biosynthesis inhibitor glyphosate in a dose dependent manner. One and 3 mM of glyphosate inhibited 70% to 80% of growth while complete growth inhibition was observed at 6 and 10 mM (Fig. 14A). However, complete growth restoration was observed when culture was supplemented with phenylalanine (150 µM), tyrosine and anthranilate (tryptophan precursor) while growth was not restored with supplementation of phenylalanine and tyrosine or phenylalanine, tyrosine and aniline (Fig. 14B).

3.1.7.2 Effect of glyphosate on indoles production by R. benzoatilyticus JA2

Glyphosate inhibited production of indoles in aniline exposed (25 mM) culture in a dose dependent manner (Fig. 15A) and 1 mM of glyphosate inhibited 80% of indoles production (Fig. 15A). Production of indoles was not inhibited by glyphosate in anthranilate exposed cultures of *R. benzoatilyticus* JA2 while in case of aniline exposed culture inhibition was observed (Fig. 15B).

3.1.7.3 Inhibition of tryptophan, indole-3-acetic acid and indole-3-aldehyde by glyphosate

Glyphosate significantly decreased the levels of tryptophan (41µg.250 ml^{-1}), IAA (38 µg.250 ml^{-1}) and IAld (15.8 µg.250 ml^{-1}) in aniline exposed cultures while in the absence of glyphosate, tryptophan (438 µg.250 ml^{-1}), IAA (245 µg.250ml^{-1}) and IAld (113 µg.250 ml^{-1}) levels were high (Fig.16). Production of tryptophan, IAA and IAld was inhibited by glyphosate in aniline exposed cultures of *R .benzoatilyticus* JA2.

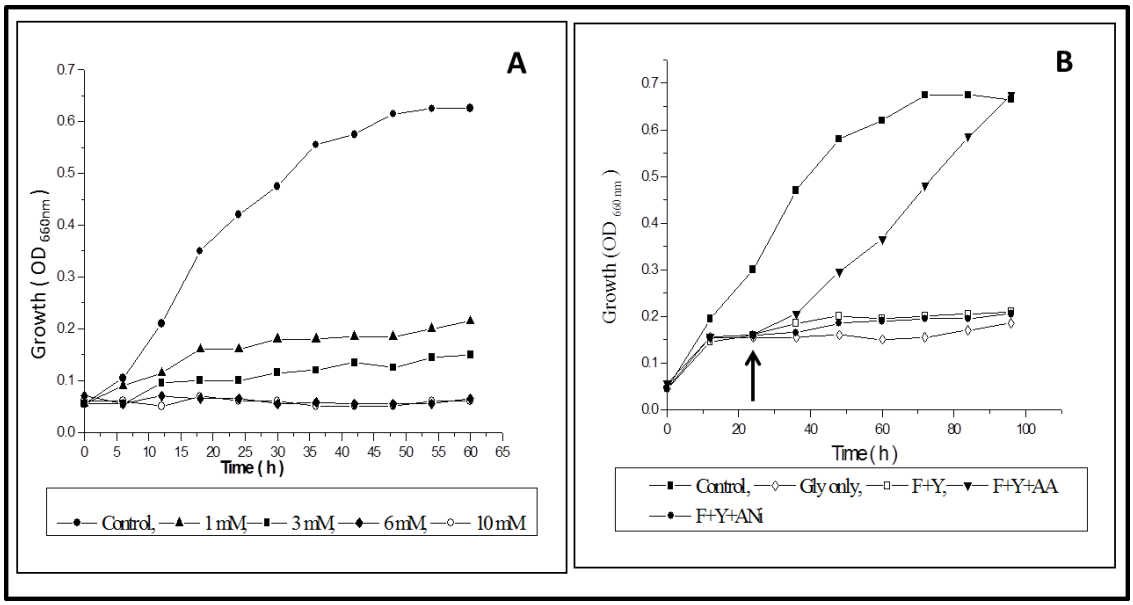

Fig. 14. Effect of glyphosate on growth of *R. benzoatilyticus* JA2.

Inhibition of growth by glyphosate (**A**) and restoration of growth by aromatic amino acids (or its precursors) in *R. benzoatilyticus* JA2 (**B**).

Growth conditions were similar as described under Fig. 8, except for supplementation of different concentrations of glyphosate to media.

Data represents mean of three independent experiments carried out in duplicates. Arrow mark indicates the time point at which the aromatic amino acids or its precursors (150µM) were supplemented to the culture.
Gly, glyphosate; F, phenylalanine; Y, tyrosine; AA, anthranilate; ANi, aniline.

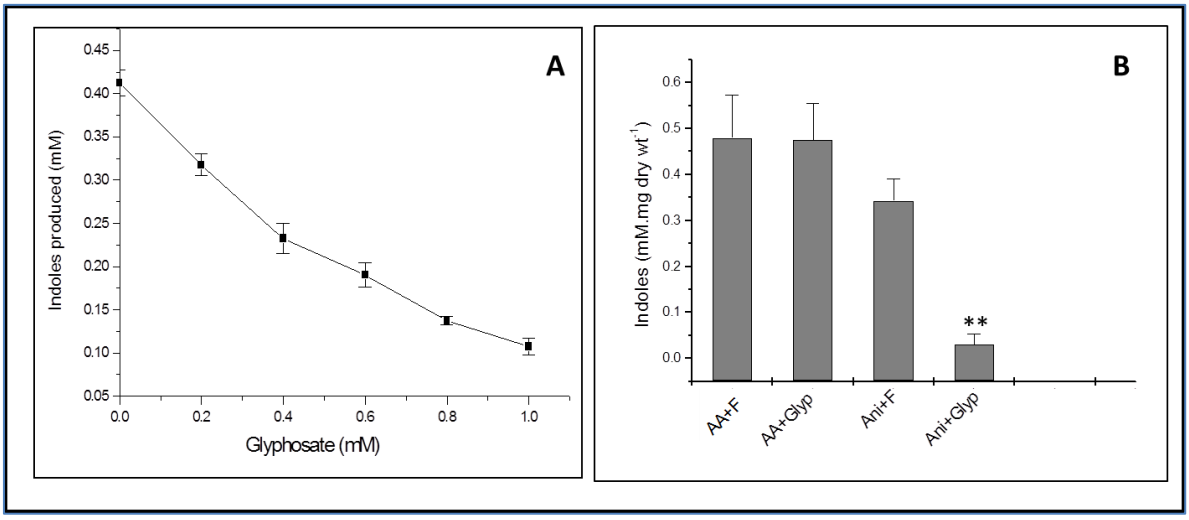

Fig. 15. Effect of glyphosate on indoles production by *R. benzoatilyticus* JA2.

Inhibition of production of indoles in aniline exposed cultures (**A**) and effect of glyphosate on production of indoles in anthranilate treated cultures of *R. benzoatilyticus* JA2 (**B**).

Experimental conditions were similar as described under Fig. 8 except for supplementation of glyphosate (1mM) to culture during aniline/anthranilate exposure and indoles were measured by Salper's reagent.

Data represents mean ± standard deviation of three independent experiments done in duplicates. *, *p* value < 0.005. AA, anthranilate; Glyp, glyphosate; Ani, aniline; F, fumarate.

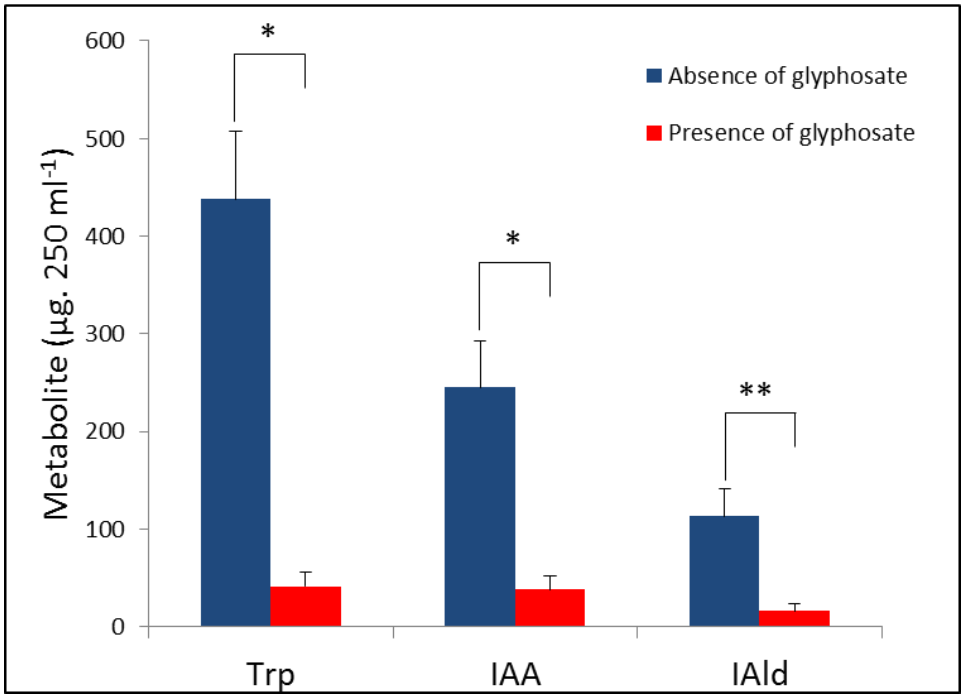

Fig. 16. Inhibition of Trp, IAA and IAld production by glyphosate in aniline exposed cultures of *R. benzoatilyticus* JA2.

Experimental conditions were similar as described under Fig. 15, except for supernatant was fractionated and analysed by HPLC for quantification.

Data expressed as mean ± standard deviation of three independent experiments. *, $p < 0.05$; **, $p < 0.005$ obtained from Student's *t*-test.

3.1.8 Probing of indoles biosynthesis by stable isotope labeled aniline feeding

Rubrivivax benzoatilyticus JA2 culture was exposed to deuterium labeled and unlabeled aniline to know whether aniline is a precursor for indoles biosynthesis or not. If aniline acts as precursor for indoles biosynthesis, indole metabolite will incorporate four deuterium atoms (mass of deuterium= 2 a.m.u) from labeled aniline and the mass of indole nucleus will increase by 4 mass units compared to unlabeled (aniline feeding) (Fig.17). Increase of 4 mass units was not observed in tryptophan mass spectrum obtained from labeled aniline fed culture (tryptophan molecular ion mass 205.0$[M+H]^+$) compared to that of mass spectrum of unlabeled (molecular ion mass 205.1$[M+H]^+$) (Fig. 18A, B). Similarly, four mass units increase was not observed in mass spectrum of IAA (molecular ion mass 176.0$[M+0]^+$; Fig. 19A, B) and indole-3-aldehyde (molecular ion mass 144.0$[M-H]^-$; Fig. 19C, D) of labeled aniline fractions compared to that of mass spectrum of unlabeled fractions (IAA molecular ion mass 176.0$[M+H]^+$; IAld 144.0$[M-H]^-$).

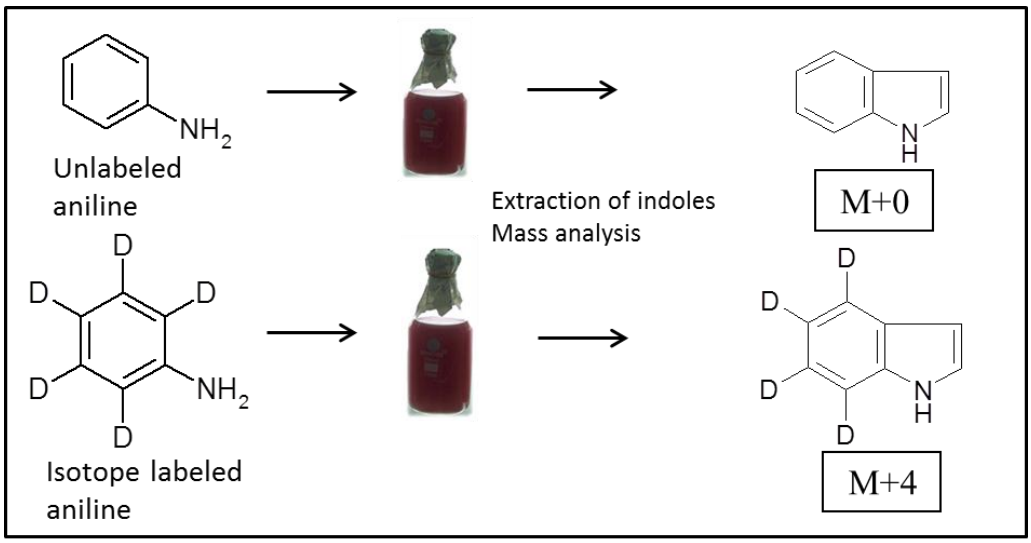

Fig. 17. Schematic representation of stable isotope labeled aniline precursor feeding in *R. benzoatilyticus* JA2.

M, (*m/z*); D, Deuterium atom; 0, no deuterium atoms incorporated; 4, maximum number of deuterium atoms incorporation possible.

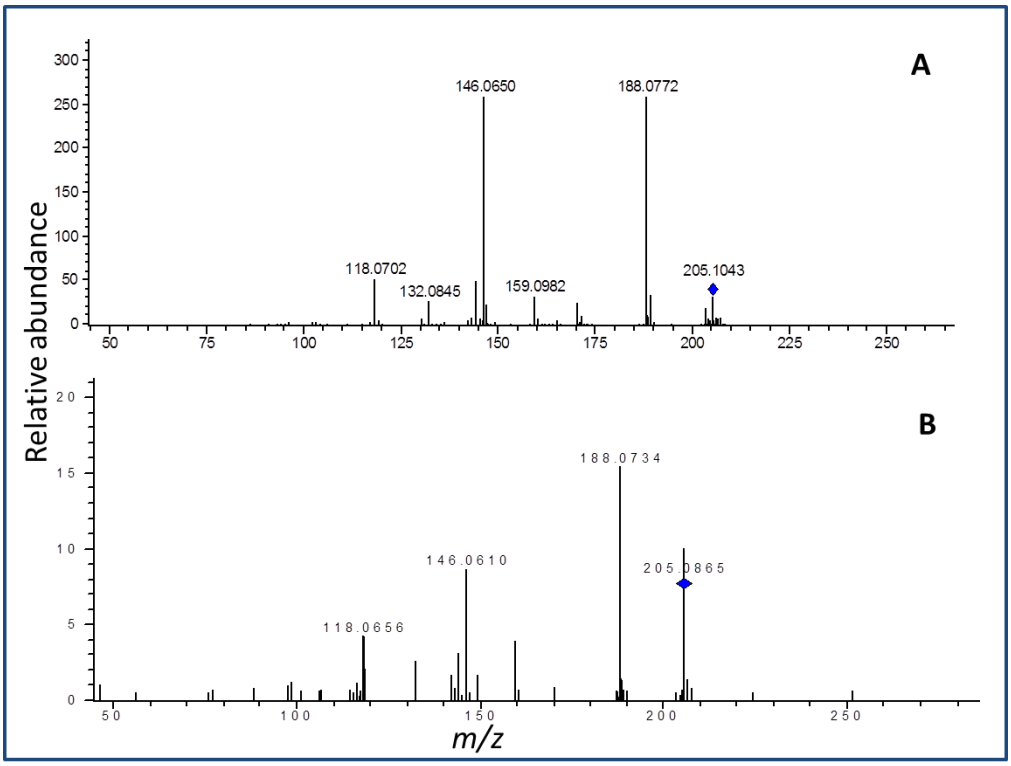

Fig. 18. Isotope labeled aniline precursor feeding of *R. benzoatilyticus* JA2 to probe tryptophan biosynthesis.

Mass spectrum of tryptophan from unlabeled aniline fed culture (**A**) and mass spectrum of tryptophan from labeled aniline fed cultures of *R. benzoatilyticus* JA2 (**B**).

Experimental conditions were same as described under Fig. 8, except for culture was fed with isotope labeled or unlabeled aniline and supernatant was collected, fractionated and subjected to mass analysis.

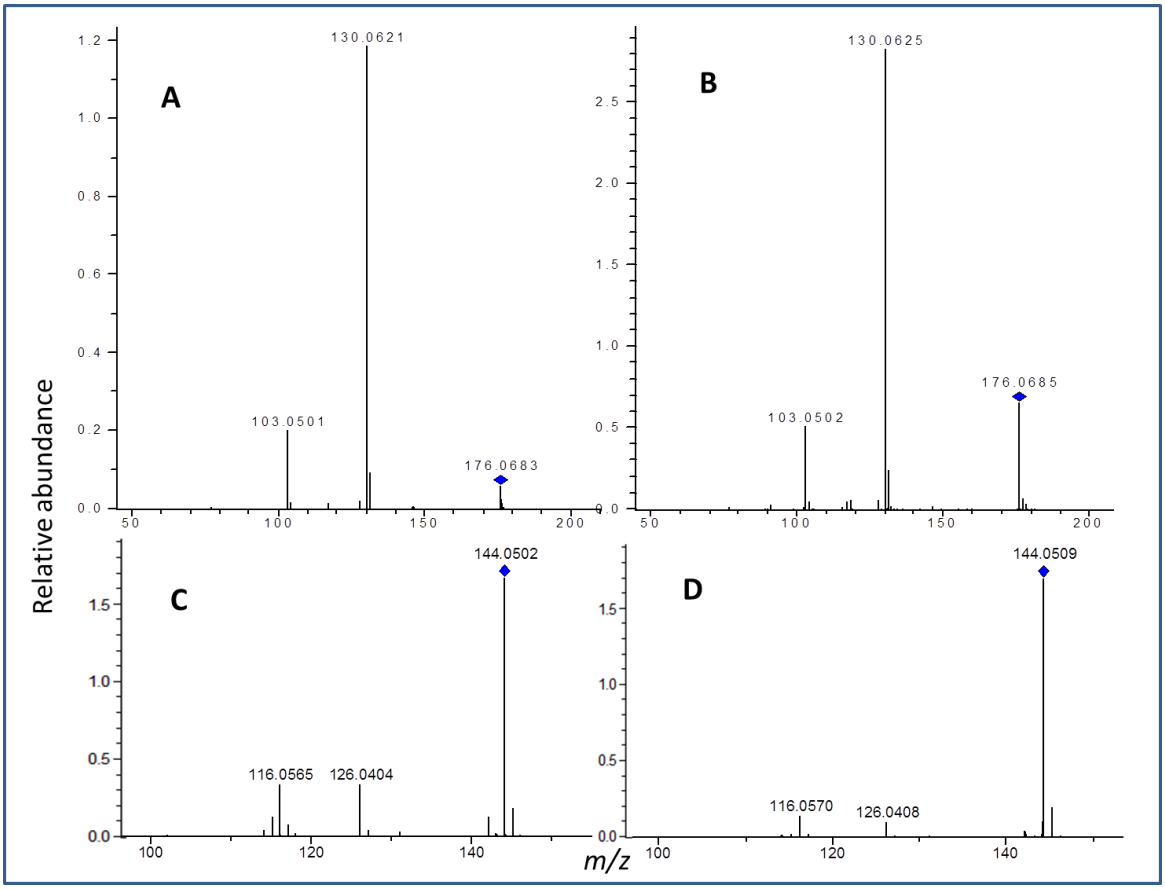

Fig. 19. Isotope labeled aniline precursor feeding of *R.benzoatilyticus* JA2 to probe indoles biosynthesis.

Mass spectrum of IAA from unlabeled aniline fed culture (**A**) and from labeled aniline fed culture (**B**). Mass spectrum of IAld from unlabelled aniline fed culture (**C**) from labeled aniline fed culture (**D**).

Experimental conditions were same as described under Fig. 8, except for culture was fed with isotope labeled or unlabeled aniline and supernatant was collected, fractionated and subjected to mass analysis.

3.1.9 Role of fumarate in indoles biosynthesis by *R. benzoatilyticus* JA2

3.1.9.1 Fumarate enhanced indoles production

Indoles production by *R. benzoatilyticus* JA2 was observed only when culture was exposed to aniline along with carbon source fumarate, while fumarate alone did not induce indoles production (data not shown). *Rubrivivax benzoatilyticus* JA2 was exposed to aniline with and without supplementation of fumarate to know the role of fumarate in indoles production. Tryptophan (462 µg.250 ml^{-1}), IAA (117 µg.250 ml^{-1}) and IAld (72 µg.250 ml^{-1}) levels were high in fumarate supplemented aniline exposed cultures while in the absence of fumarate, tryptophan (236 µg.250 ml^{-1}), IAA (42.5 µg.250 ml^{-1}) and IAld (72 µg.250 ml^{-1}) levels were low (Fig. 20A). Production of tryptophan, IAA and IAld was significantly high when resting cells supplemented with fumarate were exposed to aniline compared to that of without of fumarate feeding (Fig. 20B). Production of tryptophan, IAA and IAld was low when resting cells were exposed to aniline compared to growing cells (data not shown). Production of tryptophan, IAA and IAld was decreased by 50-65% in the absence of fumarate by growing cells while with the resting cells production was decreased by 85-90%.

3.1.9.2 Probing of indoles biosynthesis by stable isotope labeled fumarate feeding

Rubrivivax benzoatilyticus JA2 culture was exposed to deuterium labeled and unlabeled fumarate to know whether fumarate is a precursor for indoles biosynthesis or not. If fumarate acts as precursor for indoles biosynthesis mass of indole metabolites will increase due to incorporation of deuterated fumarate. Based on number of deuterium atoms incorporated, a metabolite may have isotopologues ranging from M+0 to M+n (M, molecular ion mass; 0,1,2…. n, number of deuterium atoms incorporated), (Fig. 21). Isotopologues of tryptophan 206[M+1], 207[M+2], 208[M+3] were observed in mass spectrum of tryptophan obtained from labeled fumarate fed cultures while no such isotopologues were observed from unlabeled fumarate fed cultures (Fig. 22A, B).

Isotopologues of IAA 177[M+1], 178[M+2], 179[M+3] (Fig. 23B) and IAld 147[M+0], 148[M+1], 149[M+3] (Fig. 23D) were observed in mass spectrum of IAA and IAld, respectively from labeled fumarate fed cultures while such isotopologues were not observed from unlabeled fumarate fed cultures (Fig. 23A, C). High ratio of M+1, M+2 isotopologues were observed in labeled tryptophan, IAA and IAld compared to that of unlabeled. Isotopologues M+3 and M+4 were observed only in labeled metabolites while they were absent in unlabeled (Fig. 24A). Isotopic abundance of tryptophan, IAA and IAld was significantly high in labeled fumarate fed cultures compared to that of unlabled (Fig. 24B). Detection of isotopologues and high isotopic abundance in labeled fumarate fed cultures confirms that fumarate as precursor of indole metabolites.

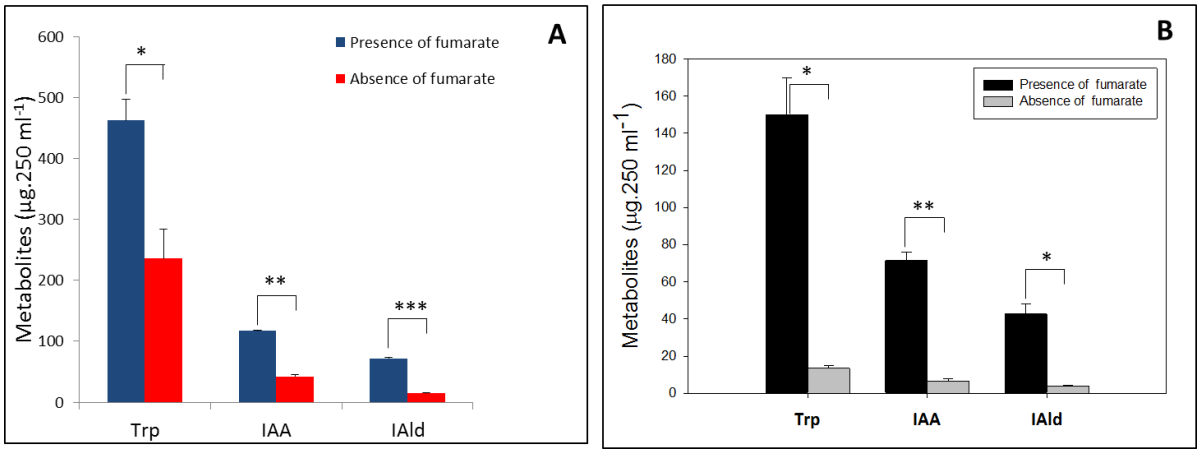

Fig. 20. Fumarate enhanced production of indole derivatives in aniline induced cultures of *R. benzoatilyticus* JA2.

Fumarate enhanced Trp, IAA and IAld production by growing (**A**) and resting cells (**B**).

Experimental conditions were same for growing cells as described under Fig. 8, except for without supplementation of fumarate. Resting cells growth conditions were same as growing cells except for after 48 h photoheterotrophic growth culture was harvested under sterile conditions finally cell pellet was suspended in mineral medium and exposed to aniline with and without supplementation of fumarate, supernatant fractionated and metabolites analysed by HPLC.

Data expressed as mean ± standard deviation of three independent experiments. *, $p < 0.05$, **, $p < 0.005$ and ***, $p < 0.0005$ obtained from Student's *t*-test.

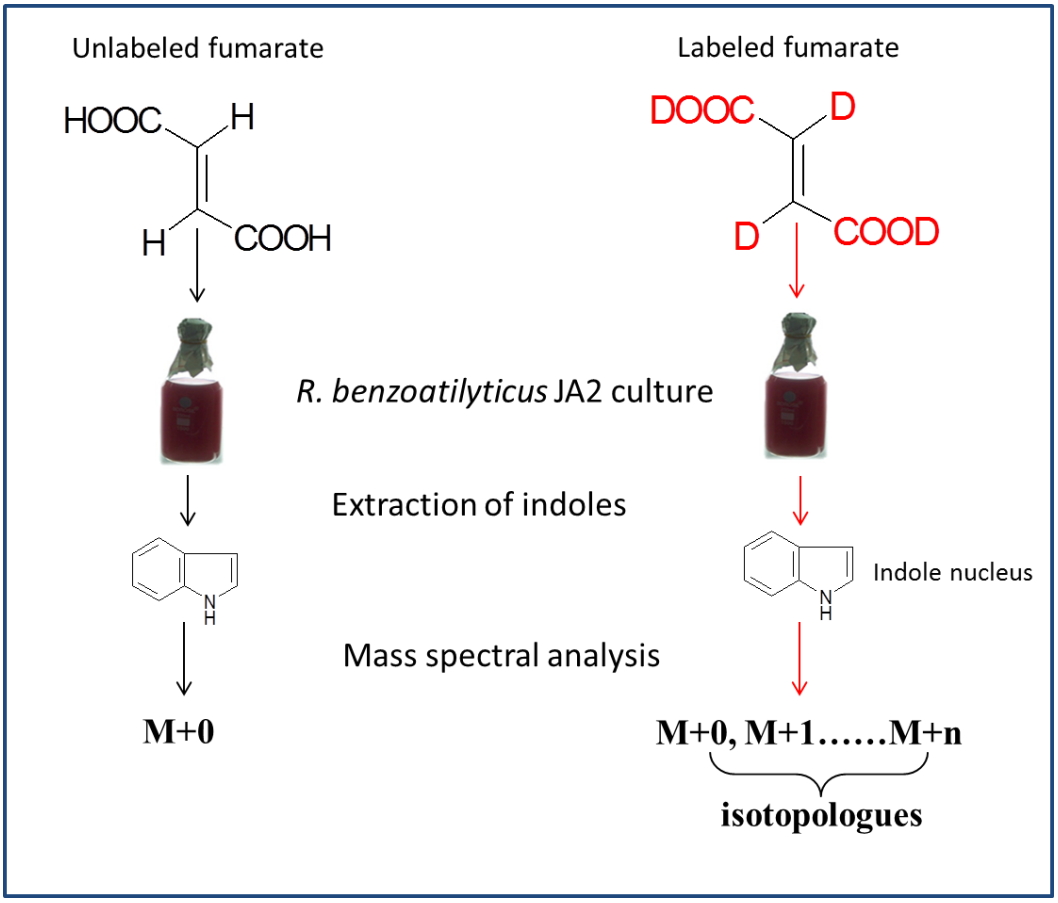

Fig. 21. Schematic representation of stable isotope labeled fumarate precursor feeding of *R. benzoatilyticus* JA2.

D, deuterium atom; M, molecular ion mass (*m/z*); 0, no stable isotope incorporation; n, number of stable isotope atoms incorporated.

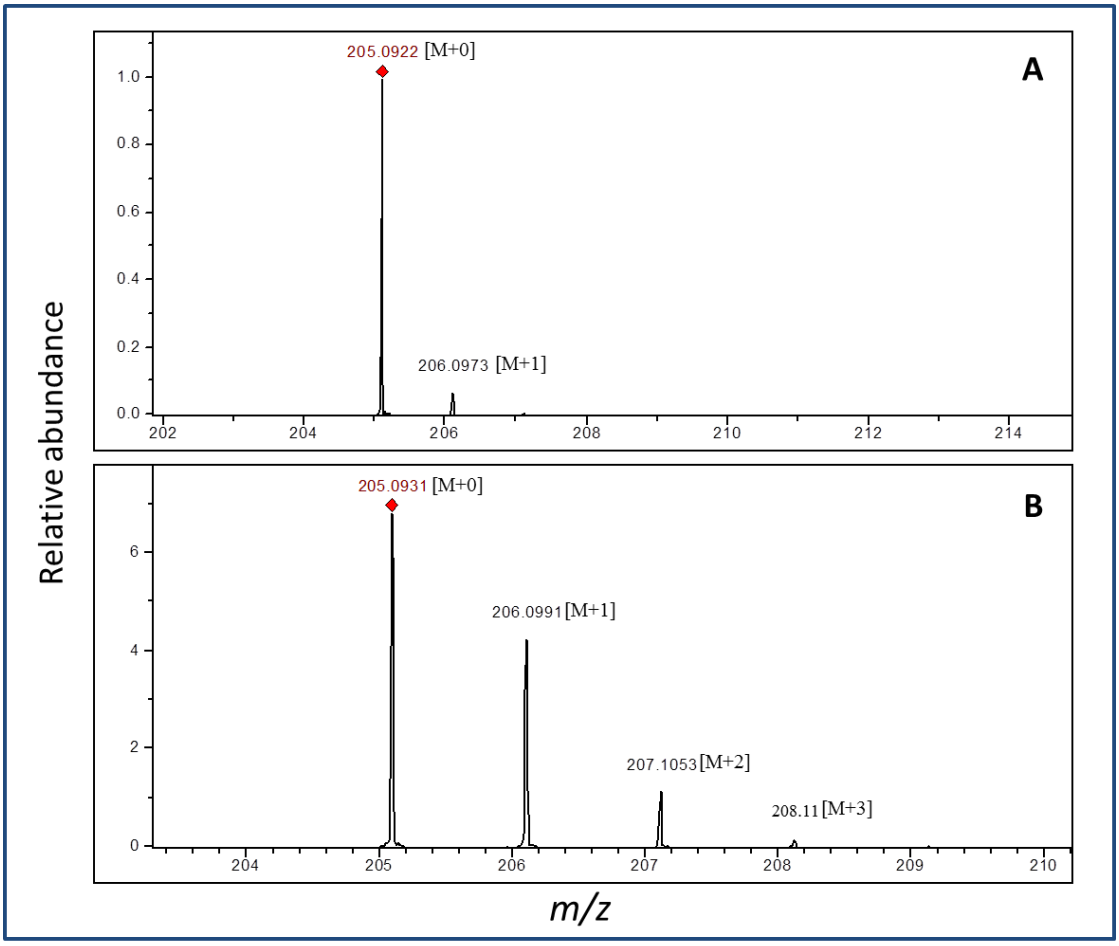

Fig .22. Probing of tryptophan biosynthesis by isotope labeled fumarate precursor feeding.

Mass spectrum of tryptophan obtained from unlabelled fumarate fed cultures (**A**) and from labeled fumarate fed cultures (**B**).

M+0 to M+3, isotopologues of tryptophan; M, molecular ion mass (*m/z*); 0, 1, 2, 3, number of stable isotope atoms incorporated.

Experimental conditions were same as described under Fig. 8 except during aniline exposure culture was fed with unlabeled or isotope labeled fumarate and culture was harvested, supernatant fractionated and analysed by LCMS.

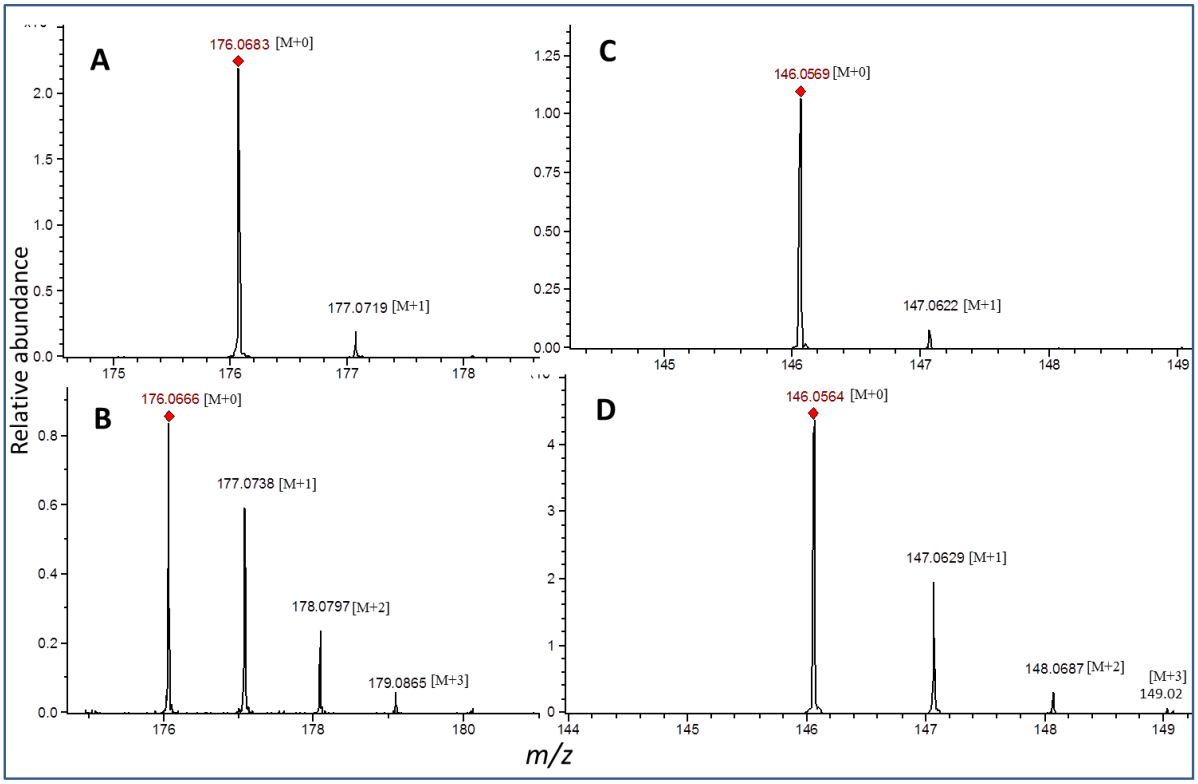

Fig. 23. Probing into aniline induced indoles biosynthesis by isotope labeled fumarate precursor feeding of *R. benzoatilyticus* JA2.

Mass spectra of the IAA obtained from unlabeled fumarate fed culture (**A**) and from labeled fumarate fed culture (**B**). Mass spectrum of IAld from unlabeled fumarate fed culture (**C**) and from labeled fumarate fed culture (**D**).

M+0 to M+3, isotopologues of respective metabolites; M, molecular ion mass (*m/z*); 0, 1, 2, 3, number of stable isotope atoms incorporated.

Experimental conditions were same as described under Fig. 22.

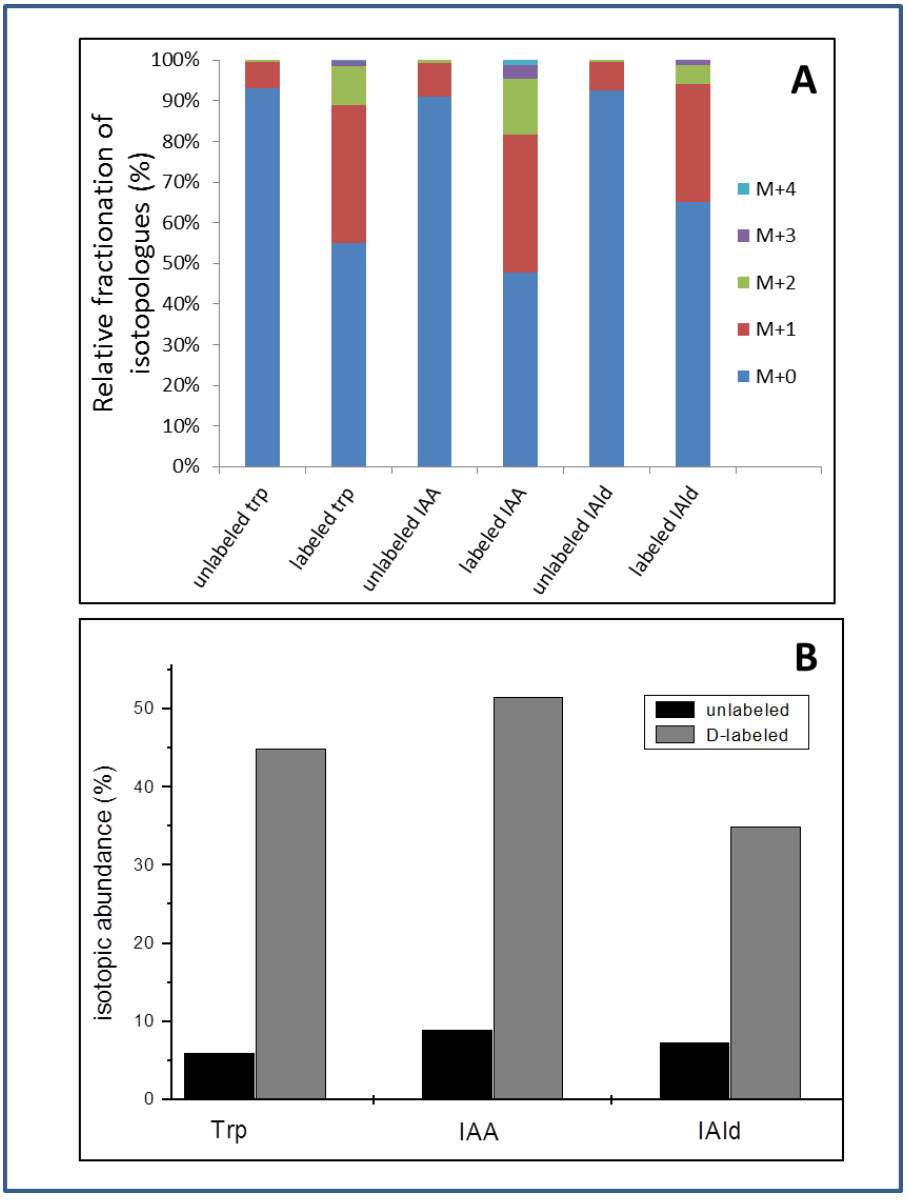

Fig. 24. Isotopic enrichment of Trp, IAA and IAld from labeled fumarate fed cultures of *R. benzoatilyticus* JA2.

Relative isotopic fractionation of isotopologues of Trp, IAA and IAld (**A**).

Total isotopic abundance of Trp, IAA and IAld from unlabeled and labeled fumarate fed cultures of *R. benzoatilyticus* JA2 (**B**).

M+1 to M+4 indicate different isotopologues of metabolites.

Peak areas of isotopologues were obtained from LCMS of labeled and unlabeled fumarate fed culture were used to calculate isotopic enrichment.

3.1.10 Anthranilate synthase activity of *R. benzoatilyticus* JA2

Anthranilate synthase participates in first committed step of tryptophan biosynthesis and it is a rate limiting step. To know the anthranilate synthase levels, enzyme activity was performed with cell free extracts of aniline exposed and unexposed cultures. Product formation was not observed when reaction mixture was incubated with the pre-denatured enzyme source (Fig. 25A) while product (anthranilate) formation was observed when reaction mixture was incubated for 1 h with active enzyme source (Fig. 25B). Specific activity of anthranilate synthase was significantly high (78.5 U. mg protein^{-1}) in aniline exposed cultures compared to that of unexposed (24.7 U. mg protein^{-1}) (Fig. 25C).

3.1.11 Tryptophan aminotransferase (TAT) and tryptophan 2-monooxygenase (TMO) activities

Tryptophan aminotransferase and tryptophan 2-monooxygenase participate in first step of tryptophan catabolism leading to the formation IAA. To know the levels of TAT and TMO, enzyme activities were performed with cell free extracts of aniline exposed and unexposed cultures. Specific activities of tryptophan aminotransferase (12.2 U. mg protein^{-1}) and monooxygenase (7.8 U. mg protein $^{-1}$) were significantly high in aniline exposed cultures compared to that of unexposed (aminotransferase, 4.9 U; monooxygenase, 2.8 U.mg.protein^{-1}) (Fig. 26).

3.1.12 Real time PCR (qRT-PCR) analysis of shikimate pathway genes

Real time PCR analysis of 3-deoxy-D-arabinoheptulosonate 7-phosphate (DAHP) synthase, chorismate synthase, chorismate mutase, anthranilate synthase, tryptophan synthase-β subunit genes was performed to check the transcript levels of these genes in aniline exposed and unexposed cells. Chorismate mutase (5.5 folds) and anthranilate synthase (5.6 folds) genes were up-regulated in aniline exposed cells compared to control (Fig. 27) while no significant change in expression of DAHP synthase, chorismate synthase, tryptophan synthase-β genes was observed after 60 min of aniline exposure.

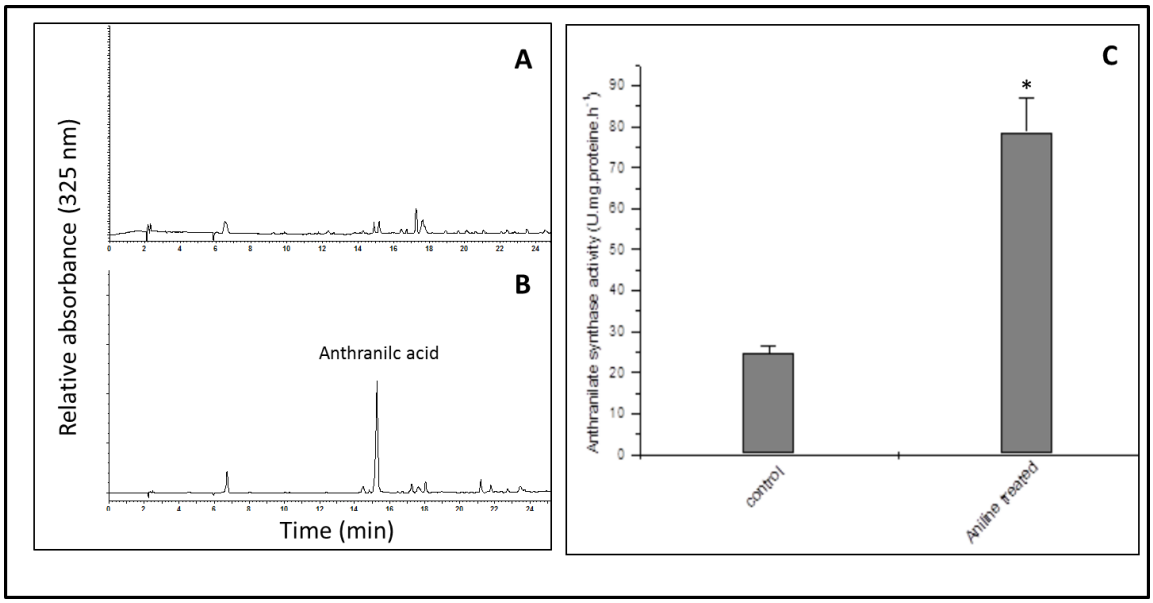

Fig. 25. Anthranilate synthase activity of *R. benzoatilyticus* JA2.

HPLC chromatogram of ethyl acetate fraction obtained from anthranilate synthase activity with denatured enzyme **(A)** and 1 h incubation with enzyme (**B**). Product anthranilic acid peak with R_t 14.5 was observed.

Specific activity of the anthranilate synthase in *R. benzoatilyticus* JA2 (**C**).

Growth conditions were similar as described under Fig. 8. Enzyme assay contained 1mM chorismate, 1mM glutamine, 0.05 mM $MgCl_2$ and cell free extract incubated at 37 $^{\circ}$C for 1h and analysed by HPLC.

Data represents mean ± standard deviation of the three independent experiments done in duplicates. *, *p* value < 0.05 from Student's *t*-test.

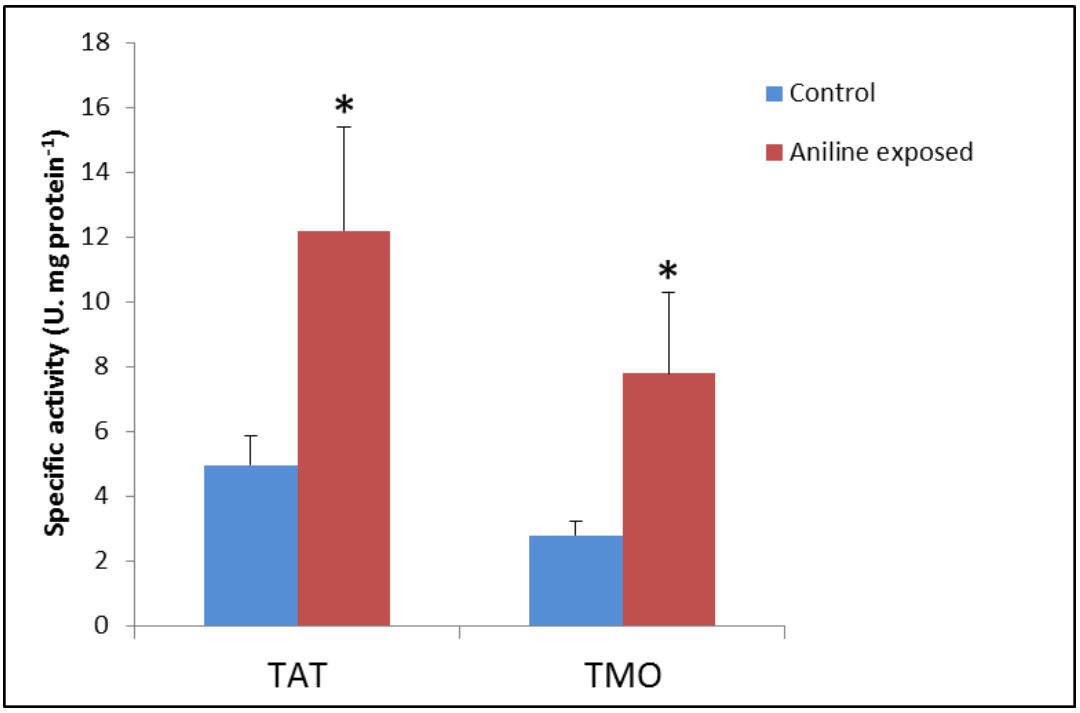

Fig. 26. Tryptophan aminotransferase (TAT) and tryptophan 2-monooxygenase (TMO) activities in *R. benzoatilyticus* JA2.

Growth conditions were similar as described under Fig. 8.

Enzyme assay contained tryptophan (1mM), 2-oxoglutarate (1mM) and 0.05 M PLP for aminotransferase activity, monooxygenase assay contained tryptophan (1 mM) alone and cell free extract. Reaction mixture was incubated at 37 °C for 1 h and the product analysed.

Data represent mean ± standard deviation of three independent experiments.*, $p < 0.05$ obtained from Student's *t* test.

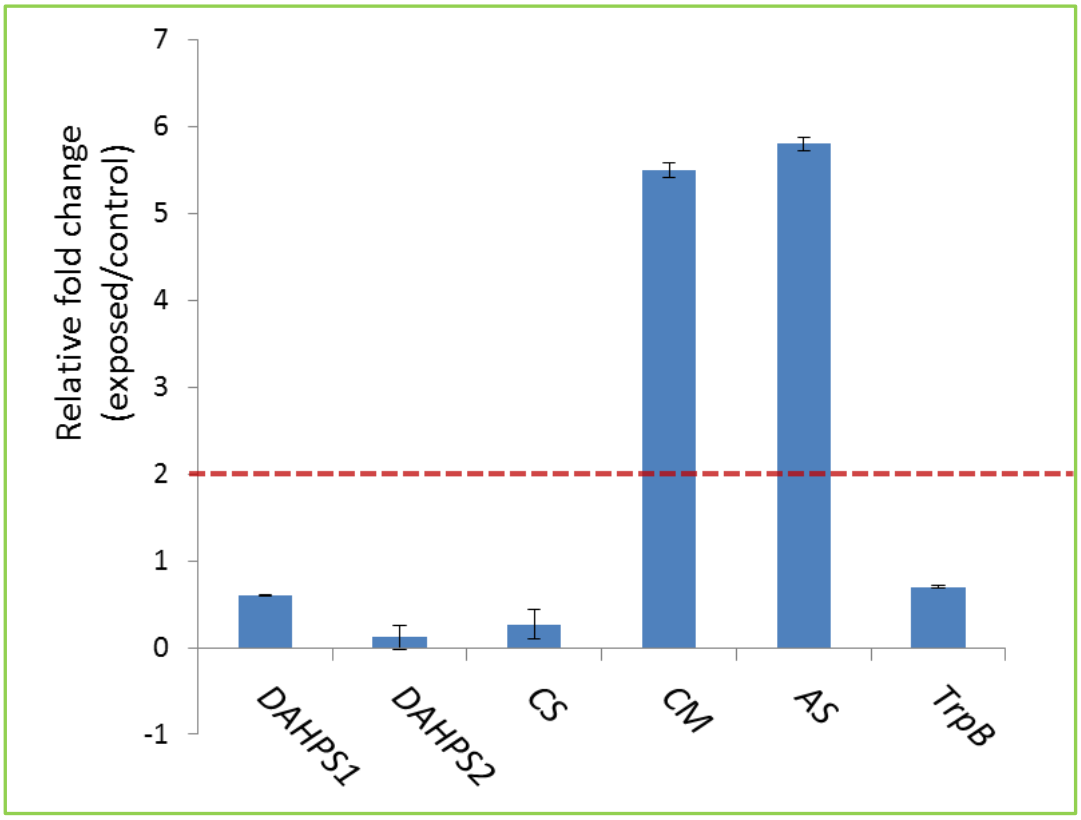

Fig. 27. Real time PCR analysis of shikimate pathway genes of *R. benzoatilyticus* JA2.

Transcript levels are expressed as relative fold change (exposed/control). Dotted lines indicate significant fold change value (2 fold). *DAHPS*, 3-deoxy-D-arabinoheptulosonate 7-phosphate synthase; *CS*, chorismate synthase; *CM*, chorismate mutase; *AS*, anthranilate synthase; *TrpB*, tryptophan synthase β subunit.

Experimental conditions are same as described under Fig. 8 except for the culture was harvested at 60 min after aniline exposure, RNA was isolated and reverse transcribed and analysed by qRT-PCR. Data represents mean standard deviation of duplicate reactions from two independent experiments.

3.1.13 Tryptophan catabolism and indole-3-acetic acid biosynthesis by *R.benzoatilyticus* JA2

3.1.13.1 Time course of tryptophan utilization and indoles production

Tryptophan supplemented photoheterotrophic cultures of *R. benzoatilyticus* JA2 produced indoles with simultaneous utilization of tryptophan (Fig. 28A). Production of indoles was observed within 6 h of tryptophan supplementation and near stoichiometric yields of indoles (0.84 mM) were produced with utilization of 0.82 mM of tryptophan.

3.1.13.2 Identification of indole derivatives

Twenty five chromatographically distinct peaks were detected by HPLC analysis of the ethyl acetate fraction obtained from tryptophan supplemented cultures, of which 17 metabolites had absorption at 270-280 nm (Fig. 28B). Further, peak eluent was collected and tested for presence of indole derivatives by Salper's reagent, among which 15 metabolites were positive for indoles test (data not shown). Six metabolites were identified based on their retention time (R_t), UV absorption spectrum and co-elution with authentic standards (Table. 2) these metabolites include; indole -3-acetamide (R_t 14.5 min), indole -3-aldehyde (R_t 17.5 min), IAA (R_t 18.55 min), indole -3-carboxylic acid (R_t 18.9 min), indole 3-acetonitrile (R_t 23.1 min), and indole (R_t 24.6 min).

Metabolites identified by HPLC were confirmed by mass analysis. Indolic fraction mass analysis detected molecular ion mass of 175$[M]^+$, 146$[M]^+$, 176$[M]^+$, 162$[M]^+$, 158$[M]^+$, and 118$[M]^+$ corresponding to the, indole-3-acetamide, indole-3-aldehyde, IAA, indole 3-carboxylic acid, indole-3-acetonitrile, and indole, respectively (Table. 2). Three metabolites were identified as methoxyindole-3-aldehyde (R_t 15.2 min; 176$[M+H]^+$), methoxyindole-3-acetic acid (R_t 17.9 min; mass 206$[M+H]^+$), and trisindoline (R_t 26.2 min; mass, 362$[M-H]^-$) based on their molecular ion mass, mass fragmentation pattern, and absorption spectra while other three metabolites remained unidentified (Table. 2).

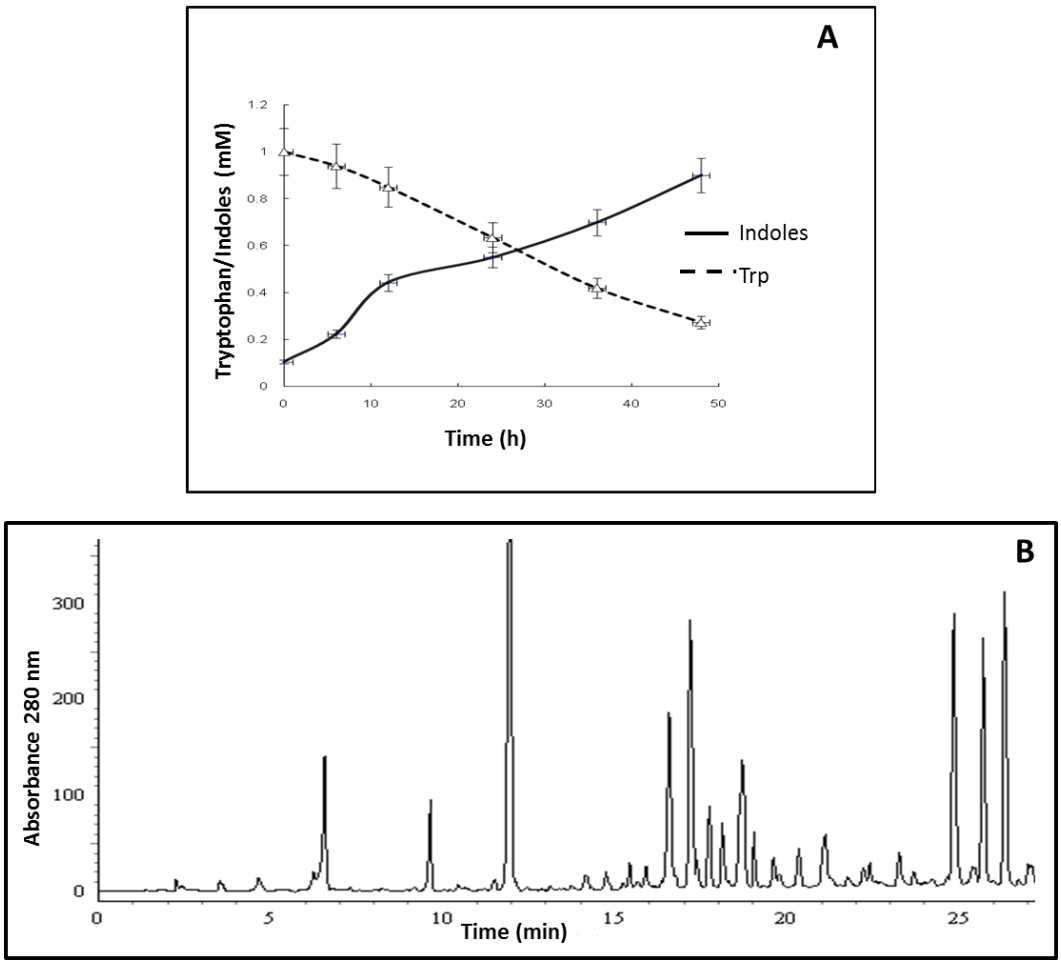

Fig. 28. Tryptophan catabolism in *R. benzoatilyticus* JA2

Utilization of Trp and production of indoles by *R. benzoatilyticus* JA2 (**A**).

HPLC chromatogram of the ethyl acetate fraction obtained from tryptophan induced culture of *R. benzoatilyticus* JA2 (**B**).

Malate grown mid log phase culture (0.25 OD $_{660nm}$) was used as inoculum (10%) and the culture was grown for 48 h photoheterotrophically then 1mM of sterile Trp was supplemented and incubated for 48 h or sample was drown at regular intervals for analysis. Indoles were measured by Salper's reagent and the profiling was done by HPLC. Trp, tryptophan.

Table.2. Identification of indole metabolites from tryptophan exposed culture supernatants

R_t (min)	UV max (nm)	Mass (m/z) and mass fragmentation	Indole derivatives
14.5	214, 226, 273, 278	175$[M+H]^+$ [175, 158,130]	Indol-3-acetamide
15.2	214, 227, 240, 279, 288	176$[M+H]^+$ [176, 166, 146]	Methoxyindole-3-aldehyde
15.7	214, 241, 258, 298	203$[M-H]^-$ [203 186, 146, 130]	Ud
17.0	215, 262, 277, 288	187$[M-H]^-$ [187, 160, 116]	Ud
17.5	214, 243, 260, 290	146$[M+H]^+$ [146,118]	Indole-3-aldehyde
17.9	222, 234, 273	206$[M+H]^+$ [206, 188,176,146,130, 115]	Methoxy-indoleacetic acid
18.55	215, 273, 278, 288	176$[M+H]^+$ [176, 146, 130]	Indole-3-acetic acid
18.9	220, 283	162$[M+H]^+$ [162, 144,118]	Indole-3-carboxylic acid
23.1	214, 242, 280	157$[M+H]^+$ [157, 130,]	Indole-3-acetonitrile
24.6	214, 270, 276, 287	118$[M+H]^+$	Indole
25.5	214, 228, 274, 278,289	258$[M+H]^+$	Ud
26.2	215, 228, 280, 288	362$[M+H]^-$ [362, 246, 158]	Trisindoline

R_t, retention time from HPLC chromatogram (Fig. 29); UV max, absorption spectra; Ud, unidentified metabolites; $[M+H]^+$, positive ion mode; $[M-H]^-$, negative ion mode.

Experimental conditions were same as described under Fig. 28 except for the indolic fraction was analysed by LCMS.

3.1.13.3 Probing of indole-3-acetic acid biosynthesis by stable isotope tryptophan feeding

Rubrivivax benzoatilyticus JA2 culture was fed with labeled and unlabeled tryptophan, culture supernatant was extracted with ethyl acetate and analysed by LCMS. Tryptophan was labeled with five deuterium atoms on its indole nucleus (L-trptophan-d_5 [indole-d_5] Cambridge Isotopes) and any metabolite produced from labeled tryptophan will have five deuterium atoms in it. Mass analysis of labeled and unlabeled fractions indicated incorporation of labeled tryptophan into indole metabolites which was evident from the increase in the molecular ion mass of labeled metabolites by 5 units. Incorporation of labeled tryptophan into indole 3-acetamide and IAA was observed by an increase in their molecular ion mass from 175$[M+0]^+$ (Fig. 29A) to 180$[M+5]^+$ (Fig. 29B) and 176$[M+0]^+$ (Fig. 29C) to181$[M+5]^+$ (Fig. 29D), respectively.

3.1.13.4 Tryptophan 2-monooxygenase activity of *R. benzoatilyticus* JA2

Tryptophan 2-monooxygenase catalyses the formation of indole-3-acetamide from tryptophan which eventually leads to IAA biosynthesis. Tryptophan 2-monooxygenase activity was demonstrated using cell free extracts of *R. benzoatilyticus* JA2 and the product was detected by HPLC analysis. Product formation (indole-3-acetamide) was observed when cell free extract was incubated with reaction mixture containing tryptophan while no such product was observed with pre-denatured protein (Fig. 30). Indole-3-acetic acid was also detected along with indole-3-acetamide in monooxygenase assay (Fig. 30).

3.1.13.5 Indole-3-actic acid biosynthetic pathways in *R. benzoatilyticus* JA2

Indole-3-acetamide (IAM) mediated IAA biosynthetic pathway was observed in *R. benzoatilyticus* JA2 which was evident from detection of metabolites IAM and IAA. Further this pathway was confirmed by detection of tryptophan 2-monooxygenase activity in cell free extracts. Indole-3-acetonitrile was also detected in culture supernatants which leads to formation of IAA and this indicate indole-3-acetontrile routed IAA biosynthesis (Fig. 31). Indole-3-pyruvate mediated pathway was reported by Kumavth *et al* (2010) in *R. benzoatilyticus* JA2 and apart from the IAA biosynthesis, tryptophanase catalysed indole formation was also observed in *R. benzoatilyticus* JA2. Based on detection of metabolites, stable isotope labeling, enzyme activities and published literature tryptophan catabolic pathway is proposed in *R. benzoatilyticus* JA2 (Fig. 31).

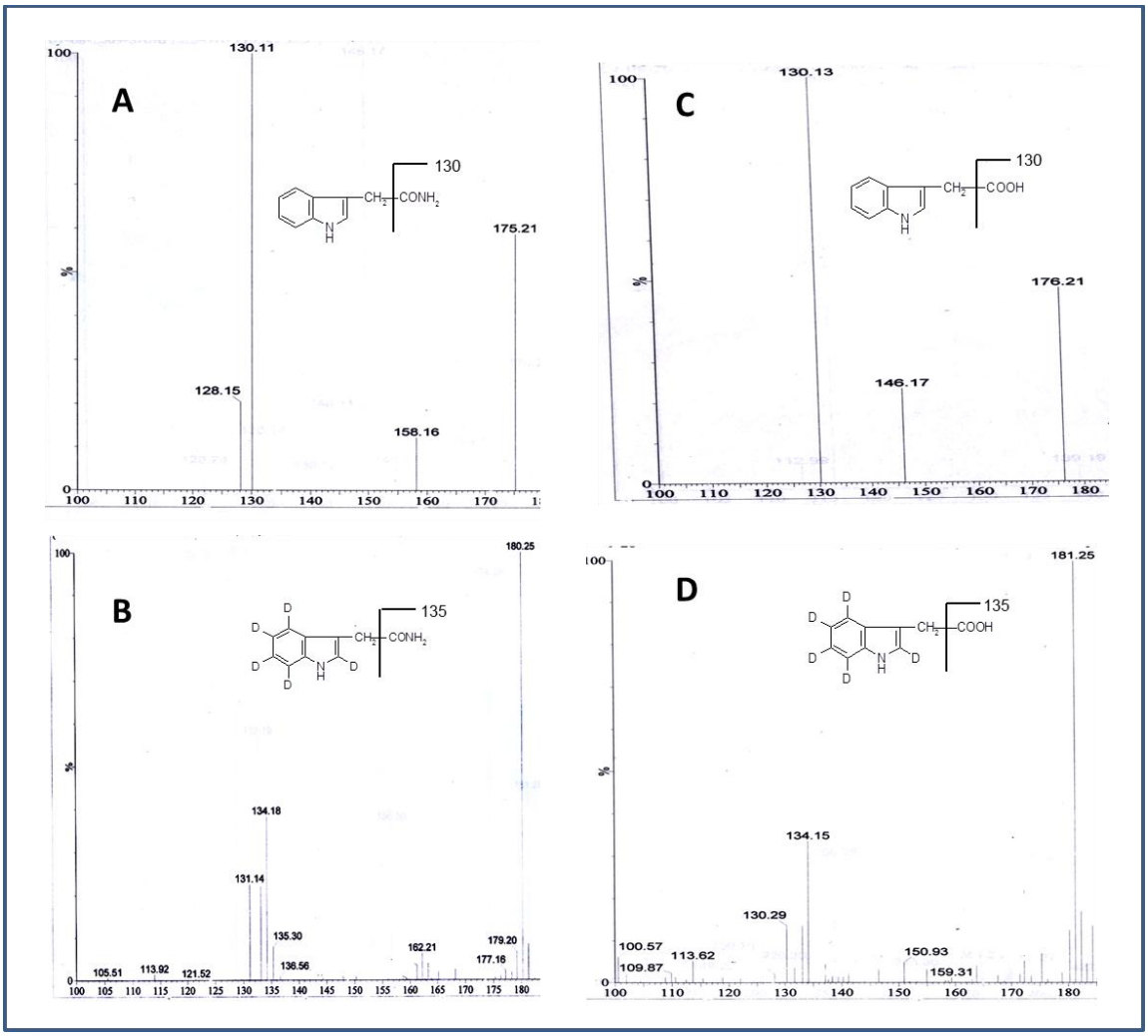

Fig. 29. Probing of indole-3-acetic acid biosynthesis by stable isotope tryptophan feeding

Mass spectrum of indole-3-acetamide from unlabeled fraction (**A**) and from laleled fraction (**B**). Mass spectrum of indole-3-acetic acid from unlabled fraction (**C**) and from labeled fraction (**D**). Insert shows fragmentation pattern of metabolite.

Experimental conditions were same as described under Fig. 28, except for the supplementation of labeled and unlabeled tryptophan to culture and supernatant was collected, extracted by ethyl acetate and mass analysis was done.

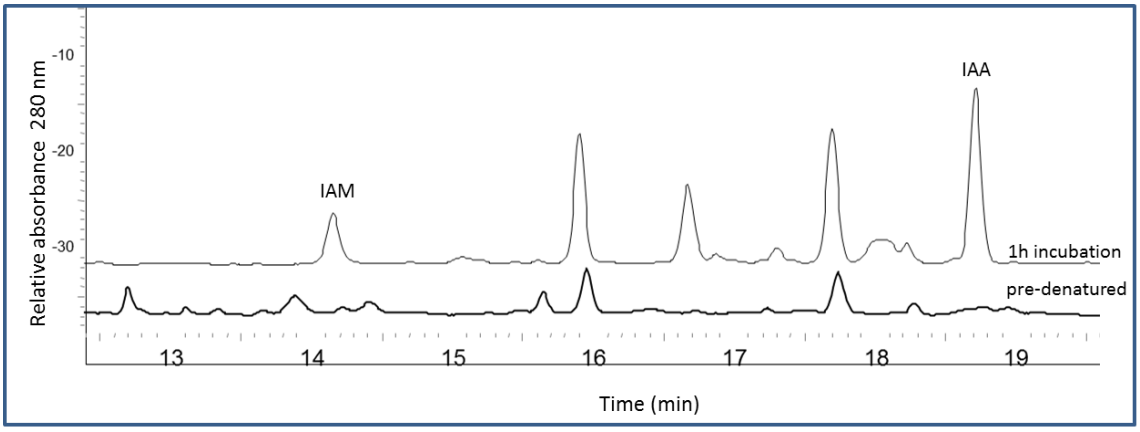

Fig. 30. HPLC chromatogram of tryptophan 2-monooxygenase activity in *R. benzoatilyticus* JA2.

IAM and IAA formation was observed as products. IAM, indoleacetamide; IAA, indole-3-acetic acid. Experimental conditions were similar as described under Fig. 26.

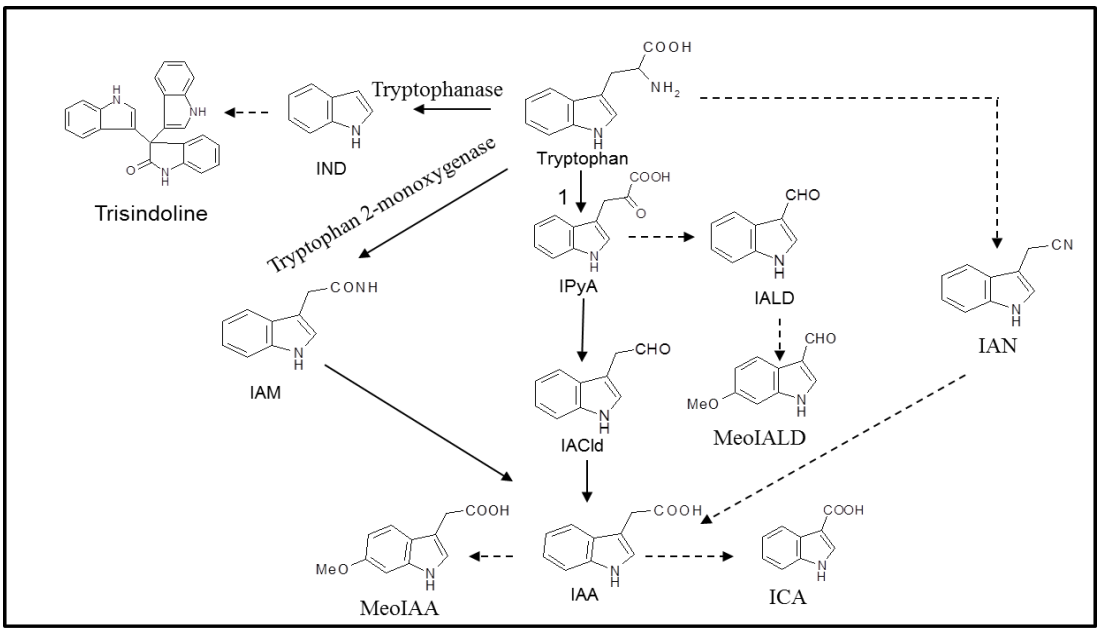

Fig. 31. Proposed pathway of the tryptophan catabolism in *R. benzoatilyticus* JA2.

Solid arrow indicate reaction confirmed based on enzyme activity and metabolite identification, dashed arrow indicate plausible reaction based on metabolite identification.

IAN, indoleacetonitrile; IND, indole; IAM,indole-3acetamide; IACld, indole-3-acetaldehyde; IAA, indole-3-acetic acid; ICA,indolecarboxylic acid; IPyA,indolepyruvic acid; Meo, methoxy group; 1, aminotransferase pathway in *R. benzoatilyticus* JA2 (Kumavath *et al* 2010).

3.1.14 pH regulated indoles biosynthesis by *R. benzoatilyticus* JA2

3.1.14.1 Effect of glucose on indoles production

Malate or glucose grown culture of *R. benzoatilyticus* JA2 was exposed to tryptophan (1mM), anthranilate (1 mM) and aniline (25 mM) for indoles production. Indoles production was high (tryptophan, 0.6 mM; anthranilate, 0.45; aniline, 0.41 mM) in malate grown cultures compared to those of glucose grown for all three exposed conditions tryptophan, (0.14 mM), anthranilate, (0.07) aniline, (0.04 mM) (Fig. 32A). Inhibition of indoles production was observed only when culture was grown on glucose. However, indoles production was not inhibited when malate grown culture (aniline exposed) was supplemented with glucose (Fig. 32B).

3.1.14.2 Influence of carbon sources on indoles production in aniline exposed cultures

Glucose inhibited the indoles production in *R. benzoatilyticus* JA2 and to evaluate the effect of other carbon sources, *R. benzoatilyticus* JA2 was grown on different sugar and non-sugar carbon sources. All the tested carbon sources supported the growth of *R. benzoatilyticus* JA2 (Table.3) and biomass yields were high in glucose (0.8 mg dry wt ml^{-1}). pH of the culture was high (8.4-8.6) in non-sugar carbon sources while pH was low (6.4-6.6) in sugar carbon sources (Table. 3). Indoles production was significantly high (0.28-0.4 mM.mg dry wt^{-1}) in cultures grown on non-sugar carbon sources compared to those on sugars (0.04-0.07 mM.mg dry wt^{-1}) (Table. 3). Sugar carbon sources inhibited the indoles production in aniline exposed cultures.

3.1.14.3 Time course of indoles production and pH of the culture supernatant

Production of indoles increased with time in malate and glucose grown cultures exposed to aniline and production was high at 48 h (Fig. 33B). However, indoles production was low in glucose grown cultures (0.09 mM) compared to those of malate (0.4 mM). pH of the glucose grown culture (6.4) and malate grown culture (8.4) remained constant throughout the experiment (Fig. 33A).

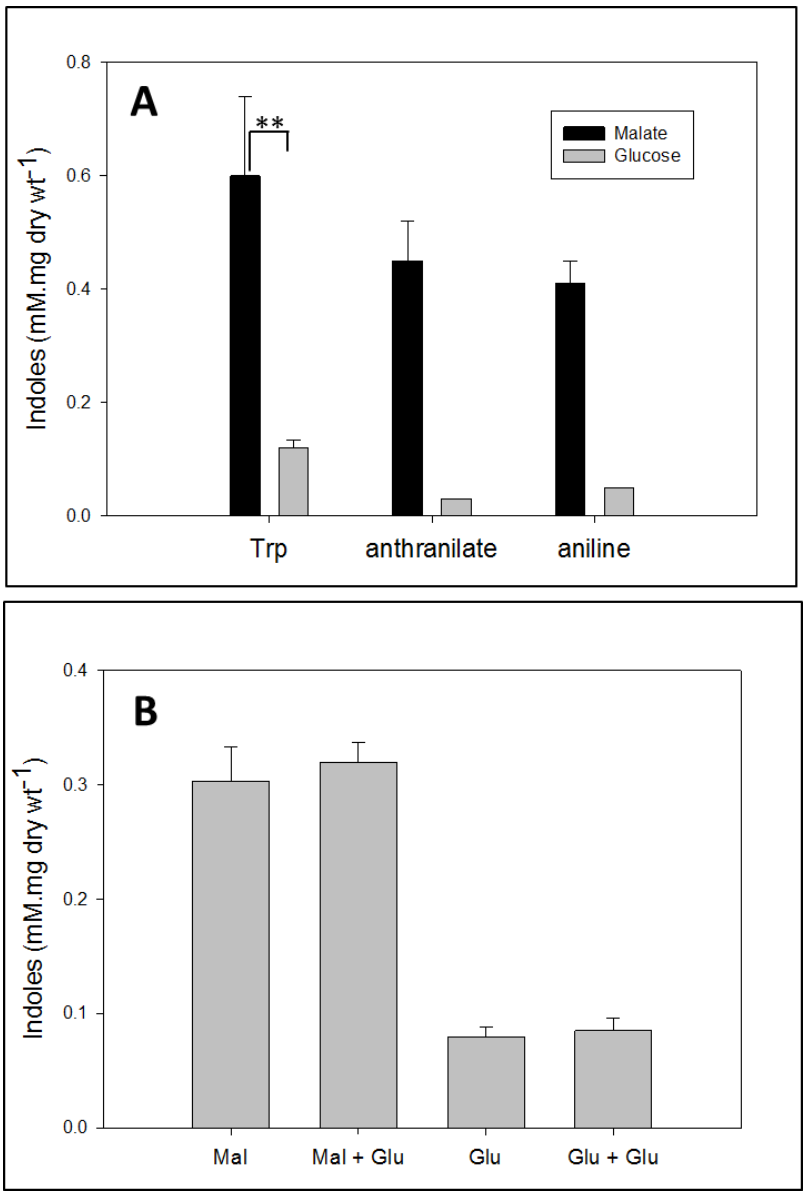

Fig. 32. Inhibition of indoles production by glucose in *R. benzoatilyticus* JA2.

Inhibition of indoles production by glucose in tryptophan, anthranilate and aniline exposed cultures of *R. benzoatilyticus* JA2 (**A**).

Glucose as carbon source inhibits production of indoles in aniline exposed culture of *R. benzoatilyticus* JA2 (**B**).

Malate grown mid log phase culture (0.25 OD $_{660nm}$) was used as inoculum (10%). Culture was grown photoheterotrophically for 48 h on malate or glucose as carbon source and during aniline exposure 22 mM of glucose was added, incubated for 48 h and indoles were measured.

Data expressed as mean ± standard deviation of three independent experiments done in duplicates. *, *p* value < 0.003. Mal, malate; Glu, glucose.

Table.3. Effect of carbon sources on indoles production and final pH of culture filtrate in *R. benzoatiltyicus* JA2

Carbon source (22mM)	Biomass yield (mg .dry wt.ml^{-1})	Final pH of the culture filtrate	Total Indoles production (mM.mg dry wt^{-1})
Malate	0.43 ± 0.03	8.4	0.4
Fumarate	0.4 ± 0.02	8.5	0.34
Pyruvate	0.43 ± 0.04	8.5	0.37
Succinate	0.34 ± 0.1	8.6	0.28
Glucose	0.82 ± 0.05	6.6	0.05
Fructose	0.42 ± 0.06	6.4	0.05
Mannose	0.34 ± 0.01	6.5	0.04
Maltose	1	6.4	0.07

Malate grown mid log phase culture (0.25 OD $_{660nm}$) of *R. benzoatilyticus* JA2 was used as inoculum (10%) for experiment and culture was grown on respective carbon sources (22 mM) for 48 h, exposed to aniline (25 mM), fumarate (13 mM). After incubation for 48 h photoheterotrophically supernatant was analysed for indoles production and final pH.

Data represents mean ± standard deviation three independent experiments carried out in duplicates.

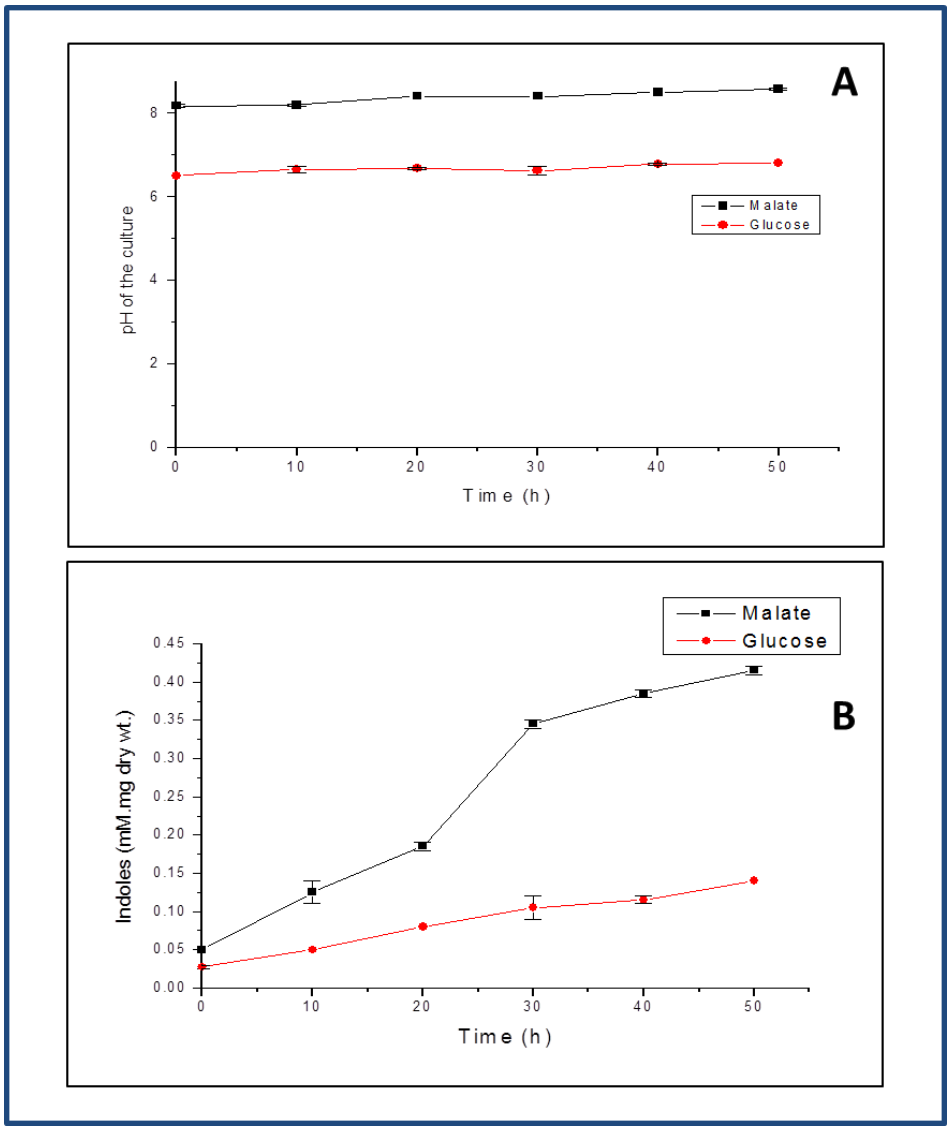

Fig. 33. Effect of carbon sources on production of the indoles and pH of the culture supernatant of *R. benzoatilyticus*.

Effect of the carbon sources on pH of the culture (**A**) and on indoles production over period of time (**B**).

Malate grown mid log phase culture (0.25 OD $_{660nm}$) was used as inoculum and culture was grown photoheterotrophically for 48 h on malate or glucose as carbon source and then exposed to aniline, incubated for 48 h and supernatant analysed for indoles.

Data expressed as mean ± standard deviation of three independent experiments done in duplicates.

3.1.14.4 Effect of pH on indoles productions

To evaluate the role of pH on indoles production, pH reversal experiment was done where, the malate culture pH was adjusted from 8.4 to 6.4, while the glucose was adjusted from 6.4 to 8.4. Indoles production was inhibited in malate culture at pH 6.4, while in glucose culture at pH 8.4 indoles production was observed (Fig. 34A), which confirms the role of pH on indoles production by *R. benzoatilyticus* JA2. Further, both malate and glucose grown cultures were suspended in buffers of pH 6.4 and 8.4. Indoles production was observed only in 8.4 pH buffer but no indoles production was observed at 6.4 pH irrespective of the carbon sources used for growth (Fig. 34B). Further, buffers with different pH strengths effected the indoles production in *R. benzoatilyticus* JA2 (Fig. 35A) where acidic pH was able to inhibit the indoles production and alkaline pH induced indoles production which was maximum at 8.5 (Fig. 35A).

3.1.14.5 Role of Cyclic AMP in indoles production

Cyclic AMP relieves the catabolic repression of glucose in bacteria (Gorke and Stulke, 2008) and to know whether cyclic AMP can relieve the inhibition of indoles production by glucose, experiment was performed. Cyclic AMP at various concentrations could not relieve the inhibitory effect of glucose on indoles production (Fig. 35B) further confirming that indoles production in *R. benzoatilyticus* JA2 not under catabolic repression.

3.1.14.6 HPLC metabolic profiling of indolic fractions

Indolic fractions from aniline exposed cell suspension of pH 6.4 and pH 8.4 were analysed by HPLC to detect indole metabolites. HPLC analysis acidic fractions detected a peak (R_t 9.45 min) corresponding to tryptophan only in pH 8.4 cell suspensions while in pH 6.4 no detectable amounts tryptophan was observed (Fig. 36A). Indole-3-acetic acid (R_t 18.7 min) was detected in HPLC chromatograms of pH 6.4 and pH 8.4 fractions (Fig. 37A) and levels of IAA were high (38 µg.mg dry wt ml^{-1}) in pH 8.4 fractions compared to pH 6.4 fractions (5 µg.mg dry wt ml^{-1}). HPLC analysis of the neutral fractions detected peak (R_t 17.3 min) corresponding to IAld (Fig. 36B) and a high level of IAld (1.2 µg.mg dry wt ml^{-1}) was observed in pH 8.4 cultures compared to pH 6.4 (70 µg.mg dry wt ml^{-1}). Tryptophan, IAA and IAld production was decreased in aniline exposed cultures at pH 6.4.

3.1.14.7 Tryptophan catabolising enzyme activities of malate and glucose grown cultures

Tryptophan aminotransferase, tryptophanase and tryptophan monooxygenase are involved in tryptophan catabolism leading to the formation of indole derivatives. All three enzyme activities were carried out in malate and glucose cultures exposed to aniline. Specific activities of tryptophan monooxygenase (10.3 U.mg protein^{-1}) and tryptophanase (3.5 U.mg protein^{-1}) were significantly high in aniline exposed cultures grown on malate compared to that of glucose (monooxygenase, 5.5 U; tryptophanase 1.5 U.mg protein^{-1}) while no significant decrease was observed in aminotransferase activity (Fig. 37).

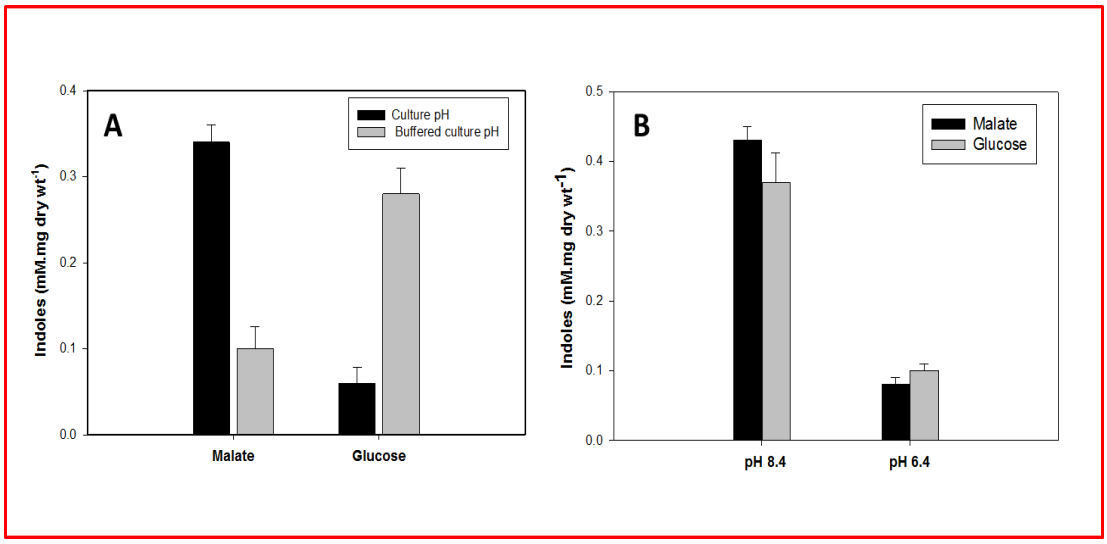

Fig. 34. pH regulation of the indoles production in *R. benzoatilyticus* JA2.

Inhibition of indoles production by pH in growing (**A**) and resting cells (**B**).

Experimental conditions were same as described under Fig. 33, except for malate grown culture pH was adjusted to 6.0 and glucose grown to 8.0 and then exposed to aniline. Culture was incubated for 48 h and supernatant analysed for indoles.

Resting cells experimental conditions were same as of growing cells except for after 48 h of phototrophic growth culture was harvested under sterile condition and cell pellet was suspended in phosphate buffer pH of 6.4 and 8.4.

Data expressed as mean ± standard deviation of three independent experiments done in duplicates.

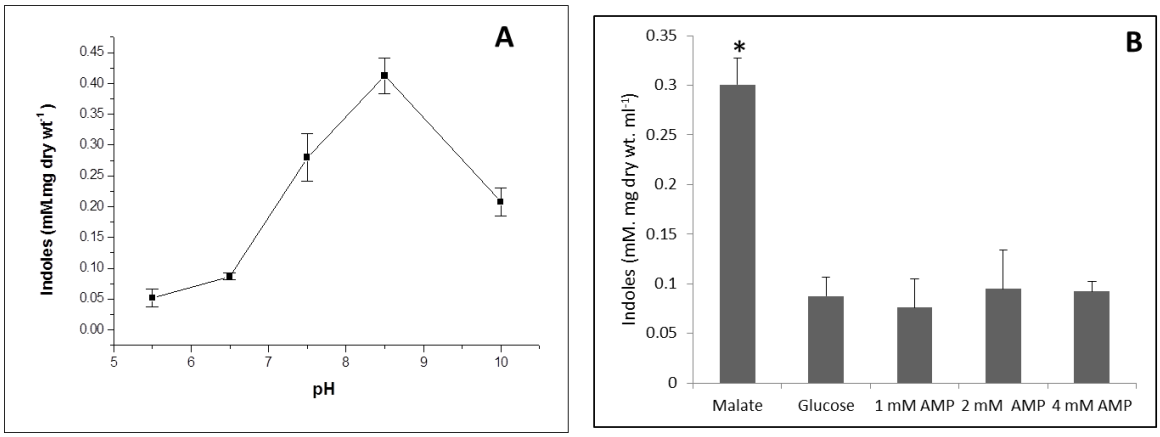

Fig.35. Effect of pH and cyclic AMP in indoles production of *R. benzoatilyticus* JA2.

Effect of pH (**A**) and cyclic AMP (**B**) on production indoles by *R. benzoatilyticus* JA2

Experimental conditions were same as described under Fig. 34 except, for the after 48h of growth culture was harvested; cell pellet was suspended in buffers of different pH.

For cyclic AMP experiment different concentrations (1-4 mM) of cyclic AMP was added during aniline exposure.

Data expressed as mean ± standard deviation of three independent experiments done in duplicates. *, $p < 0.05$.

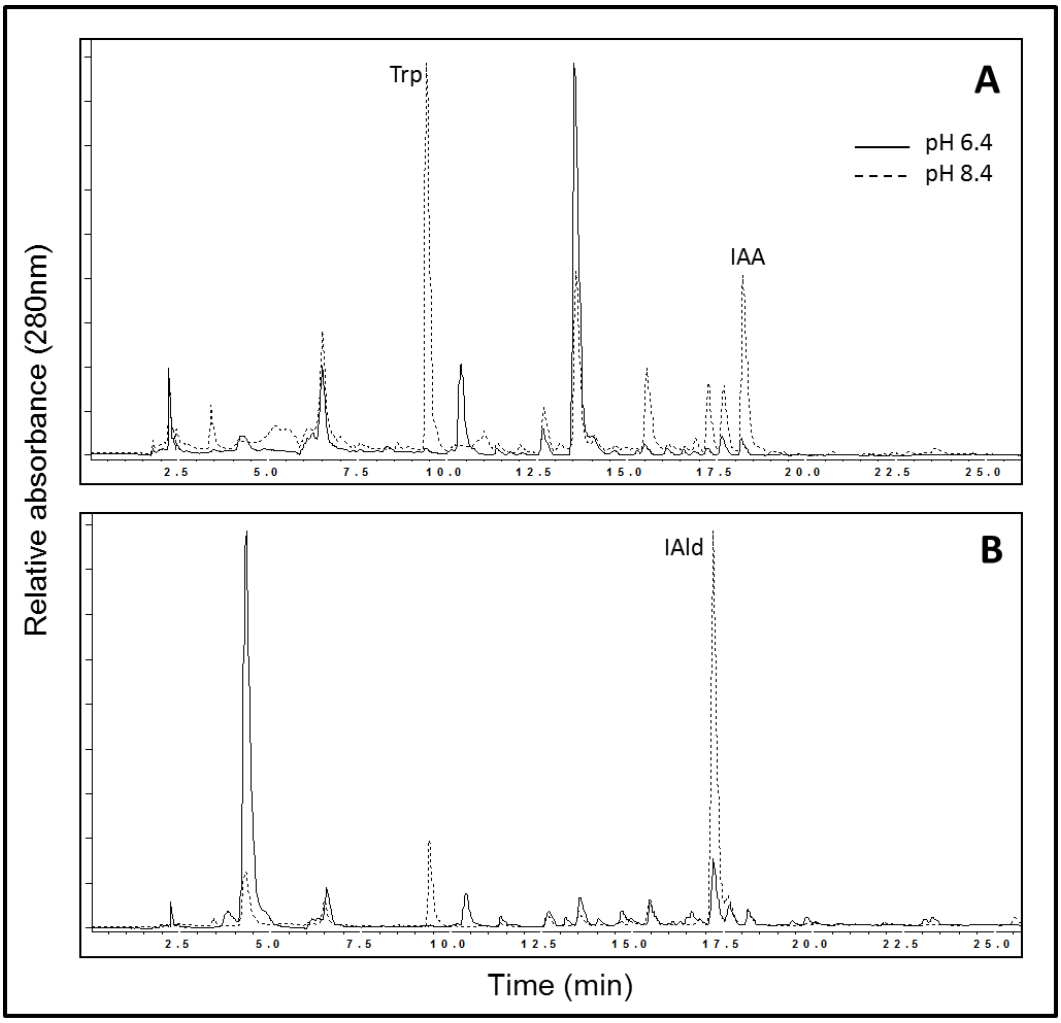

Fig. 36. Metabolic profiling of indolic fractions from aniline exposed cultures of *R.benzoatilyticus* JA2 at different pH.

HPLC chromatogram of acidic fractions showing trp and IAA (**A**) and neutral fractions showing IAld (**B**).

Experimental conditions were same as described under Fig. 35 except, for after 48 h aniline exposure, cell were harvested and of the culture supernatant was fractionated, analysed by HPLC.

Solid line chromatograms indicate indolic fractions from culture pH of 6.4 and dotted line from culture pH of 8.4. Trp, tryptophan; IAA, indole-3-acetic acid; IAld, indole-3-aldehyde.

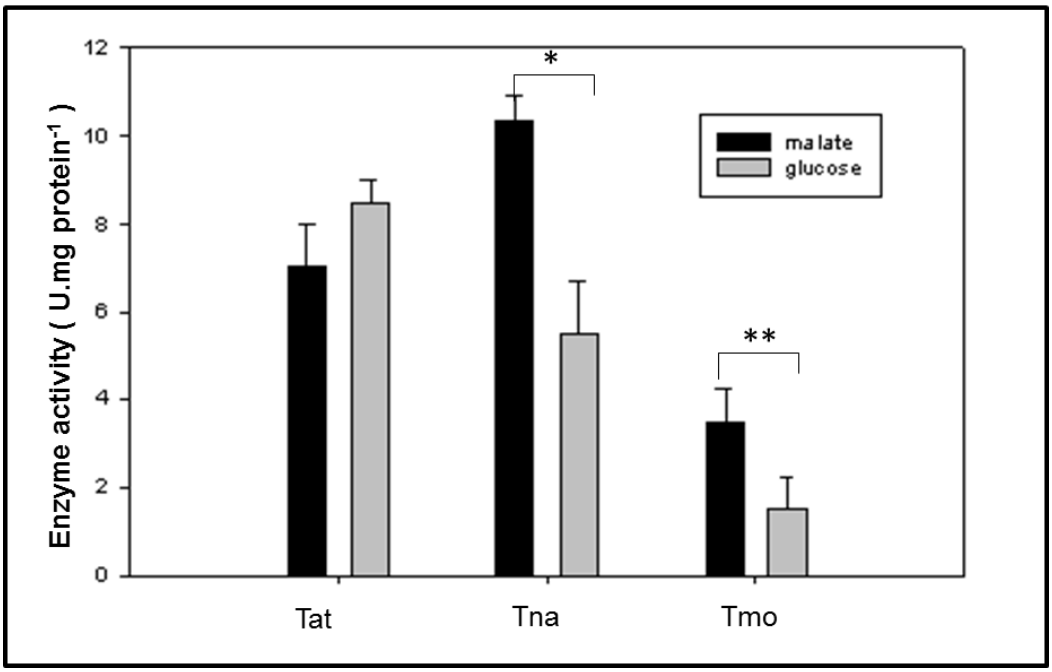

Fig. 37. Tryptophan catabolizing enzyme activities in *R.benzoatilyticus* JA2.

Experimental conditions were same as described under Fig. 33 except, for the culture after 48 h of exposure to aniline was harvested and cell free extract was prepared for enzyme analysis. Enzyme assay conditions were similar as described under Fig.27.

Data represents mean ± standard deviation of three independent experiments and * $p < 0.05$; **, $p < 0.007$. Tat, tryptophan aminotransferase; Tna, tryptophanase; Tmo, tryptophan 2-monooxygenase.

3.2 Metabolomic and proteomic responses of *R. benzoatilyticus* JA2 to aniline stress

3.2.1 Metabolomic responses of *R. benzoatilyticus* JA2 to aniline stress

3.2.1.1 *Growth and aniline tolerance of Rubrivivax benzoatilyticus* JA2

Photoheterotrophic growth of *R. benzoatilyticus* JA2 on aniline as sole sources of carbon and nitrogen or as carbon or nitrogen source could not be demonstrated. Doubling time of aniline exposed culture was 10.8 h, and 5 and 10 mM of aniline has not influenced the doubling time, while at 15 and 20 mM doubling time was 18 h, 27 h respectively (Fig. 38A). Minimum inhibitory concentration (MIC) of aniline was 30 mM and IC50 was 22.5 mM (Fig. 38B) when *R. benzoatilyticus* JA2 was grown photoheterotrophically on malate mineral medium along with aniline.

3.2.1.2 GC-MS based metabolic profiling and metabolite identification

Gas chromatography mass spectrometry (GC-MS) based metabolomics approach was employed to decipher the metabolic responses of *R. benzoatilyticus* JA2 to aniline stress. Intracellular metabolites (endometabolome) of control and aniline exposed cells were extracted, derivatised (silylation; BSTFA+TMCS) and analysed by GC-MS. Metabolites were identified by comparing the mass spectrum of metabolites to national institute of standards and technology (NIST) library, Golm metabolome database (*www.gmd.mpimp-golm.mpg.de*) and by some authentic standards. Relative metabolites concentration was determined by peak area of metabolites. Data was normalised and subjected to multivariate statistical analysis to identify the hidden patterns. Complete experimental scheme was illustrated in Fig. 39**.**

Gas chromatography mass spectrometric analysis of intracellular metabolites from control and aniline exposed cells of *R. benzoatilyticus* JA2 revealed a total of 161 metabolites. Only 61 metabolites were identified based on data base, authentic standards and 100 metabolites remained unknown. Identified metabolites include aliphatic organic acids, amino acids and their derivatives, sugars, nucleotides, fatty acids, amines and aromatic acids. Forty three metabolites were found common in control as well as aniline exposed conditions while 8 metabolites were found only in control and 10 metabolites only in aniline exposed cells (Fig. 40). Sugars, amino acids and their derivatives, fatty acids and TCA cycle intermediates were more differentially detected in control and aniline exposed cells.

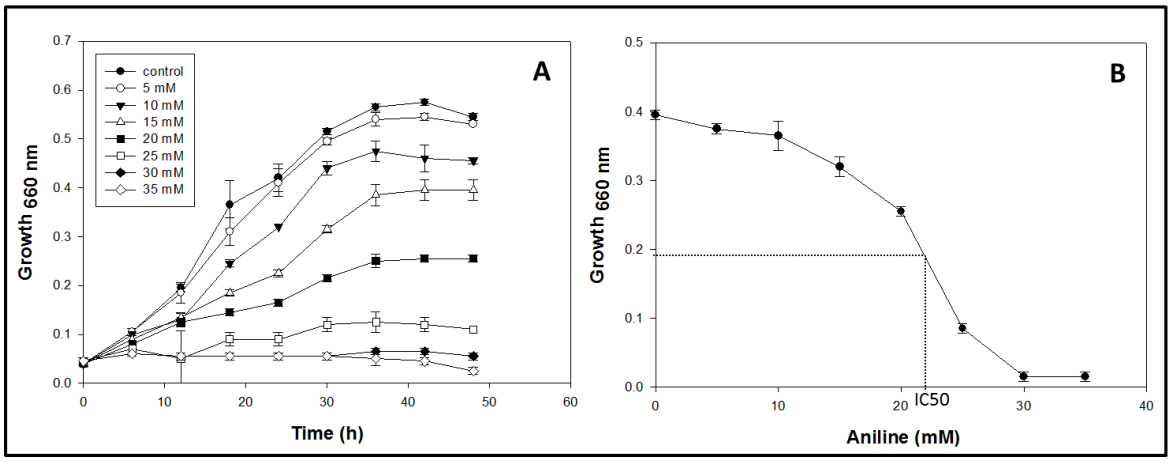

Fig. 38. Effect of aniline on growth of *R. benzoatilyticus* JA2.

Growth in presence of aniline **(A)** and IC50 and MIC of aniline **(B).**

Malate grown mid log phase culture (OD_{660nm} 0.25) of *R. benzoatilyticus* JA2 was used as inoculum (10%) and culture was grown on malate medium supplemented with different concentrations of aniline and incubated for 48 h photoheterotrophically. Growth was measured at 660 nm.

Intersect with dotted line on Y-axis indicate IC50 of aniline. Data represents mean ± standard deviation of three independent experiments done in duplicates. MIC, Minimum inhibitory concentration.

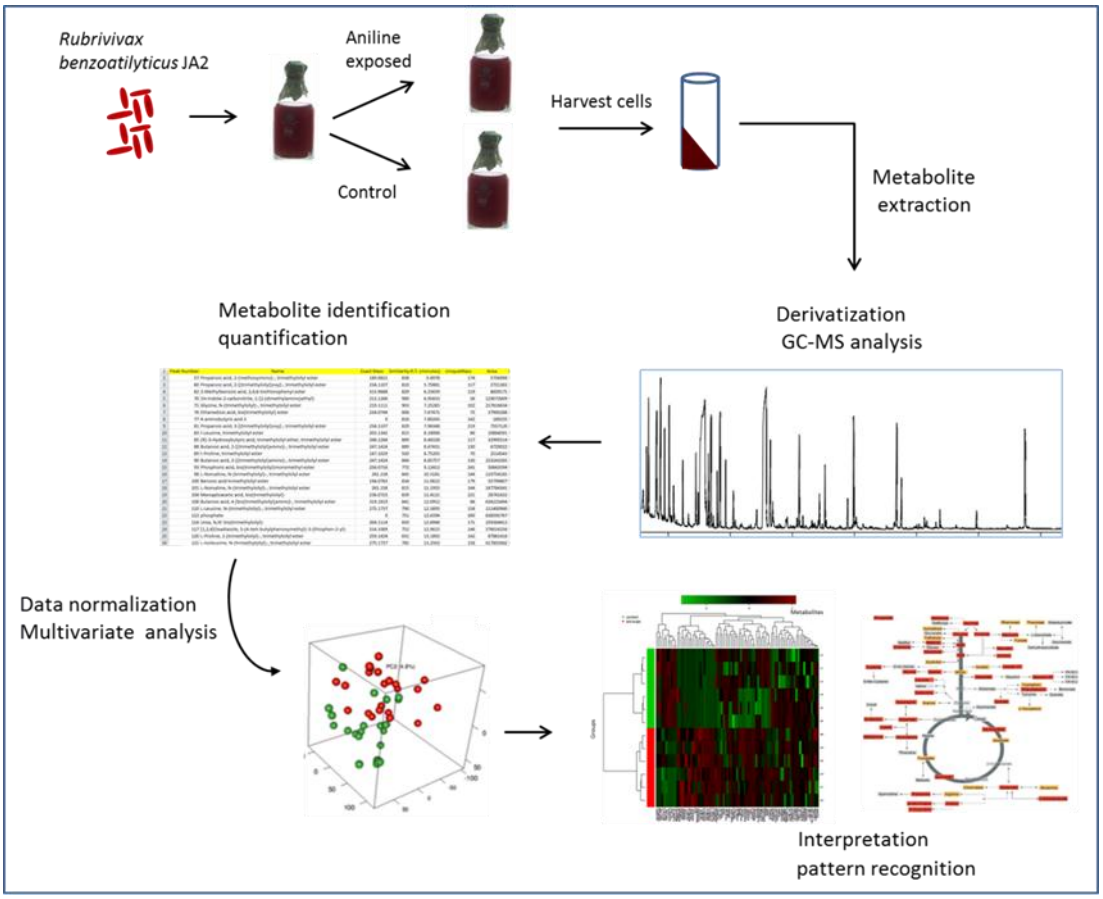

Fig. 39. Schematic representation of GC-MS metabolic profiling of *R. benzoatilyticus* JA2.

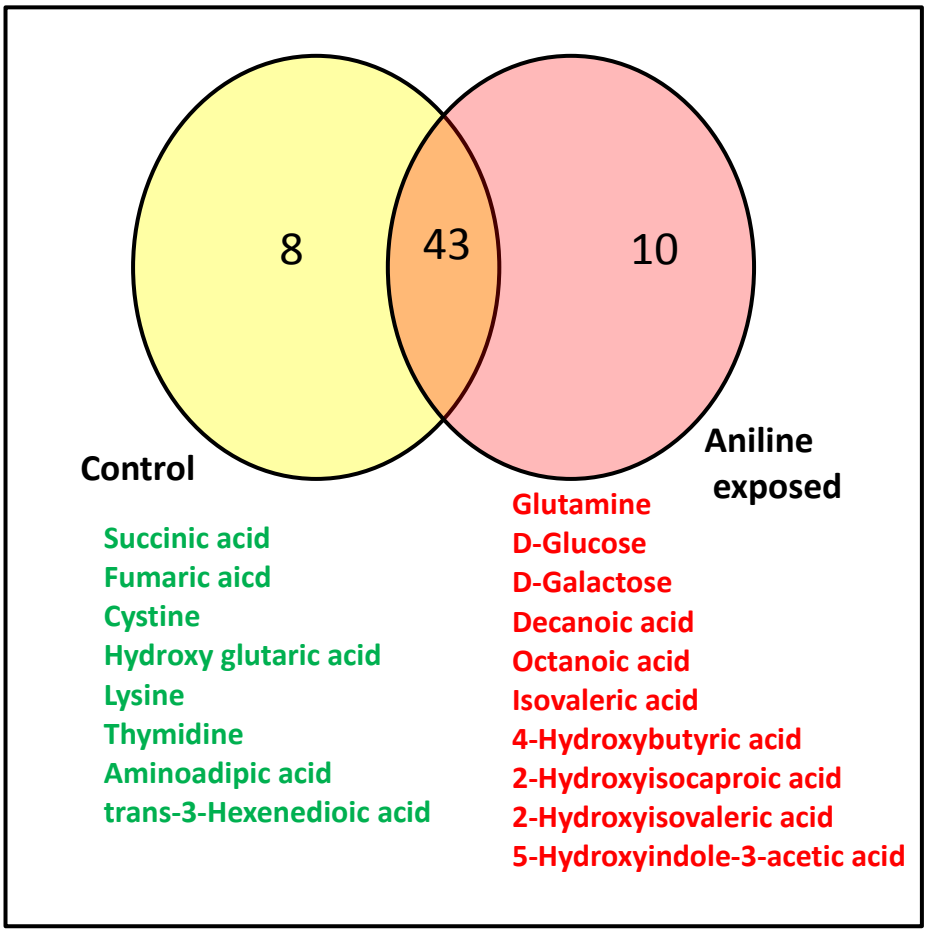

Fig. 40. Venn diagram showing shared, unique metabolites of control and aniline exposed cell of *R. benzoatilyticus* JA2.

Metabolites denoted in green found only in control and red belongs to aniline exposed cells.

Malate grown mid log phase culture (OD_{660nm} 0.25) of *R. benzoatilyticus* JA2 was used as inoculum (10%) and culture was grown on malate medium for 48 h photoheterotrophically then exposed to aniline (25 mM), fumarate (13 mM). After 48 h of growth under photoheterotrophic conditions culture was harvested, lyophilised.

Intracellular metabolites were extracted, derivatized and analysed by GC-MS. Metabolites were identified by comparing the spectra to the NIST library (similarity >750) and Golm metabolome database (http://gmd.mpimp-golm.mpg.de/). Data was normalised by dry weight of the culture and data represents mean of the three independent experiments done in duplicates.

3.2.1.3 Hierarchical cluster analysis (HCA) of metabolites of control and aniline exposed cells

Hierarchical clustering analysis of metabolites from control and aniline exposed cells was performed to identify the response patterns. Groups or metabolites with similar kind of response pattern cluster together in HCA analysis. Control and aniline exposed metabolomes were separated from each other forming two distinct clusters while all aniline exposed metabolomes were clustered together. Similarly, all the control metabolomes were grouped together (Fig. 41). Based on their response patterns metabolites were clustered into five groups. Group I includes metabolites whose concentration was high in control cells, group II includes metabolites whose concentration was high in aniline exposed cells and group IV, V include metabolites 1whose concentration was same in control and aniline exposed cells (Fig. 41). HCA analysis indicated metabolic dissimilarity between control and aniline exposed cells.

3.2.1.4 Principal component analysis (PCA)

Gas chromatography mass spectrometry data was subjected to PCA analysis to identity significant metabolic differences between control and aniline exposed cells. Principal component analysis is an unsupervised, reductive statistical method used in metabolomics to decipher the maximum metabolic variations and it separates samples from each other based on their differences. Samples clustered closely indicate metabolically similar and one stood away indicate metabolic dissimilarity. Five component PCA analyses explained 90% of the variance, 74.1% of variation was explained by principle component1 (PC1) and 10.4% by PC2. Control and aniline exposed samples were clearly separated from each other by PCA analysis (Fig. 42A) indicating metabolic differences in control and aniline exposed cells.

3.2.1.5 Partial least square discrimination analysis (PLS-DA)

Partial least square discrimination analysis was performed to further confirm the metabolic variations and to identify the key metabolic features responsible for metabolic difference. Partial least square discrimination analysis is a supervised statistical method employed for differentiating the groups based on pre-assigned class. In PLS-DA samples from different groups are classified into different class. Control and aniline exposed cells

were clearly separated in three principal components by PLS-DA analysis (Fig. 42B). R^2 value for this model was 0.9 which indicated goodness of fit and Q^2 was 0.85 which indicates goodness of predictability. High values of R^2 and Q^2 indicate that this model is representative of true differences in metabolomes.

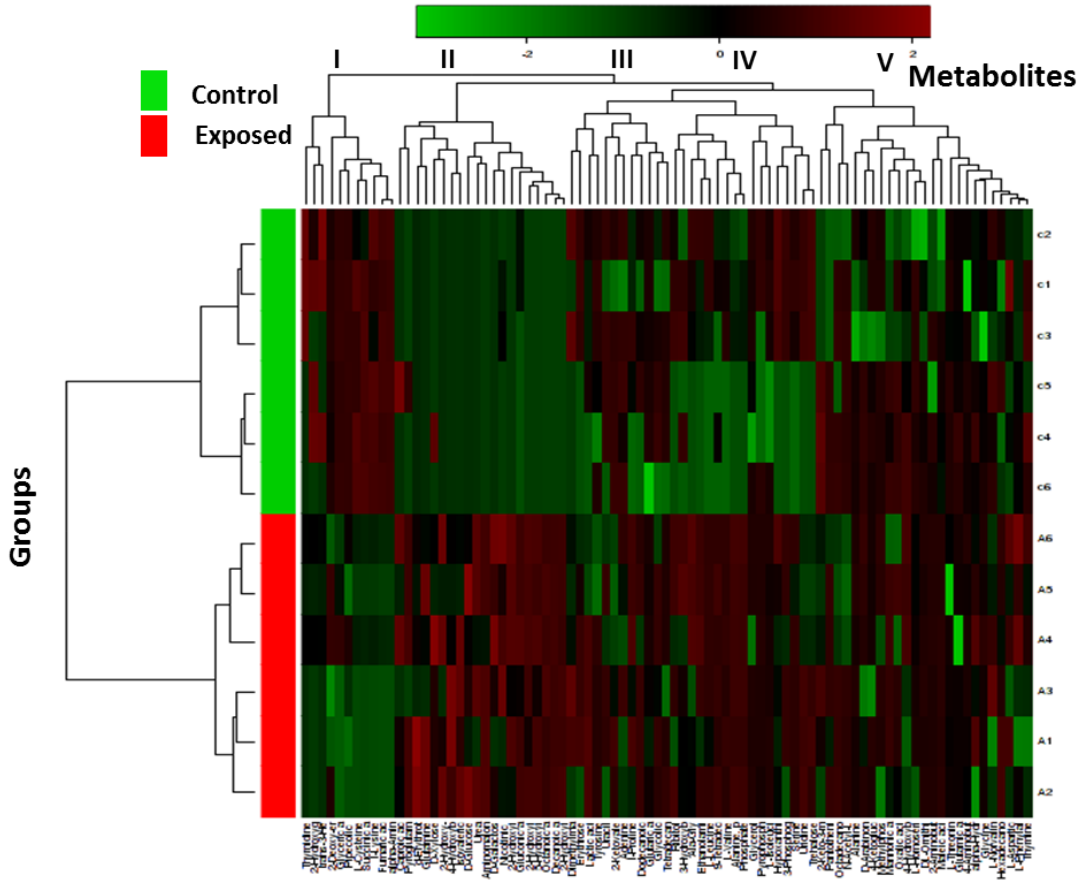

Fig. 41. Hierarchical clustering analysis of metabolites associated with control and aniline exposed cultures.

C1-C6 indicates control and A1-A6 aniline exposed cultures. Clustering was performed using Pearson correlation as the distance matrix by MetaboAnalyst (www.metaboanalyst.ca/MetaboAnalyst/faces/Home.jsp). Metabolites in red indicate high concentration and green as low concentration.

Data obtained from GC-MS analysis as described under Fig. 40 was used for HCA analysis. Data was normalised by dry weight of the culture, statistical normalization was done by quantile approach and data was log transformed (log_2) by using Metaboanalyst. Data represents mean of the three independent experiments done in duplicates.

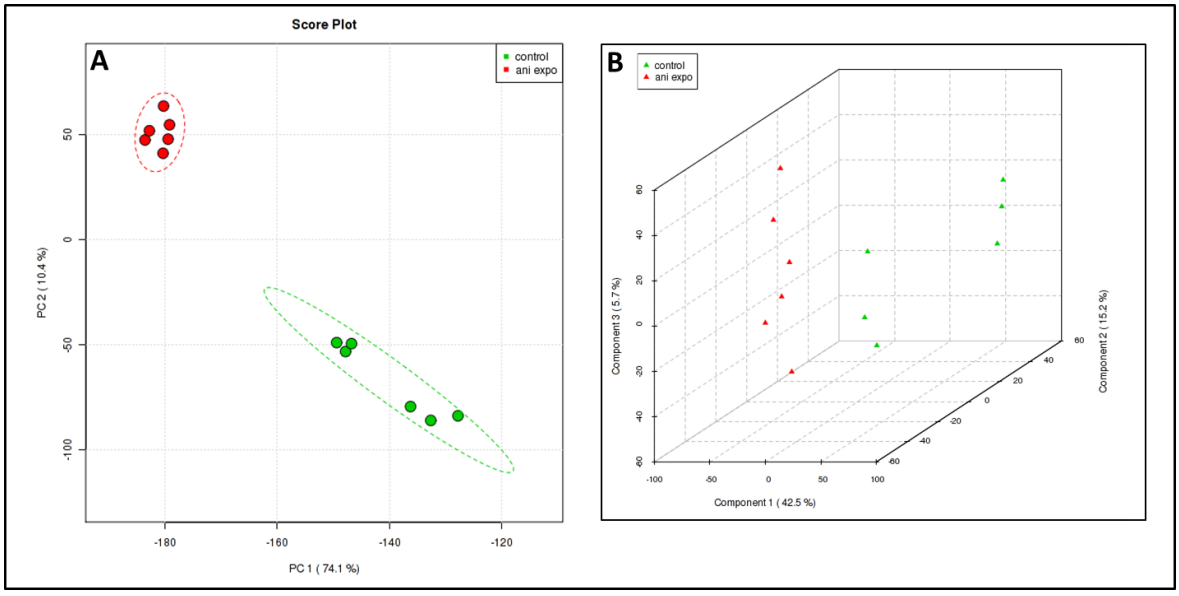

Fig. 42. Principal component analysis (PCA) (A) partial least square discriminant (PLS-DA) (B) scatter plot analysis of control and aniline exposed cultures of *R. benzoatilyticus* JA2.

Normalised data obtained from GC-MS analysis as described under Fig. 41 was subjected to PCA, PLS-DA analysis using MetaboAnalyst.

3.2.1.6 Important metabolic features identification

Variables importance on projection (VIP) score was obtained from PLS-DA model and VIP scores were used to identify key metabolic features significant for group separation. Metabolites with VIP score >1 was considered to have a statistically significant contribution to the model. Thirty metabolites were identified as significant (VIP >1) from VIP score plot along with their relative concentrations in control and aniline exposed cells (Fig. 43). Fatty acids, TCA cycle intermediates, carbohydrates, amino acid and their derivatives were largely responsible for group separation in model. Pipecolic acid, cysteine, lysine, glyceric acid, succinic acid, fumaric acid and aminoadipic acid concentrations were high in control compared to aniline exposed cells. Glucose, galactose, gluconic acid, octanoic acid, decanoic acid, 5-hydroxyindole-3-acetic acid, phosphate, glutamine, ethanolamine, 4-hydroxybutyrate and serine concentrations were high in aniline exposed cells compared to control (Fig. 43).

3.2.1.7 Relative fold change of metabolites in aniline exposed cells

Statistical analysis was performed to identify metabolites that are significantly regulated in aniline exposed cells of *R. benzoatilyticus* JA2. Metabolite was considered statistically significant if fold change (aniline exposed/control) was greater than 2 and *p* value less than 0.05. Thirty one metabolites were identified whose response was altered significantly by aniline stress. Relative concentration of 21 metabolites was high in aniline exposed cells while 10 metabolites concentration was low compared to that of control (Fig. 44). Relative metabolite fold changes were significantly high for carbohydrates, fatty acids, amino acids and their derivatives and organic acids of aniline exposed cells. D-xylose, glucose, gluconic acid, galactose levels were increased in aniline exposed cells compared to control (Fig. 44). Decanoic acid, octanoic acid 9-tertradecenoic acid concentrations were high while hexenedioic acid concentration was low in aniline exposed cells. 4-hydroxybutyric acid, 5- hydroxyindole-3-acetic acid, glutamine, valine, phosphate and urea levels increased in aniline exposed cells (Fig. 44). Succcinic acid, fumaric acid, lysine, thymidine, cysteine concentrations decreased upon aniline exposure.

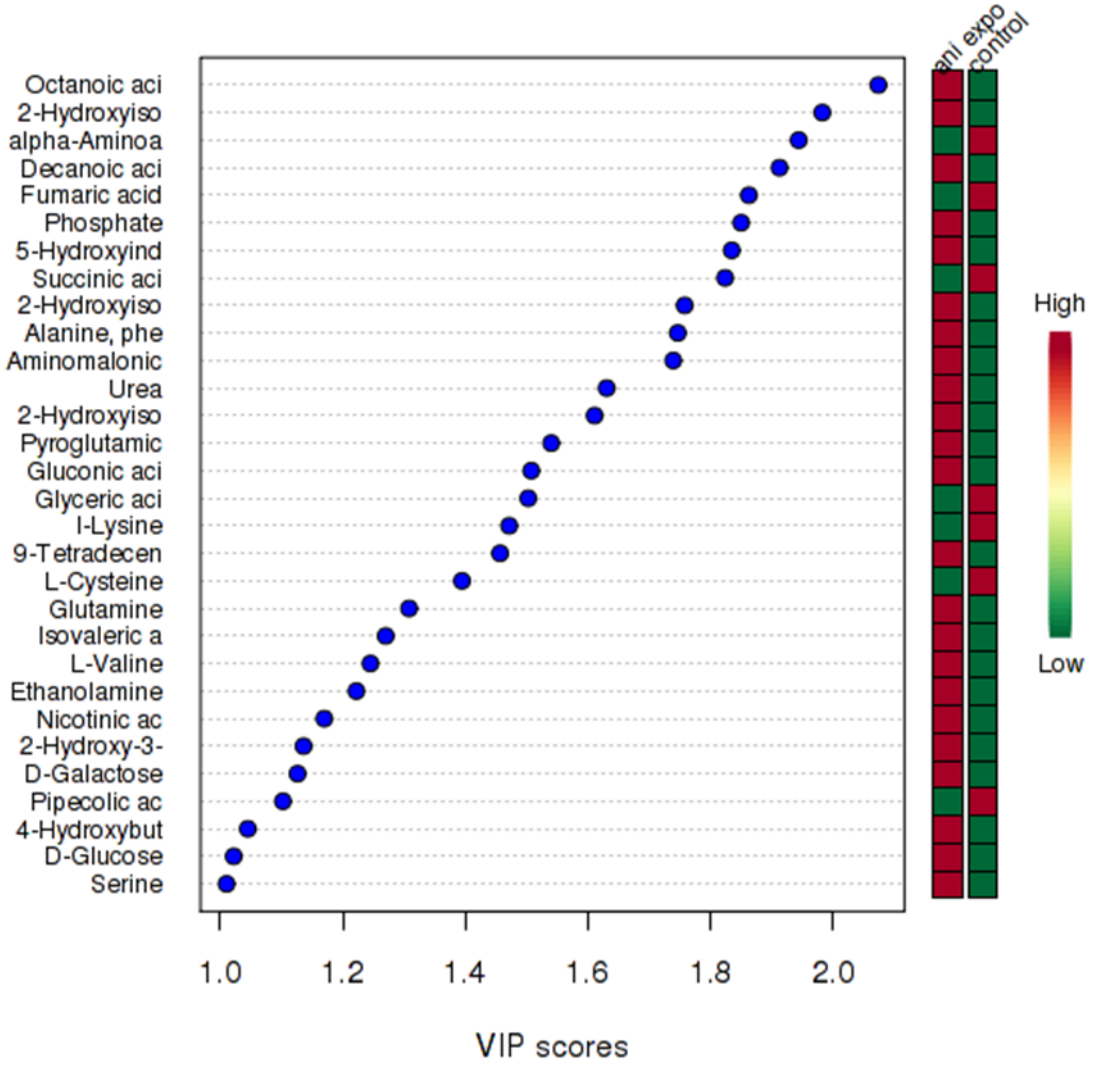

Fig. 43. Variable importance on projection (VIP) scores of the metabolites obtained from PLS-DA analysis of control and aniline exposed cultures.

Coloured boxes on right side indicate relative abundance of metabolites between control and treated conditions. Metabolites with VIP > 1.0 was considered to be of significant.

Data processing parameters were same as described under Fig. 42 and the same data was subjected to VIP analysis by using MetaboAnalyst.

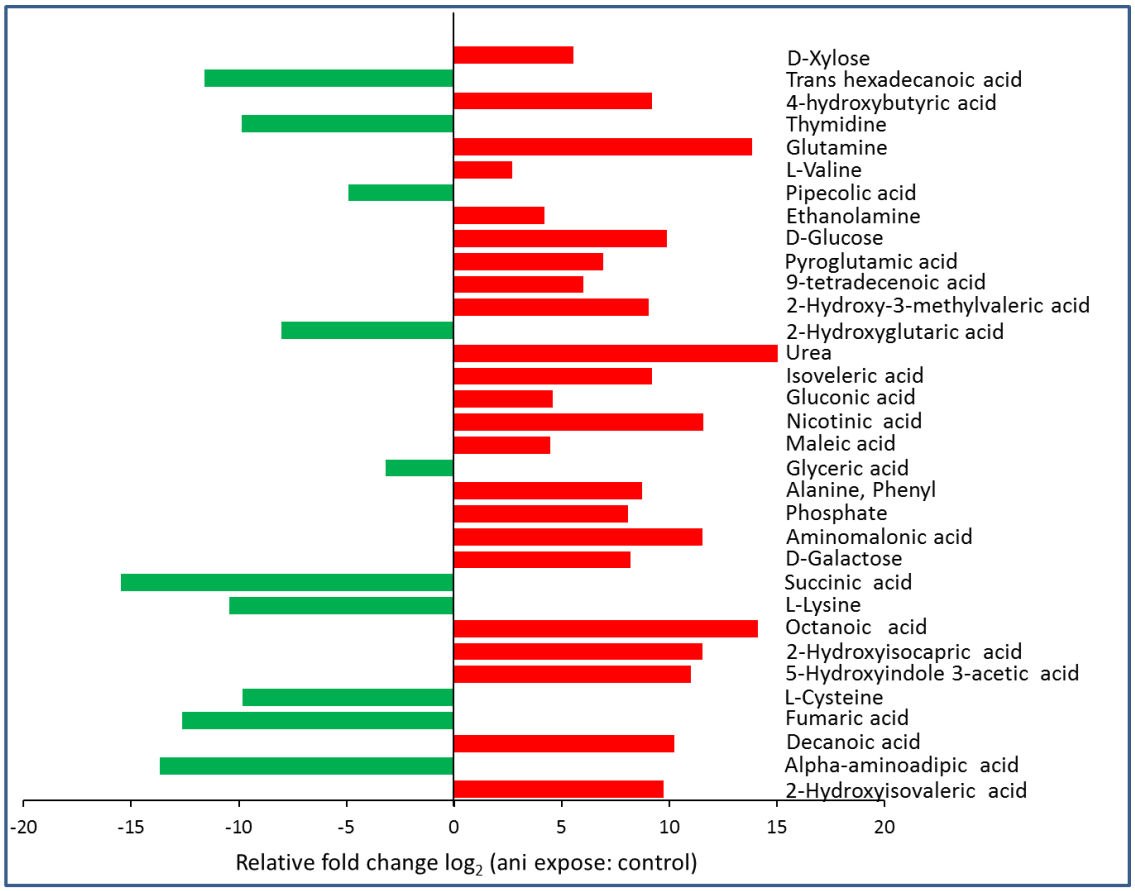

Fig. 44. Relative fold change of metabolites from aniline exposed cultures of *R. benzoatilyticus* JA2.

Metabolites with significant fold change (aniline/control) > 2.0 and *p*-value <0.05 were considered for data analysis. Relative fold change correspond to peak area of the metabolites of aniline exposed/control cultures. Fold change analysis was performed by using MetaboAnalyst.

Data obtained from GC-MS analysis as described under Fig. 40 was $\log_2$ transformed and subjected to Student's *t*-test by using Metaboanalyst.

3.2.1.8 Functional annotation of differentially regulated metabolites

Differentially regulated metabolites (with significant fold change) were annotated to their respective metabolic pathways according to KEGG database (*www.genome.jp/kegg*) to identify metabolic pathways affected by aniline stress. Amino acid metabolism was highly (29%) affected by aniline stress followed by carbohydrate metabolism (14%) and fatty acid metabolism (12%). Butanoate (6%), nucleic acid (6%), nitrogen (6%) tricarboxylic acid cycle (6%) and vitamins-cofactors metabolisms were also affected by aniline stress (Fig. 45). Tryptophan metabolism, secondary metabolites biosynthesis (6%) lipid (3%) and glutathione (3%) metabolisms were among the metabolic pathways influenced by aniline stress in *R. benzoatilyticus* JA2 (Fig. 45).

3.2.1.9 Effect of aniline on fatty acid composition of *R. benzoatilyticus* JA2

Fatty acid composition analysis of aniline exposed and unexposed (control) cell was done to monitor any apparent change in fatty acid content due to aniline stress. $C_{16:0}$ (30-35 mol%) and $C_{16:1}$ (31-41 mol%) were two major fatty acids identified in aniline exposed as well as unexposed cultures of *R. benzoatilyticus* JA2 along with other minor fatty acids (Table. 4). Total saturated fatty acid content was increased (65.4%) in aniline exposed cultures compared to control (52.6%) and total unsaturated fatty acids decreased in aniline exposed cultures (34.6%) compared to unexposed (46.9%). Saturated to unsaturated fatty acid ratio increased from 1.12 to 1.9 in aniline exposed cells compared to those unexposed (Table. 4). 3-Hydroxydecanoic acid ($C_{10:0}$3OH) content was also high in aniline exposed cells compared to control. High saturated fatty acids content in aniline exposed cultures indicate decreased membrane fluidity and rigidification of membrane.

3.2.1.10 Polyhydroxyalkanoates accumulation in *R. benzoatilyticus* JA2

Polyhydroxyalkanoates (PHAs) accumulation in aniline exposed cells was observed by staining with Nile red, a lipophilic fluorophore followed by confocal laser microscopy. Zero to one PHA granule (intensive red spots) in unexposed (Fig. 46A, B) and one to three PHA granules in aniline exposed cells were observed by Nile red staining (Fig. 46C, D). PHAs content was significantly high (72.1 µg.mg dry wt^{-1}) in aniline exposed cells compared to unexposed (16.6 µg.mg dry wt^{-1}).

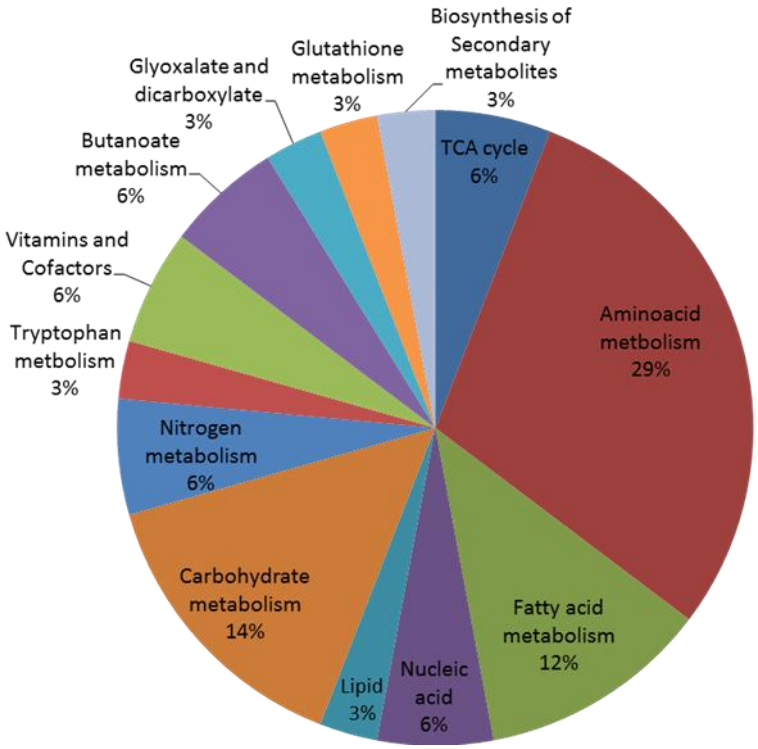

Fig. 45. Functional classification of differential regulated metabolites of aniline exposed cultures of *R. benzoatilyticus* JA2.

Metabolites with fold change (aniline/control) >2.0 and *p*-value ($p < 0.05$) were considered for analysis. Functional classification was done according to KEGG database (http://www.genome.jp/kegg/pathway.html.)

Metabolites identified as significant by fold change analysis described under Fig. 44 were used for functional classification according to KEGG.

Table.4. Whole cell fatty acid composition of *R. benzoatilyticus* JA2

Fatty acid	mol%		
	Control (No solvent)	Aniline treated	*p*-value
$C_{10:0}$	0.5 ± 0.2	1.2 ± 0.3	0.30
$C_{10:0}$ 3OH	7.8 ± 0.5	10.2 ± 0.2	0.09
$C_{12:0}$	7.6 ± 0.4	10.4 ± 0.4	0.07
$C_{14:0}$	4.0 ± 0.1	6.5 ± 0.1	0.12
$C_{16:0}$	30.7 ± 1.0	35.7 ± 0.4	0.03
$C_{16:1}\omega7c/\ \omega6c$	41.6 ± 0.3	31.0 ± 1.0	0.02
$C_{18:1}\omega7c$	4.8 ± 0.2	2.2 ± 0.4	0.05
Total	100	100	
Sat/Unsat	1.12	1.90	

Malate grown mid log phase culture (OD_{660nm} 0.25) of *R. benzoatilyticus* JA2 was used as inoculum (10%) and culture was grown on malate medium for 48 h photoheterotrophically then exposed to aniline (25 mM), fumarate (13 mM), after 48 h of growth under photoheterotrophic conditions culture was harvested, lyophilised and analysed by gas chromatography.

Data represents mean ± standard deviation of three independent experiments. *p*-value was obtained from Student's *t*-test. Sat, saturated; Unsat, unsaturated.

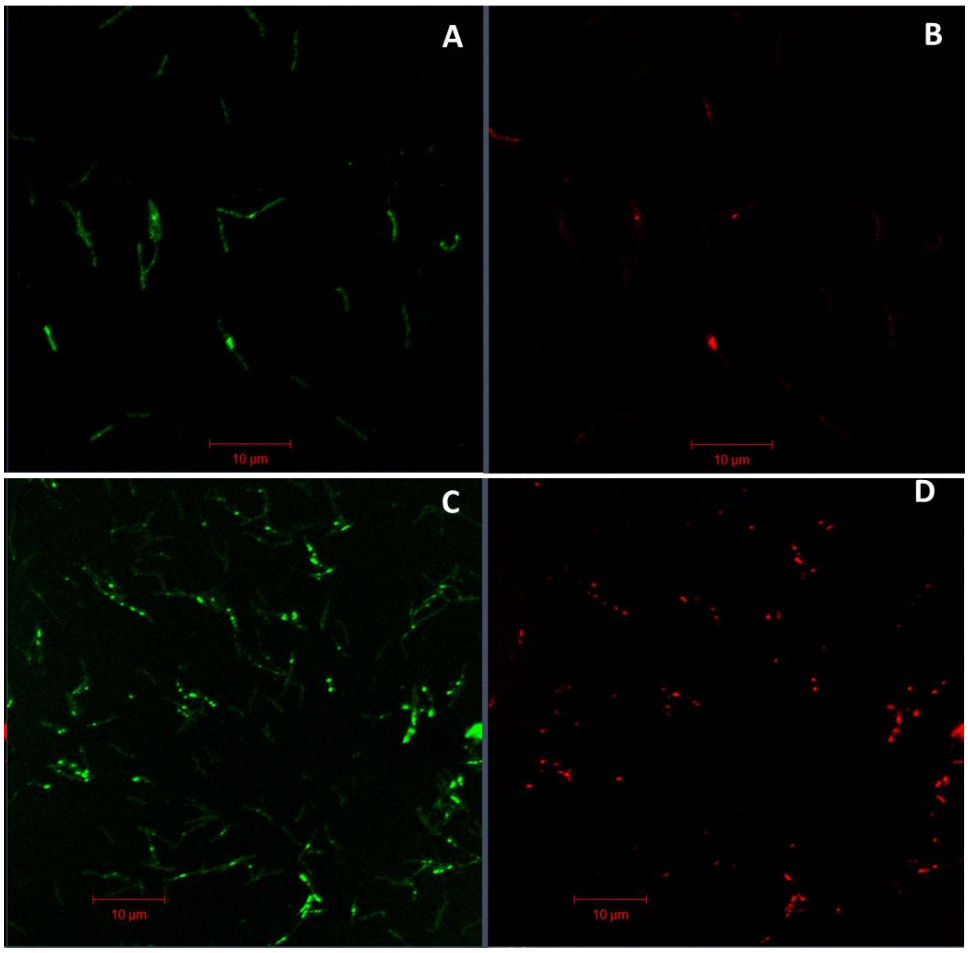

Fig. 46. Confocal laser scanning microscopic studies of PHA accumulation by *R. benzoatilyticus* JA2.

Confocal micrographs of control cells stained with FDA **(A)**, Nile red **(B)** aniline exposed cells stained with FDA **(C)** and Nile red **(D)**. Darkly stained red colour bodies indicate PHA

Malate grown mid log phase culture (OD_{660nm} 0.25) of *R. benzoatilyticus* JA2 was used as inoculum (10%) and culture was grown on malate medium for 48 h photoheterotrophically then exposed to aniline (25 mM), fumarate (13 mM), after 48 h of growth under photoheterotrophic conditions, cells were stained with respective dyes and analysed. FDA, Fluorescene diacetate; PHA, Polyhydroxyalkanoates.

3.2.1.11 Identification of PHAs of the *R. benzoatilyticus* JA2

Analysis of the PHAs by ^{13}C and ^{1}H NMR revealed characteristic chemical shift signals of -C=O-, -CH-, -CH_2 and -CH_3 corresponds to different types of carbon atoms present in PHAs (Fig. 47A, B). FTIR analysis revealed band at 1452 cm^{-1}corresponds to the asymmetrical deformation of the C–H bond in -CH_2 groups, band at 1379 cm^{-1} is of -CH3 groups. The band at 1725 cm^{-1} correspond to stretching of the -C=O- bond and a series of bands located at 1000–1300 cm^{-1} correspond to the stretching of the -C–O- bond of the ester group (Fig. 47C). Based on NMR and FTIR analysis PHAs produced by *R. benzoatilyticus* JA2 were identified as polyhydroxybutyrates (PHBs) and all the spectra were well in accordance with standard PHBs (Oliveira *et al*., 2007).

3.2.1.12 Extracellular polymeric substance (EPS) production

Extracellular polymeric substance (EPS) formation was observed in aniline exposed cells while no such formation was observed in unexposed cells by scanning electron microscopic analysis (Fig. 48A, B). Aniline exposed culture was viscous and often formed aggregates. These aggregates were stained with fluorescent dyes and analyzed by CLSM to detect EPS components and their distribution. Nucleic acids, proteins, lipids and β-polysaccharides were detected in aggregates by staining with fluorescent dyes (Fig. 49B-E). Polysaccharides, proteins were distributed evenly in aggregates while lipids distribution was uneven. Extracellular polymeric substance formation and its distribution in aggregates of *R. benzoatilyticus* JA2 was confirmed by SEM and CLSM analysis.

3.2.1.12b Characterization of extracellular polymeric substance

Purified EPS was analysed by ^{13}C solid state NMR and FTIR to identify the major structural components of EPS. Solid state NMR analysis revealed characteristic chemical shift signals of lipids and aliphatic acids (0-45 ppm), proteins (45-65 and 160-200 ppm), carbohydrates (65-110 ppm), and nucleic acids (110-160 ppm) (Fig. 50A) (Metzger *et al*., 2009). Glycosidic bond resonance (95-106 ppm) observed in NMR spectrum corresponds to α and β linkage of monomers in EPS (Jiao *et al*., 2010). Bands at 1000-1200 cm^{-1} in FTIR spectrum corresponds to (–COC–) group vibration in the cyclic structures of carbohydrates, sharp bands at 1245-1270 cm^{-1} corresponds to phosphate group in nucleic acids. Intense bands at 1530-1670 cm^{-1} correspond to amide I (–CO–) and amide II (–NH –) in proteins and minor band at 2930-2970 cm^{-1} were of symmetric, asymmetric vibrations of –CH– in lipids (Fig. 50B) (Sheng *et al*., 2006).

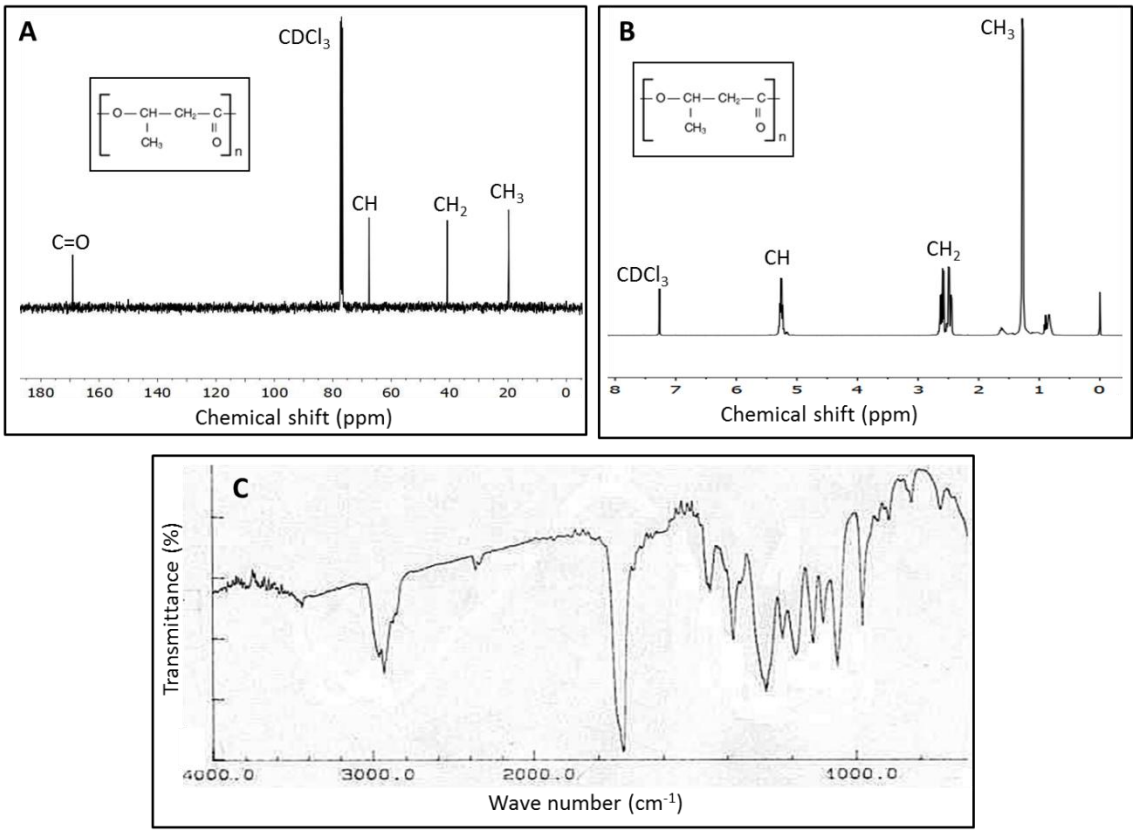

Fig. 47. Polychem analysis of polyhydroxyalkanoates of *R. benzoatilyticus* JA2.

^{13}C NMR spectrum **(A)** ^{1}H NMR spectrum **(B)** and IR spectrum(**C**) of polyhydroxyalkanoates produced by aniline exposed culture of *R. benzoatilyticus* JA2. Insert polyhydroxybutyrate structure.

Experimental conditions were similar as described under Fig. 46, except after 48 h of growth culture was harvested and PHA were purified and analysed. PHA, polyhydroxyalkanoates.

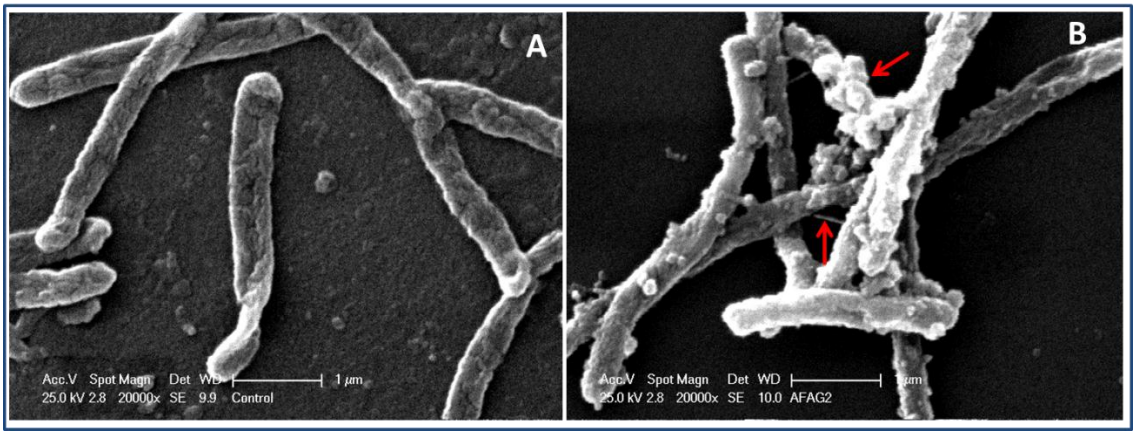

Fig. 48. Scanning electron micrograph of control cell (A) and EPS producing cells (B) of *R. benzoatilyticus* JA2.

Experimental conditions were similar as described under Fig. 46, except for cells were harvested and fixed for scanning electron microscopy. EPS, extracellular polymeric substances. Arrows indicate different forms of EPS.

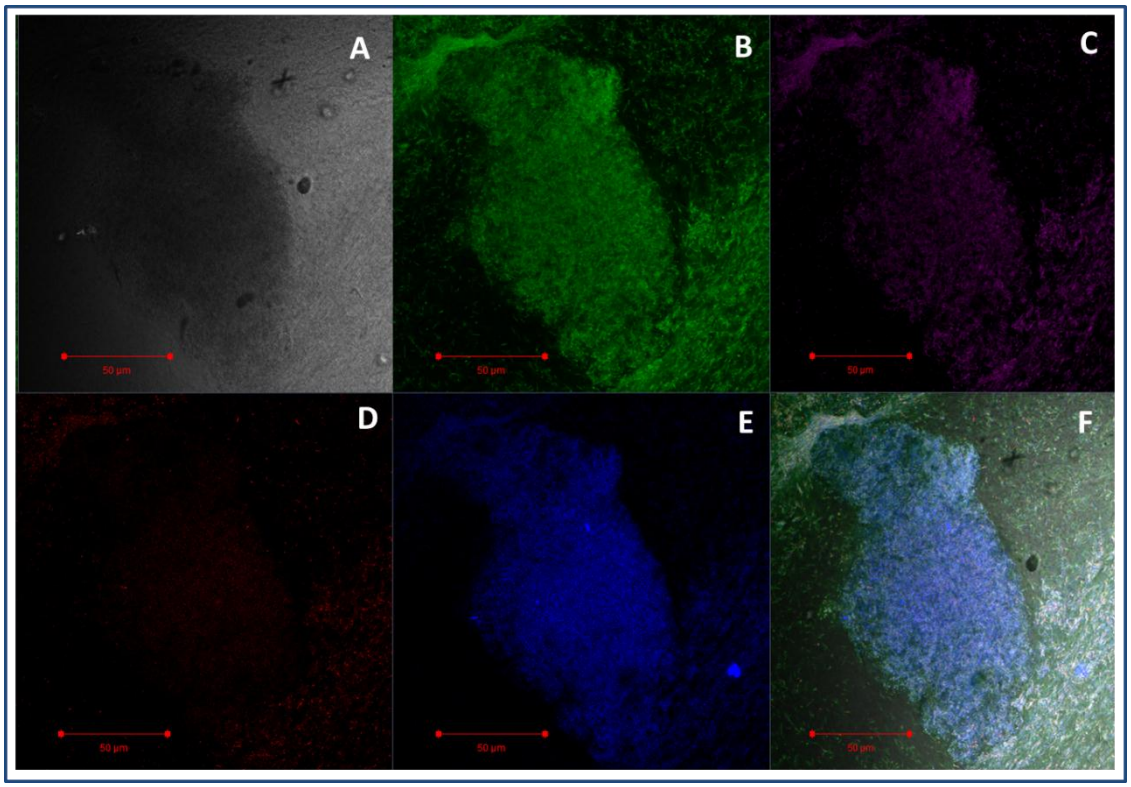

Fig. 49. Confocal laser scanning microscopic analysis of the cell aggregates of *R. benzoatilyticus* JA2.

Confocal image of aggregate (A), aggregate stained with SYTOX green (B), TRITC (C), Nile red (D), calcofluor white (E) and merged image (F).

Experimental conditions were same as described under Fig. 46, except for the aggregates were removed and stained with SYTOX green for nucleic acids, TRITC (Tetramethyl Rhodamine Isothiocyanate) for amines (proteins), nile red for lipids and calcofluor white for polysaccharides and analysed.

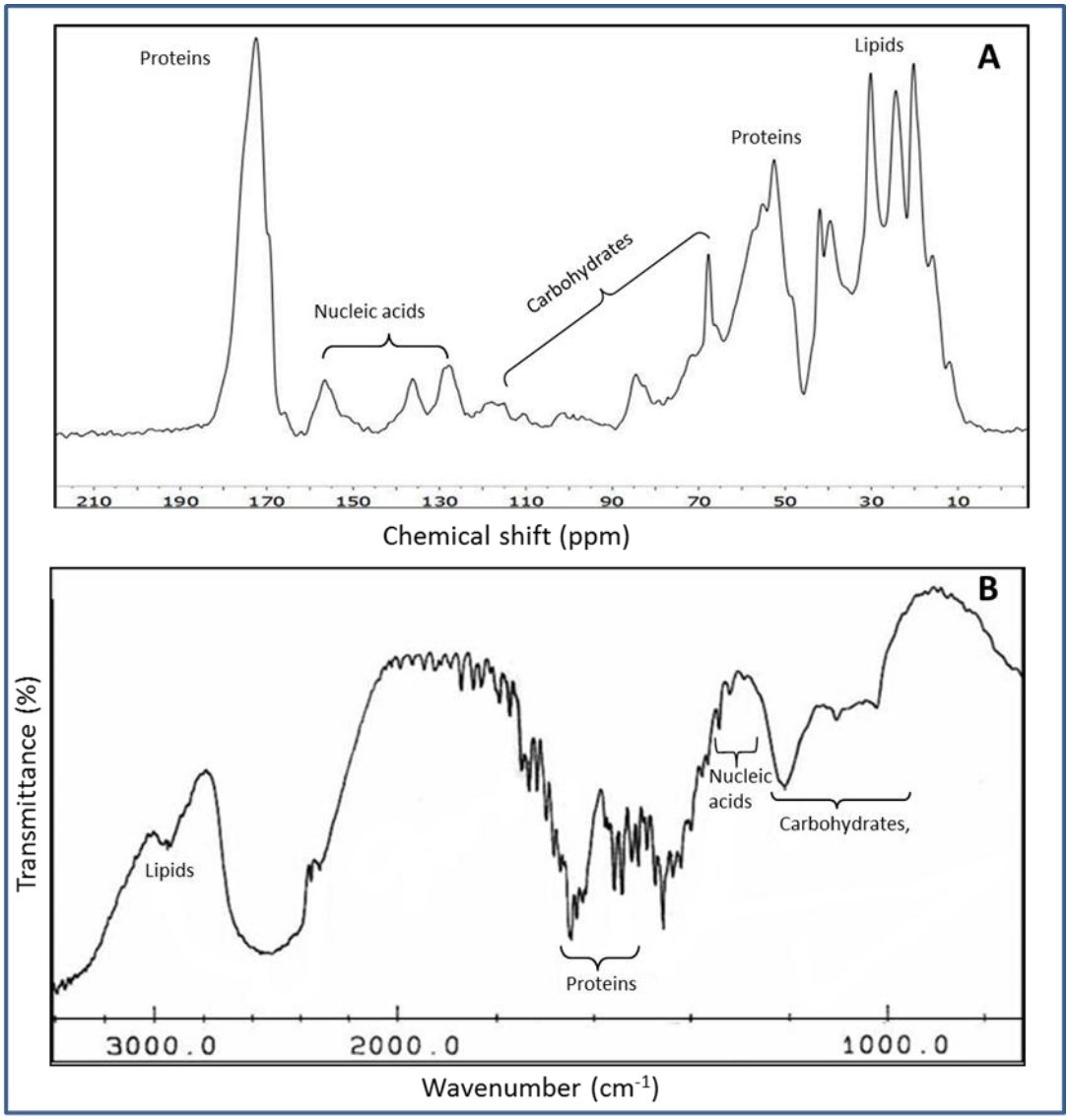

Fig. 50. 13-C Solid state NMR spectrum (A) and IR spectrum (B) of the purified EPS.

Experimental conditions were similar as described under Fig. 46, except for after 48 h cells were harvested and EPS was isolated and analysed.

NMR and FTIR analysis suggest that carbohydrates, proteins, nucleic acids and lipids as structural components of EPS and it has α, β linkage of polysaccharides.

Purified EPS was analysed by energy dispersive X-ray spectroscopic (EDAX) for its organic and inorganic constituents. EPS had more organic content (93%) than inorganic (7%) and carbon being the highest (65%) followed by oxygen (19%) and nitrogen (9%). Phosphate content was high (4%) and potassium, calcium, magnesium were low (<1%) (Fig. 51A). Macromolecular composition of EPS has carbohydrates as major component (545 µg.mg EPS dry wt^{-1}) followed by proteins (290 µg. mg EPS dry wt^{-1}.), others (100 µg. mg EPS dry wt^{-1} humic substance, lipids, organic acids) and DNA (64 µg. mg EPS dry wt^{-1}) (Fig. 51B).These results indicate that EPS to be heterogeneous polymer of carbohydrates, proteins, nucleic acids and lipids.

Nine fatty acids were detected by fatty acid methyl esters (FAME) analysis of purified EPS and 3-Hydroxydecanoic acid ($C_{10:0}$3OH), dodecanoic acid ($C_{12:0}$) content was high (35 and 28.9 mol%) (Table. 5). EPS consisted of more short chain fatty acids (70 mol%) and cells consisted of more long chain fatty acids (75 mol%). 3-Hydroxydecanoic acid, dodecanoic acid content was high and hexadecanoic acid ($C_{16:0}$), hexadecenoic ($C_{16:1}$) content was low in EPS compared to membrane fatty acids (Table. 5).

3.2.1.12c GC-MS metabolic profiling of EPS

Purified EPS was hydrolysed, derivatized, and analysed by GC-MS, metabolites were identified by comparing the mass spectra to NIST library (similarity >750) and by some standards. Eight sugar monomers, ninteen amino acids and their derivatives, five nucleotides, five fatty acid and two organic acids were detected by GCMS analysis (Table. 6). Polysaccharide of EPS consisted of glucosamine (30 mol%), ketogluconic acid (30 mol%), glucose (23 mol%), rhamnose (7 mol%), methyl glucose (7 mol%) and trace amounts (<2 mol%) of mannonic acid and arabinose as monomers (Fig. 52). Extracellular polymeric substance of *R. benzoatilyticus* JA2 consists of heteropolysaccharide as indicated by GC-MS analysis. Detection of sugars, amino acids, nucleotides and fatty acids by NMR, FTIR, GC-MS confirms the presence of polysaccharides, proteins, nucleic acids and fatty acids as components of EPS.

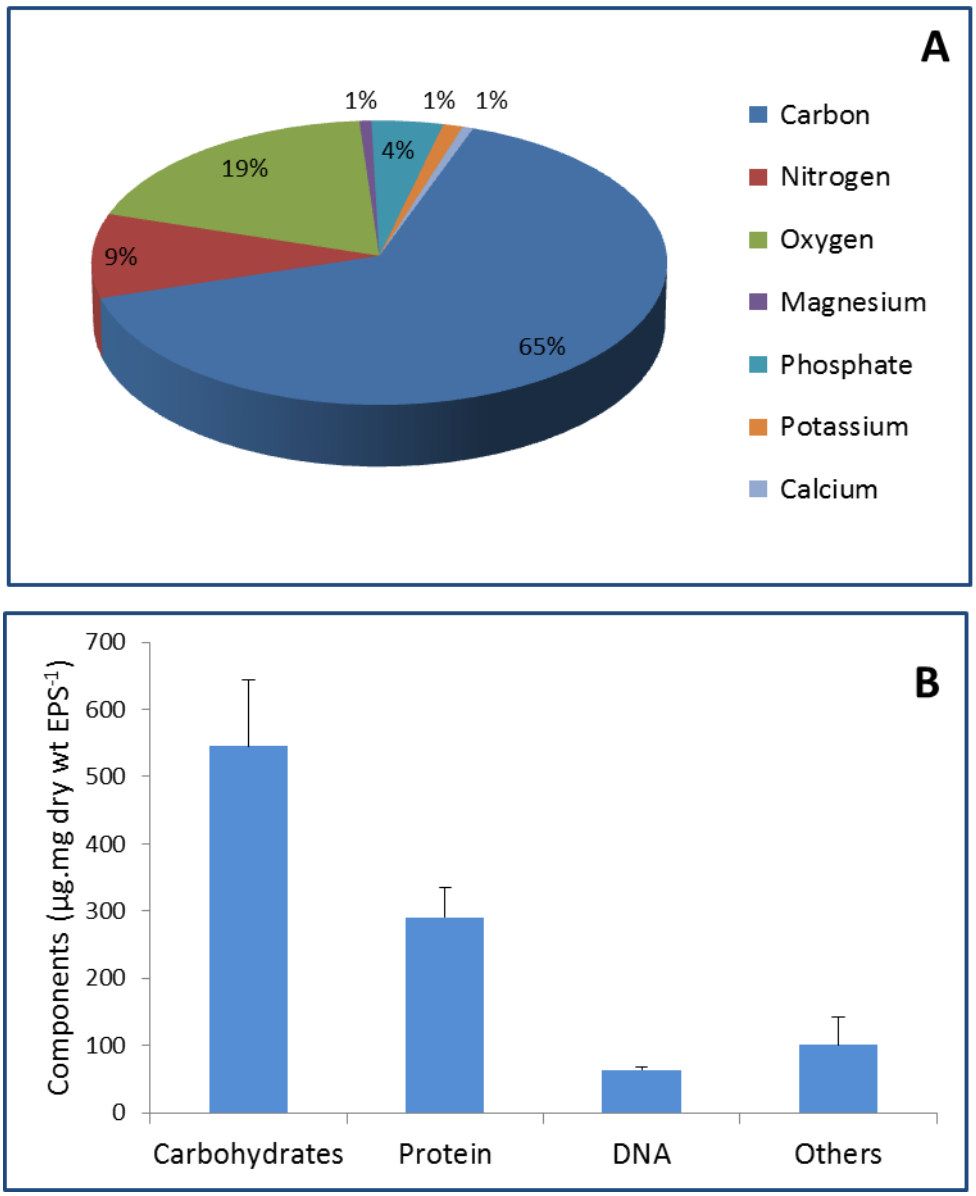

Fig. 51. Macromolecular composition of extracellular polymeric substances of *R. benzoatilyticus* JA2.

Energy dispersive X-ray analysis of EPS (**A**) and quantification of protein, carbohydrate, DNA, and others **(B).** EPS, extracellular polymeric substances.

Experimental conditions were similar as described under Fig. 46, except for after 48 h cells were harvested and EPS was isolated and analysed. Data represents mean ± standard deviation of three independent experiments.

Table. 5. Fatty acid composition of extracellular polymeric substances

Fatty acid	mol%	
	Anilne treated cells	EPS
$C_{10:0}$	1.0 ± 0.8	5.6 ± 2.2
$C_{10:0}$3OH	9.6 ± 2.5	35.0 ± 8.5
$C_{11:0}$	Nd	0.5 ± 0.1
$C_{12:0}$	8.4 ± 4.2	28.9 ± 8.0
$C_{13:0}$	Nd	0.6 ± 0.2
$C_{14:0}$	6.5 ± 0.9	7.0 ± 0.5
$C_{16:0}$	31.4 ± 7.2	4.4 ± 3.1
$C_{16:1}$ω 7c/ ω 6c	34.5 ± 3.9	1.6 ± 0.1
$C_{18:1}$ω 7c	3.0 ± 0.6	1.6 ± 0.3

Experimental conditions were same as described under Fig. 51, except of the purified EPS was analysed for fatty acid by gas chromatography. Data expressed as ± mean standard deviation of three independent experiments. nd, not detected.

Table. 6. Identification of metabolites of EPS of *R. benzoatilyticus* JA2 based on GCMS analysis

Metabolite	Exact mass	Derivatised mass and fragmentation	mol (%)
Amino acids			
Glycine	75.0	219.1 [204, 146, 102, 73]	1.24
Alanine	89.0	233.1 [128, 75, 43]	0.15
Leucine	131.1	203.1 [146, 86]	0.22
Isoleucine	131.1	275.1 [260, 218, 158, 100]	0.57
Serine	105	321.1 [279, 204, 148, 100, 73]	0.96
Proline	115.1	259.1 [216, 142, 73]	0.63
Cysteine	121.1	337.1 [220, 147, 102, 73]	0.07
Ornithine	132.1	348.2 [204, 142, 115, 102, 73]	0.38
Homocysteine	135.1	351.7 [234, 128,100, 73]	0.05
Tyrosine	181.1	397.1 [354, 280, 218, 179, 147, 100, 73]	0.62
Lysine	146.1	362.2 [362, 230, 156, 128, 84]	1.69
Aspartic acid	133.1	349.6 [232, 174, 147, 73]	0.05
N-acetyl-glutamine	188.1	476.9 [203, 147, 100, 73]	0.18
Tryptophan	204.2	348.1 [202, 130, 73]	3.85
Phenylalanine	165.1	309.1 [266, 218, 192, 147,100, 73]	3.66
Threonine	119.1	263.1 [219, 117, 57]	0.35
Methionine	149.2	293.1 [219, 202, 176, 128, 100, 73]	0.68
Valine	117.1	189.1 [146, 72]	0.11
N-acetyl-lysine	188.2	404.2 [375, 257, 174, 147, 73]	0.07
Carbohydrates			
Glucose	180.6	540.2 [204, 147, 103, 73]	1.15
Glucosamine	179.1	467.2 [204, 131, 103,73]	0.96
Keto-gluconic acid	195.1	554.2 [437, 303, 217, 147, 103, 73]	1.98
2-O-methyl-α-D-glucose	194.18	409.2 [191,146,73]	0.26
2,4-di-O-methyl-D-glucose	208.1	424.1 [191, 146, 73]	0.21
Rhamnose	164.1	452.2 [204, 147, 133, 73]	0.24
Mannonic acid	196.1	466.2 [292, 217, 147,103,73]	0.16
Arabinose	150.1	438.2 [319, 305, 217, 191, 147, 103, 73]	0.01
Nucleotides			
Uracil	112.0	256.1 [241, 147, 99, 73]	2.0
Thymine	126.1	270.1 [255, 185,147, 113, 73]	0.66
Cytosine	111.0	255.4 [254, 240, 170, 125, 98, 73]	0.15
Guanine	151.1	376.6 [352, 264, 147, 99, 73]	0.1
Adenine	135.1	279.4 [264, 192, 138, 73]	0.25
Fatty /organic acids			
Succinic acid	118.0	262.1 [247, 172, 147, 73]	0.49
Aminomalonic acid	119.0	335.1 [320, 292, 248, 218, 174, 147, 73]	0.52
3-Hydroxydodecanedioic acid	246.3	462.2 [331, 275, 233, 147, 101, 73]	3.85
Hexadecanoic acid	256.4	328.2 [313, 117, 75]	3.69
Heptadecanoic acid	270.4	342.2 [327, 201, 117, 75]	0.24
Octadecanoic acid	284.4	356.3 [341, 313, 201, 117, 73]	0.85
Eicosanoic acid	312.5	384.3 [369, 201, 117,73]	0.08

Experimental conditions were same as described under Fig. 52, Sample was derivatised with BSTFA+TMCS and analysed by GCMS. Metabolites were identified by comparing the mass spectra with the NIST library (similarity >750). BSTFA imparts 74 Da mass per active hydrogen group in molecule.

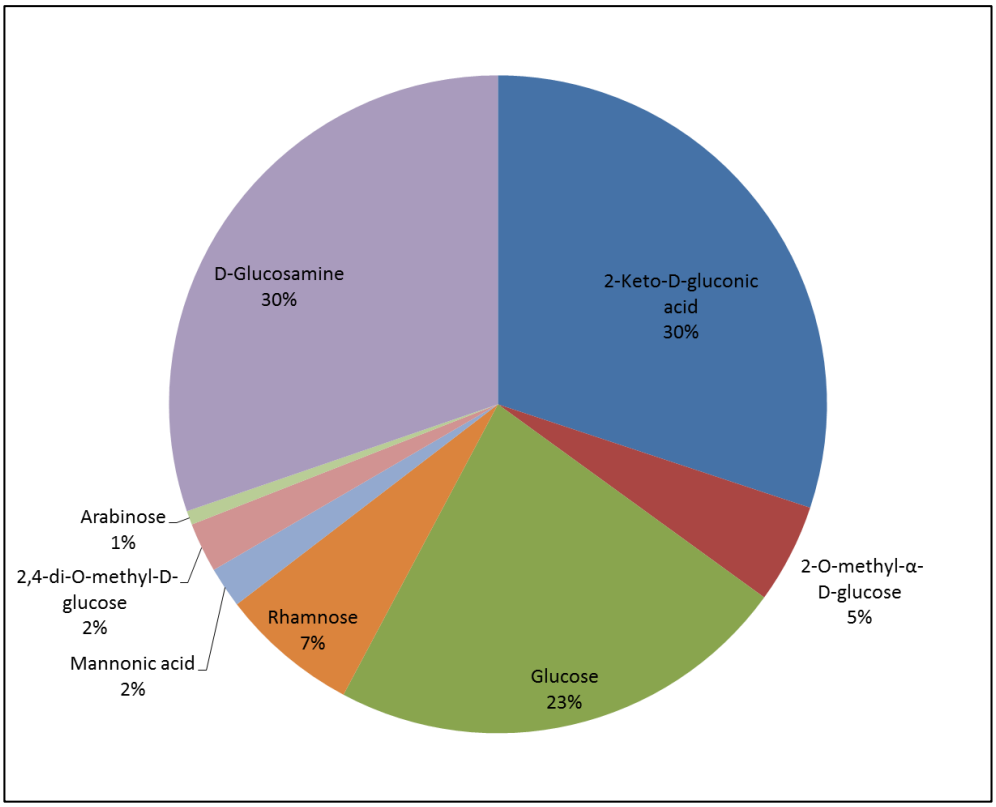

Fig. 52. GC-MS based carbohydrate composition of EPS produced by *R. benzoatilyticus* JA2.

Experimental conditions were same as described under Fig. 46, except for purified EPS was hydrolysed, derivatized and analysed by GC-MS. Metabolite area was used to determine mol (%)

3.2.2 Proteomic responses of *Rubrivivax benzoatilyticus* JA2 to aniline stress

3.2.2.1 Proteomic inventory of *Rubrivivax benzoatilyticus* JA2

Comparative proteomic analysis was done to decipher the molecular responses of *R. benzoatilyticus* JA2 to aniline stress at functional level. Isobaric Tag Relative and Absolute Quantification (iTRAQ) technique was employed for proteomic studies. Total proteome was isolated from three aniline exposed and one control culture, digested with trypsin and each peptide pool was labelled with one isobaric tag (control-114, aniline exposed-115,116 and 117). Equal amounts of labeled peptide pools were mixed from all four conditions and fractionated by strong cation exchange chromatography. Fractionated peptides were separated by reverse phase chromatography and separated peptides were subjected to mass analysis. Peptide mass finger printing was used to identify the protein and reporter ions for quantification. Methodology used in this study was illustrated in Fig. 53.

Proteins isolated from control and aniline exposed cells were subjected to SDS-PAGE analysis (12.5%) before iTRAQ analysis (Fig. 54A). Total of 750 proteins were detected by iTRAQ analysis of the proteome which correspond to 16% of total the theoretical proteome (3,898 protein coding genes of *R. benzoatilyticus* JA2) of *R. benzoatilyticus* JA2 (Fig. 54B). Identified proteins were subjected to *in silico* analysis for theoretical molecular weight, isoelectric point (pI) and hydropathy analysis (www.expasy.org). Molecular weight verses isoelectric point map indicated two clusters of proteins with pI of 4.5 to 7.0 and 9.0 to11, respectively (Fig. 55A). Hydrophilic (31.5%) and hydrophobic (68.5%) proteins were detected by grand average hydropathy (GRAVY) analysis of proteins (Fig. 55B). Correlation analysis of the iTRAQ identified proteins of biological replicates was done to evaluate their reproducibility. Fold change analysis of total identified proteins indicate many proteins levels were unchanged (Fig. 56A). Linear regression analysis between biological replicates (1 and 2) had a correlation coefficient value (R, R^2) of R=0.84, R^2= 0.721 which indicate data was reproducible (Fig. 56B).

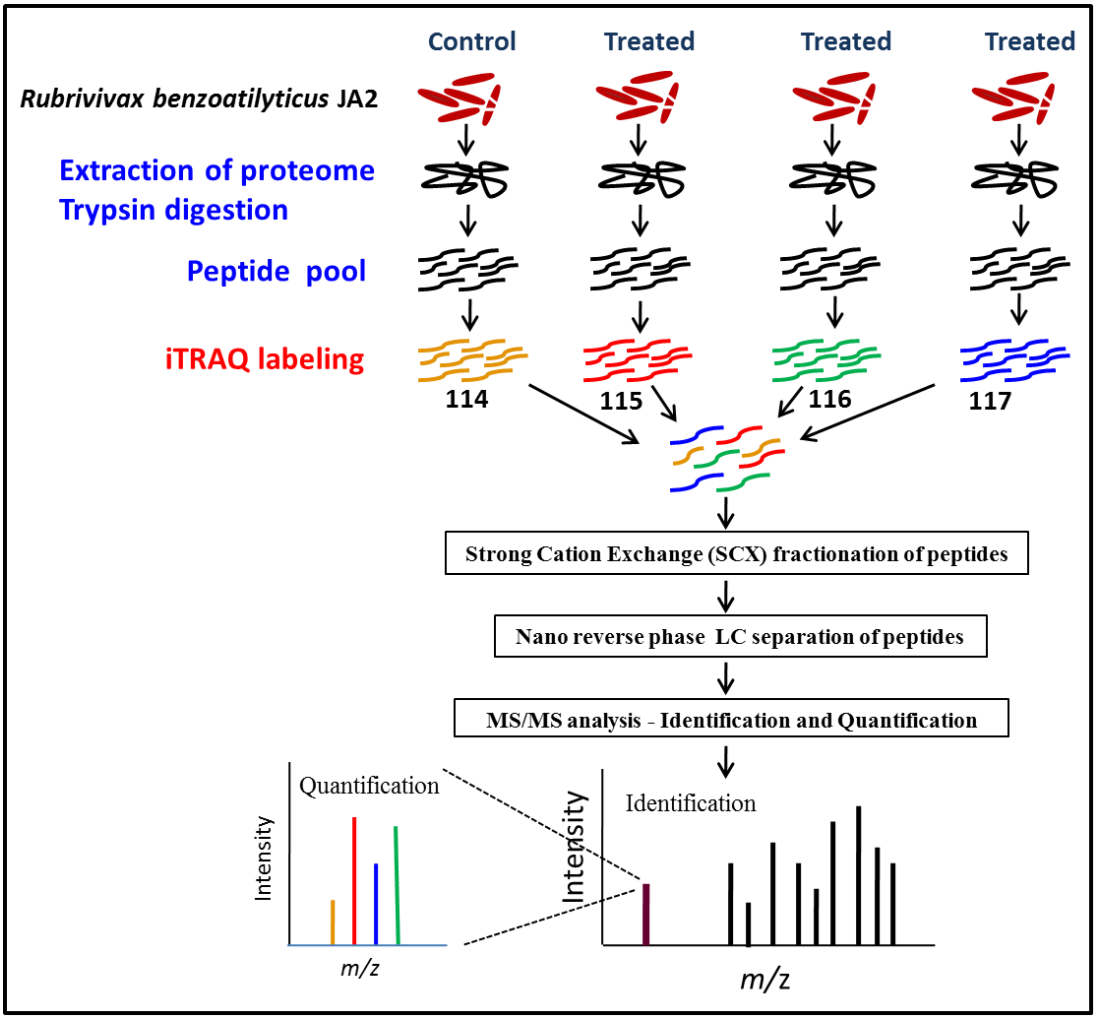

Fig. 53. Schematic representation of isotopic tags relative and absolute quantitation (iTRAQ) based proteome analysis of *R. benzoatilyticus* JA2.

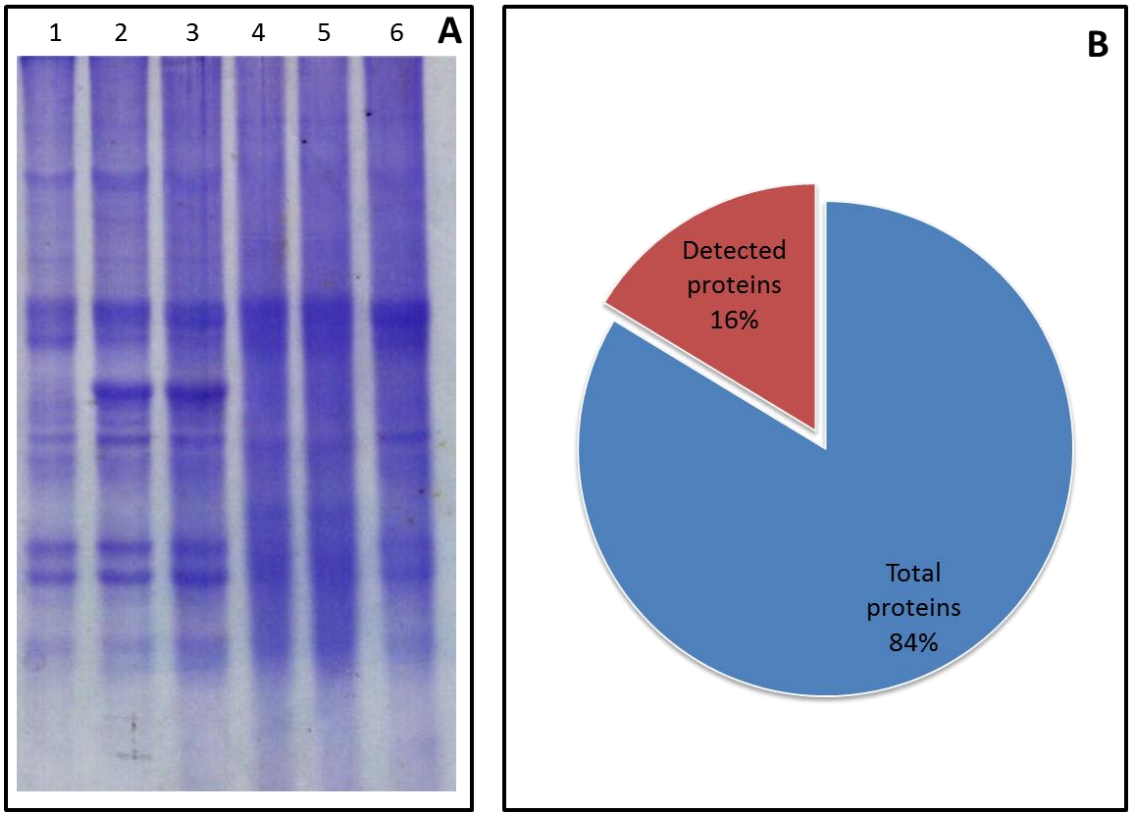

Fig. 54. SDS-PAGE analysis of the *R. benzoatilyticus* JA2 proteome **(A)** and proteins identified by iTRAQ analysis of *R. benzoatilyticus* JA2 proteome **(B)**.

Lane 1, 2, 3 were proteins from control cells and 3, 4, 5 from aniline exposed cells and proteins were run on 12.5% SDS-PAGE.

Experimental conditions were same as described under Fig. 46, except for the culture was harvested and proteins were isolated, lyophilised and analysed by iTRAQ (isobaric tags relative and absolute quantitation. Proteins were identified and quantified by using ProteinPilot 2.0. Data represents of three independent experiments.

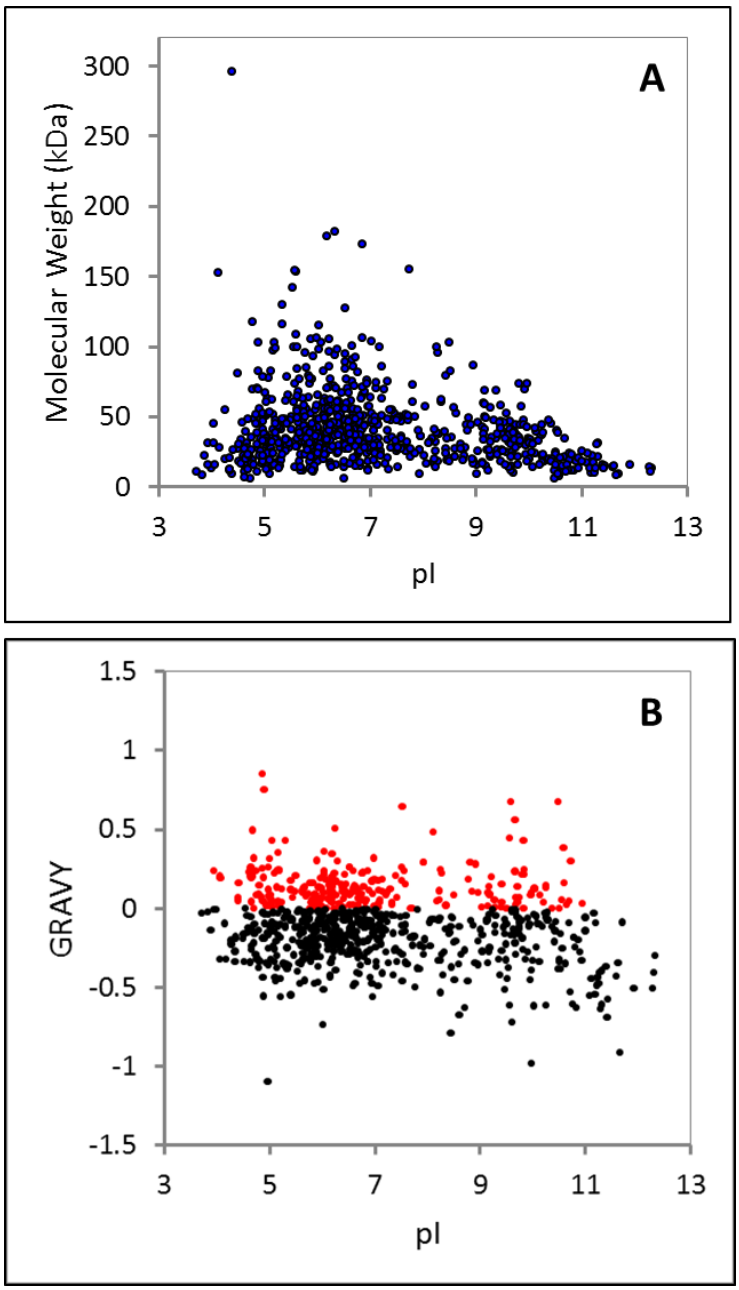

Fig. 55. Map of molecular weight versus isoelectric point (pI) **(A)**, hydropathy versus pI **(B)** of all proteins identified by iTRAQ analysis of the *R. benzoatilyticus* JA2 proteome.

Proteins identified by iTRAQ analysis as described under Fig. 54 were subjected to molecular weight, pI analysis by ExPASy tool (www.expasy.org), and GRAVY (grand average of hydropathy) by Sequence Manipulation Suite (www.bioinformatics.org/sms2/protein_gravy).

Red circles indicate hydrophobic (positive GRAVY) and black circles hydrophilic (negative GRAVY).

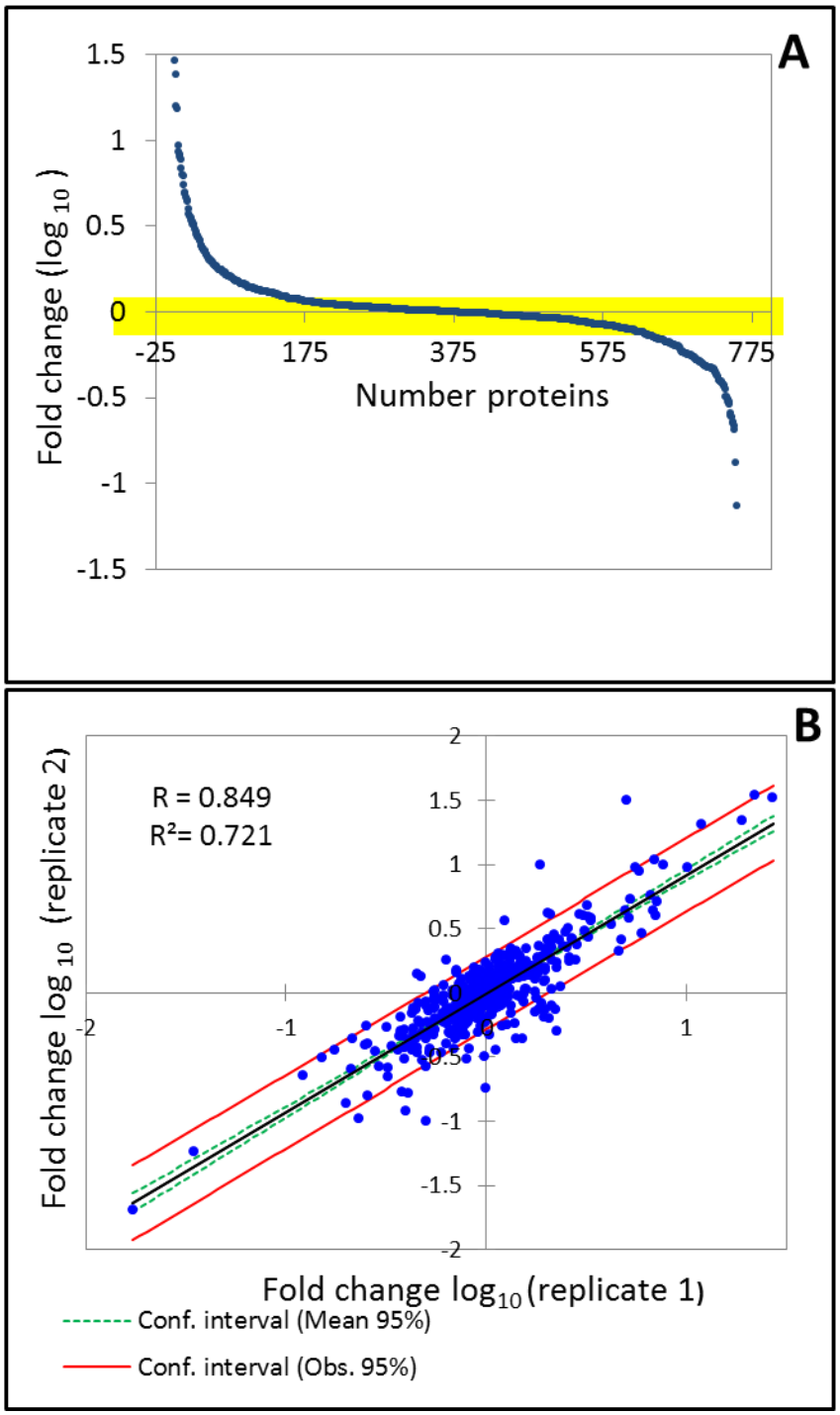

Fig. 56. Fold change analysis of the total proteins identified from iTRAQ analysis **(A)** Correlation analysis of the iTRAQ identified proteins of two biological replicates from *R. benzoatilyticus* JA2 **(B)**.

Proteins identified by iTRAQ analysis as described under Fig. 54 were used for linear regression analysis. Fold change correspond to protein ratios (aniline exposed/ control) from iTRAQ analysed samples were log transformed (log_{10}) and plotted by Xcel stat.

3.2.2.2 Differential regulated proteins identification

Proteins identified (750) by iTRAQ analysis were subjected to volcano plot analysis to identify differentially regulated proteins. A protein was considered differentially regulated if the ratio (aniline exposed/control) less than 0.8 (down regulated) or greater than 1.2 (up-regulated) in at least two biological replicated with *p* value of less than 0.05. Total of 114 proteins were identified as differentially regulated proteins from volcano plot (Fig. 57) of which 58 proteins were up-regulated (aniline exposed/control ratio <1.2) and 56 proteins were down regulated (aniline exposed/control ratio <0.8) in aniline exposed cells.

3.2.2.3 Functional classification of differential regulated proteins

Differentially regulated proteins (114) were classified into different functional groups according to KEGG database (*http://www.genome.jp/kegg/*) to identify molecular or cellular processes modulated by aniline stress. Differential regulated proteins were grouped under 16 functional categories, largely belonging to general cellular metabolism, transcription, translation, membrane transport, signal transduction, stress, replication, folding sorting and degradation of proteins (Fig. 58). Proteins related to membrane transport were highly regulated followed by proteins related to central carbon metabolism, folding and sorting, hypothetical proteins, metabolism of vitamins-cofactors, amino acid, energy, nucleotide metabolism, transcription and translation were differential regulated (Fig. 58). Proteins related to signal transduction, stress, biosynthesis of secondary metabolites were up regulated while lipid metabolism and replication and repair were down-regulated (Fig. 58).

Among the up regulated proteins 21% were related to folding sorting and degradation of proteins followed by membrane transport (16%), hypothetical (10%), translation (9%) and metabolism of cofactors and vitamins (9%), stress related proteins (7%), transcription (5%), signal transduction (5%), carbohydrate metabolism were (5%) (Fig. 59A). Biosynthesis of secondary metabolites, glycan biosynthesis, amino acid metabolism related proteins were up regulated by 3% while energy and nucleotide metabolism was up regulated by 2% (Fig. 59A). Among the down regulated proteins 27% were related to tricarboxylic acid cycle metabolism followed by membrane transport (22%), amino acid metabolism (9%), lipid metabolism (7%) and replication and repair mechanism (7%), nucleotide (6%), and hypothetical proteins (5%) (Fig. 59B).

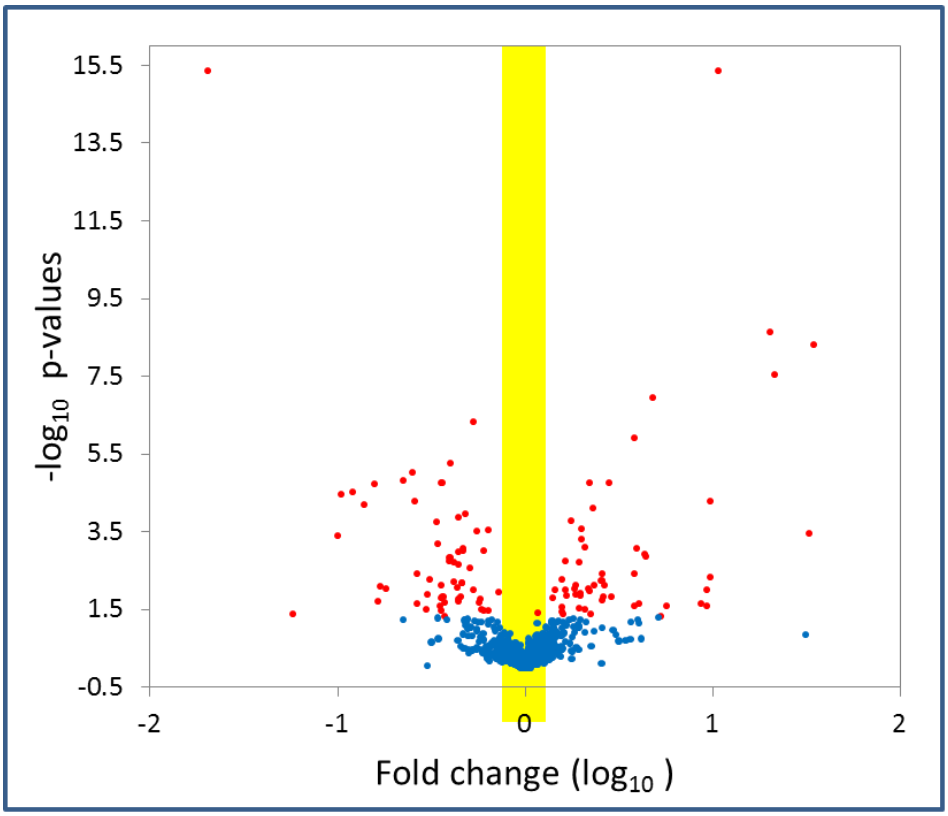

Fig. 57. Volcano plot of iTRAQ identified proteins of *R. benzoatilyticus* JA2.

Red circles indicate proteins with statistically significant *p*-value (<0.05), on X-axis positive log values indicate up-regulation and negative values down regulation. Colour shaded (yellow) region indicate no fold change. Fold change correspond to protein ratios of aniline exposed/control cultures. Log_{10} >0.08 was considered up regulated (ratio > 1.2) and log_{10} < -0.1 was considered down regulated (ratio< 0.8)

Data processing parameters were similar as described under Fig. 56.

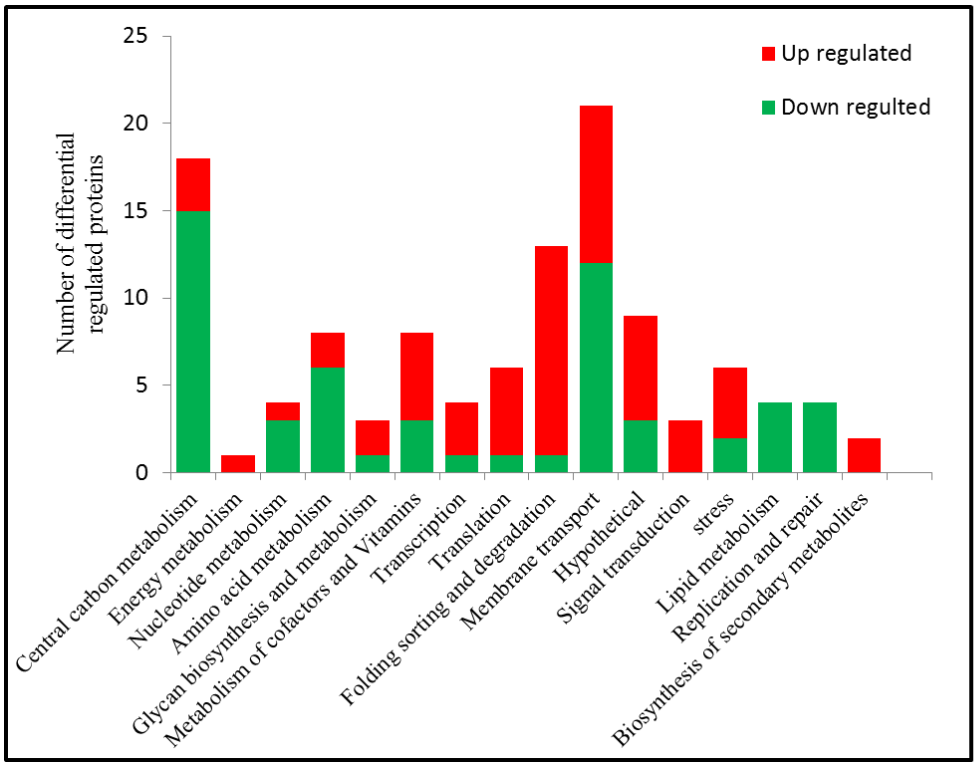

Fig. 58. Functional classification of differential regulated proteins of *R. benzoatilyticus* JA2 identified by iTRAQ analysis.

Functional classification was done according to KEGG (Kyoto Encyclopedia of Genes and Genomes database, www.genome.jp/kegg/)

Differential regulated proteins identified by volcano plot analysis as described under Fig. 57 were functionally annotated.

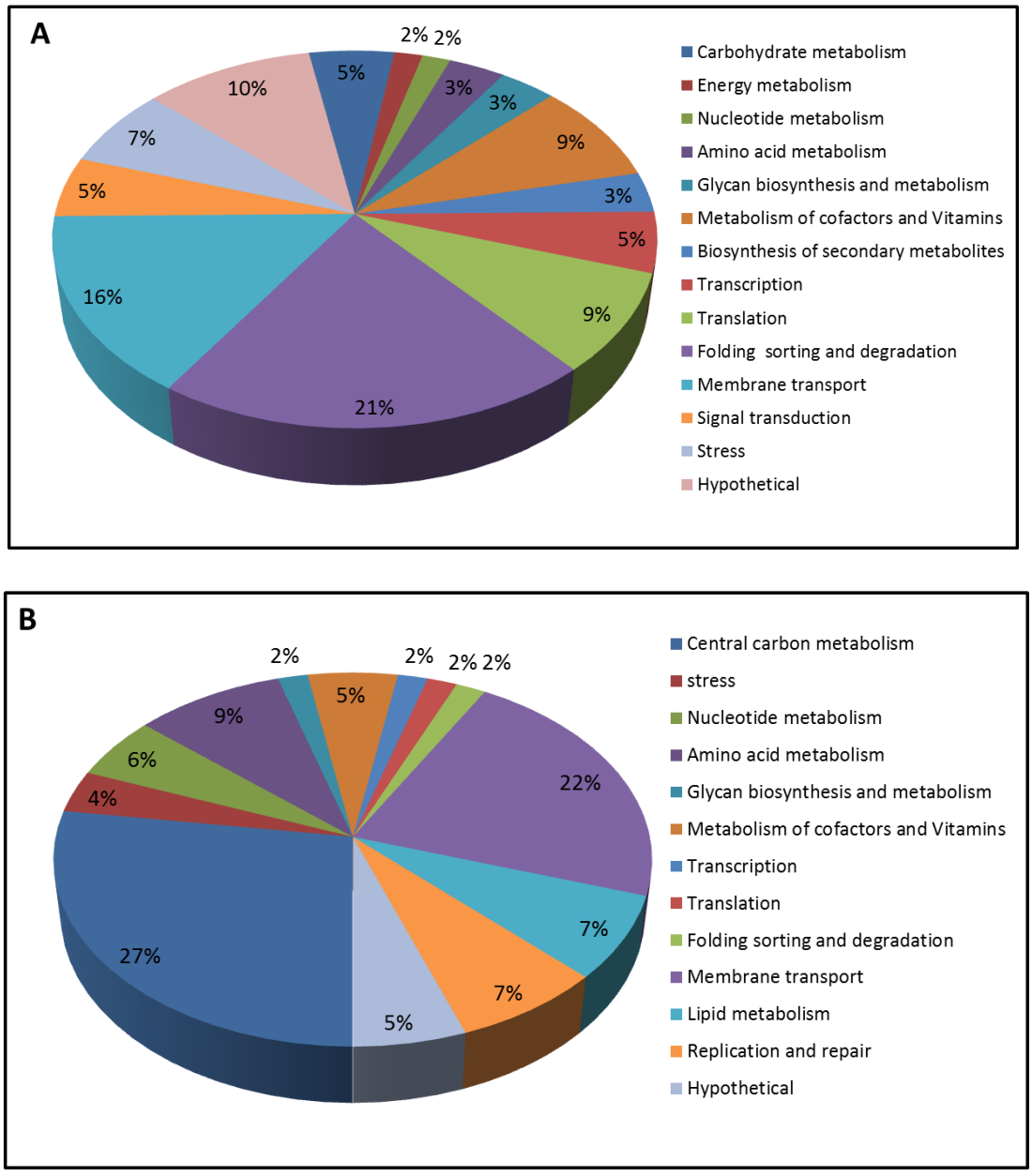

Fig. 59. Functional categories of up-regulated and down-regulated proteins of *R. benzoatilyticus* JA2.

Functional categories of up-regulated proteins **(A)** and down-regulation **(B)** Data processing parameters were same as described under Fig. 58.

3.2.2.4 Cellular responses of *R. benzoatilyticus* JA2 to aniline stress

3.2.2.4a Heat shock proteins (molecular chperones)

Heat shock proteins are family of proteins involved in protein folding, sorting degradation of miss folded proteins. Class I heat shock proteins GroEL, GroES, Dnak and co-chaperone DnaJ were up regulated in aniline exposed cells (Table. 7). Two Hsp 20 and putative heat shock proteins were also up regulated. Class III heat shock proteins such as caseinolytic protease ClpA, ClpP, ClpB were up regulated to aniline stress (Table. 7). Class VI heat shock protein Lon protease was significantly up regulated in aniline induced stress.

3.2.2.4b Membrane transport

Proteins related to membrane transport were highly differential regulated to aniline stress. Resistance-nodulation-cell division (RND) efflux pumps related outer membrane proteins, acraflavin resistance protein and putative efflux proteins were up regulated (Table. 7). Putative ABC transporter, phosphate-binding periplasmic (pbp) ABC transporter, translocation protein TolB and polar amino acid transporters were up regulated (Table. 7). Vitamin B_{12} transporter, maltose ABC transporter periplasmic protein, maltoporin and many extracellular solute-binding proteins were down regulated (Table. 7)

3.2.2.4c Transcription and translation

Transcription machinery was up regulated along with some transcriptional regulators to aniline stress. Transcription termination factor Rho, antiteriminator NusG proteins were up regulated. Nitrogen regulatory protein P-II, two component transcriptional regulator, nucleoside diphosphate kinase regulator(Rnk), histone-like nucleoid-structuring protein (H-NS) and two component LuxR family transcriptional regulator were up regulated in aniline exposed cells (Table. 7). Proteins related to translation such as 50S and 30S subunit were up regulated and trigger factor, a chaperone associated with translation was also up regulated to aniline stress (Table. 7).

3.2.2.4d Replication and repair

Proteins related to replication and repair such as DNA gyrase β-subunit, DNA topoisomerase III, and RecA were down regulated to aniline stress (Table. 7).

3.2.2.4e Signal transduction

Histidine kinase, putative histidine kinase and PAS/PAC hybrid histidine kinase putative high potential iron-sulfur (hipip) signal peptide proteins were up regulated while response regulator receiver modulated metal dependent phosphohydrolase was down regulated in aniline exposed cells (Table. 7).

3.2.2.4f Stress related proteins

Universal stress protein (UspA), type I antifreeze protein (HlyD), alkaline phosphatase, putative nitrite/sulfite reductase, leucyl aminopeptidase and phasin family proteins were up regulated (Table. 7) while putative cytochrome c peroxidase, catalase/hydroperoxidase HPI(I) and YceI family proteins were down regulated to aniline stress (Table. 7).

3.2.2.4g Metabolism

Tryptophan biosynthesis related proteins such as 3-dehydroquinate dehydratase, anthranilate synthase, tryptophan synthase α, β subunits were up regulated to aniline stress. Proteins related to gluconeogenesis/glycolysis and pentose phosphate pathway were up regulated (Table. 7). Isopropylmalate dehydrogenase, dihydrodipicolinate synthase of lysine biosynthesis, acetylserine sulfhydrylase of cysitne/methionine biosynthesis and carbamoyl-phosphate synthase of arginine biosynthesis were up-regulated (Table. 7). Proteins involved in chlorophyll biosynthesis and carotenoid biosynthesis proteins 4-hydroxy-3-methylbut-2-enyl diphosphate reductase, phytoene dehydrogenase were up regulated to aniline stress (Table. 7). All the TCA cycle proteins were down regulated except for fumarate hydrolyase (fumarase) in aniline exposed cells. (Table. 7). Proteins related β-oxidation pathway of fatty acids, all the proteins of histidine catabolism were down regulated to aniline stress (Table. 7) Isovaleryl-CoA dehydrogenase, 3-oxoacid CoA-transferase involved in branched chain amino acid degradation, lysine decorboxylase, acetyl-CoA C-acetyltransferase of lysine degradation and glycine cleavage system proteins of glycine catabolism were down regulated (Table. 7) Zinc and iron dependent alcohol dehydrogenase and aldehyde dehydrogenase were down-regulated (Table. 7).

3.2.2.4h Hypothetical proteins

Fifteen percentage of differential regulated proteins belonged to hypothetical proteins of *R. benzoatilyticus*. Six hypothetical proteins were up-regulated and 4 hypothetical proteins were down-regulated (Table.7).

Table. 7. Proteins identified by iTRAQ analysis of aniline exposed cells

Accession No.	Protein description	Unused Prot Score	Seq %Coverage	No. Peptides	Avg fold change (log_{10}) ± S.D
Up-regulated proteins					
	Membrane transport				
gi|332111082	Porin	70.96	93.69	107	0.265 ±0.0
gi|332111811	extracellular solute-binding protein	55.01	82.03	54	0.202 ±0.12
gi|332108171	extracellular ligand-binding receptor	51.02	83.42	46	0.414 ±0.14
gi|332109169	translocation protein TolB	23.01	46.77	13	0.216 ±0.07
gi|332109520	putative ABC transporter ATP-binding protein	22.22	45.85	11	0.302 ±0.04
gi|332112675	putative transport/efflux trans membrane protein	8.97	40.61	4	0.537 ±0.10
gi|332107790	RND efflux system outer membrane lipoprotein	12.18	38.84	6	0.694 ±0.13
gi|332107789	RND family efflux transporter MFP subunit	10.56	38.99	6	0.650 ±0.04
gi|332112674	acriflavin resistance protein	3.61	15.28	2	0.210 ±0.05
gi|332107601	polar amino acid transporter substrate-binding protein	33.17	72.96	24	0.645 ±0.06
gi|332109964	putative phosphate-binding periplasmic (pbp) ABC transporter protein	18.11	47.98	10	0.414 ±0.06
	Translation and ribosomal biogenesis				
gi|332111964	30S ribosomal protein S1	42.44	52.54	26	0.180 ±0.01
gi|332107879	50S ribosomal protein L5	13.29	62.58	9	0.268 ±0.02
gi|332108095	50S ribosomal protein L10	13.01	69.19	6	0.386 ±0.06
gi|332107867	50S ribosomal protein L4	12.33	67.96	7	0.368 ±0.02
gi|332112447	SSU ribosomal protein S2P	12.75	73.28	11	0.328 ±0
	Folding, sorting, protein turnover and chaperones				
gi|332108332	chaperonin GroEL	108.85	90.81	124	0.902 ±0.11
gi|332112473	molecular chaperone DnaK	54.91	64.07	39	0.601 ±0.08
gi|332107934	*heat shock protein DnaJ domain-containing protein*	*2.06*	*8.869*	*1*	*0.374 ±0.12*
gi|332112673	trigger factor	37.41	67.43	22	0.506 ±0.17

gi|332112761	ATP-dependent chaperone ClpB	36.27	42.48	21	1.184 ±0.11
gi|332110107	ATP-dependent Clp protease, ATP-binding subunit clpA	26.69	40.39	14	0.738 ±0.09
gi|332108331	co-chaperonin GroES	16.7	97.92	22	0.506 ±0.08
gi|332112474	putative heat shock protein	11.33	51.7	8	0.289 ±0.05
gi|332112670	endopeptidase La (Lon)	24.03	24.16	13	0.972 ±0.03
gi|332107864	heat shock protein Hsp20	6.02	36.67	4	0.930 ±0.16
gi|332107863	heat shock protein Hsp20	3.87	52.76	3	0.920 ±0.14
gi|332111751	*ATP-dependent Clp protease proteolytic subunit ClpP*	*5.21*	*27.86*	*3*	*0.176 ±0.03*
	Transcription				
gi|332109975	transcription termination factor Rho	18.22	31.12	12	0.272 ±0.02
gi|332108098	transcription antitermination protein NusG	14.59	58.55	7	0.230 ±0.05
gi|332110564	nitrogen regulatory protein P-II	15.46	69.64	12	0.392 ±0.03
gi|332112530	two component transcriptional regulator	9.04	43.16	6	0.889 ±0.10
gi|332112137	nucleoside diphosphate kinase regulator	19.87	94.24	17	0.381 ±0.07
gi|332108399	*two component LuxR family transcriptional regulator*	*15.99*	*51.21*	*10*	*0.254±0.002*
gi|332109848	*histone-like nucleoid-structuring protein H-NS*	*6.86*	*59.26*	*4*	*0.554 ±0.06*
	Signal transduction				
gi|332112529	histidine kinase	5.68	15.32	3	0.669 ±0.09
gi|332109370	putative high potential iron-sulfur (hipip) signal peptide protein	23.41	79	23	0.357 ±0.03
gi|332111998	*PAS/PAC sensor hybrid histidine kinase*	*2.51*	*9.47*	*2*	*0.22 ±0.05*
	Metabolism				
gi|332108614	*tartrate/fumarate subfamily Fe-S type hydro-lyase subunit alpha*	*16.02*	*36.22*	*9*	*0.196 ±0.17*
gi|332108124	*3-isopropylmalate dehydrogenase*	*20.85*	*47.38*	*14*	*0.250 ±0.17*
gi|332112501	*dihydrodipicolinate synthase*	*10.72*	*45.24*	*6*	*0.144 ±0.06*
gi|332108062	*anthranilate synthase*	*5.68*	*15.38*	*3*	*0.131 ±0.06*
gi|332112027	*3-dehydroquinate dehydratase*	*2.04*	*19.33*	*1*	*0.139 ±0.03*
gi|332107639	tryptophan synthase subunit beta	14.31	34.46	8	0.317 ± 0.10
gi|332107638	*tryptophan synthase subunit alpha*	*12.27*	*36.8*	*8*	*0.302 ±0.01*
gi|332111680	*O-acetylhomoserine/O-acetylserine sulfhydrylase*	*16.94*	*35.32*	*12*	*0.264 ±0.02*
gi|332109954	carbamoyl-phosphate synthase large subunit	12.66	20.17	7	0.330 ±0.16
gi|332107971	Transketolase	25.14	42.77	14	0.297 ±0.05
gi|332109881	UTP-glucose-1-phosphate	14.87	53.47	7	0.264 ±0

	uridylyltransferase				
gi|332111092	*Enolase*	*39.01*	*76.11*	*27*	*0.200 ±0.11*
gi|332107479	*phosphoglycerate mutase 1 family protein*	*21.47*	*62.5*	*12*	*0.218 ±0.002*
gi|332108491	*phosphoenolpyruvate carboxykinase*	*39.66*	*58.52*	*34*	*0.130 ±0.00*
gi|332110123	phosphoenolpyruvate carboxylase	25.51	36.29	14	0.216 ±0.01
gi|332107849	*glucose/ribitol dehydrogenase family protein*	*8.03*	*44.27*	*7*	*0.157 ±0.04*
gi|332108599	*fructose-1,6-bisphosphatase*	*3.67*	*8.95*	*2*	*0.1 ±0.01*
gi|332112586	*ribulose-phosphate 3-epimerase*	*2.49*	*22.22*	*1*	*0.216 ±0.10*
gi|332108363	Magnesium protoporphyrin IX monomethyl ester anaerobic oxidative cyclase	34.75	43.24	20	0.180 ±0.06
gi|332112588	ribulose bisphosphate carboxylase	24.51	58.42	21	0.396 ±0.07
gi|332109934	light-independent protochlorophyllide reductase subunit B	18.79	32.84	9	0.300 ±0.03
gi|332109935	light-independent protochlorophyllide reductase subunit N	16.44	55.97	9	0.465 ±0.04
gi|332111602	inosine-5'-monophosphate dehydrogenase	19.2	42.24	11	0.118 ±0.07
gi|332112046	*F0F1 ATP synthase subunit beta*	*49.42*	*75.32*	*42*	*0.20 ±0.12*
gi|332110897	glutamate-1-semialdehyde aminotransferase	15.63	30.93	12	0.353 ±0.05
gi|332109939	phytoene dehydrogenase	13.24	31.19	7	0.177 ±0.04
gi|332112545	4-hydroxy-3-methylbut-2-enyl diphosphate reductase	14.92	47.37	8	0.412 ±0.06
gi|332112609	formyltetrahydrofolate deformylase	13.35	36.73	8	0.524 ±0.05
	Stress related proteins				
gi|332109836	alkaline phosphatase	27.9	61.49	20	0.21 ±0.01
gi|332108189	leucyl aminopeptidase	9.09	34.97	5	0.898 ±0.13
gi|332108594	type I antifreeze protein:HlyD family secretion protein	13.89	60.11	8	0.80 ±0.03
gi|332110028	UspA domain-containing protein	12.91	70.75	7	0.284 ±0.07
gi|332112133	putative nitrite/sulfite reductase	12.42	34.56	6	0.572 ±0.04
gi|332112139	phasin family protein	24.79	88.11	21	1.385 ±0.13
	Hypothetical				
gi|332111542	hypothetical protein -14391	62.86	88.54	67	0.184 ±0.09
gi|332112531	hypothetical protein- 18423	19.22	73.63	27	1.194 ±0.19
gi|332111968	hypothetical protein-16522	15.53	65.17	11	0.348 ±0.05
gi|332112538	hypothetical protein-18458	8.55	38.43	6	1.461 ±0.04

gi|332110122	hypothetical protein-10509	5.11	14.14	3	0.838 ±0.12
gi|332109527	hypothetical protein-08990	2.83	16.33	2	0.141 ±0.07
Down-regulated proteins					
	Membrane transport				
gi|332110081	vitamin B12 transporter btuB precursor, putative	119.08	85.14	131	-0.226 ±0.11
gi|332109158	extracellular solute-binding protein family 5	57.34	69.42	62	-0.326 ±0.15
gi|332112514	gram-negative type outer membrane porin protein	37.62	70.07	28	-0.396 ±0.04
gi|332109200	maltose ABC transporter periplasmic protein	33.99	56.17	18	-0.298 ±0.14
gi|332111191	extracellular solute-binding protein	31.26	59.13	17	-0.333 ±0.08
gi|332109205	maltoporin	30.75	53.54	27	-0.412 ±0.06
gi|332108709	polypeptide-transport-associated domain-containing protein	23.13	47.59	14	-0.258 ±0.13
gi|332111726	extracellular solute-binding protein, family 7	22.46	59.25	15	-0.613 ±0.05
gi|332109141	extracellular solute-binding protein family 1	20.58	52.4	13	-0.332 ±0.06
gi|332108070	putative substrate-binding periplasmic (pbp) ABC transporter protein	14.95	49	12	-0.525 ±0.10
gi|332107729	extracellular solute-binding protein	10.26	39.19	7	-0.568 ±0.21
	Transcription				
gi|332108092	DNA-directed RNA polymerase subunit beta	57.99	43.29	32	-0.150 ±0.10
gi|332108093	DNA-directed RNA polymerase subunit beta	39.55	31.54	22	-0.162 ±0.04
gi|332111578	response regulator receiver modulated metal dependent phosphohydrolase	7.01	18.88	4	-0.346 ±0.05
gi|332108087	elongation factor Tu	55.08	70.89	58	-0.266 ±0.09
	Replication and repair				
gi|332111369	recA protein	16.95	50.86	12	-0.776 ±0.11
gi|332108198	DNA gyrase subunit B	16.25	24.13	8	-0.322 ±0.12
gi|332107966	DNA topoisomerase III	7.74	12.04	4	-0.288 ±0.09
	Metabolism				
gi|332110008	bifunctional aconitate hydratase 2/2-methylisocitrate dehydratase	88.24	70.45	70	-1.346 ±0.15

gi|332109442	isocitrate lyase	61.37	90.26	72	-1.728 ±0.05
gi|332110006	malate dehydrogenase	42.77	86.59	38	-0.512 ±0.22
gi|332110104	isocitrate dehydrogenase	34.84	53.83	23	-0.20 ±0.10
gi|332109999	type II citrate synthase	22.88	47.02	20	-0.494 ±0.13
gi|332112657	2-oxoglutarate dehydrogenase E1 component	22.76	24.37	11	-0.254 ±0.03
gi|332110002	succinate dehydrogenase subunit A	19.36	37.35	9	-0.392 ±0
gi|332110001	*succinate dehydrogenase subunit B*	*4.98*	*33.33*	*4*	*-0.406 ±0.24*
gi|332111365	*succinyl-CoA synthetase subunit alpha*	*12.16*	*42.42*	*7*	*-0.202 ±0.04*
gi|332109996	succinyl-CoA synthetase subunit beta	15.77	39.12	10	-0.372 ±0.07
gi|332109333	dihydrolipoamide dehydrogenase	7.49	25.21	4	-0.398 ±0.07
gi|332107739	urocanate hydratase	106.27	79.93	171	-0.438 ±0.14
gi|332109412	Acetyl-CoA C-acetyltransferase	34.22	71.9	28	-0.26 ±0.11
gi|332107742	imidazolonepropionase	25.82	55.75	19	-0.374 ±0.05
gi|332111131	aromatic amino acid aminotransferase	22.31	51.75	15	-0.284 ±0.07
gi|332111195	glycine cleavage system T protein	20.1	49.6	12	-0.250 ±0.13
gi|332108035	isovaleryl-CoA dehydrogenase	13.22	30.1	7	-0.436 ±0.19
gi|33211130	3-oxoacid CoA-transferase subunit B	12.71	46.95	8	-0.306 ±0.03
gi|332112707	lysine decarboxylase	9.18	20.79	4	-0.318 ±0.12
gi|332107740	histidine utilization repressor	9.23	44.12	5	-0.524 ±0.20
gi|332107743	*N-formylglutamate amidohydrolase*	*18.07*	*58.17*	*13*	*-0.283 ±0.04*
gi|332107744	*N-formimino-L-glutamate deiminase*	*17.87*	*39.91*	*11*	*-0.405 ±0.11*
gi|332108287	Zn-dependent alcohol dehydrogenase	66.28	92.88	84	-0.284 ±0.10
gi|332110433	iron-containing alcohol dehydrogenase	24.69	46.64	15	-0.312 ±0.10
gi|332112569	aldehyde dehydrogenase	20.44	37.75	13	-0.782 ±0.18
gi|332111321	putative long-chain-fatty-acid--CoA ligase protein	23.45	41.26	13	-0.606 ±0.12
gi|332109379	3-ketoacyl-(acyl-carrier-protein) reductase	14.53	49.39	10	-0.513 ±0.05
	3-hydroxyacyl-CoA dehydrogenase		14.53	4	-0.650 ±0.15

gi|332109506	NAD-binding protein	6.01			
gi|332108616	acetyl-coenzyme A synthetase	30.57	46.36	20	-0.265 ±0.16
gi|332108688	phosphoribosylaminoimidazole-succinocarboxamide synthase	28.7	69.67	19	-0.328 ±0.09
gi|332109910	2-desacetyl-2-hydroxyethyl bacteriochlorophyllide A dehydrogenase, putative	22.91	60.12	11	-0.250 ±0.06
gi|332107463	hydroxyethylthiazole kinase	21.07	57.61	24	-0.66 ±0.22
gi|332107461	phosphomethylpyrimidine kinase	20.05	55.36	12	-0.804 ±0.24
gi|332107567	deoxyxylulose-5-phosphate synthase	13.33	20.7	6	-0.648 ±0.41
	Oxidative stress and stress				
gi|332112542	catalase/hydroperoxidase HPI(I)	21.91	29.48	12	-0.324 ±0.05
gi|332107843	putative cytochrome c peroxidase	13.75	39.46	7	-0.348 ±0.07
gi|332111699	carboxyl-terminal protease	4.4	20.04	2	-0.448 ±0.18
gi|332111727	YceI family protein	10.17	48.15	6	-0.350 ±0.13
	Hypothetical				
gi|332111537	hypothetical protein-14366	18.95	45.64	12	-0.685 ±0.10
gi|332111078	hypothetical protein -12317	26.57	68.94	20	-0.242 ±0.10
gi|332111376	hypothetical protein -13569	4.7	42.44	3	-0.405 ±0.06

Unused ProtScore is a measure of the protein confidence for a detected protein, calculated from the peptide confidence for peptides from spectra that are not already completely ‘‘used’’ by higher scoring winning proteins. ProtScore = 2log (1-Percent Confidence/100). The corresponding Percent Confidence of ProScore 2.0 is 99%.

% Seq coverage, the percentage of matching amino acids from identified peptides having confidence greater than 0, divided by the total number of amino acids in the sequence.

Fold change, Protein ratio of aniline exposed to control (unexposed) and the ratio were $\log_{10}$ transformed values are mean ± standard deviation of three biological replicates. Data was obtained from iTRAQ analysis of control and aniline exposed proteomes.

DISCUSSION

4.0 Discussion

Bacteria are remarkable in adapting to the changing environmental conditions and this enable them to thrive in diverse habitats. One such changing environmental condition is pollution, brought by release of chemical compounds into biosphere through ever increasing anthropogenic activities. Many of the chemical compounds released into the environment are foreign (xenobiotic) to bacteria and are toxic, interfere with cellular processes eventually leading to the cell death (Wijte *et al*., 2010). Bacteria employ various strategies to overcome these adverse conditions and thrive in xenobiotic stress (Ramos *et al.*, 2002; Segura *et al*., 2012). Some bacteria degrade, utilize xenobiotic compounds as sole source of energy for their growth and degradation/transformation of xenobiotics is compound/species specific process (Ramos *et al*., 2002). Although some bacteria are unable to degrade xenobiotic compounds but they adopt various tolerance (stress response) mechanisms to combat the xenobiotic stress (Wijte *et al*., 2010). Stress response/tolerance involve various mechanisms which are not yet fully understood (Dominguez-Cuevas *et al*., 2006).

Aniline is an anthropogenic aromatic compound mainly used in various industrial applications (Liu *et al*., 2002). Aniline is persistent, recalcitrant and toxic compound widely distributed in the environment (Liu *et al*., 2002; Liang *et al*., 2005). On one hand, aniline acts as potential source of carbon for bacteria and on the other hand aniline is toxic and exerts stress on bacteria (Liang *et al*., 2005; Aruoja *et al*., 2011). Many bacteria capable of degrading aniline were isolated and their degradation pathways were well studied (Kahng *et al.*, 2000; Liang *et al*., 2005). Degradation/detoxification of the toxic compounds is considered as one of the mechanisms of toxic compounds tolerance (Ramos *et al*., 2002). Majority of the aniline degrading bacteria so far reported tolerate aniline up to 5-10 mM (Kim *et al*., 2004) except for a few species of *Delftia sp.* AN3 tolerating up to 50 mM (Liu *et al*., 2002). However, stress response and tolerance mechanisms of bacteria to aniline in both degraders and non-degraders are yet to be deciphered. On the other hand production of indoles in presence of aniline or its derivatives was reported in purple bacteria (Shanker *et al*., 2006). However, biosynthetic pathway of indoles in aniline exposed cell yet to be investigated. In the present study we employed systems approach to decipher the indoles biosynthesis and stress response mechanisms of *R. benzoatilyticus* JA2 to aniline stress.

Aniline induced indoles biosynthesis and its regulation

Aniline or its derivatives (Table.1) could not support the growth of *R. benzoatilyticus* JA2 as sole source of carbon or nitrogen (data not shown). Though aniline has not supported growth of the *R. benzoatilyticus* JA2 as carbon/energy source, strain JA2 tolerated high (25 mM) concentrations of aniline with MIC value of 30 mM. Aniline exposed cells of *R. benzoatilyticus* JA2 produced indoles and no such indoles formation was found in control culture (aniline unexposed). Indoles production was observed only with aniline and anthranilate but not with other aniline derivatives (Table. 1) which may be due to regeoselectivity as observed in case of anilines transformation to acetanilide by *Bacillus cereus* PDa-1 (Takenaka *et al*., 2006). Tryptophan, IAA and indole-3-aldehyde (IAld) were identified as major indole metabolites in aniline exposed cells (Fig. 9, 10 and 11 and this indicate possible active biosynthesis or accumulation of indoles. Similarly, formation of indole was observed when sulphate reducing bacteria were exposed to diphenylamines (Drzyzga and Blotevogel, 1997) or nitrodiphenylamines (Drzyzga *et al*., 1996) and *Rhodobacter sphaeroides* OU5 produced indole metabolites in presence of anthranilate (2-aminobenzoate) (Sunayana *et al*., 2005) or aniline (Shanker *et al*., 2006). Although biosynthesis of indoles from aniline or its derivative (anthranilate) was proposed in previous studies, the proposed pathway(s) were remained speculative.

Aromatic metabolites including indoles are *de novo* biosynthesised *via* shikimate pathway which operates in plants, fungi and bacteria (Maeda and Dudareva, 2012). When *De novo* biosynthesis of aromatic amino acids (shikimate) was inhibited by glyphosate (N-(phosphonomethyl) glycine), growth of *R. benzoatilyticus* JA2 ceased and complete growth restoration was observed when the culture was supplemented with phenylalanine, tyrosine and anthranilate (natural precursor of trp). However, growth was not restored when anthranilate was replaced with aniline (speculated precursor of trp) along with other aromatic amino acids. Moreover, glyphosate inhibited indoles production in aniline exposed cells in a dose dependent manner (Fig. 15A). Taken together these results suggest that aniline may not be a precursor for indoles biosynthesis and shikimate pathway may be involved in the biosynthesis of indoles in aniline exposed cells. Shikimate pathway is source for all three aromatic amino acids biosynthesis and for many plant, bacterial secondary metabolites (Gosset, 2009). Indoles are one such aromatic metabolites biosynthesised from shikimate pathway either in tryptophan dependent or independent manner (Spaepen *et al*., 2007). Further, to evaluate the role of aniline in indoles

biosynthesis, stable isotope precursor feeding experiments were done. Mass analysis of tryptophan, IAA and IAld from the labeled aniline fed cultures revealed no signals of labeled aniline incorporation into indole metabolites (Fig.18, 19) and this result suggest that aniline is not a precursor for indoles biosynthesis. Glyphosate mediated inhibition of indoles production and no stable isotope labeling of indoles suggest *de novo* biosynthesis of indoles *via* shikimate pathway. Previous report by Shanker *et al* (2006) suggested that presence of carbon source such as TCA cycle intermediates is required for indoles biosynthesis during aniline exposure in *Rhodobacter sphaeroides* OU5. Fumarate supplementation significantly enhanced the production of tryptophan, IAA and IAld compared to without supplementation during aniline exposure of strain JA2 (Fig. 20) and these results indicate that aniline induced indoles biosynthesis is dependent on carbon source availability. Stable isotope fumarate feeding of aniline exposed cells revealed incorporation of fumarate into tryptophan, IAA, IAld and MS/MS fragmentation analysis of the labeled indole metabolites revealed incorporation of stable atoms in indole nucleus (Fig. 22, 23). Isotopes labeled fumarate feeding experiments confirm that fumarate is indeed a precursor for indoles biosynthesis and forms a basic carbon skeleton of indoles. Though the aniline is not a precursor for indoles biosynthesis, aniline stress induced indoles biosynthesis in *R. benzoatilyticus* JA2 *via* shikimate pathway.

Aniline stress also induced tryptophan/indoles production in other purple nonsulfur bacteria (data not shown) possibly indicating a wide spread response to aniline stress. Stress induced indoles production was reported in some bacteria for example, antibiotic stress induced indole production in *E. coli* (Kuczynska-Wisnik *et al*., 2010; Han *et al*., 2011) and nutritional, environmental stress triggered IAA biosynthesis in *Azospirillum brasilense* SM (Mahindra and Sheela, 2009). Stress induced indole metabolites production was also observed in some eukaryotes such as yeast upon ethanol stress, oxidative stress caused by acifluorfen (herbicide) induced indolic compound (camalexin) biosynthesis *via* shikimate pathway in *Arabidopsis thaliana* (Zhao *et al*., 1998). In the present study, we found tryptophan or its derivatives production to toxic chemical stress and to the best of our knowledge this is the first report of indoles production to a toxic compound stress in bacteria. GC-MS data suggested modulation of tryptophan metabolism by aniline stress and this is well in accordance with the increased levels of tryptophan, other indole derivatives in aniline exposed cultures (Fig. 13C, D). However, biosynthesis of aromatic metabolites is stringently regulated at transcriptional and translational level in bacteria

(Panina *et al*., 2001; Gosset, 2009). Overproduction of tryptophan/indoles requires flux of carbon towards shikimate pathway in general (Ikeda, 2006). Carbon flux from common aromatic pathway (shikimate pathway) towards tryptophan biosynthesis is regulated by anthranilate synthase (TrpE) which catalyses the conversion of chorismate to anthranilate, a first committed step in indole/tryptophan biosynthesis (Maeda and Dudareva, 2012). Anthranilate synthase (TrpE) is the key enzyme of tryptophan biosynthesis as it is subject to transcriptional and feedback regulation by tryptophan (Panina *et al*., 2001), up-regulation of *TrpE* gene is key for fluxing carbon towards tryptophan production (Gu *et al*., 2012). Anthranilate synthase activity was significantly high in aniline induced cultures compared to control (Fig. 25C) and relative transcript levels of anthranilate synthase gene (*TrpE*) increased 5 folds after 60 min exposure to aniline (Fig. 27). Up-regulation of *TrpE* gene and its enzyme activity in aniline exposed cells corroborate well with accumulation of tryptophan and indoles in strain JA2. Similarly, overexpression of *TrpE* or feedback insensitive *TrpE* genes resulted in overproduction of tryptophan or its related metabolites in plants (Matsuda *et al*., 2005; Morino *et al*., 2005) as well as in bacteria (Ikeda, 2006; Gu *et al*., 2012).

Further, proteome analysis of aniline exposed cells revealed up-regulation of TrpE, tryptophan synthase α (TrpA), tryptophan synthase β (TrpB) subunits (Table. 7) which are pivotal for tryptophan synthesis and these results correlate well with accumulation of tryptophan in strain JA2. Up-regulation of tryptophan biosynthesis related genes were observed in *Salmonella enterica sv typhimurium* during biofilm formation (Hamilton *et al*., 2009) and in *Saccharomyces cerevisiae* upon ethanol stress (Hirasawa *et al*., 2007). Recent study on inactivation of the tryptophan attenuator and promoter swapping of *E. coli* resulted in increased transcription of trp operon genes and accumulation of tryptophan (Gu *et al*., 2012). Overproduction of tryptophan also dependents on availability of precursors (Ikeda, 2006) and tryptophan biosynthesis requires products of four other pathways such as erythrose-4-phosphate (E4P), ATP, phosphoribosyl pyrophosphate (PRPP), two phosphoenolpyruvate (PEP) molecules, L-glutamine, and L-serine (Xie *et al*., 2003). GC-MS metabolic profiling of aniline exposed cells revealed elevated levels of glutamine, pentose sugars and this indicate possible up-regulation of carbohydrate metabolism. Furthermore, this was supported by up-regulation of proteins related to pentose phosphate pathway (PPP) and gluconeogenesis in aniline exposed cells (Table. 7) and these pathways provide E4P, PEP and PRPP for aromatic metabolites biosynthesis

(Shen *et al.*, 2012). Proteomic analysis of aniline exposed cells revealed up-regulation of transketolase (tkt) phosphoenolpyruvate carboxykinase (pck) (Table. 7) and they are involved in synthesis of PEP, E4P. Overexpression of *tkt and pck* genes implicated in overproduction of aromatic compounds/tryptophan by providing precursors such as E4P and PEP (Gosset, 2009; Shen *et al*., 2012). Simultaneous overexpression of transketolase (*tkt*) (pentose phosphate pathway), PEP synthase (*pps*) resulted in higher yields of tryptophan in *E. coli* (Ikeda, 2006; Shen *et al*., 2012) and increased pool of E4P and PEP enhanced the production of tryptophan in bacteria (Gu *et al*., 2012). Surprisingly, in the present study other genes/proteins related to shikimate pathway were not up-regulated by aniline stress except for dehydroquinate synthase (Table.7). Several evidences suggests that modulation of genes involved in rate limiting steps are good enough to drive the carbon flux into a metabolic pathway (Gosset, 2009), in case of tryptophan biosynthesis it is anthranilate synthase which is rate limiting one (Ikeda, 2006). In the present study we found up-regulation of anthranilate synthase gene and accumulation of tryptophan to aniline stress. Extensive genetic manipulations and strain improvement methods were employed for overproduction of aromatic metabolites in general and tryptophan production in particular as their production is stringently regulated at all levels (Ikeda, 2006; Gosset, 2009; Gu *et al*., 2012). Interestingly in the present study aniline stress induces accumulation of tryptophan, indoles in spite of their complex biosynthetic and regulatory mechanisms reported in bacteria. Genome sequence of *R. benzoatilyticus* JA2 revealed presence of complete set of genes for aromatic amino acid (shikimate pathway) biosynthesis (Mohammed *et al*., 2011) however, organization of these genes and their regulation is not studied. Genomic insights of *R. benzoatilyticus* JA2 revealed that tryptophan biosynthetic genes are organized into two separate clusters possible as split-pathway operon (data not shown) and similar kind of split-operons organization was observed in other bacteria also (Xie *et al*., 2003). However, regulation of split-pathway Trp operon is not studied completely.

Organization of trp genes and their regulation vary greatly in bacteria and this is governed largely by life style/selective pressure under which bacteria thrive (Xie *et al*., 2003; Merino *et al*., 2008). Further, tryptophan beyond as precursor for proteins, it also serves other functions such as precursor for pigments, antibiotics and secondary metabolites at different physiological/developmental stages and this necessitates different regulatory mechanisms other than sensing tryptophan for protein synthesis (Xie *et al*.,

2003; Merino *et al*., 2008). In the present study overproduction of tryptophan was not observed in control (aniline unexposed) culture, indicating that tryptophan production is plausibly under some kind of regulation. However, aniline stress induces tryptophan overproduction in strain JA2 and thus it is tempting to speculate that tryptophan/indoles accumulation is possibly due to de-regulation of tryptophan biosynthesis or different kind of regulatory mechanism enabling cell to overproduce indoles. Furthermore, though phenylalanine, tyrosine and tryptophan share common metabolic pathway (shikimate pathway) aniline stress induced only tryptophan or its related metabolites production in strain JA2. Although it is unclear how tryptophan alone is biosynthesised in aniline stress we speculate plausible metabolic flux of carbon towards tryptophan biosynthesis. However, aromatic metabolites biosynthesis and its regulation is not studied in *R. benzoatilyticus* JA2 and gaining insights of these mechanisms is of particular interest in context of overproduction of aromatic compounds. Correlation between tryptophan production and IAA accumulation was observed in aniline exposed cells of *R. benzoatilyticus* JA2. Furthermore, tryptophan aminotransferase, tryptophan 2-monooxygenase activities were significantly high in aniline exposed cells (Fig. 26) which involve in tryptophan dependent IAA biosynthesis (Manulis *et al*., 1994; Spaepen *et al*., 2007). Tryptophan dependent IAA biosynthesis is predominant in many bacteria (Spaepen *et al*., 2007) and IAA production was also reported from some photosynthetic bacteria from indole/tryptophan. Induction of tryptophan catabolizing enzymes coupled well with IAA production and this suggests their plausible role in IAA biosynthesis from tryptophan in aniline exposed cells of strain JA2.

IAA biosynthesis in *R. benzoatilyticus* JA2

Tryptophan induces IAA and related indole metabolites production in many bacteria. *R. benzoatilyticus* JA2 was unable to grow on tryptophan as sole source of carbon however, strain JA2 transforms tryptophan to indole metabolites. Based on HPLC, LCMS analysis of tryptophan exposed culture, nine indole metabolites were identified of which six were IAA related metabolites this indicate metabolic diversity of tryptophan catabolism in strain JA2 (Table. 2). Further tryptophan stable isotope feeding experiments confirmed that tryptophan is indeed a precursor for identified indole metabolites as evidenced from labeling pattern (Fig. 30). Identification of indole-3-acetamide and tryptophan 2-monooxygenase activity in *R. benzoatilyticus* JA2 confirms the indole-3-acetamide (IAM) dependent IAA biosynthesis. Formation of indole-3-acetonitrile in

tryptophan exposed cultures and presence of nitrilase genes in the genome of *R. benzoatilyticus* JA2 suggest a possible indole-3-acetonitrile (IAN) pathway of IAA biosynthesis. Indole-3-pyruvic acid mediated IAA biosynthesis was reported in *R. benzoatilyticus* JA2 previously (Kumavath *et al*., 2010) and in the present study two tryptophan dependent IAA biosynthetic pathways (IAM and IAN) were identified in *R. benzoatilyticus* JA2 (Fig. 31). Multiple pathways of IAA biosynthesis were reported in bacteria (Gutierrez *et al*., 2009) and present study also indicates plausible degeneracy of IAA biosynthesis in *R. benzoatilyticus* JA2. Tryptophan dependent IAA biosynthesis is predominant in many bacteria except for *Azospirillum brasilence* where tryptophan independent IAA biosynthesis was observed (Spaepen *et al*., 2007). However, IAA production upon tryptophan supplementation and isotope labeled tryptophan feeding experiments suggest that IAA biosynthesis in *R. benzoatilyticus* JA2 is tryptophan dependent.

pH dependent regulation of indoles in *R. benzoatilyticus* JA2

Indoles are aromatic natural products produced by plants and microorganisms mainly from tryptophan. Wide variety of indolic compounds are produced by bacteria such as IAA, indole, indigo, violaceine, rebeccaamycine, trisindolin, isatin, indolmycin and indole terpenoids (Lee and Lee, 2010). Production of indoles was regulated by various endogenous and exogenous cues in bacteria (Spaepen *et al*., 2007; Lee and Lee, 2010; Han *et al*., 2011). *Rubrivivax benzoatilyticus* JA2 produces indoles from tryptophan, anthranilate and during aniline exposure. However, production of indoles was repressed when culture was grown on glucose as carbon source in strain JA2 (Fig. 32A). Similarly, presence of glucose in the medium repressed the indole formation in *E.coli*, tryptophan catabolism in *Bacillus* (Isaacs *et al*., 1994) and this phenomenon is called catabolic repression (Gorke and Stulke, 2008). In contrast to this, even after complete loss of glucose from media indoles production was not observed in *R. benzoatilyticus* JA2 and moreover, addition of glucose to malate grown culture has not resulted in repression of indoles. Furthermore, cyclic AMP (catabolic repression reliever) has not relieved the glucose mediated repression (Fig. 35B) suggesting that indoles production by *R. benzoatilyticus* JA2 may not be under glucose catabolite repression. Glucose can also effect the secondary metabolites production by catabolic repression independent mechanism in which, bacterial growth on metabolisible sugars like glucose decreases the culture pH by producing organic acids, which in turn regulates the production of

secondary metabolites (Haavik, 1974; Sole *et al*., 2000). Indoles production was repressed when culture pH was at 6.2-6.4 while pH of 8.4.-8.6 had no effect on indoles production irrespective of carbon source used for growth (Fig. 34). These results probably indicate that pH is regulating indoles production rather than carbon sources. Further, repression of indoles production at acidic pH (4.5-6.4) and induction of indoles production at alkaline pH (7-8.4) of the culture (Fig. 35A) confirms the role of pH in regulating indoles production by strain JA2. Production of secondary metabolites, penicillin (Espeso *et al*., 1993), prodigiosin (Sole *et al*., 1994), bacitracin (Haavik, 1974) were regulated by pH. Tryptophan, IAA and IAld levels were low at culture pH of 6.4 compared to that of 8.4 pH and this corroborates well with repression of indoles at pH 6.4 in strain JA2. Tryptophan catabolism and indoles production markedly effected by culture pH in pig faecal bacteria when grown on fructo-oligosaccharides, where acidic pH decreases the tryptophan catabolism (Xu *et al*., 2002). Repression of indoles production in glucose cultures of *R. benzoatilyticus* JA2 is plausibly due to low levels of tryptophan aminotransferase, tryptophan 2-monooxygenase and tryptophanase activities (Fig. 37) which are implicated in indoles production. Similarly, decreased production of indole, at acidic pH in intestinal bacteria was implicated to low levels of tryptophanase and indole-3-pyruvate lyase activities at acidic pH (Kim *et al*., 1995). Indoles production and tryptophan catabolism in *R. benzoatilyticus* JA2 is independent of carbon catabolic repression and the results suggest that like many of the secondary metabolites production by fungi is regulated by pH (Penalva *et al*., 2008), production of indoles by *R. benzoatilyticus* JA2 is under pH regulatory circuit and this is the first of its kind of report in anoxygenic photosynthetic bacteria.

Role of tryptophan or its derivatives (indoles) in plant development and defence is well established (Kang *et al*., 2009; Kazan and Manners, 2009). Though wide array of indolic compounds are produced by microorganisms their physiological role was discovered recently (Dudler and Eberl, 2006; Lee and Lee, 2010). Indoles act as an intraspecies, interspecies (Lee *et al*., 2007) inter kingdom signalling molecule. Some of the indoles produced by bacteria are implicated in biofilm formation, plasmid maintenance, cell division, stress tolerance, virulence, pathogenicity and drug resistance (Lee and Lee, 2010). In *Saccharomyces cerevisiae* ethanol stress enhanced the expression of tryptophan biosynthetic genes and overproduction of tryptophan enhanced the stress tolerance to ethanol (Hirasawa *et al*., 2007). Tryptophan biosynthesis in *Salmonella* was

implicated in biofilm formation and survival under different conditions (Hamilton *et al*., 2009). Exposure of *E. coli* to antimicrobial compounds prompted indole production and this was implicated in antibiotic resistance (Poole, 2012). Indole production also enhanced the acid resistance in *E. coli* (Hirakawa *et al*., 2010) and drug resistance in *Salmonella enterica sv typhimurium* (Nikaido *et al*., 2012). Stress induces IAA production in *Azospirillum brasilense* SM (Mahindra and Sheela, 2009) and in the present study we found IAA production in *R. benzoatilyticus* JA2 to aniline stress. Indole-3-acetic acid stimulated exopolysaccharide, biofilm formation and also enhanced the tolerance to several stress conditions (heat and cold shock, UV-irradiation, osmotic and acid shock and oxidative stress), to different toxic compounds in *E. coli* K12, (antibiotics, detergents and dyes) (Bianco *et al*., 2006). In the present study we found aniline stress induces tryptophan and its derivatives biosynthesis in *R. benzoatilyticus* JA2, we also found correlation between extracellular polymer substance formation and indoles production in strain JA2 (data not shown). EPS formation was implicated in bacterial stress tolerance (Halan *et al*., 2011). Consistent with the notion that indoles role in cell survival under stress, we speculate production of indoles in *R. benzoatilyticus* JA2 may have fitness benefit to bacteria under aniline stress.

Metabolic responses of *R. benzoatilyticus* JA2 to aniline stress

Increasing number of evidences suggest that environmental perturbations modulate metabolism in bacteria and metabolic remodelling enable the cell to survive under stress conditions. In the present study GC-MS based metabolic profiling was employed to decipher the global metabolic responses of strain JA2 to aniline stress. GC-MS based metabolic profiling followed by multivariate analysis such as HCA, PCA and PLS-DA revealed metabolic variations between control and aniline exposed cells (Fig. 41, 42). Similarly, nicotine stress in *Pseudomonas* sp HF-1 caused metabolic dissimilarities between control and nicotine stressed cells (Ye *et al*., 2012a). Heat stress in *E. coli* (Ye *et al*., 2012b), copper stress in *Pseudomonas fluorescens* ATCC 13525 (Booth *et al*., 2011) and nitrosative stress in *Pseudomonas fluorescens*13525 (Auger *et al*., 2011) induced marked metabolic variations between control and stressed cells. Differentially regulated metabolites of aniline exposed cells were identified by variable importance on projection (VIP) and *t*-test analysis, which are extensively used in field of metabolomics (Booth *et al*., 2011; Ye *et al*., 2012b). Functional annotation of differential metabolites revealed amino acid, carbohydrate, fatty acid, nitrogen, TCA cycle, butanoate, nucleic acid,

vitamin/cofactor, lipid and tryptophan metabolisms were mainly influenced by aniline stress (Fig. 45).

Amino acid metabolism was highly influenced by aniline at both metabolic and proteome levels and increased pools of amino acids or their derivatives are likely due to breakdown of denatured proteins or possibly due to *de novo* synthesis under stress (Ye *et al*., 2012b). Proteins related to amino acid biosynthesis (lysine, cysteine/methionine, arginine, tryptophan) were up-regulated and amino acid catabolism (branched chain amino acid, lysine, glycine entire histidine catabolism operon) proteins were down regulated to aniline stress (Table. 7) and this may be a possible mechanism to maintain the intracellular amino acids pool to meet the demands of increased proteins synthesis under stress (Miller *et al*., 2009). Amino acids on one hand are precursors for synthesis of proteins on the other hand they are also involved in the cell protection during stress. Elevated levels of glutamine, glutamate were observed in aniline stress (Fig. 44) and glutamate activates ClpB which is involved in disaggregation of proteins (Ye *et al*., 2012b). Glutamate is also a precursor for the synthesis of stress related metabolites, such as aminobutyrate and polyamines. Increased pools of saturated fatty acids (decanoic acid, octanoic acid) and decreased pool of unsaturated fatty acid (trans-hexadecanoic acid) were found in metabolome of aniline exposed cells. Further, fatty acid methyl esters analysis of aniline exposed cells revealed significantly high saturated to unsaturated fatty acid ratio (Table. 4) and this indicate a plausible tolerance mechanism to toxic compounds (Mrozik *et al*., 2004). High saturated to unsaturated fatty acid ratio decreases the membrane fluidity prevents entry of the toxic compounds into the cell and this is one of the effective mechanisms of toxic compound tolerance found in many bacteria (Ramos *et al*., 2002).

An elevated level of hydroxybutyric acid was observed in aniline exposed cells and hydroxybutyric acid is a precursor for polyhydroxyalkanoates (PHAs) in bacteria (Sudesh *et al*., 2000). Wide variety of stress conditions trigger accumulation of polyhydroxyalkanoates in bacteria and enhances the bacterial tolerance to stress (Susana castro *et al*., 2010). In agreement with previous studies of PHAs accumulation under stress, aniline exposed cells of *R. benzoatilyticus* JA2 accumulated significantly high levels of PHAs compared to control (Fig. 46). Further, this was supported by phasin family proteins up-regulation to aniline stress (Table. 7), which are involved in regulation of PHAs synthesis and formation, thus considered as markers of PHAs accumulation (York *et al*., 2001; Trautwein *et al*., 2008). Chemical characterization revealed PHAs of *R.*

benzoatilyticus JA2 as polyhydroxybutyrates (PHBs). Role of PHAs in stress tolerance is well reported in bacteria (Pham *et al*., 2004; Zhao *et al*., 2007) and accumulation of PHAs by *R. benzoatilyticus* JA2 may have a role in aniline tolerance.

Aniline exposed culture of *R. benzoatilyticus* JA2 becomes more viscous and often forms aggregates (data not shown), this kind of behaviour is possible due to formation of extracellular polymeric substance (EPS) as observed in some bacteria to stress (Chen *et al*., 2007; Halan *et al*., 2011). Further, formation of EPS by *R. benzoatilyticus* JA2 to aniline stress was confirmed by SEM (Fig. 48) and confocal microscopic (Fig. 49) analysis. Chemical characterization of EPS revealed it as heterogeneous mixture of polysaccharides, proteins, nucleic acids and lipids as observed in many EPS forming bacteria (Chen *et al*., 2007). EPS of *R. benzoatilyticus* is composed of 70% carbohydrates with glucose, glucosamine and gluconic acids as major monomers. EPS production requires continuous supply of precursors mainly carbohydrates and GC-MS analysis revealed that carbohydrate metabolism is highly influenced by aniline stress (Fig. 45). Further, we found xylose, glucose, gluconic acid and galactose levels were high in aniline exposed cells (Fig. 44) indicating possible increase of pentose phosphate, gluconeogenesis pathways. Proteome analysis revealed up-regulation of many proteins related to pentose phosphate, gluconeogenesis pathway (Table.7) further strengthening the view of enhanced carbohydrate metabolism. Pentose phosphate pathway and gluconeogenesis plausibly flux carbon flow to EPS synthesis and provide carbohydrate monomers for EPS production in *R. benzoatilyticus* JA2 as observed elsewhere in *Salmonella* during biofilm formation (White *et al*., 2010). EPS formation was also observed in other bacteria when exposed to heavy metals and toxic compounds (phenol, glutaraldehyde) (Fang *et al*., 2002) and styrene induced EPS formation in *Pseudomonas* (Halan *et al*., 2011). EPS formation was implicated in toxic compound resistance and tolerance to adverse conditions (Halan *et al*., 2011) and we speculate EPS formation by *R. benzoatilyticus* JA2 may enhance its tolerance to aniline stress.

Low levels of TCA cycle metabolites were found in aniline exposed cells (GC-MS metabolic profiling) indicating a possible down regulation of TCA cycle metabolism (Fig. 44). Further, this was supported by proteome analysis where all the proteins related to TCA cycle metabolism were down regulated (Table. 7). Down regulation of TCA cycle metabolism was observed in some bacteria as an adaptive mechanism to stress, for example toluene stress in *Pseudomonas* (Dominguez-Cuevas *et al*., 2006), heat stress in *E.*

coli (Ye *et al*., 2012b) and ethanol stress in S*taphylococcus epidermidis 1457* (Sadykov *et al*., 2010). Recent evidences suggests that TCA cycle acts as a signaling component in signal transduction under stress and modulates adaptation to stress (Sadykov *et al*., 2010) . In the present study we speculate down regulation of TCA cycle metabolism may flux the carbon towards biosynthesis of EPS, or indoles or an adaptive response to stress which has to be investigated. Metabolism of cofactor and vitamins was modulated both at metabolic (Fig. 45) and proteome level to aniline stress possible to meet the demands of active biosynthesis under stress (Fig. 58). Low levels of nucleosides were found in aniline exposed cells (Fig. 44) and further, proteome analysis indicated down regulation of replication and repair mechanisms (Table. 7). Growth of *R. benzoatilyticus* JA2 was stopped after aniline exposure and this correlates with the down regulation of replication. Taken together these results suggest down regulation of replication and repair as plausible energy conservation mechanism as observed in bacteria under stress (Ye *et al*., 2012b). Aniline stress also modulated the nitrogen, lipid, glyoxylate, and secondary metabolism of *R. benzoatilyticus* JA2 (Fig. 45) however due to lack of supporting data we could not explain their physiological relevance in the present study. Metabolic profiling of aniline exposed cells revealed a metabolic shift and remodelling of metabolism plausibly an adaptive response to aniline stress by *R. benzoatilyticus* JA2. Increasing evidences suggests that metabolic reprogramming and metabolic adaptions play significant role in bacterial tolerance to stress (Jozefczuk *et al*., 2010; White *et al*., 2010; Ye *et al*., 2012b).

Molecular responses to aniline stress

Survival of bacteria under diverse environmental conditions largely depends on sensing the changes and bringing up the necessary responses or adaptions at all levels of cellular processes. Proteomic analysis of the aniline exposed cells revealed up-regulation of histidine kinase, PAS/PAC hybrid histidine kinases (Table. 7) and these proteins are part of two component signal transduction system involved in sensing the environmental stimuli, thereby modulate gene expression for survival (Mascher *et al*., 2006). Transcriptional machinery was modulated to aniline stress and transcription factors such as H-NS (histone-like nucleotide structuring protein), Rnk (nucleoside diphosphate kinase regulator), LuxR and unknown two component transcription regulator were up-regulated (Table. 7). H-NS and LuxR are global transcription regulators and H-NS was implicated in regulation of metabolism, stress tolerance and biofilm formation in *E. coli* (Erol *et al*., 2006; Sanchez-Torres *et al*., 2010). Rnk regulator is involved in regulation of energy

metabolism (Shankar *et al*., 1995), proteins such as inosine-5'-monophosphate dehydrogenase, FoF1-ATP synthase were up-regulated (Table. 7) and this possibly indicate increased energy metabolism to stress. Nitrogen regulatory protein P-II, involved in regulation of nitrogen metabolism was up-regulated to aniline stress and possible indicating change in nitrogen metabolism. Further, supporting this GC-MS metabolic profiling revealed that nitrogen metabolism was influenced by aniline (Fig. 45). Adaptation to stress requires synthesis of proteins, in support of this we found up-regulation of proteins related to translation machinery such as 50S, 30S ribosomal subunits and trigger factor (Table. 7). This result suggests that active translation machinery is operating in aniline stress and synthesis of new proteins may enable stress tolerance.

Twelve proteins related to protein folding, sorting and degradation (Heat shock) were up-regulated in aniline exposed cells of *R. benzoatilyticus* JA2 which is 21% up-regulated proteins. Heat shock proteins such as GroES, GroEL, DnaK, DnaJ, Hsp20 and ClpB, were up-regulated to aniline stress (Table. 7). Heat shock proteins play a critical role in folding of newly synthesised proteins and refolding of misfolded proteins (Matallana-Surget *et al*., 2012). Similarly, heat shock proteins were up-regulated in *Pseudomonas putida* KT2440 to toluene, xylene and methyl benzoic acid stress (Segura *et al*., 2005; Dominguez-Cuevas *et al*., 2006). Accumulation of heat shock proteins in *Pseudomonas putida* strain R2 increased toluene resistance (Kobayashi *et al*., 2010). Overexpression of GroESL enhanced the solvent tolerance in *Lactobacillus paracasei* NFBC 338 (Kobayashi *et al*., 2010). In contrast to chaperones we found upregulation of ATP dependent ClpA, ClpP and Lon proteases in aniline exposed cells (Table. 7) they play critical role in degradation of irreversibly damaged/denatured proteins (Desmond *et al*., 2004). ATP dependent proteases such as ClpP and Lon proteases are implicated in stress tolerance in bacteria (Kruger *et al*., 2000). Chaperones and proteases are involved in protein quality control during stress, (Gerth *et al*., 1998). Up-regulation of different heat shock proteins in strain JA2 indicates their possible role in tolerance to aniline.

Membrane transport proteins (38%) are highly differential regulated to aniline stress mainly ABC transporters, porins, extracellular solute binding proteins and RND family proteins are up-regulated. RND efflux pumps and ABC transport proteins are implicated in extrusion of toxic compounds (Segura *et al*., 2012). RND family efflux

pumps are considered to be most important for solvent tolerance in Gram-negative bacteria (Ramos *et al*., 2002; Segura *et al*., 2012). Extrusion of solvent/toxic compounds from cell is considered as one of the effective mechanisms of solvent tolerance in bacteria (Aeschlimann, 2003; Fernandes *et al*., 2003). Up-regulation of proteins related to toxic compound extrusion such as RND efflux pumps, acriflavine resistance protein and putative efflux pump to aniline stress (Table. 7) indicate their possible role in extrusion of aniline and thereby enhancing the tolerance of *R. benzoatilyticus* JA2 to aniline. Stress related proteins such as alkaline phosphatase, universal stress protein (UspA), anti freezing protein and aminopeptidase were up-regulated to aniline stress (Table. 7). Surprisingly, oxidative stress related proteins such as catalase and peroxidase were down-regulated. Proteome analysis of aniline exposed cells revealed that among differential regulated proteins 15% were hypothetical proteins. Six hypothetical proteins were highly up-regulated (Table. 7) and accumulation of these proteins in aniline stress suggest their possible role in cell survival. Proteome analysis revealed differential regulation of several other proteins mainly of metabolism, transport and others with unspecified functions whose relevance could not be predicted in the present study with available data.

CONCLUSIONS

5.0 Conclusions

Successful colonization and survival of bacteria under extreme conditions require adaptations at all functional levels. One such extreme condition is created by xenobiotic compounds and bacteria degrade xenobiotic compounds for growth or adopt various stress response mechanisms to overcome the deleterious effects of toxic compounds. A systems approach is required to understand the complex stress response/adaptation mechanisms of the bacteria. Present study employed an integrated metabolomic and proteomics approach to decipher the stress responses of *R. benzoatilyticus* JA2 to aniline. Though aniline did not support the growth of strain JA2 as carbon or nitrogen source, it induced global metabolic changes. Marked metabolic variations between control and aniline exposed cells were evident from modulation of amino acid, carbohydrate, fatty acid, nucleic acid, nitrogen cycle, TCA, co-factor-vitamin, butanoate and tryptophan metabolism.

Aniline induced tryptophan and indoles biosynthesis *via* shikimate pathway in strain JA2 which was fumarate dependent and this was corroborated with up-regulation of tryptophan biosynthesis related proteins. Tryptophan catabolism and indoles production in strain JA2 is under pH regulatory circuit. Aniline stress induced secretion of extracellular polymeric substances (EPS) indicate a possible role of EPS in tolerating toxic compounds like aniline. Accumulation of polyhydroxybutanoates (PHBs) and phasin proteins to aniline stress indicates an adaptive response of strain JA2. More saturated fatty acids in the membranes of strain JA2 suggest a plausible membrane adaptation.

Differential regulation of membrane transport, folding sorting and degradation, transcription, translation, signal transduction, stress, replication and repair mechanisms indicate stress adaptive response of strain JA2 to aniline stress. Up-regulation of signal transduction, transcription and translation machinery suggest their possible role in sensing the environmental changes and in orchestrating gene expression, protein synthesis to thrive under stress (Fig. 60). Up-regulation of proteins related to energy metabolism to aniline stress indicates increased energy demand during stress adaptation. Up-regulation of gluconeogenesis, pentose phosphate pathway related proteins to aniline stress indicate a plausible metabolic flux of carbon towards EPS and tryptophan biosynthesis (Fig. 60).

Down regulation of proteins related to replication repair, β-oxidation of fatty acids and entire TCA cycle metabolism suggests a possible energy conservation mechanism to aniline stress (Fig. 60). Differential regulation of membrane transport proteins indicates export or import of specific molecules under stress. Up-regulation of proteins related to RND efflux pumps to aniline stress indicates a plausible toxic compound extrusion system in strain JA2 (Fig. 60). Up-regulation of heat shock proteins to aniline stress suggests their role in maintaining the protein quality control under stress and possible enhancement of tolerance to toxic compound (Fig. 60). Differential regulation of hypothetical proteins to aniline stress indicating their possible role in stress response.

Integrated metabolomic and proteomic approach revealed snapshot of metabolic and molecular responses of strain JA2 to aniline stress (Fig. 60). Aniline induces a global metabolic remodeling in strain JA2 leading to biosynthesis of fatty acids, PHAs, EPS, indoles and modulation of other metabolic pathways possibly as an adaptive mechanism. *Rubrivivax benzoatilyticus* JA2 employed multiple stress tolerance mechanisms such as membrane adaptation, toxic compound extrusion, EPS formation, heat shock proteins, PHAs accumulation and general stress related proteins to survive under aniline stress (Fig. 60). However, physiological relevance of some of the metabolic and proteomic responses to aniline stress could not be predicted in the present study. Multiple stress tolerance mechanisms observed in strain JA2 were also implicated in other bacterial systems, however, the physiological relevance and the mechanisms of aniline stress tolerance in strain JA2 are yet to be revealed. Present study sheds light on the possible potential targets of aniline tolerance in strain JA2.

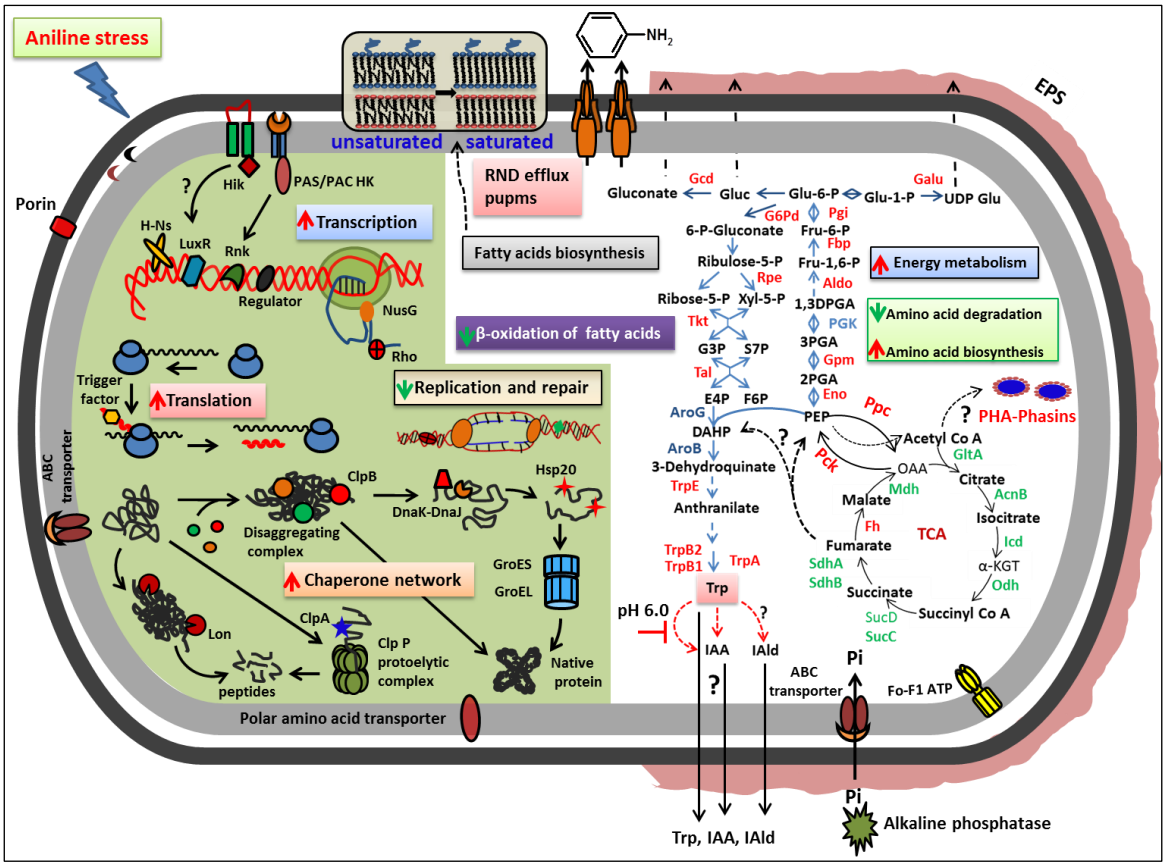

Fig. 60 Model depicting the metabolomic and proteomic responses of *R. benzoatilyticus* JA2 to aniline stress.

Model was generated by integrating the physiology, metabolomic and proteomic data. Functions of proteins or metabolites were assigned according to KEGG database (*www.genome.jp/**kegg***). Metabolic pathways were constructed based on bacterial metabolic pathways of KEGG and genome analysis of *R. benzoatilyticus* JA2.

Solid up arrows in red indicate up-regulation, down arrows in green indicate down regulation of cellular process. Proteins in red indicate up-regulation, green down regulation and blue indicate proteins whose levels were unchanged. Dotted arrows denote multiple steps in pathway; ?, unknown mechanism or reactions.

SucC, SucD, succinate synthase sub units; SdhA, B, succinate dehydrogenase subunits; Fh, fumarate hydratase; Mdh, malate dehydrogenase; GltA, citrate synthase; AcnB, aconitase; Icd, isocitrate dehydrogenase; Odh, oxoglutarate dehydrogenase; Pck, phosphoenolpyruvate carboxykinase; Ppc, phosphoenolpyruvate carboxylase; Eno, enolase; Gpm, glycerophosphomutase; PGk, Phosphoglycerate kinase; Aldo, aldolase, Fbp, fructose bisphosphatase; Pgi, phosphoglucoisomerase; Gcd, glucose dehydrogenase; G6Pd, glucose-6-phosphate dehydrogenase; Galu, UTP-glucose-1-phosphate uridyltransferase; Rpe, ribulose-5-phosphate epimerase; Tkt, Transketolase; Tal, transaldolase; AroG, 3-deoxy-D-arabinoheptulosonate 7-phosphate synthase; AroB, 3-dehydroquinate synthase; TrpE, anthranilate synthase; TrpA,TrpB, tryptophan synthase subunits.

REFERENCES

6.0 References

Aeschlimann, J.R. (2003) The role of multidrug efflux pumps in the antibiotic resistance of *Pseudomonas aeruginosa* and other gram-negative bacteria. Insights from the Society of Infectious Diseases Pharmacists. *Pharmacotherapy* **23**: 916-924.

Aruoja, V., Sihtmae, M., Dubourguier, H.C., and Kahru, A. (2011) Toxicity of 58 substituted anilines and phenols to algae *Pseudokirchneriella subcapitata* and bacteria *Vibrio fischeri*: comparison with published data and QSARs. *Chemosphere* **84**: 1310-1320.

Auger, C., Lemire, J., Cecchini, D., Bignucolo, A., and Appanna, V.D. (2011) The metabolic reprogramming evoked by nitrosative stress triggers the anaerobic utilization of citrate in *Pseudomonas fluorescens*. *PLoS One* **6**: e28469.

Azizan, K.A., Baharum, S.N., and Mohd Noor, N. (2012) Metabolic profiling of *Lactococcus lactis* under different culture conditions. *Molecules* **17**: 8022-8036.

Baumgarten, T., Sperling, S., Seifert, J., von Bergen, M., Steiniger, F., Wick, L.Y., and Heipieper, H.J. (2012a) Membrane Vesicle Formation as a Multiple-Stress Response Mechanism Enhances *Pseudomonas putida* DOT-T1E Cell Surface Hydrophobicity and Biofilm Formation. *Appl Environ Microbiol* **78**: 6217-6224.

Baumgarten, T., Vazquez, J., Bastisch, C., Veron, W., Feuilloley, M.G., Nietzsche, S. et al. (2012b) Alkanols and chlorophenols cause different physiological adaptive responses on the level of cell surface properties and membrane vesicle formation in *Pseudomonas putida* DOT-T1E. *Appl Microbiol Biotechnol* **93**: 837-845.

Behrends, V., Ryall, B., Zlosnik, J.E., Speert, D.P., Bundy, J.G., and Williams, H.D. (2012) Metabolic adaptations of *Pseudomonas aeruginosa* during cystic fibrosis chronic lung infections. *Environ Microbiol*. doi: 10.1111/j.1462-2920.2012.02840.x.

Bianco, C., Imperlini, E., Calogero, R., Senatore, B., Amoresano, A., Carpentieri, A. et al. (2006) Indole-3-acetic acid improves *Escherichia coli*'s defences to stress. *Arch Microbiol* **185**: 373-382.

Boon, N., Goris, J., De Vos, P., Verstraete, W., and Top, E.M. (2001) Genetic diversity among 3-chloroaniline- and aniline-degrading strains of the Comamonadaceae. *Appl Environ Microbiol* **67**: 1107-1115.

Booth, S.C., Workentine, M.L., Wen, J., Shaykhutdinov, R., Vogel, H.J., Ceri, H. et al. (2011) Differences in metabolism between the biofilm and planktonic response to metal stress. *J Proteome Res* **10**: 3190-3199.

Bradford, M.M. (1976) A rapid and sensitive method for the quantitation of microgram quantities of protein utilizing the principle of protein-dye binding. *Anal Biochem* **72**: 248-254.

Brennan, R.J., and Schiestl, R.H. (1997) Aniline and its metabolites generate free radicals in yeast. *Mutagenesis* **12**: 215-220.

Burton, K. (1956) A study of the conditions and mechanism of the diphenylamine reaction for the colorimetric estimation of deoxyribonucleic acid. *Biochem J* **62**: 315-323.

Campanac, C., Pineau, L., Payard, A., Baziard-Mouysset, G., and Roques, C. (2002) Interactions between biocide cationic agents and bacterial biofilms. *Antimicrob Agents Chemother* **46**: 1469-1474.

Cao, B., Shi, L., Brown, R.N., Xiong, Y., Fredrickson, J.K., Romine, M.F. et al. (2011) Extracellular polymeric substances from *Shewanella* sp. HRCR-1 biofilms: characterization by infrared spectroscopy and proteomics. *Environ Microbiol* **13**: 1018-1031.

Carmona, M., Zamarro, M.T., Blazquez, B., Durante-Rodriguez, G., Juarez, J.F., Valderrama, J.A. et al. (2009) Anaerobic catabolism of aromatic compounds: a genetic and genomic view. *Microbiol Mol Biol Rev* **73**: 71-133.

Cerniglia, C.E., Freeman, J.P., and Van Baalen, C. (1981) Biotransformation and toxicity of aniline and aniline derivatives of cyanobacteria. *Arch Microbiol* **130**: 272-275.

Chen, M.Y., Lee, D.J., Tay, J.H., and Show, K.Y. (2007) Staining of extracellular polymeric substances and cells in bioaggregates. *Appl Microbiol Biotechnol* **75**: 467-474.

de Sa Alves, F.R., Barreiro, E.J., and Fraga, C.A. (2009) From nature to drug discovery: the indole scaffold as a 'privileged structure'. *Mini Rev Med Chem* **9**: 782-793.

Delomenie, C., Fouix, S., Longuemaux, S., Brahimi, N., Bizet, C., Picard, B. et al. (2001) Identification and functional characterization of arylamine N-acetyltransferases in eubacteria: evidence for highly selective acetylation of 5-aminosalicylic acid. *J Bacteriol* **183**: 3417-3427.

Desmond, C., Fitzgerald, G.F., Stanton, C., and Ross, R.P. (2004) Improved stress tolerance of GroESL-overproducing *Lactococcus lactis* and probiotic *Lactobacillus paracasei* NFBC 338. *Appl Environ Microbiol* **70**: 5929-5936.

Dettmer, K., Aronov, P.A., and Hammock, B.D. (2007) Mass spectrometry-based metabolomics. *Mass Spectrom Rev* **26**: 51-78.

Dominguez-Cuevas, P., Gonzalez-Pastor, J.E., Marques, S., Ramos, J.L., and de Lorenzo, V. (2006) Transcriptional tradeoff between metabolic and stress-response programs in *Pseudomonas putida* KT2440 cells exposed to toluene. *J Biol Chem* **281**: 11981-11991.

Donlon, B.A., Razo-Flores, E., Field, J.A., and Lettinga, G. (1995) Toxicity of N-substituted aromatics to acetoclastic methanogenic activity in granular sludge. *Appl Environ Microbiol* **61**: 3889-3893.

Drzyzga, O., and Blotevogel, K.H. (1997) Microbial Degradation of Diphenylamine Under Anoxic Conditions. *Curr Microbiol* **35**: 343-347.

Drzyzga, O., Schmidt, A., and Blotevogel, K. (1996) Cometabolic transformation and cleavage of nitrodiphenylamines by three newly isolated sulfate-reducing bacterial strains. *Appl Environ Microbiol* **62**: 1710-1716.

Dudler, R., and Eberl, L. (2006) Interactions between bacteria and eukaryotes via small molecules. *Curr Opin Biotechnol* **17**: 268-273.

Dunlop, M.J. (2011) Engineering microbes for tolerance to next-generation biofuels. *Biotechnol Biofuels* **4**: 32.

Erol, I., Jeong, K.C., Baumler, D.J., Vykhodets, B., Choi, S.H., and Kaspar, C.W. (2006) H-NS controls metabolism and stress tolerance in *Escherichia coli* O157:H7 that influence mouse passage. *BMC Microbiol* **6**: 72.

Espeso, E.A., Tilburn, J., Arst, H.N., Jr., and Penalva, M.A. (1993) pH regulation is a major determinant in expression of a fungal penicillin biosynthetic gene. *EMBO J* **12**: 3947-3956.

Fan, X., Wang, J., Soman, K.V., Ansari, G.A., and Khan, M.F. (2011) Aniline-induced nitrosative stress in rat spleen: proteomic identification of nitrated proteins. *Toxicol Appl Pharmacol* **255**: 103-112.

Fang, H.H., Xu, L.C., and Chan, K.Y. (2002) Effects of toxic metals and chemicals on biofilm and biocorrosion. *Water Res* **36**: 4709-4716.

Fernandes, P., Ferreira, B.S., and Cabral, J.M. (2003) Solvent tolerance in bacteria: role of efflux pumps and cross-resistance with antibiotics. *Int J Antimicrob Agents* **22**: 211-216.

Flemming, H.C., Neu, T.R., and Wozniak, D.J. (2007) The EPS matrix: the "house of biofilm cells". *J Bacteriol* **189**: 7945-7947.

Galan, B., Dinjaski, N., Maestro, B., de Eugenio, L.I., Escapa, I.F., Sanz, J.M. et al. (2012) Nucleoid-associated PhaF phasin drives intracellular location and segregation of polyhydroxyalkanoate granules in *Pseudomonas putida* KT2442. *Mol Microbiol* **79**: 402-418.

Gerth, U., Kruger, E., Derre, I., Msadek, T., and Hecker, M. (1998) Stress induction of the *Bacillus subtilis* clpP gene encoding a homologue of the proteolytic component of the Clp protease and the involvement of ClpP and ClpX in stress tolerance. *Mol Microbiol* **28**: 787-802.

Glaeser, J., and Klug, G. (2005) Photo-oxidative stress in *Rhodobacter sphaeroides*: protective role of carotenoids and expression of selected genes. *Microbiology* **151**: 1927-1938.

Gorenflo, V., Steinbuchel, A., Marose, S., Rieseberg, M., and Scheper, T. (1999) Quantification of bacterial polyhydroxyalkanoic acids by Nile red staining. *Appl Microbiol Biotechnol* **51**: 765-772.

Gorke, B., and Stulke, J. (2008) Carbon catabolite repression in bacteria: many ways to make the most out of nutrients. *Nat Rev Microbiol* **6**: 613-624.

Gosset, G. (2009) Production of aromatic compounds in bacteria. *Curr Opin Biotechnol* **20**: 651-658.

Graham, T.L. (1991) A rapid, high resolution high performance liquid chromatography profiling procedure for plant and microbial aromatic secondary metabolites. *Plant Physiol* **95**: 584-593.

Grodowska, K., and Parczewski, A. Organic solvents in the pharmaceutical industry. *Acta Pol Pharm* **67**: 3-12.

Grodowska, K., and Parczewski, A. (2010) Organic solvents in the pharmaceutical industry. *Acta Pol Pharm* **67**: 3-12.

Gromova, M., and Roby, C. (2010) Toward *Arabidopsis thaliana* hydrophilic metabolome: assessment of extraction methods and quantitative 1H NMR. *Physiol Plant* **140**: 111-127.

Gu, P., Yang, F., Kang, J., Wang, Q., and Qi, Q. (2012) One-step of tryptophan attenuator inactivation and promoter swapping to improve the production of L-tryptophan in *Escherichia coli*. *Microb Cell Fact* **11**: 30.

Gutierrez, C.K., Matsui, G.Y., Lincoln, D.E., and Lovell, C.R. (2009) Production of the phytohormone indole-3-acetic acid by estuarine species of the genus *Vibrio*. *Appl Environ Microbiol* **75**: 2253-2258.

Haavik, H.I. (1974) Studies on the formation of bacitracin by *Bacillus licheniformis*: role of catabolite repression and organic acids. *J Gen Microbiol* **84**: 321-326.

Habe, H., and Omori, T. (2003) Genetics of polycyclic aromatic hydrocarbon metabolism in diverse aerobic bacteria. *Biosci Biotechnol Biochem* **67**: 225-243.

Halan, B., Schmid, A., and Buehler, K. (2011) Real-time solvent tolerance analysis of *Pseudomonas* sp. strain VLB120{Delta}C catalytic biofilms. *Appl Environ Microbiol* **77**: 1563-1571.

Halan, B., Buehler, K., and Schmid, A. (2012) Biofilms as living catalysts in continuous chemical syntheses. *Trends Biotechnol* **30**: 453-465.

Hamilton, S., Bongaerts, R.J., Mulholland, F., Cochrane, B., Porter, J., Lucchini, S. et al. (2009) The transcriptional programme of *Salmonella enterica serovar typhimurium* reveals a key role for tryptophan metabolism in biofilms. *BMC Genomics* **10**: 599.

Han, T.H., Lee, J.H., Cho, M.H., Wood, T.K., and Lee, J. (2011) Environmental factors affecting indole production in *Escherichia coli*. *Res Microbiol* **162**: 108-116.

Hirakawa, H., Hayashi-Nishino, M., Yamaguchi, A., and Nishino, K. (2010) Indole enhances acid resistance in *Escherichia coli*. *Microb Pathog* **49**: 90-94.

Hirasawa, T., Yoshikawa, K., Nakakura, Y., Nagahisa, K., Furusawa, C., Katakura, Y. et al. (2007) Identification of target genes conferring ethanol stress tolerance to *Saccharomyces cerevisiae* based on DNA microarray data analysis. *J Biotechnol* **131**: 34-44.

Ikeda, M. (2006) Towards bacterial strains overproducing L-tryptophan and other aromatics by metabolic engineering. *Appl Microbiol Biotechnol* **69**: 615-626.

Isaacs, H., Jr., Chao, D., Yanofsky, C., and Saier, M.H., Jr. (1994) Mechanism of catabolite repression of tryptophanase synthesis in *Escherichia coli*. *Microbiology* **140** (Pt 8): 2125-2134.

Jiao, Y., Cody, G.D., Harding, A.K., Wilmes, P., Schrenk, M., Wheeler, K.E. et al. (2010) Characterization of extracellular polymeric substances from acidophilic microbial biofilms. *Appl Environ Microbiol* **76**: 2916-2922.

Jones, E., and Fox, V. (2003) Lack of clastogenic activity of aniline hydrochloride in the mouse bone marrow. *Mutagenesis* **18**: 283-285.

Jozefczuk, S., Klie, S., Catchpole, G., Szymanski, J., Cuadros-Inostroza, A., Steinhauser, D. et al. (2010) Metabolomic and transcriptomic stress response of *Escherichia coli*. *Mol Syst Biol* **6**: 364.

Kahng, H.Y., Kukor, J.J., and Oh, K.H. (2000) Characterization of strain HY99, a novel microorganism capable of aerobic and anaerobic degradation of aniline. *FEMS Microbiol Lett* **190**: 215-221.

Kang, K., Kim, Y.S., Park, S., and Back, K. (2009) Senescence-induced serotonin biosynthesis and its role in delaying senescence in rice leaves. *Plant Physiol* **150**: 1380-1393.

Kazan, K., and Manners, J.M. (2009) Linking development to defense: auxin in plant-pathogen interactions. *Trends Plant Sci* **14**: 373-382.

Kim, E.A., Kim, J.Y., Kim, S.J., Park, K.R., Chung, H.J., Leem, S.H., and Kim, S.I. (2004) Proteomic analysis of *Acinetobacter lwoffii* K24 by 2-D gel electrophoresis and electrospray ionization quadrupole-time of flight mass spectrometry. *J Microbiol Methods* **57**: 337-349.

Kim, S.I., Kim, S.J., Nam, M.H., Kim, S., Ha, K.S., Oh, K.H. et al. (2002) Proteome analysis of aniline-induced proteins in *Acinetobacter lwoffii* K24. *Curr Microbiol* **44**: 61-66.

Kim, Y.G., Lee, J.H., Cho, M.H., and Lee, J. (2011) Indole and 3-indolylacetonitrile inhibit spore maturation in *Paenibacillus alvei*. *BMC Microbiol* **11**: 119.

Kobayashi, Y., Ohtsu, I., Fujimura, M., and Fukumori, F. (2010) A mutation in dnaK causes stabilization of the heat shock sigma factor sigma32, accumulation of heat shock proteins and increase in toluene-resistance in *Pseudomonas putida*. *Environ Microbiol* **13**: 2007-2017.

Konopka, A., Knight, D., and Turco, R.F. (1989) Characterization of a *Pseudomonas* sp. Capable of Aniline Degradation in the Presence of Secondary Carbon Sources. *Appl Environ Microbiol* **55**: 385-389.

Kotte, O., Zaugg, J.B., and Heinemann, M. (2010) Bacterial adaptation through distributed sensing of metabolic fluxes. *Mol Syst Biol* **6**: 355.

Kruger, E., Witt, E., Ohlmeier, S., Hanschke, R., and Hecker, M. (2000) The clp proteases of Bacillus subtilis are directly involved in degradation of misfolded proteins. *J Bacteriol* **182**: 3259-3265.

Kubota, H., Senda, S., Nomura, N., Tokuda, H., and Uchiyama, H. (2008) Biofilm formation by lactic acid bacteria and resistance to environmental stress. *J Biosci Bioeng* **106**: 381-386.

Kuczynska-Wisnik, D., Matuszewska, E., Furmanek-Blaszk, B., Leszczynska, D., Grudowska, A., Szczepaniak, P., and Laskowska, E. (2010) Antibiotics promoting oxidative stress inhibit formation of *Escherichia coli* biofilm via indole signalling. *Res Microbiol* **161**: 847-853.

Kumavath, R.N., Ramana Ch, V., and Sasikala, C. (2010a) Production of phenols and alkyl gallate esters by *Rhodobacter sphaeroides* OU5. *Curr Microbiol* **60**: 107-111.

Kumavath, R.N., Ramana Ch, V., and Sasikala, C. (2010b) L-Tryptophan catabolism by *Rubrivivax benzoatilyticus* JA2 occurs through indole 3-pyruvic acid pathway. *Biodegradation* **21**: 825-832.

Larimer, F.W., Chain, P., Hauser, L., Lamerdin, J., Malfatti, S., Do, L. et al. (2004) Complete genome sequence of the metabolically versatile photosynthetic bacterium *Rhodopseudomonas palustris*. *Nat Biotechnol* **22**: 55-61.

Lee, H.H., Molla, M.N., Cantor, C.R., and Collins, J.J. (2010) Bacterial charity work leads to population-wide resistance. *Nature* **467**: 82-85.

Lee, J., Jayaraman, A., and Wood, T.K. (2007a) Indole is an inter-species biofilm signal mediated by SdiA. *BMC Microbiol* **7**: 42.

Lee, J., Bansal, T., Jayaraman, A., Bentley, W.E., and Wood, T.K. (2007b) Enterohemorrhagic *Escherichia coli* biofilms are inhibited by 7-hydroxyindole and stimulated by isatin. *Appl Environ Microbiol* **73**: 4100-4109.

Lee, J.H., and Lee, J. (2010) Indole as an intercellular signal in microbial communities. *FEMS Microbiol Rev* **34**: 426-444.

Lee, J.H., Cho, M.H., and Lee, J. (2011) 3-indolylacetonitrile decreases *Escherichia coli* O157:H7 biofilm formation and *Pseudomonas aeruginosa* virulence. *Environ Microbiol* **13**: 62-73.

Liang, Q., Takeo, M., Chen, M., Zhang, W., Xu, Y., and Lin, M. (2005) Chromosome-encoded gene cluster for the metabolic pathway that converts aniline to TCA-cycle intermediates in *Delftia tsuruhatensis* AD9. *Microbiology* **151**: 3435-3446.

Liu, P., and Nester, E.W. (2006) Indoleacetic acid, a product of transferred DNA, inhibits vir gene expression and growth of *Agrobacterium tumefaciens* C58. *Proc Natl Acad Sci U S A* **103**: 4658-4662.

Liu, Z., Yang, H., Huang, Z., Zhou, P., and Liu, S.J. (2002) Degradation of aniline by newly isolated, extremely aniline-tolerant *Delftia* sp. AN3. *Appl Microbiol Biotechnol* **58**: 679-682.

Loffler, C., Eberlein, C., Mausezahl, I., Kappelmeyer, U., and Heipieper, H.J. (2010) Physiological evidence for the presence of a cis-trans isomerase of unsaturated fatty acids in *Methylococcus capsulatus* Bath to adapt to the presence of toxic organic compounds. *FEMS Microbiol Lett* **308**: 68-75.

Maeda, H., and Dudareva, N. (2012) The shikimate pathway and aromatic amino Acid biosynthesis in plants. *Annu Rev Plant Biol* **63**: 73-105.

Manulis, S., Shafrir, H., Epstein, E., Lichter, A., and Barash, I. (1994) Biosynthesis of indole-3-acetic acid via the indole-3-acetamide pathway in *Streptomyces* spp. *Microbiology* **140** (Pt 5): 1045-1050.

Mascher, T., Helmann, J.D., and Unden, G. (2006) Stimulus perception in bacterial signal-transducing histidine kinases. *Microbiol Mol Biol Rev* **70**: 910-938.

Matallana-Surget, S., Joux, F., Wattiez, R., and Lebaron, P. (2012) Proteome Analysis of the UVB-Resistant Marine Bacterium *Photobacterium angustum* S14. *PLoS One* **7**: e42299.

Matsuda, F., Yamada, T., Miyazawa, H., Miyagawa, H., and Wakasa, K. (2005) Characterization of tryptophan-overproducing potato transgenic for a mutant rice anthranilate synthase alpha-subunit gene (OASA1D). *Planta* **222**: 535-545.

Merino, E., Jensen, R.A., and Yanofsky, C. (2008) Evolution of bacterial trp operons and their regulation. *Curr Opin Microbiol* **11**: 78-86.

Metzger, U., Lankes, U., Fischpera, K., and Frimmel, F.H. (2009) The concentration of polysaccharides and proteins in EPS of *Pseudomonas putida* and *Aureobasidum pullulans* as revealed by 13C CPMAS NMR spectroscopy. *Appl Microbiol Biotechnol* **85**: 197-206.

Miller, C.D., Pettee, B., Zhang, C., Pabst, M., McLean, J.E., and Anderson, A.J. (2009) Copper and cadmium: responses in *Pseudomonas putida* KT2440. *Lett Appl Microbiol* **49**: 775-783.

Mohammed, M., Isukapatla, A., Mekala, L.P., Eedara Veera Venkata, R.P., Chintalapati, S., and Chintalapati, V.R. (2011) Genome sequence of the phototrophic betaproteobacterium *Rubrivivax benzoatilyticus* strain JA2T. *J Bacteriol* **193**: 2898-2899.

Morino, K., Matsuda, F., Miyazawa, H., Sukegawa, A., Miyagawa, H., and Wakasa, K. (2005) Metabolic profiling of tryptophan-overproducing rice calli that express a feedback-insensitive alpha subunit of anthranilate synthase. *Plant Cell Physiol* **46**: 514-521.

Mrozik, A., Piotrowska-Seget, Z., and Labuzek, S. (2004) Changes in whole cell-derived fatty acids induced by naphthalene in bacteria from genus *Pseudomonas*. *Microbiol Res* **159**: 87-95.

Murakami, S., Nakanishi, Y., Kodama, N., Takenaka, S., Shinke, R., and Aoki, K. (1998) Purification, characterization, and gene analysis of catechol 2,3-dioxygenase from the aniline-assimilating bacterium *Pseudomonas* species AW-2. *Biosci Biotechnol Biochem* **62**: 747-752.

Nikaido, E., Giraud, E., Baucheron, S., Yamasaki, S., Wiedemann, A., Okamoto, K. et al. (2012) Effects of indole on drug resistance and virulence of *Salmonella enterica serovar typhimurium* revealed by genome-wide analyses. *Gut Pathog* **4**: 5.

Oh, S., Go, G.W., Mylonakis, E., and Kim, Y. (2012) The bacterial signalling molecule indole attenuates the virulence of the fungal pathogen *Candida albicans*. *J Appl Microbiol* **113**: 622-628.

Oliveira, F.C., Dias, M.L., Castilho, L.R., and Freire, D.M. (2007) Characterization of poly(3-hydroxybutyrate) produced by *Cupriavidus necator* in solid-state fermentation. *Bioresour Technol* **98**: 633-638.

Panina, E.M., Vitreschak, A.G., Mironov, A.A., and Gelfand, M.S. (2001) Regulation of aromatic amino acid biosynthesis in gamma-proteobacteria. *J Mol Microbiol Biotechnol* **3**: 529-543.

Panina, E.M., Vitreschak, A.G., Mironov, A.A., and Gelfand, M.S. (2003) Regulation of biosynthesis and transport of aromatic amino acids in low-GC Gram-positive bacteria. *FEMS Microbiol Lett* **222**: 211-220.

Penalva, M.A., Tilburn, J., Bignell, E., and Arst, H.N., Jr. (2008) Ambient pH gene regulation in fungi: making connections. *Trends Microbiol* **16**: 291-300.

Pham, T.H., Webb, J.S., and Rehm, B.H. (2004) The role of polyhydroxyalkanoate biosynthesis by *Pseudomonas aeruginosa* in rhamnolipid and alginate production as well as stress tolerance and biofilm formation. *Microbiology* **150**: 3405-3413.

Pluvinage, B., Dairou, J., Possot, O.M., Martins, M., Fouet, A., Dupret, J.M., and Rodrigues-Lima, F. (2007) Cloning and molecular characterization of three arylamine N-acetyltransferase genes from *Bacillus anthracis*: identification of unusual enzymatic properties and their contribution to sulfamethoxazole resistance. *Biochemistry* **46**: 7069-7078.

Poole, K. (2012) Bacterial stress responses as determinants of antimicrobial resistance. *J Antimicrob Chemother* **67**: 2069-2089.

Powell, L.E. (1964) Preparation of Indole Extracts from Plants for Gas Chromatography and Spectrophotofluorometry. *Plant Physiol* **39**: 836-842.

Priester, J.H., Horst, A.M., Van de Werfhorst, L.C., Saleta, J.L., Mertes, L.A., and Holden, P.A. (2007) Enhanced visualization of microbial biofilms by staining and environmental scanning electron microscopy. *J Microbiol Methods* **68**: 577-587.

Quillaguaman, J., Guzman, H., Van-Thuoc, D., and Hatti-Kaul, R. (2010) Synthesis and production of polyhydroxyalkanoates by halophiles: current potential and future prospects. *Appl Microbiol Biotechnol* **85**: 1687-1696.

Ramos, J.L., Duque, E., Rodriguez-Herva, J.J., Godoy, P., Haidour, A., Reyes, F., and Fernandez-Barrero, A. (1997) Mechanisms for solvent tolerance in bacteria. *J Biol Chem* **272**: 3887-3890.

Ramos, J.L., Duque, E., Gallegos, M.T., Godoy, P., Ramos-Gonzalez, M.I., Rojas, A. et al. (2002) Mechanisms of solvent tolerance in gram-negative bacteria. *Annu Rev Microbiol* **56**: 743-768.

Reyes, L.H., Almario, M.P., and Kao, K.C. (2011) Genomic library screens for genes involved in n-butanol tolerance in *Escherichia coli*. *PLoS One* **6**: e17678.

Sadykov, M.R., Zhang, B., Halouska, S., Nelson, J.L., Kreimer, L.W., Zhu, Y. et al. (2010) Using NMR metabolomics to investigate tricarboxylic acid cycle-dependent signal transduction in *Staphylococcus epidermidis*. *J Biol Chem* **285**: 36616-36624.

Sanchez-Torres, V., Maeda, T., and Wood, T.K. (2010) Global regulator H-NS and lipoprotein NlpI influence production of extracellular DNA in *Escherichia coli*. *Biochem Biophys Res Commun* **401**: 197-202.

Sasikala, C., and Ramana, C.V. (1998) Biodegradation and metabolism of unusual carbon compounds by anoxygenic phototrophic bacteria. *Adv Microb Physiol* **39**: 339-377.

Schnell, S., Bak, F., and Pfennig, N. (1989) Anaerobic degradation of aniline and dihydroxybenzenes by newly isolated sulfate-reducing bacteria and description of *Desulfobacterium anilini*. *Arch Microbiol* **152**: 556-563.

Scribner, J.D., Fisk, S.R., and Scribner, N.K. (1979) Mechanisms of action of carcinogenic aromatic amines: an investigation using mutagenesis in bacteria. *Chem Biol Interact* **26**: 11-25.

Segura, A., Molina, L., Fillet, S., Krell, T., Bernal, P., Munoz-Rojas, J., and Ramos, J.L. Solvent tolerance in Gram-negative bacteria. *Curr Opin Biotechnol* **23**: 415-421.

Segura, A., Godoy, P., van Dillewijn, P., Hurtado, A., Arroyo, N., Santacruz, S., and Ramos, J.L. (2005) Proteomic analysis reveals the participation of energy- and stress-related proteins in the response of *Pseudomonas putida* DOT-T1E to toluene. *J Bacteriol* **187**: 5937-5945.

Segura, A., Molina, L., Fillet, S., Krell, T., Bernal, P., Munoz-Rojas, J., and Ramos, J.L. (2012) Solvent tolerance in Gram-negative bacteria. *Curr Opin Biotechnol* **23**: 415-421.

Shankar, S., Schlictman, D., and Chakrabarty, A.M. (1995) Regulation of nucleoside diphosphate kinase and an alternative kinase in *Escherichia coli*: role of the sspA and rnk genes in nucleoside triphosphate formation. *Mol Microbiol* **17**: 935-943.

Shanker, V., Rayabandla, S.M., Kumavath, R.N., Chintalapati, S., and Chintalapati, R. (2006) Light-dependent transformation of aniline to indole esters by the purple bacterium *Rhodobacter sphaeroides* OU5. *Curr Microbiol* **52**: 413-417.

Shen, T., Liu, Q., Xie, X., Xu, Q., and Chen, N. (2012) Improved production of tryptophan in genetically engineered *Escherichia coli* with TktA and PpsA overexpression. *J Biomed Biotechnol* 2012: 605219. doi:10.1155/2012/605219

Sheng, G.P., Yu, H.Q., and Wang, C.M. (2006) FTIR-spectral analysis of two photosynthetic hydrogen-producing [corrected] strains and their extracellular polymeric substances. *Appl Microbiol Biotechnol* **73**: 204-210.

Shimada, K., Itoh, Y., Washio, K., and Morikawa, M. (2012) Efficacy of forming biofilms by naphthalene degrading *Pseudomonas stutzeri* T102 toward bioremediation technology and its molecular mechanisms. *Chemosphere* **87**: 226-233.

Sikkema, J., de Bont, J.A., and Poolman, B. (1995) Mechanisms of membrane toxicity of hydrocarbons. *Microbiol Rev* **59**: 201-222.

Sole, M., Rius, N., and Loren, J.G. (2000) Rapid extracellular acidification induced by glucose metabolism in non-proliferating cells of *Serratia marcescens*. *Int Microbiol* **3**: 39-43.

Sole, M., Rius, N., Francia, A., and Loren, J.G. (1994) The effect of pH on prodigiosin production by non-proliferating cells of *Serratia marcescens*. *Lett Appl Microbiol* **19**: 341-344.

Spaepen, S., Vanderleyden, J., and Remans, R. (2007) Indole-3-acetic acid in microbial and microorganism-plant signaling. *FEMS Microbiol Rev* **31**: 425-448.

Steunou, A.S., Astier, C., and Ouchane, S. (2004) Regulation of photosynthesis genes in *Rubrivivax gelatinosus*: transcription factor PpsR is involved in both negative and positive control. *J Bacteriol* **186**: 3133-3142.

Sunayana, M.R., Sasikala, C., and Ramana Ch, V. (2005) Rhodestrin: a novel indole terpenoid phytohormone from *Rhodobacter sphaeroides*. *Biotechnol Lett* **27**: 1897-1900.

Suzuki, H., Ohnishi, Y., and Horinouchi, S. (2007) Arylamine N-acetyltransferase responsible for acetylation of 2-aminophenols in *Streptomyces griseus*. *J Bacteriol* **189**: 2155-2159.

Takenaka, S., Mulyono, Sasano, Y., Takahashi, Y., Murakami, S., and Aoki, K. (2006) Microbial transformation of aniline derivatives: regioselective biotransformation and detoxification of 2-phenylenediamine by *Bacillus cereus* strain PDa-1. *J Biosci Bioeng* **102**: 21-27.

Tang, J. (2011) Microbial metabolomics. *Curr Genomics* **12**: 391-403.

Tomas, C.A., Welker, N.E., and Papoutsakis, E.T. (2003) Overexpression of groESL in *Clostridium acetobutylicum* results in increased solvent production and tolerance, prolonged metabolism, and changes in the cell's transcriptional program. *Appl Environ Microbiol* **69**: 4951-4965.

Trautwein, K., Kuhner, S., Wohlbrand, L., Halder, T., Kuchta, K., Steinbuchel, A., and Rabus, R. (2008) Solvent stress response of the denitrifying bacterium "*Aromatoleum aromaticum*" strain EbN1. *Appl Environ Microbiol* **74**: 2267-2274.

Tremaroli, V., Workentine, M.L., Weljie, A.M., Vogel, H.J., Ceri, H., Viti, C. et al. (2009) Metabolomic investigation of the bacterial response to a metal challenge. *Appl Environ Microbiol* **75**: 719-728.

Udaondo, Z., Duque, E., Fernandez, M., Molina, L., Torre Jde, L., Bernal, P. et al. (2012) Analysis of solvent tolerance in Pseudomonas putida DOT-T1E based on its genome sequence and a collection of mutants. *FEBS Lett* **586**: 2932-2938.

Vangnai, A.S., and Petchkroh, W. (2007) Biodegradation of 4-chloroaniline by bacteria enriched from soil. *FEMS Microbiol Lett* **268**: 209-216.

Webby, C.J., Jiao, W., Hutton, R.D., Blackmore, N.J., Baker, H.M., Baker, E.N. et al. (2010) Synergistic allostery, a sophisticated regulatory network for the control of aromatic amino acid biosynthesis in *Mycobacterium tuberculosis*. *J Biol Chem* **285**: 30567-30576.

White, A.P., Weljie, A.M., Apel, D., Zhang, P., Shaykhutdinov, R., Vogel, H.J., and Surette, M.G. (2010) A global metabolic shift is linked to *Salmonella* multicellular development. *PLoS One* **5**: e11814.

Wijte, D., van Baar, B.L., Heck, A.J., and Altelaar, A.F. (2010) Probing the proteome response to toluene exposure in the solvent tolerant *Pseudomonas putida* S12. *J Proteome Res* **10**: 394-403.

Xie, G., Keyhani, N.O., Bonner, C.A., and Jensen, R.A. (2003) Ancient origin of the tryptophan operon and the dynamics of evolutionary change. *Microbiol Mol Biol Rev* **67**: 303-342, table of contents.

Xu, Z.R., Hu, C.H., and Wang, M.Q. (2002) Effects of fructooligosaccharide on conversion of L-tryptophan to skatole and indole by mixed populations of pig fecal bacteria. *J Gen Appl Microbiol* **48**: 83-90.

Yanofsky, C. (2007) RNA-based regulation of genes of tryptophan synthesis and degradation, in bacteria. *RNA* **13**: 1141-1154.

Ye, Y., Wang, X., Zhang, L., Lu, Z., and Yan, X. (2012a) Unraveling the concentration-dependent metabolic response of *Pseudomonas* sp. HF-1 to nicotine stress by (1)H NMR-based metabolomics. *Ecotoxicology* **21**: 1314-1324.

Ye, Y., Zhang, L., Hao, F., Zhang, J., Wang, Y., and Tang, H. (2012b) Global metabolomic responses of *Escherichia coli* to heat stress. *J Proteome Res* **11**: 2559-2566.

York, G.M., Junker, B.H., Stubbe, J.A., and Sinskey, A.J. (2001) Accumulation of the PhaP phasin of *Ralstonia eutropha* is dependent on production of polyhydroxybutyrate in cells. *J Bacteriol* **183**: 4217-4226.

Zhao, J., Williams, C.C., and Last, R.L. (1998) Induction of *Arabidopsis* tryptophan pathway enzymes and camalexin by amino acid starvation, oxidative stress, and an abiotic elicitor. *Plant Cell* **10**: 359-370.

Zhao, Y.H., Li, H.M., Qin, L.F., Wang, H.H., and Chen, G.Q. (2007) Disruption of the polyhydroxyalkanoate synthase gene in *Aeromonas hydrophila* reduces its survival ability under stress conditions. *FEMS Microbiol Lett* **276**: 34-41.

PUBLICATIONS

Curr Microbiol (2010) 61:285–290
DOI 10.1007/s00284-010-9609-2

Aniline-Induced Tryptophan Production and Identification of Indole Derivatives from Three Purple Bacteria

Md. Mujahid · Ch. Sasikala · Ch. V. Ramana

Received: 7 January 2010 / Accepted: 4 February 2010 / Published online: 21 February 2010

Abstract Growth on aniline by three purple non-sulfur bacteria (*Rhodospirillum rubrum* ATCC 11170, *Rhodobacter sphaeroides* DSM 158, and *Rubrivivax benzoatiliticus* JA2) as nitrogen, or carbon source could not be demonstrated. However in its presence, production of indole derivatives was observed with all the strains tested. At least 14 chromatographically (HPLC) distinct peaks were observed at the absorption maxima of 275–280 nm from aniline induced cultures. Five major indoles were identified based on HPLC and LC–MS/MS analysis. While tryptophan was the major common metabolite for all the three aniline induced cultures, production of indole-3-acetic acid was observed with *Rvi. benzoatilyticus* JA2 alone, while indole-3-aldehyde was identified from *Rvi. benzoatilyticus* JA2 and *Rba. sphaeroides* DSM 158. Indole-3-ethanol was identified only from *Rsp. rubrum* ATCC 1170 and anthranilic acid was identified from *Rba. sphaeroides* DSM 158.

Introduction

Aniline is a primary aromatic amine widely used in the manufacturing of plastic, dyes, paints, herbicides, and pesticides. Biogenesis of aniline through microbiological transformation of nitroaromatic compounds and from aniline-based pesticides [11] augments its release into the environment which was mainly thought to be due to industrial effluents [3, 7]. Aniline is toxic, mutagenic and hence its fate in the environment is of serious concern [12]. Aniline can either be degraded by microorganisms under oxic [8]/anoxic [8, 21] environments or transformed into compounds like; acetanilide, formanilide, phenylhdroxylamine, nitrobenzene, and *N*-methylaniline [6, 13]. Though there are reports of indole derivatives production [4, 25] in aniline presence, these indole derivatives were not characterized and need attention since microbiological activation process is more dangerous than the initial substrates [1]. In the present communication, we extended our work [25] in identifying the indole derivatives produced by purple bacteria in the presence of aniline.

Md. Mujahid · Ch. V. Ramana (✉)
Department of Plant Sciences, School of Life Sciences, University of Hyderabad, P.O. Central University, Hyderabad 500 046, India
e-mail: r449@sify.com; chvrsl@uohyd.ernet.in

Ch. Sasikala
Bacterial Discovery Laboratory, Center for Environment, Institute of Science and Technology, JNT University, Kukatpally, Hyderabad 500 085, India
e-mail: sasi449@yahoo.ie

Materials and Methods

Organisms and Growth Conditions

Rhodobacter sphaeroides DSM158^T, *Rhodospirillum rubrum* ATCC 11170^T, and *Rubrivivax benzoatiliticus* JA2^T were grown photoheterotrophically (anaerobic, 30°C; light 2,400 lux) in a mineral medium [2] supplemented with malate (22 mM) as carbon source and ammonium chloride (7 mM) as nitrogen source in fully filled screw cap test tubes (10 × 100 mm)/reagent bottles (250 ml) at pH 6.8, 30°C and at a light intensity of 30 μE m^{-2} s^{-1}. An elevated (10 g l^{-1}) level of yeast extract was used for the growth of *Rsp. rubrum*. Malate and ammonium chloride were replaced with aniline when aniline was used as carbon or nitrogen source.

Aniline Induction Assay

Bacteria were allowed to grow photoheterotrophically for 48 h to which, autoclaved aniline or its derivatives and fumarate were added to give a final concentration of 25 and 13 mM, respectively. Phototrophic incubations were continued for further 48 h and the cells were harvested by centrifugation (10000 rpm, 10 min at 4°C) and the supernatant was used for estimation of indoles, aniline, and for the extraction of metabolites. Data pertain to the experiments done in duplicates and form three independent experiments.

Extraction of Metabolites

Culture supernatant was concentrated to dryness under vacuum in rotary flash evaporator (Heidolph, Germany) at 45°C. After complete dryness, the brown residue was fractionated according to the protocol used by Powell [16]. The acidic, aqueous, basic, and neutral fractions were tested for the presence of indoles using Sapler's reagent [5]. Fractions were evaporated to dryness using flash evaporator, redissolved in methanol (1 ml), filtered (0.22 μm membrane), and used for HPLC and mass spectral analysis.

HPLC Analysis

HPLC analysis was performed on Shimadzu (LC- 20AT) system equipped with photodiode array detector and Phenomenex C-18 column (Luna, 5 μm, 250 × 4.6 mm). Gradient method was employed for separation of metabolites for 30 min. Acetic acid (1% v/v) and acetonitrile were used as mobile phase. Linear gradient of 0–55% acetonitrile for 25 min followed by step increase to 100% acetonitrile held for 3 min and finally returns to 1% acetic acid wash. Flow rate was 1.5 ml/min; injection volume was 20 μl, and the metabolites were detected at 230, 280, and 350 nm. UV spectra were recorded by photodiode array detector and metabolites were quantified with reference to the peak areas of known concentrations of authentic standards.

ESI–LC–MS/MS Analysis

Mass analysis was performed on MicroTOF-Q (Brukars deltanoics) mass spectrometer coupled to HPLC (Agilent 1200 series) equipped with UV–VIS detector. Metabolites were separated on reverse phase column (water's C-18, 5 μm, 150 × 4.6 mm). HPLC conditions were as same as described above, except the flow rate was 0.8 ml/min and detection was done at 280 nm, with a post column split effluent was introduced into electro spray ionization (ESI) ion source (80°C, Cone voltage 15–25 V). ESI (+) ion mode was used to detect molecular ion mass ($[M]^+$) and fragmentation was obtained by collision energy of 5–20 eV depending upon the nature of the molecule. Mass spectra were recorded from 50 to 1000 Da.

Results and Discussion

Utilization of Aniline for Growth by Purple Bacteria

Growth of the three purple non-sulfur bacteria could not be demonstrated when aniline (1 mM) was used as sole source of carbon or nitrogen (data not shown). Utilization of aniline (0.4 mM) was observed with *Rvi. benzoatilyticus* and 95% of the cells of the tested purple bacteria were viable even at 25 mM aniline. There are no reports so far (to our knowledge) on the photosynthetic bacteria that can grow at the expense of aniline as carbon source. However, aniline supported growth of a few other bacteria as a sole source of carbon or nitrogen [8]. Although aromatic hydrocarbon catabolism and subsequent utilization for growth is restricted to a few purple non-sulfur bacteria [17], their ability to transform some of the aromatic compounds is interesting [20].

Production of Indole Derivatives by Purple Bacteria

Ten species of five genera of purple non-sulfur bacteria (*Rubrivivax gelatinosus* ATCC 17011, *Rhodospirillum rubrum* ATCC 11170, *Rhodopseudomonas faecalis* JCM 11668, *Pheospirillum sp.*JA 317, *Rhodopseudomonas palustris* ATCC 17001, *Rhodobacter sphaeroides* ATCC 17023, *Rhodobacter maris* JA 276, *Rhodobacter aesturii* JA 296, *Rhodobacter azatoformensis* KA 25, *Rhodobacter* JA 192, *Rhodobacter sp.*) were tested for production of indole derivatives in the presence of aniline (25 mM). Production of indole derivatives was observed with all the 10 aniline-induced strains, while the same was not observed in control (without aniline induction; data not shown). *Rhodobacter sphaeroides* DSM 158, *Rhodospirillum rubrum* ATCC 11170, *Rubrivivax gelatinosus* ATCC 17011, and *Rubrivivax benzoatilyticus* JA2 produced high (0.34–0.45 mM) concentrations of indole derivatives. These results indicated that aniline-induced indole derivatives production could be wide spread among anoxygenic photosynthetic bacteria.

Production of Indole Derivatives from Aniline Derivatives

Except for aniline and 2-aminobenzoate-induced cultures, indole derivatives production was not observed from 10 different aniline derivatives tested (aniline, 2-aminobenzoate, 3-

aminobenzoate, sulphanilate, 4-nitroaniline, 4-bromoaniline, 4-aminophenol, 1,2-diaminophenol, 2,6-dicholoroaniline, 3, 5-dimethylaniline). One possible reason for the specificity of aniline(s) could be due to the regioselectivity as observed in case of transformation of aniline derivatives to acetanilide by *Bacillus cereus* [24].

Identification of Indole Derivatives

Rubrivivax benzoatilyticus JA2

Total yields of indole derivatives (0.34 mM) were in near stoichiometry to the aniline consumed (0.4 mM). Five chromatographically distinct peaks were observed from the aqueous fraction of aniline induced *Rvi. benzoatilyticus* JA2. Peak with retention time (R_t) of 9.5 min was identified as tryptophan (Fig. 1a, b), which had identical UV absorption spectrum and co-eluted with standard. Mass spectral analysis of this metabolite shown a molecular ion peak at 205$[M]^+$, MS/MS fragmentation 205$[M]^+$, 188$[M–NH_3]^+$, 146, 118 (Fig. 2a) which was well in accordance with the mass spectrum of authentic tryptophan.

Neutral and acidic fractions of *Rvi. benzoatilyticus* JA2 gave positive test (orange-pink color with Salper's reagent) for indole derivatives, while the aqueous fraction was negative. HPLC analysis of acidic and neutral fractions of *Rvi. benzoatilyticus* JA2 indicated 5 and 7 chromatographically distinct peaks, respectively. Major metabolite of acidic fraction had a R_t of 19.3 min and was identified as indole 3-acetic acid (IAA); (Fig. 3a) which was authenticated by co-elution and by identical UV absorption spectrum using standard. Further, molecular ion peak of 176$[M]^+$ and MS/MS fragmentation 176$[M]^+$,130$[M–COOH]^+$; (Fig. 2b) confirmed the major metabolite of acidic fraction as IAA. Production of IAA from indole was reported in *Rba. sphaeroides* OU5 earlier [19]. The neutral

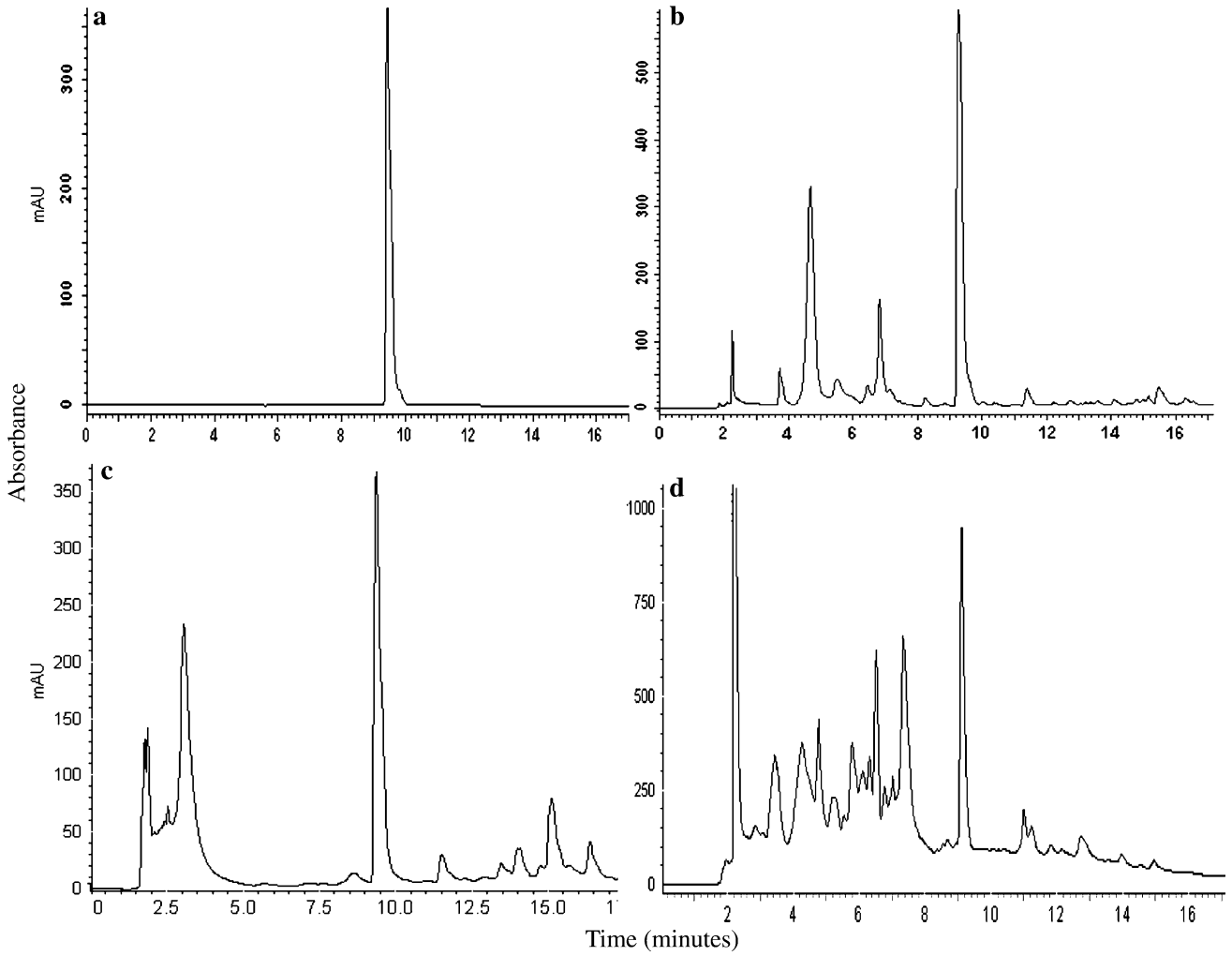

Fig. 1 HPLC chromatograms of aqueous fractions obtained from aniline-induced culture supernatants. Authentic tryptophan (**a**), *Rvi. benzoatilyticus* JA2 fraction (**b**), *Rba. sphaeroides* DSM 158 fraction (**c**), and *Rsp. rubrum* fraction (**d**). Peak at 9.5 min (R_t) corresponds to tryptophan

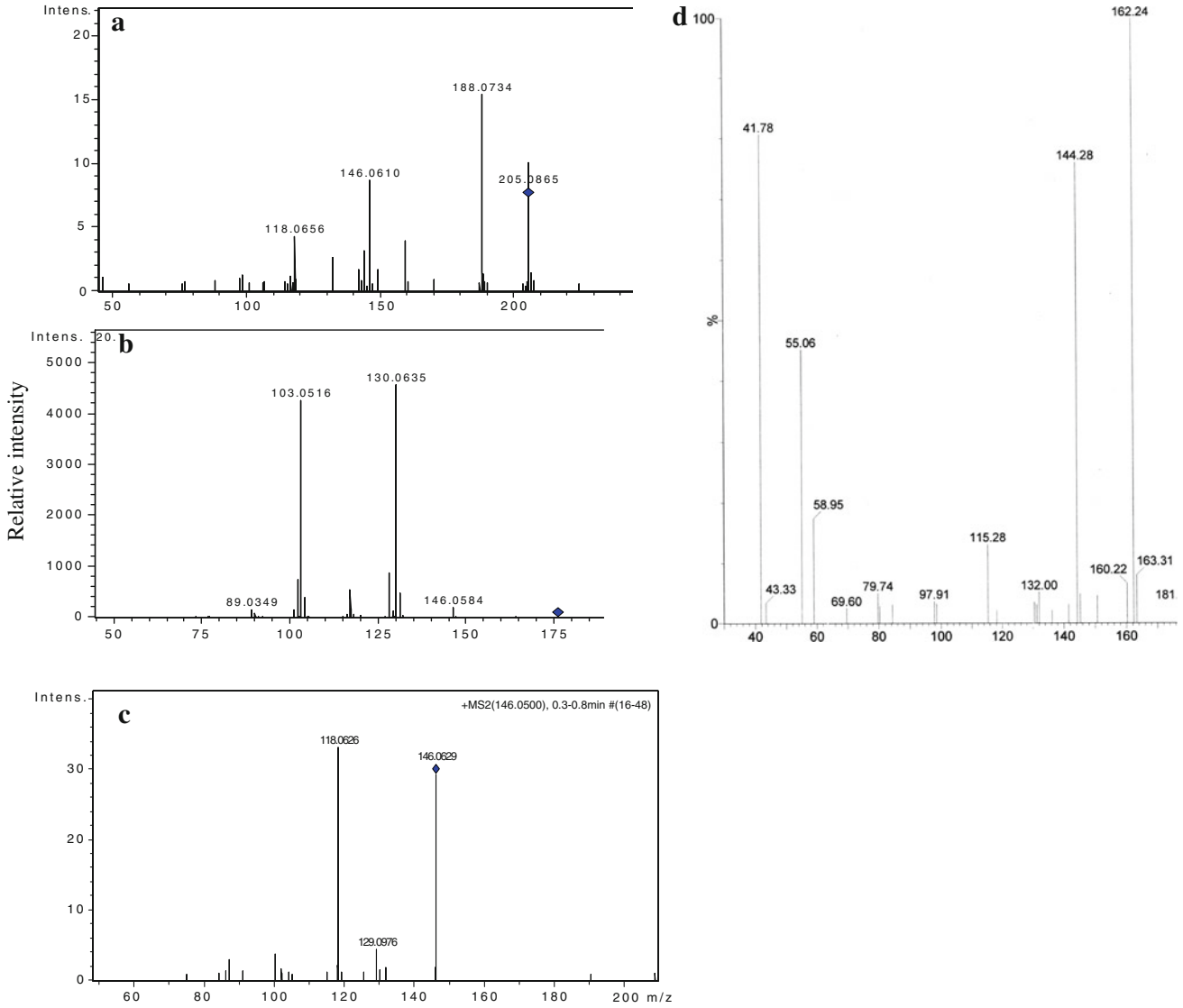

Fig. 2 Mass spectra of different indole metabolites obtained from mass analysis of HPLC peaks corresponding to indole metabolites obtained from aniline-induced cultures of all three purple bacteria. Representative mass spectrum of tryptophan (**a**), mass spectra of IAA (**b**), IAld (**c**), and IET (**d**)

fraction had a major metabolite with 18.7 R_t which was identified as indole-3-aldehyde based on its co-elution with authentic indole-3-aldehdye (Fig. 3b) and from the mass spectral analysis (molecular ion peak of 146[M]$^+$, MS/MS fragmentation 146[M]$^+$, 129[M–OH]$^+$, 118[M–CHO]$^+$ (Fig. 2c). Though indole-3-acetic acid and indole-3-aldehyde were also produced in control (without aniline), the concentration of these metabolites was significantly high (3-fold) in presence of aniline (Fig. 3a, b), while tryptophan could not be detected in control.

Rhodobacter sphaeroides DSM 158

Aqueous and neutral (but not acidic) fractions obtained from aniline-induced cultures of *Rba. sphaeroides* DSM158 gave positive for indole derivatives test. Eight chromatographically (HPLC) distinct peaks were observed from the aqueous fraction. Peak with R_t 9.5 min was identified as tryptophan based on its identical retention time (Fig. 1c) and after co-elution with authentic tryptophan standard. Mass analysis of this metabolite indicated a molecular ion peak at 205[M]$^+$ confirming the metabolite as tryptophan. The other metabolite with 15.1 min (R_t) having a UV λ_{max} of 226, 238, 288 with a molecular ion peak at 210[M]$^+$ and MS/MS fragmentation 210[M]$^+$, 192, 164, 150,146 could not be identified. Of the nine chromatographically distinct peaks, from acidic fraction of *Rba. sphaeroides* DSM 158, a peak with 14.6 min (R_t) was identified as anthranilic acid based on its retention time (Fig. 3c), co-elution with authentic anthranilic acid and mass spectral analysis of this metabolite

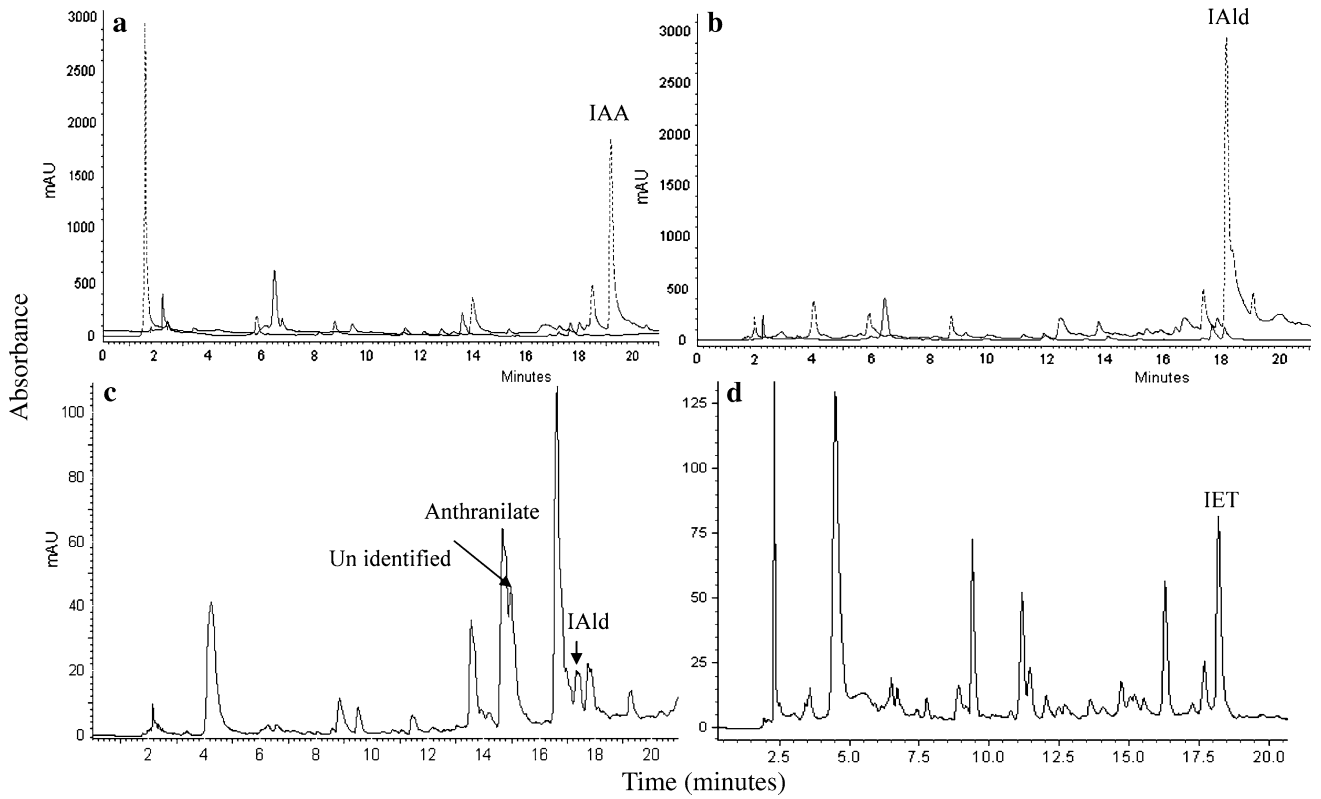

Fig. 3 HPLC chromatograms of various fraction obtained from aniline induced culture supernatants. Acidic (**a**), neutral fractions (**b**) from *Rvi. benzoatilyticus* JA2; acidic fraction (**c**) from *Rba. sphaeroides* DSM 158; neutral fraction (**d**) from *Rsp. rubrum* ATCC 11170. *IAA* Indole-3-acetic acid, *IAld* indole-3-aldehyde, *IET* indole-3-ethanol. *Dotted line* chromatograms are from aniline-induced culture supernatant and *solid line* chromatograms are from control culture supernatant

shown a molecular ion peak of 138$[M]^+$ with MS/MS fragmentation 138$[M]^+$, 120$[M–OH]^+$. Anthranilic acid production was observed only in aniline induced cultures (even not from tryptophan) of *Rba. sphaeroides* DSM 158 but not with other two strains. Anthranilic acid is an intermediate in indole biosynthesis as well in the indole or tryptophan degradation in bacteria [9].

Rhodospirillum rubrum ATCC 11170

Neutral fraction HPLC analysis of *Rsp. rubrum* ATCC 11170 had seven chromatographically distinct peaks. R_t of 18.1 min (Fig. 3d) was identical with that of authentic indole-3-ethanol (IET) and co-eluted with standard. Mass spectral analysis of metabolite corresponding to the indole-

Table 1 Indole derivatives identified from aniline-induced culture supernatants of all three species of purple bacteria

Compound	R_t (min)	UV λ_{Max}	m/z	Concentration (μg ml^{-1})		
				*Rvi. benzoatilyticus*JA2	*Rba. sphaeroides* DSM158	*Rsp. rubrum* 11170
Tryptophan	9.5	227, 272, 278, 287	205$[M]^+$	3.0	2.5	2.9
IAA	19.1	228, 273, 279, 288	176$[M]^+$	0.9	nd	nd
IAld	18.7	214, 243, 260, 297	146$[M]^+$	0.3	1.5	nd
IET	18.1	215, 225, 281	162$[M]^+$	nd	nd	0.6
Anthranilate	14.6	219, 241, 341	138$[M]^+$	nd	3.75	nd
Unidentified	15.1	226, 238, 288	210$[M]^+$	nd	ud	nd

nd not detected, *ud* un determined

3-ethanol indicated a molecular ion peak of 162[M]$^+$ with MS/MS fragmentation of 162[M]$^+$, 144[M–HOH]$^+$, 132, 117 (Fig. 2d) and it was identical to that of authentic mass spectrum of IET and this metabolite was identified as IET. HPLC analysis of aniline-induced fractions of *Rsp. rubrum* indicated eight chromatographically distinct peaks of which peak at 9.5 (R_t) was identified as trytophan (Fig. 1d) based on its identical retention time with authentic tryptophan and mass analysis revealed a molecular ion peak at 205 which is consistent with authentic tryptophan.

From the aniline-stressed bacterial cultures, indole [4] or indole esters [15, 23, 25] were identified, while five (Table 1) other indole derivatives are recognized in this study, as against a number of unidentified. Physiological stress induces the formation of indole [10] or its derivatives [14] in bacteria and production of indoles by the purple bacteria could be due to the physiological response to aniline. Tryptophan was identified as a major metabolite under aniline stress by purple bacteria, which was otherwise possible only with regulatory mutants [22] or by providing precursors [18].

Conclusions

It is premature to conclude from the experimental data if aniline would be the precursor for the observed indole derivatives or these are produced due to stress response. However, evidence of utilization of aniline (0.4 mM) and near stoichiometric yield of indole derivatives by *Rvi. benzoatilyticus* JA2 support [4] the possibility of an alternate pathway in the biosynthesis of indoles directly from aniline. To the best of our knowledge, this is the first report of tryptophan production under stress induced by aromatic compounds.

Acknowledgments Md. Mujahid thanks CSIR, Government of India for the award of JRF. Facilities used under the FIST and CAS supported by DST and UGC, Government of India, respectively, are duly acknowledged.

References

1. Alexander M (1999) Biodegradation and bioremediation. Academic press, San Diego
2. Biebl H, Pfennig N (1981) Isolation of members of the family *Rhodospirillaceae*. In: Starr MP, Stolp H, Truper HG, Balows A, Schlegel HG (eds) The prokaryotes. Springer, New York
3. Chengbin X, Jun N, Hai Y, Xundong S, Jiye HU (2009) Biodegradation of aniline by a newly isolated *Delftia* sp. XYJ6. Chin J Chem Eng 17:500–505
4. Drazyga O, Schmid A, Blotevogel KH (1996) Cometabolic transformation and cleavage of nitrodiphenylamines by three newly isolated sulfate-reducing bacterial strains. Appl Environ Microbiol 62:1710–1716
5. Gordon SA, Paleg LG (1957) Quantitative measurement of indole acetic acid. Plant Physiol 10:37–48
6. Harvey PJ, Companella BF, Castro PM, Harms H, Lichtfouse E, Schaffner AR, Smrek S, Wesck-Reichhart D (2002) Phytoremediation of polyaromatic hydrocarbons, aniline and phenols. Environ Sci Pollut Res Int 9:29–47
7. Junminx L, Zexin J, Binbin Y (2010) Isolation and characterization of aniline degradation slightly halophilic bacterium, *Erwinia sp*. StrainHSA6. Microbiol Res (in press). doi:10.1016/j.micres.2009.09.003
8. Kahng HY, Kukor JJ, Oh KH (2000) Characterization of strain HY99, a novel microorganism capable of aerobic and anaerobic degradation of aniline. FEMS Microbiol Lett 190:215–221
9. Kurnasov O, Jablonski L, Polanuyer B, Dorrestein P, Begley T, Osterman A (2003) Aerobic tryptophan degradation pathway in bacteria: novel kynurenine formamidase. FEMS Microbiol Lett 227:219–227
10. Lee J, Lee JH (2010) Intercellular signal indole in microbial community. FEMS Microbiol Rev (in press). doi:10.1111/j.1574-6976.2009.00204.x
11. Liang Q, Takeo M, Chen M, Zhang W, Xu Y, Lin M (2005) Chromosome encoded gene cluster for the metabolic pathway that converts aniline to TCA-cycle intermediates in *Delftia tsuruthatenesis* AD9. Microbiology 151:3435–3446
12. Liu Z, Yang H, Huang Z, Zhou P, Liu SJ (2002) Degradation of aniline by newly isolated, extremely aniline-tolerant *Delftia* sp. AN3. Appl Microbiol Biotechnol 58:682–689
13. Lyons CD, Katz S, Bartha R (1984) Mechanisms and pathways of aniline elimination from aquatic environments. Appl Environ Microbiol 48:491–496
14. Mandira M, Sheela S (2009) Stress-responsive indole-3-acetic acid biosynthesis by *Azospirillum brasilense* SM and its ability to modulate plant growth. Eur J Soil Biol 45:73–80
15. Nanda D, Sasikala Ch, Ramana ChV (2000) Light dependent transformation of anthranilate to indole by *Rhodobacter sphaeroides* OU5. J Ind Microbiol Biotechnol 24:219–221
16. Powell LE (1964) Preparation of indole extracts from plants for gas chromatography and spectrophotofluorometry. Plant Physiol 39:836–842
17. Rajasekhar N, Sasikala Ch, Ramana ChV (1999) Photometabolism of indole by purple non-sulfur bacteria. Ind J Microbiol 39:39–44
18. Rajasekhar N, Sasikala Ch, Ramana ChV (1999) Photoproduction of L-tryptophan from indole and glycine by *Rhodobacter sphaeroides* OU5. Biotechnol Appl Biochem 30:209–212
19. Rajasekhar N, Sasikala Ch, Ramana ChV (1999) Photoproduction of indole-3-acetic acid by *Rhodobacter sphaeroides* from indole and glycine. Biotechnol Lett 21:543–545
20. Sasikala Ch, Ramana ChV (1998) Biodegradation and metabolism of unusual carbon compounds by anoxygenic phototrophic bacteria. Adv Microb Physiol 39:339–377
21. Schnell S, Schink B (1991) Anaerobic aniline degradation via reductive deamination of 4-aminobenzoyl-CoA *Desulfobacterium anilini*. Arch Microbiol 155:183–190
22. Sugimoto S, Shiio I (1982) Tryptophan synthase and production of L-tryptophan in regulatory mutants. Agric Biol Chem 46:2711–2718
23. Sunayana MR, Sasikala Ch, Ramana ChV (2005) Production of novel indole esters from 2-aminobenzoate by *Rhodobacter sphaeroides* OU5. J Ind Microbiol Biotechnol 32:41–45
24. Takenaka S, Sasanao MY, Takahashi Y, Murakami S, Aoki K (2006) Microbial transformation of aniline derivatives: regioselective biotransformation and detoxification of 2-phenylenediamine by *Bacillus cereus* strain PDa-1. J Biosci Bioeng 102:21–27
25. Vijay S, Sunayana MR, Ranjith NK, Sasikala Ch, Ramana ChV (2006) Light dependent transformation of aniline to indole esters by the purple bacterium *Rhodobacter sphaeroides* OU5. Curr Microbiol 52:413–417

Appl Microbiol Biotechnol (2011) 89:1001–1008
DOI 10.1007/s00253-010-2951-2

Production of indole-3-acetic acid and related indole derivatives from L-tryptophan by *Rubrivivax benzoatilyticus* JA2

Md. Mujahid · Ch. Sasikala · Ch. V. Ramana

Received: 22 September 2010 / Revised: 8 October 2010 / Accepted: 9 October 2010 / Published online: 24 October 2010

Abstract *Rubrivivax benzoatilyticus* JA2 produces indoles with simultaneous utilization of L-tryptophan. Fifteen chromatographically distinct indole derivatives were detected from the L-tryptophan-supplemented cultures of *R. benzoatilyticus* JA2. Nine of these were identified as, indole 3-acetamide, Methoxyindole-3-aldehyde, indole 3-aldehyde, methoxyindole-3-acetic acid, indole 3-acetic acid, indole-3-carboxylic acid, indole-3-acetonitrile, indole, and trisindoline. Tryptophan stable isotope feeding confirmed the indoles produced are from the supplemented L-tryptophan. Indole 3-acetic acid is one of the major products of L-tryptophan catabolism by *R. benzoatilyticus* JA2 and its production was influenced by growth conditions. Identification of indole 3-acetamide and tryptophan monooxygenase activity suggests indole 3-acetamide routed IAA biosynthesis in *R. benzoatilyticus* JA2. The study also indicated the possible multiple pathways of IAA biosynthesis in *R. benzoatilyticus* JA2.

Keywords *Rubrivivax benzoatilyticus* · Indole 3-acetic acid · Indole · L-Tryptophan · Catabolism · Metabolite probe

M. Mujahid · C. V. Ramana (✉)
Department of Plant Sciences, School of Life Sciences,
University of Hyderabad, P.O. Central University,
Hyderabad 500 046, India
e-mail: r449@sify.com

C. Sasikala
Bacterial Discovery Laboratory, Center for Environment, IST,
J NT University,
Kukatpally,
Hyderabad 500 085, India
e-mail: sasi449@yahoo.ie

Introduction

Plant growth-promoting rhizobacteria (PGPR) promote plant growth by various mechanisms, which mainly include; nitrogen fixation, mineral solubilization, sidorophore, and plant growth hormone production (Glick et al. 1999). Hormones like auxins (indole 3-acetic acid [IAA]), abscisic acid (ABA), cytokines, and ethylene (Boiero et al. 2007; Bloemberg and Lugtenberg 2001) are produced by many PGPR strains. Indole 3-acetic acid is the principle hormone which regulates various developmental and physiological processes in plants. Plant growth stimulation by rhizobacteria is attributed to their ability to produce IAA (Tsavkelova et al. 2007), thus IAA production is considered as a key trait for the selection of PGPR, and strains, which produce IAA, are of great importance (Ali et al. 2009; Patten and Glick 1996). Members of the genera *Azospirillum*, *Pseudomonas*, *Rhizobium*, *Acetobacter*, *Azatobacter,* and *Bacillus* produce IAA and are effectively used to enhance plant growth and productivity of crop plants (Patten and Glick 1996; Idris et al. 2007).

Wide range of bacteria colonizes the plant rhizosphere and one such group is the anoxygenic photosynthetic bacteria (Elbadry et al. 1999), which are widely distributed in the oxic/anoxic environments and their ideal niches are the paddy soils (Elbadry et al. 1999; Feng et al. 2009). Being metabolically versatile (Imhoff and Trüper 1992) and capable of producing plant growth-promoting hormones, these bacteria are receiving attention as good candidates of biofertilizers (Sasikala and Ramana 1995), particularly for paddy (Feng et al. 2009; Gamal-Eldin and Elbanna 2010). However, the role of anoxygenic phototrophic bacteria in the plant growth promotion and production of plant growth

regulators like IAA is poorly understood. In the present communication, we investigated the L-tryptophan catabolism and production of IAA by *Rubrivivax benzoatilyticus* JA2, which was isolated from the rhizosphere of a flooded paddy (Ramana et al. 2006).

Materials and methods

Organisms and growth conditions

R. benzoatilyticus JA2^T and other strains were grown photoheterotrophically (anaerobic, 30 °C; light 2,400 lux) in a mineral medium (Kalyan Chakravarthy et al. 2007) supplemented with malate (22 mM) as carbon source and ammonium chloride (7 mM) as nitrogen source in fully filled screw-cap test tubes (10×100 mm)/reagent bottles (250 ml) at pH 6.8, 30 °C and at a light intensity of 30 $\mu E \cdot m^{-2} \cdot s^{-1}$. Ammonium chloride was replaced with tryptophan when tryptophan was used as a nitrogen source.

Tryptophan induction assay

Bacteria were allowed to grow photoheterotrophically (anaerobically) or light/dark aerobically for 48 h to which, sterile tryptophan was added to give a final concentration of 1 mM and in case of stable isotope feeding experiments, 0.5 mM. Aerobic growth was performed in 250-ml flasks, which were incubated in a shaker at 150 rpm and at 30 °C. After incubation of 48 h, cells were harvested by centrifugation (10,000 rpm, 10 min at 4 °C). The supernatant was used for estimation of indoles, tryptophan and for the extraction of metabolites. All the experiments were done in duplicates as three independent experiments.

Extraction of indole metabolites

Culture supernatant was acidified to pH 2.5 with 5N HCl and the metabolites were extracted thrice with equal volumes of ethyl acetate. The ethyl acetate layers were pooled and evaporated to dryness under vacuum in rotary flash evaporator (Heidolph, Germany) at 45 °C. After complete dryness, the brown residue was dissolved in methanol (1 ml), filtered (0.22-μm membrane), and used for HPLC and mass spectral analysis.

Analytical methods

Total indoles were estimated by Salper's reagent (Gordon and Paleg 1957) from the culture supernatant and tryptophan was estimated by HPLC.

Table 1 IAA produced by different purple nonsulfur bacteria

Organisms	IAA production ($\mu g \cdot ml^{-1}$)
Rubrivivax gelatinosus ATCC17011^T	13±2
Rubrivivax benzoatilyticus JA2	21.6±2.8
Rhodopseudomonas fecalis JCM11668^T	9.9±3
Rhodopseudomonas palustris DSM123^T	9.6±2
Pheospirillum oryzae JA317^T	1.5±0.5
Rhodobacter sphaeroides DSM158^T	9.1±1
Rhodobacter maris JA276^T	4.5±1.2
Rhodobacter aesturii JA296^T	1.5±0.35
Rhodobacter azotoformans KA25^T	4.6±0.8
Rhodobacter johrii JA192^T	3.3±1
Rhodobacter megalophilus JA194^T	6.5±1.2

Data presented mean standard deviation (±) of two independent experiments

^{T} Type strains

HPLC analysis

HPLC analysis was performed on Shimadzu (LC-20AT) system equipped with photodiode array detector and phenomenex C-18 column (Luna, 5 μm, 250×4.6 mm). Gradient method was employed for separation of metabolites for 30 min. Acetic acid (1% *v*/*v*) and acetonitrile were used as mobile phase. Linear gradient of 0–55% acetonitrile for 25 min followed by step increase to 100% acetonitrile held for 3 min and finally return to 1% acetic acid wash. Flow rate was 1.5 $ml \cdot min^{-1}$; injection volume was 20 μl and the metabolites were detected at 230, 280, and 350 nm.

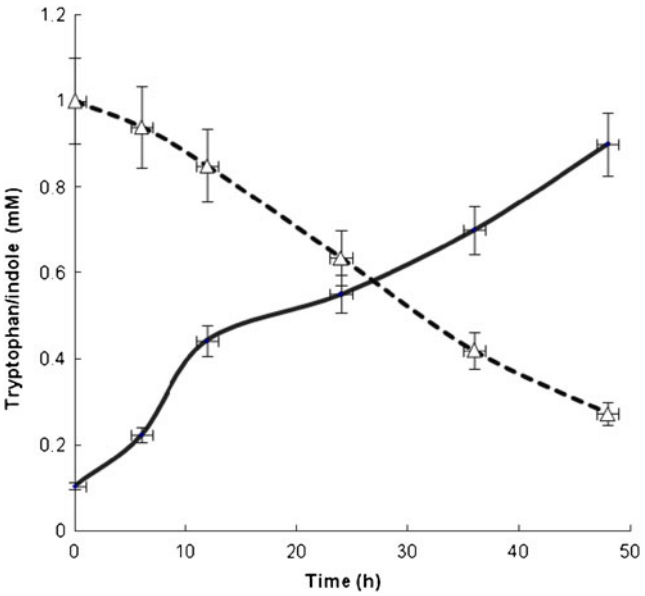

Fig. 1 Tryptophan utilization and production of indoles by *R. benzoatilyticus* JA2. *Solid line*, tryptophan; *dashed line*, indoles. Data represents mean±standard deviation of three independent experiments

Table 2 Identification of indole derivatives from the culture supernatant of *R. benzoatilyticus* JA2^T

R_t (min)	UV max (nm)	Mass (*m*/*z*) fragmentation	Indole derivatives	mole%
14.5	214, 226, 273, 278	175$[M+H]^+$ [175, 158,130]	Indole 3-acetamide	1.0
15.2	214, 227, 240, 279, 288	176$[M+H]^+$ [176, 166, 146]	Methoxyindole 3-aldehdye	0.6
15.7	214, 241, 258, 298	203$[M-H]^-$ [203 186, 146, 130]	Ud	1.9
16.6	238,270, 289	Ni	Ud	10.0
17.0	215, 262, 277, 288	187$[M-H]^-$ [187, 160,116]	Ud	10.2
17.5	214, 243, 260, 290	146$[M+H]^+$ [146,118]	Indole 3-aldehyde	4.5
17.9	222, 234, 273	206$[M+H]^+$ [206, 188,176,146,130.115]	Methoxyindole 3-acetic acid	2.8
18.55	215, 273, 278, 288	176$[M+H]^+$ [176, 146, 130]	Indole 3-acetic acid	12.0
18.9	220, 283	162$[M+H]^+$ [162, 144,118]	Indole 3-carboxylic acid	2.5
19.5	214, 237, 275	Ni	Ud	1.6
21.1	268, 276, 286	Ni	Ud	4.0
23.1	214, 242, 280	157$[M+H]^+$ [157, 130,]	Indole 3-acetonitrile	2.5
24.6	214, 270, 276, 287	118$[M+H]^+$	Indole	15.8
25.5	214, 228, 274, 278,289	258$[M+H]^+$	Ud	12.6
26.2	215, 228, 280, 288	362$[M+H]^-$ [362,246,158]	Trisindoline	18.0

Ud unidentified; *Ni* not ionized

UV spectra were recorded by photodiode array detector and metabolites were quantified with reference to the peak areas of known concentrations of authentic standards.

ESI-LC-MS/MS analysis

Mass analysis was performed on MicroTOF-Q (Brukars deltanoics) mass spectrometer coupled to HPLC (Agilent 1,200 series) equipped with UV–VIS detector. Metabolites were separated on reverse phase column (Waters' C-18, 5 μm, 150×4.6 mm). HPLC conditions were as same as described above, except the flow rate was 0.8 ml·min^{-1} and detection was done at 280 nm, with a postcolumn split effluent was introduced into electro spray ionization (ESI) ion source (80 °C, Cone voltage 15–25 V). ESI (+) ion mode was used to detect molecular ion mass ($[M]^+$) and fragmentation was obtained by collision energy of 5–20 eV depending upon the nature of the molecule. Mass spectra were recorded from 50 to 1,000 Da.

Preparation of cell-free extracts

Cells of tryptophan supplemented culture were harvested by centrifugation (4 °C, 10,000×*g*, 10 min). Cell pellet was washed with Tris–HCl buffer (50 mM pH 7.8) and finally resuspended in 4 ml of same buffer. Cells were lysed by sonication with MS-70 probe (Bandelin, Model UW 2070, Germany), after sonication, lysate was centrifuged (20000×*g*, 20 min, 4 °C) clear supernatant obtained was used as source of enzyme.

Tryptophan 2-monooxygenase activity

Enzyme activity was carried out in final volume of 0.7 ml Tris buffer (50 mM, pH 7.8) contained 0.5 mM of L-tryptophan and appropriate amount of enzyme. Reaction was incubated at 37 °C for 20 min and then stopped by adding 100 μl of 5N HCl. Pre-denatured enzyme was taken as blank. Reaction mixture was centrifuged (4 °C for 10 min at 10,000×*g*) and the supernatant was collected and extracted twice with ethyl acetate. The ethyl acetate layer was pooled, evaporated to dryness under vacuum, dissolved in 50 μl methanol, and products were analyzed using HPLC.

Results

Production of IAA by purple bacteria

Except for *Rhodospirillum rubrum* ATCC11170^T, all the other 11 species of purple nonsulfur bacteria produced IAA on L-tryptophan (1 mM) supplementation and the yields are given in Table 1.

Utilization of L-tryptophan and production of indoles

Photoheterotrophically growing culture of *R. benzoatilyticus* JA2 supplemented with L-tryptophan (1 mM) produced indoles (0.87 mM) with simultaneous consumption of tryptophan (0.8 mM) for over 50 h (Fig. 1).

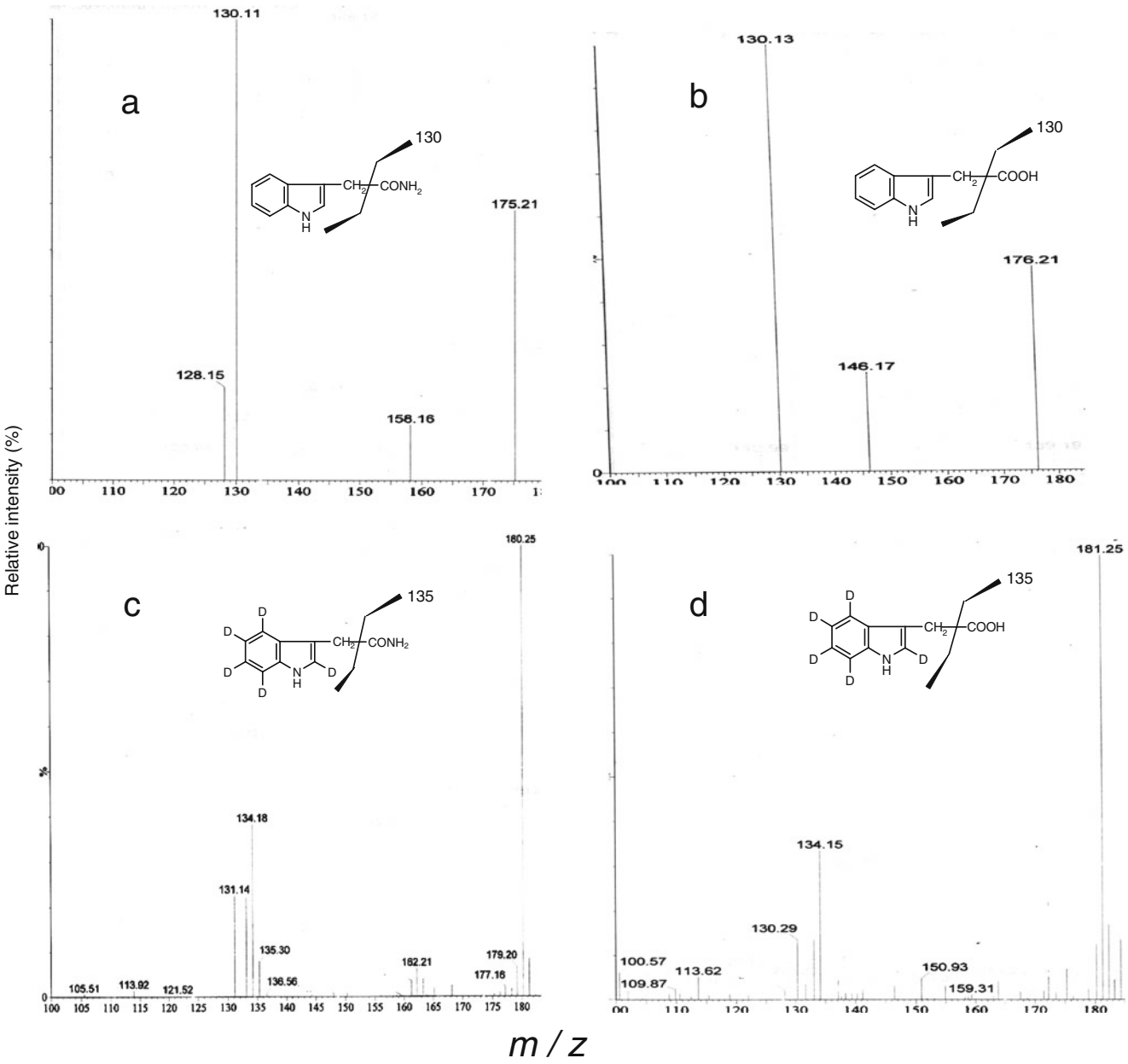

Fig. 2 LC-MS/MS analysis of IAM and IAA derived from unlabeled or labeled tryptophan-supplemented culture supernatants of *R. benzoatilyticus* JA2. Unlabeled IAM (**a**), unlabeled IAA (**b**), labeled IAM (**c**), and labeled IAA (**d**)

Identification of indole derivatives

HPLC analysis of ethyl acetate fraction obtained from L-tryptophan-supplemented culture supernatant indicated 25 chromatographically distinct peaks. Seventeen peaks had absorption at 270–280 nm, which can be depicted as due to indole nucleus. Peaks corresponding to the metabolites were collected and tested for the presence of indoles using Salper's reagent, among which, 15 peaks corresponding to the metabolites gave positive test for indoles. Nine indole derivatives were identified in total (Table 2) of which, six were confirmed based on their retention time (R_t), co-elution, UV absorption spectra identical to that of authentic standards (Table 2). These include; indole 3-acetamide (R_t 14.5 min), indole 3-aldehyde (R_t 17.5 min), IAA (R_t 18.55 min), indole 3-carboxylic acid (R_t 18.9 min), indole 3-acetonitrile (R_t 23.1 min), and indole (R_t 24.6 min). LC-MS/MS analysis of the ethyl acetate fraction has shown molecular ion peaks at 175$[M]^+$, 146$[M]^+$, 176$[M]^+$, 162$[M]^+$, 158$[M]^+$, and 118$[M]^+$ corresponding to the, indole-3-acetamide, indole-3-aldehyde, IAA, indole 3-carboxylic acid, indole-3-acetonitrile, and indole. The remaining three metabolites were identified as methoxyindole-3-aldehyde (R_t15.2 min;

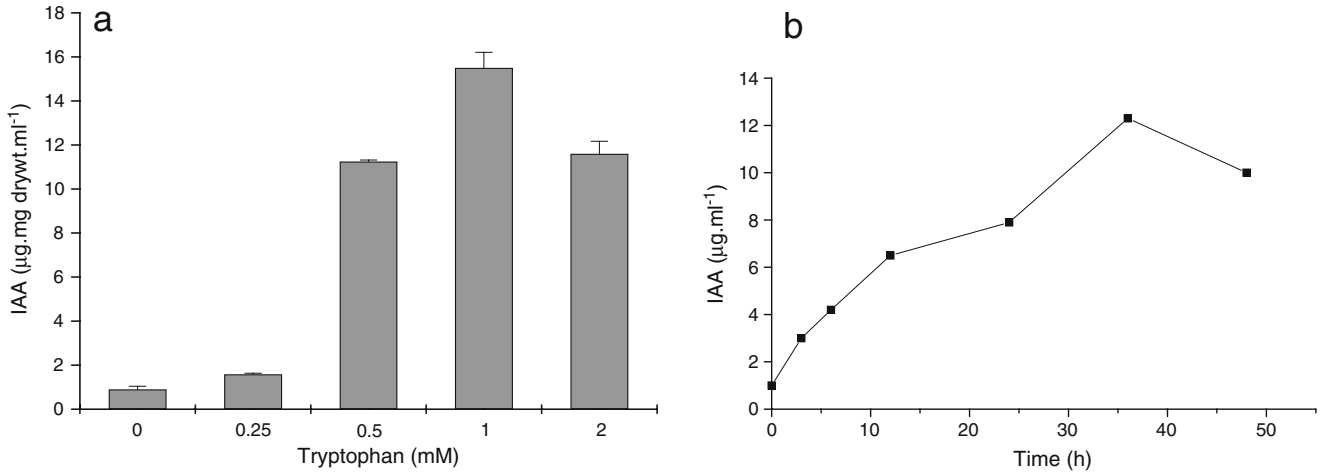

Fig. 3 Effect of tryptophan concentration on IAA production (**a**), time course of IAA production (**b**) in *R. benzoatilyticus* JA2

mass, 176[M+H]$^+$), methoxyindole-3-acetic acid (R_t 17.9 min; mass 206[M+H]$^+$), and trisindoline (R_t 26.2 min; mass, 362[M−H]$^-$) based on their molecular ion mass, mass fragmentation pattern, and absorption spectra (Ravikanth et al. 2003; Young-Man and Bernard, 2009; Pedras et al. 2008; http://www.massbank.jp). Indole 3-acetamide, methoxyindole 3-aldehyde, indole 3-carboxylic acid, indole 3-acetonitrile, indole, methoxy IAA, and trisindoline were not observed in control culture which was not supplemented with L-tryptophan.

L-Tryptophan stable isotope feeding

Deuterium-labeled L-tryptophan [L-tryptophan-d_5 (indole-d_5), 98%] was used as a metabolic probe to identify the indole metabolites, which incorporated labeled tryptophan. Culture was supplemented with 0.5-mM-labeled tryptophan and supernatant was analyzed by LC-MS. Mass analysis indicated incorporation of labeled tryptophan into indole metabolites which was evident from the increase in the molecular ion mass of labeled metabolites by 5 units. Incorporation of labeled tryptophan into indole 3-acetamide and IAA was observed (Fig. 2) by increase in their molecular ion mass from 175[M+0]$^+$ to 180[M+5]$^+$ and 176[M+0]$^+$ to 181[M+5]$^+$, respectively. Similar labeling pattern was observed with other identified indole metabolites (indolaldehyde,146[M+0]$^+$/151[M+5]$^+$; indole 3-acetonitrile, 158[M+0]$^+$/163[M+5]$^+$; indole 118 [M+0]$^+$/123 [M+5]$^+$).

Effect of L-tryptophan on IAA production

Production of IAA was observed with *R. benzoatilyticus* JA2 even in the absence of L-tryptophan (1.5 µg.ml^{-1}). However, externally supplemented L-tryptophan enhanced (12–14 µg.ml^{-1}) IAA formation which was dose (Fig. 3a) and time (Fig. 3b) dependent in *R. benzoatilyticus* JA2.

Growth conditions influence on IAA production

IAA production (12–14 µg.ml^{-1}) was enhanced when L-tryptophan supplemented to early stationary phase culture compare to control. IAA production was high (21–23 µg.ml^{-1}) in logarithmic phase culture supplemented with L-tryptophan. Production of IAA was high (32–51 µg.ml^{-1}) in aerobically grown culture compared to anaerobic (12–20 µg.ml$^{-1)}$. IAA production enhanced under light aerobic conditions compared to dark (Table 3). *R. benzoatilyticus* JA2 utilizes L-tryptophan as nitrogen source with simultaneous production of IAA, which was high compared to when used as supplement (Table 3).

Table 3 Effect of growth conditions on IAA production by *R. benzoatilyticus* JA2. Growth conditions IAA production

Growth conditions	IAA production (µg·ml^{-1})
Light anaerobic	
Control (without tryptophan)	1.05±0.5
Tryptophan supplemented[a]	
Logarithmic phase	21.6±2.8
Early stationary phase	12.3±2.51
Tryptophan as nitrogen source[b]	31.0±4.0
Dark aerobic	32.6±5.0
Light aerobic	58.1±4.6

Data represented mean±standard deviation of three independent experiments

[a] Tryptophan was amended to the mineral medium

[b] Ammonium chloride was replaced with 1 mM tryptophan as nitrogen source

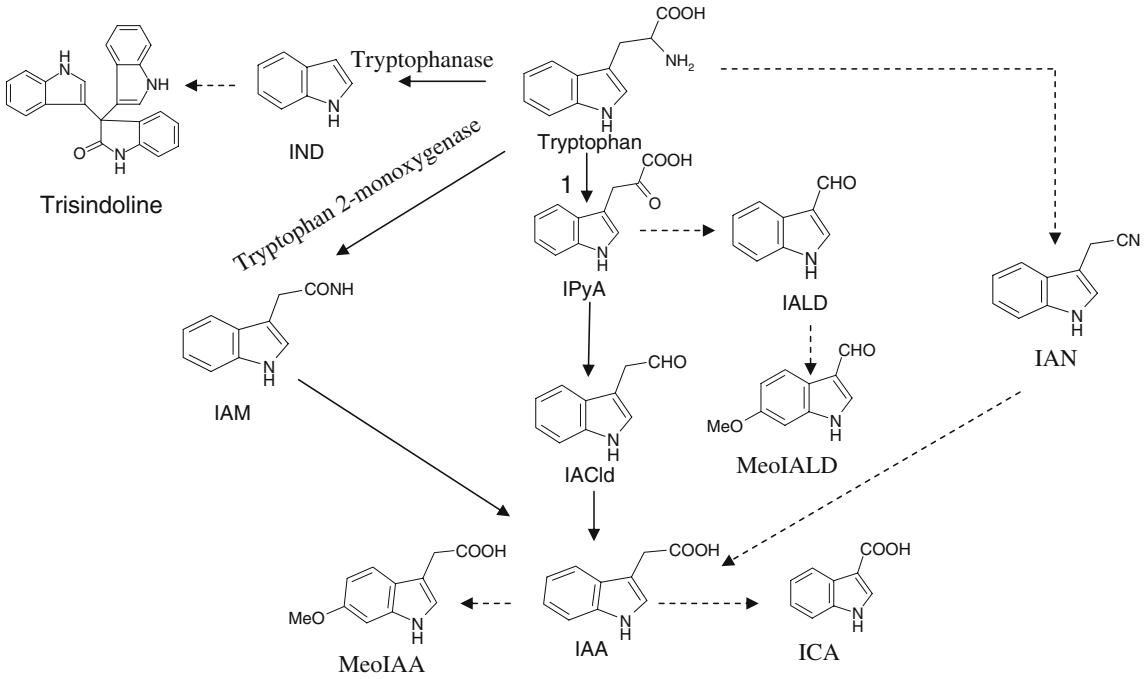

Fig. 4 Proposed L-tryptophan catabolic pathways of *R. benzoatilyticus* JA2. *Arrows with solid line* indicate pathway confirmed by enzyme assays, *arrows with dashed line* indicate pathway proposed based on previous literature. 1=IpyA pathway was confirmed in *R. benzoatilyticus* JA2 (Ranjith et al. 2010); *IpyA*, indole 3-pyruvic acid; *IND*, indole; *IAA*, indole 3-acetic acid; *IAM*, indole 3-aetamide; *IAN*, indole 3-acetonitrile; *Meo IAA*, methoxy indole 3-acetic acid; *Meo IALD*, methoxyindole 3-aldehyde; *ICA*, indole 3-carboxylic acid; *IACld*, indole 3-acetaldehyde; *IALD*, indole-3-aldehyde

Tryptophan-2 monooxygenase activity

HPLC analysis of enzyme reaction mixture indicated the formation of products having a R_t of 14.5 and 18.5 min which corresponds to indole 3-acetamide and IAA, respectively.

Discussion

Purple bacteria aid in the transformation of aromatic compounds (Sasikala and Ramana 1998). L-Tryptophan catabolites identified from the culture supernatant of *R. benzoatilyticus* JA2 in this study are; indoleacetamide, methoxyindole 3-aldehyde, indole 3-aldehyde, indole 3-acetonitrile, indole, IAA, indole 3-carboxylic acid, trisindoline, and mehtoxyindole 3-acetic acid. This is the first report of identifying indole 3-acetamide, indole 3-acetonitrile, methoxyindole 3-aldehyde, indole 3-carboxylic acid, trisindoline, indole, and methoxyindole 3-acetic acid from purple bacteria, while IAA, indole 3-aldehyde were identified from tryptophan/aniline-supplemented cultures of purple bacteria (Mujahid et al. 2010; Ranjith et al. 2010). Tryptophan stable isotope feeding experiments confirmed that tryptophan is indeed a precursor of the identified indoles as evidenced from labeling patterns (Fig. 2).

Tryptophan catabolism occurs through various pathways, culminating in the formation of indoles in bacteria

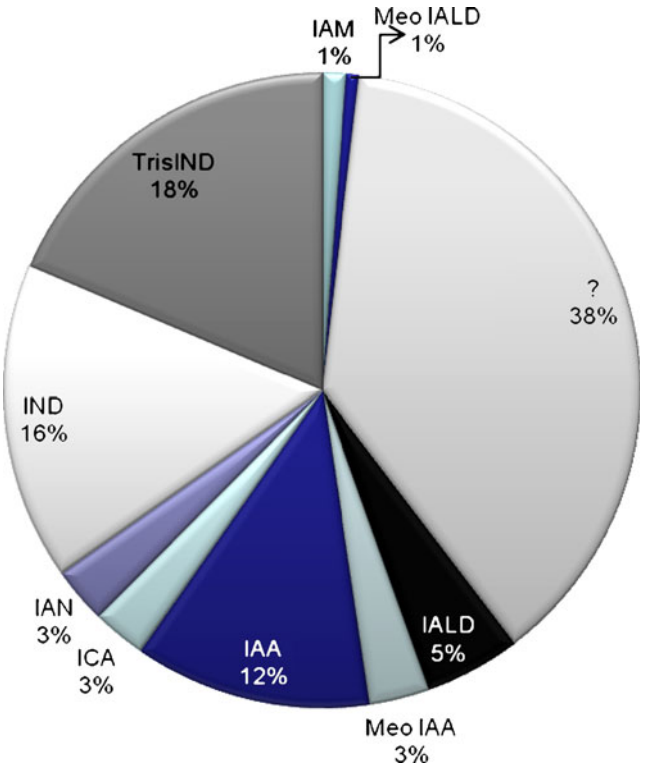

Fig. 5 Snap-shot of indole derivatives produced by *R. benzoatilyticus* JA2. Abbreviations used in the figure are defined in Fig. 4, except: *TrisIND*, Trisindoline; *question mark* (*?*), Unidentified; *percent* (*%*), mole%

(Martens and Frankenberger 1993; Prinsen et al. 1997). We observed formation of indole 3-acetonitrile, indole 3-acetamide in the present study which happened to be the intermediates of two different pathways of tryptophan dependent IAA biosynthesis (Spaepen et al. 2007). Presence of indole 3-acetamide and tryptophan 2-monooxygenase activity confirms the indole 3-acetamide pathway (Lambrecht et al. 2000) of IAA biosynthesis in *R. benzoatilyticus* JA2. Indole 3-pyruvic acid-mediated IAA biosynthesis was reported in *R. benzoatilyticus* JA2 (Ranjith et al. 2010) where L-tryptophan consumption was observed simultaneously along the growth in 6 h when used as sole source of nitrogen. In contrast to the earlier experimentation (Ranjith et al. 2010), L-tryptophan when used as supplement to the early stationary phase cultures, consumption was observed over a period of 50 h (Fig. 1). We could not detect indole 3-pyruvic acid or indole 3-acetaldehyde plausibly because of their unstable nature but we could demonstrate trytophan aminotranferase activity a key enzyme in indole 3-pyruvic acid-routed IAA biosynthesis. Multiple pathways for IAA biosynthesis were reported in bacteria (Brandl et al. 2001) and our results also indicate possible degeneracy of IAA biosynthesis in *R. benzoatilyticus* JA2. Presence of indole in the culture supernatant and tryptophanase activity (data not shown) further suggests the tryptophanse-dependent indole production (Lee et al. 2007). Indole 3-aldehyde formation could not be demonstrated from IAA in *R. benzoatilyticus* JA2 an alternative route of biosynthesis of indole 3-aldehyde was via indole 3-pyruvic acid. Indole 3-carboxylic acid formation was reported from oxidation of IAA (Davis and Gustafson 1976). Trisindoline formation was reported from indole in bacteria (Ravikanth et al. 2003; Young-Man and Bernard, 2009). Based on indole derivatives identified from the culture supernatant, we propose the possible biosynthetic routes (Fig. 4) of indole derivatives in *R. benzoatilyticus* JA2.

Production of IAA by *R. benzoatilyticus* JA2 is significantly high compared to those reported from other rhizosphere bacteria supplemented with L-tryptophan (Aslantas et al. 2007; Sarwar and Kremer 1995). IAA produced by strain JA2 represents about 12% of the total indole derivatives identified (Fig. 5). *R. benzoatilyticus* JA2 produced IAA during logarithmic and aerobic conditions and the results are in contrast of the stress factor (carbon exhaustion, oxygen tension, and entry into the stationary phase) that triggered IAA production in *Azopirillum*, *Enterobacter cloacae,* and *Pseudomanas putida* GR12-2 (Ona et al. 2005), indicating that IAA production in *R. benzoatilyticus* JA2 is independent of these factors. Production of IAA may be a common property among purple bacteria, since most strains screened were capable of producing IAA (Table 1).

Purple bacteria inhabit rhizosphere (Elbadry et al. 1999; Feng et al. 2009) and their ability to produce phytoharmones and fixing atmospheric nitrogen (Glick et al. 1999; Sasikala and Ramana 1995) probably help in growth enhancement and productivity of rice (Harada et al. 2005; Elbadry and Elbanna 1999; Elbadry et al. 1999; Gamal-Eldin and Elbanna 2010). Production of significant amount (58 $\mu g \cdot ml^{-1}$) of IAA by *R. benzoatilyticus* JA2 under different physiological conditions makes this organism suitable for IAA production under both in vitro and in vivo conditions. Further analysis of strain JA2 is required to evaluate its plant growth-promoting activity for developing the inoculums for rice.

Acknowledgements Mujahid. Md thanks CSIR, Government of India for the award of JRF/SRF. Facilities used under the FIST and CAS supported by DST and UGC, Government of India, respectively, are duly acknowledged.

References

Ali B, Sabri AN, Ljung K, Hasnain S (2009) Auxin production by plant associated bacteria: impact on endogenous IAA content and growth of *Triticum aestivum* L. Lett Appl Microbiol 48:542–547

Aslantas R, Cakmakci R, Sahin F (2007) Effect of plant growth promoting rhizobacteria on young apple tree growth and fruit yield under orchard conditions. Sci Hortic 111:371–377

Bloemberg GV, Lugtenberg BJ (2001) Molecular basis of plant growth promotion and biocontrol by rhizobacteria. Curr Opin Plant Biol 4:343–350

Boiero L, Perrig D, Masciarelli O, Penna C, Cassán F, Luna V (2007) Phytohormone production by three strains of *Bradyrhizobium japonicum* and possible physiological and technological implications. Appl Microbiol Biotechnol 74:874–880

Brandl MT, Quinones B, Lindow SE (2001) Heterogeneous transcription of an indole acetic acid biosynthetic gene in *Erwinia herbicola* on plant surfaces. Proc Natl Acad Sci USA 98:3454–3459

Davis PJ, Gustafson RPJ (1976) Formation of indole 3-carboxylic acid by *Chromobacterium violaceum*. J Bacteriol 126:544–546

Elbadry M, Elbanna Kh (1999) Response of four rice varieties to *Rhodobacter capsulatus* at seedling stage. World J Microbiol Biotechnol 15:363–367

Elbadry M, El-Bassel A, Elbanna Kh (1999) Occurrence and dynamics of phototrophic purple nonsulphur bacteria compared with other asymbiotic nitrogen fixers in rice fields of Egypt. World J Microbiol Biotechnol 15:359–362

Feng Y, Lin X, Wang Y, Zhang J, Mao T, Yin R, Zhu J (2009) Free-air CO_2 enrichment (FACE) enhances the biodiversity of purple phototrophic bacteria in flooded paddy soil. Plant Soil 324:317–328

Gamal-Eldin H, Elbanna K (2010) Field evidence for the potential of *Rhodobacter capsulatus* as biofertilizer for flooded rice. Curr Microbiol. doi:10.1007/s00284-010-9719-x

Glick BR, Patten CL, Holguin G, Penrose DM (1999) Biochemical and genetic mechanisms used by plant growthpromoting bacteria. Imperial College Press, London

Gordon SA, Paleg LG (1957) Quantitative measurement of indole acetic acid. Plant Physiol 10:37–48

Harada N, Nishiyama M, Otsuka S, Matsumoto S (2005) Effects of inoculation of phototrophic bacteria on grain yield of rice and nitrogenase activity of paddy soil in a pot experiment. Soil Sci Plant Nutr 51:361–367

Idris EE, Iglesias EJ, Talon M, Borriss R (2007) Tryptophan dependent production of indole-3-acetic acid (IAA) affects level of plant growth promotion by *Bacillus amyloliquefaciens* FZB42. Mol Plant-Microb Interact 20:619–626

Imhoff JF, Trüper HG (1992) The genus *Rhodospirillum* and related genera. In: Balows A, Trüper HG, Dworkin M, Harder W, Schleifer K-H (eds) The prokaryotes, 2nd edn. Springer-Verlag, New York, pp 2141–2155

Kalyan Chakravarthy S, Srinivas TNR, Anil Kumar P, Sasikala Ch, Ramana ChV (2007) *Roseospira visakhapatnamensis* sp. nov. and *Roseospira goensis* sp. nov. Int J Syst Evol Microbiol 57:2453–2457

Lambrecht M, Okon Y, Vande Broek A, Vanderleyden J (2000) Indole-3-acetic acid: a reciprocal signaling molecule in bacteria–plant interactions. Trends Microbiol 8:298–300

Lee J, Jayaraman A, Wood TK (2007) Indole is an inter-species biofilm signal mediated by SdiA. BMC Microbiol 7:42

Martens DA Jr, Frankenberger WT (1993) Metabolism of tryptophan in soil. Soil Biol Biochem 25:1679–1687

Mujahid MD, Sasikala Ch, Ramana ChV (2010) Aniline-induced tryptophan production and identification of indole derivatives from three purple bacteria. Curr Microbiol 61:285–290

Ona O, Impe JV, Prinsen E, Vanderleyden J (2005) Growth and indole-3-acetic acid biosynthesis of *Azospirillum brasilense* Sp245 is environmentally controlled. FEMS Microbiol Lett 246:125–130

Patten C, Glick B (1996) Bacterial biosynthesis of indole-3-acetic acid. Can J Microbiol 42:207–220

Pedras MS, Zheng QA, Strelkov S (2008) Metabolic changes in roots of the oilseed canola infected with the biotroph Plasmodiophora brassicae: phytoalexins and phytoanticipins. J Agric Food Chem 56:9949–9961

Prinsen E, Dongen WV, Esmans EL, Van Onckelen HA (1997) HPLC linked electrospray tandem mass spectrometry: a Rapid and reliable method to analyze indole 3-acetic acid metabolism in bacteria. J Mass Spectrom 32:12–22

Ramana ChV, Sasikala Ch, Arunasri K, Anil Kumar P, Srinivas TNR, Shivaji S, Gupta P, Süling P, Imhoff JF (2006) *Rubrivivax benzoatilyticus* sp. nov., an aromatic, hydrocarbon-degrading purple betaproteobacterium. Int J Syst Evol Microbiol 56:2157–2164

Ranjith NK, Ramana ChV, Sasikala Ch (2010) L-Tryptophan catabolism by *Rubrivivax benzoatilyticus* JA2 occurs through indole 3-pyruvic acid pathway. Biodegradation 21:825–832

Ravikanth V, Imelda O, Irene WD, Hartmut L (2003) New indole alkaloids from the North sea bacterium *Vibrio parahaemolyticus* Bio2491. J Nat Prod 66:1520–1523

Sarwar M, Kremer RJ (1995) Determination of bacterially derived auxins using a microplate method. Lett Appl Microbiol 20:282–285

Sasikala Ch, Ramana ChV (1995) Biotechnological potentials of anoxygenic phototrophic bacteria. II. Biopolyesters, Biopesticide, Biofuel, and Biofertilizer. Adv Appl Microbiol 41:227–278

Sasikala Ch, Ramana ChV (1998) Biodegradation and metabolism of unusual carbon compounds by anoxygenic phototrophic bacteria. Adv Microbial Physiol 39:339–377

Spaepen S, Vanderleyden J, Remans R (2007) Indole 3-acetic acid in microbial and microorganism-plant signaling. FEMS Microbiol Rev 31:425–448

Tsavkelova EA, Cherdyntseva TA, Botina SG, Netrusov AI (2007) Bacteria associated with orchid roots and microbial production of auxin. Microbiol Res 162:69–76

Young-Man K, Bernard W (2009) Production of 3-nitrosoindole derivatives by *Escherichia coli* during anaerobic growth. J Bacteriol 191:5369–5376

JOURNAL OF BACTERIOLOGY, June 2011, p. 2898–2899 Vol. 193, No. 11
0021-9193/11/$12.00 doi:10.1128/JB.00379-11

Genome Sequence of the Phototrophic Betaproteobacterium *Rubrivivax benzoatilyticus* Strain JA2$^{T\nabla}$

Mujahid Mohammed,[1] Arvind Isukapatla,[1] Lakshmi Prasuna Mekala,[1] Rama Prasad Eedara Veera Venkata,[1] Sasikala Chintalapati,[2] and Venkata Ramana Chintalapati[1]*

Department of Plant Sciences, School of Life Sciences, University of Hyderabad, P.O. Central University, Hyderabad 500 046, India,[1] and Bacterial Discovery Laboratory, Center for Environment, IST, JNT University Hyderabad, Kukatpally, Hyderabad 500 085, India[2]

Received 21 March 2011/Accepted 25 March 2011

Herein we report the draft genome sequence of a phototrophic bacterium, *Rubrivivax benzoatilyticus* strain JA2^T, which apparently is the first genome sequence report of a phototrophic member belonging to the class *Betaproteobacteria*. The unique feature of this strain is its capability to synthesize carotenoids through both spirilloxanthin and spheroidenone pathways. Strain JA2^T produces several novel secondary metabolites, and the genome insights help in understanding the unique machinery that the strain adapted.

Rubrivivax benzoatilyticus JA2^T was isolated from a flooded paddy field in South India and was found to be closely related to *Rubrivivax gelatinosus* ATCC 17011^T based on 16S rRNA gene sequence similarity (6). Extended growth modes (photo-/chemoheterotrophy and photoautotrophy) coupled with utilization of a variety of organic compounds make the strain highly metabolically flexible. *Rubrivivax benzoatilyticus* JA2^T can fix N_2 and also produces H_2. *Rubrivivax benzoatilyticus* JA2^T produces polyhydroxyalkanoates and secondary metabolites such as phenolic compounds (8) and indole derivatives (4, 5, 7). Here, we report the draft genome sequence of this bacterium, which may provide insights into the molecular aspects of its metabolic versatility.

Rubrivivax benzoatilyticus JA2^T (= ATCC BBA-35^T = JCM13220^T = MTTC7087^T) was grown photoheterotrophically on mineral medium (1) with malate (22 mM) and ammonium chloride (7 mM) as carbon and nitrogen sources, respectively. DNA was isolated with the QIAamp minikit (Qiagen), and the authenticity of the genome was confirmed by 16S rRNA gene sequencing. The genome of *Rubrivivax benzoatilyticus* JA2^T was sequenced by using the Roche 454 GS (FLX titanium) pyrosequencing platform. Sequencing resulted in a total of 262,346 high-quality reads with approximately 24× coverage of the entire genome. All of the reads were assembled by using a Newbler assembler (Roche Life Sciences), which generated 165 contigs. Functional annotation was carried out by using the BLAST tool (NCBI), identification of tRNA genes was carried out by using tRNAscan-SE (3), and identification of rRNA genes was carried out by using RNammer (2). GC content was estimated from the genome sequence.

The *Rubrivivax benzoatilyticus* JA2^T draft genome consists of a single circular chromosome of 4,130,132 bp with an average GC content of 72.77%. A total of 3,762 open reading frames (ORFs) were found in the genome where 3,210 (85.32%) are functionally annotated, 382 (10.15%) are hypothetical, and 170 (4.51%) are unknown. The numbers of genes transcribed were 1,926 from the positive strand and 1,836 from the negative strand. The coding density of the genome is 87.5%, with an average gene length of 961 bp, and the average intergenic length is 136 bp. The *Rubrivivax benzoatilyticus* JA2^T genome contains a single 16S-23S-5S operon, 46 tRNA genes, and 25 aminoacyl-tRNA synthetase genes for all 20 amino acids. The genome consisted of 56 predicted ABC transporters, 17 putative transposases, and 29 methyl-accepting chemosensory transducer genes. The *Rubrivivax benzoatilyticus* JA2^T genome has a complete set of genes for bacterial chlorophyll, carotenoid, quinone, and vitamin biosynthesis. Light-harvesting complex and reaction center-encoding genes along with Calvin-Benson cycle-dependent autotrophic CO_2 fixation genes were also located in the genome. Nitrogenase regulatory and nitrogen molybdenum-iron protein- and nitrogenase iron protein-encoding genes were predicted. Many multidrug-resistant transporter, organic solvent resistance, and aromatic compound metabolism genes were also revealed in the genome. A detailed analysis of the *R. benzoatilyticus* JA2^T genome and comparative genome analysis with other photosynthetic members will provide insights into the unique biochemical and molecular characteristics of this strain.

Nucleotide sequence accession number. The complete genome sequence was deposited in GenBank under accession number AEWG00000000.

The Department of Biotechnology, the Department of Science and Technology, the Ministry of Earth Sciences, the Council for Scientific and Industrial Research, and the Government of India are acknowledged for financial support. M.M. thanks the CSIR (India) for the Senior Research Fellowship.

We acknowledge the help of Xcelris Labs for genome sequence deposition. We thank Niyaz Ahmed, Department of Biotechnology, University of Hyderabad, for his critical suggestions.

* Corresponding author. Mailing address: Department of Plant Sciences, School of Life Sciences, University of Hyderabad, P.O. Central University, Hyderabad 500 046, India. Phone: 91 040 23134502. Fax: 91 040 23010120. E-mail: r449@sify.com.

▽ Published ahead of print on 8 April 2011.

REFERENCES

1. **Kalyan Chakravarthy, S., T. N. R. Srinivas, P. Anil Kumar, C. Sasikala, and C. V. Ramana.** 2007. *Roseospira visakhapatnamensis* sp. nov. and *Roseospira goensis* sp. nov. Int. J. Syst. Evol. Microbiol. **57:**2453–2457.
2. **Lagesen, K., et al.** 2007. RNammer: consistent annotation of rRNA genes in genomic sequences. Nucleic Acids Res. **35:**3100–3108.
3. **Lowe, T. M., and S. R. Eddy.** 1997. tRNAscan-SE: a program for improved detection of transfer RNA genes in genomic sequence. Nucleic Acids Res. **25:**955–964.
4. **Mujahid, M., C. Sasikala, and C. V. Ramana.** 2010. Aniline-induced tryptophan production and identification of indole derivatives from three purple bacteria. Curr. Microbiol. **61:**285–290.
5. **Mujahid, M., C. Sasikala, and C. V. Ramana.** 2011. Production of indole-3-acetic acid and related indole derivatives from L-tryptophan by *Rubrivivax benzoatilyticus* JA2. Appl. Microbiol. Biotechnol. **89:**1001–1008.
6. **Ramana, C. V., et al.** 2006. *Rubrivivax benzoatilyticus* sp. nov., an aromatic, hydrocarbon-degrading purple betaproteobacterium. Int. J. Syst. Evol. Microbiol. **56:**2157–2164.
7. **Ranjith, N. K., C. V. Ramana, and C. Sasikala.** 2010. L-tryptophan catabolism by *Rubrivivax benzoatilyticus* JA2 occurs through indole 3-pyruvic acid pathway. Biodegradation **21:**825–832.
8. **Ranjith, N. K., C. V. Ramana, and C. Sasikala.** 2010. Rubrivivaxin, a new cytotoxic and cyclooxygenase-I inhibitory metabolite from *Rubrivivax benzoatilyticus* JA2. World J. Microbiol. Biotechnol. doi:10.1007/s11274-010-0420-9.

Microbiological Research 167 (2012) 526–531

Contents lists available at SciVerse ScienceDirect

Microbiological Research

journal homepage: www.elsevier.de/micres

Research paper

L-Phenylalanine catabolism and L-phenyllactic acid production by a phototrophic bacterium, *Rubrivivax benzoatilyticus* JA2

M. Lakshmi Prasuna[a], Md. Mujahid[a], Ch. Sasikala[b], Ch.V. Ramana[a,*]

[a] Department of Plant Sciences, University of Hyderabad, Hyderabad 500046, India
[b] Bacterial Discovery Laboratory, Centre for Environment, IST, JNTUH, Hyderabad 500085, India

ARTICLE INFO

Article history:
Received 28 November 2011
Received in revised form 6 March 2012
Accepted 11 March 2012

Keywords:
L-Phenylalanine
L-Phenyllactate
Phenylpyruvic acid
Rubrivivax benzoatilyticus JA2

ABSTRACT

A phototrophic bacterium (*Rubrivivax benzoatilyticus* JA2) grows at the expense of L-phenylalanine as sole source of nitrogen but not as carbon source. Near stoichiometric yields of L-phenylpyruvic acid (0.4 mM) and L-phenyllactate (0.4 mM) were observed from L-phenylalanine (0.9 mM consumed). Aminotransfarase and dehydrogenase activities involved in the formation of L-phenylpyruvic acid and L-phenyllactate were demonstrated unequivocally in *Rubrivivax benzoatilyticus* JA2. Growth conditions and carbon sources had an influence on L-phenyllactate production. The process yielded a maximum of 0.92 mM L-phenyllactate from L-phenylalanine (1 mM) when fructose served as carbon source for *R. benzoatilyticus* JA2.

1. Introduction

Bacteria utilize wide variety of compounds as carbon and nitrogen sources for their growth including amino acids. Amino acids support growth of bacteria as an excellent source of nitrogen and this process of catabolism, many a times, leads to secondary metabolite production (Thierry and Maillard 2002; Kumavath et al. 2010). Utilization of aromatic amino acids as nitrogen source leads to the production of their corresponding aromatic acids and alcohols (Somers et al. 2005; Narayanan and Ramananda Rao 1974). Purple phototrophic bacteria are metabolically versatile, utilizes wide range of organic compounds as carbon and nitrogen source for their growth and few purple bacteria can also metabolize aromatic compounds (Sasikala and Ramana 1998). *Rubrivivax benzoatilyticus* JA2 is an anoxygenic photosynthetic purple nonsulfur bacterium which transforms aromatic compounds like phenylalanine, tryptophan and aniline to value added compounds (Mujahid et al. 2011; Ranjith et al. 2011). The genome of strain JA2 is now available (Mohammed et al. 2011) and a critical analysis indicated potential pathways of aromatic compound metabolism by this strain. In the present study, we made an attempt to understand the metabolism of L-phenylalanine by *R. benzoatilyticus* JA2.

2. Materials and methods

2.1. Organism and growth conditions

R. benzoatilyticus JA2 (=ATCCBAA-35) was grown photoheterotrophically on a mineral media (Kalyan et al. 2007) containing malate (22 mM) and ammonium chloride (7 mM) as carbon and nitrogen source respectively, pH 6.8 at 30 ± 2 °C and light 2400 lux, under anaerobic condition in screw cap test tubes (10 mm × 100 mm)/250 ml culture bottles. Aerobic dark growth was performed in 250 ml conical flasks under continuous agitation (150 rpm). When L-phenylalanine was added as sole source of nitrogen, ammonium chloride was replaced with 1 mM of L-phenylalanine. Growth was measured turbidometrically at 660 nm.

2.2. Analytical methods

HPLC analysis was done according to Mujahid et al. (2011) on a SHIMADZU (LC-20AT) system equipped with photodiode array (PDA) detector and Phenomenex C18 column (Luna, 5 μm, 250 mm × 4.6 mm). A linear gradient method of 30 min was used with mobile phase 1% glacial acetic acid (solvent A) and 100% acetonitrile (solvent B) for the separation of metabolites. Flow rate was 1.5 ml min^{-1}, injection volume 20 μl at 260 nm. L-Phenylalanine, phenylpyruvic acid and L-phenyllactic acid were quantified by HPLC with reference to the peak areas of known concentrations of authentic standards. Mass analysis was performed on MicroTOF-Q (Brukers deltanoics) mass spectrometer with electro spray ionization (ESI) ion source (80 °C, cone voltage 15–25 V). ESI (−) ion mode

* Corresponding author. Tel.: +91 40 23134502; fax: +91 40 23010120/45.
E-mail addresses: r449@sify.com, chvrsl@uohyd.ernet.in (Ch.V. Ramana).

0944-5013/$ – see front matter © 2012 Elsevier GmbH. All rights reserved.
doi:10.1016/j.micres.2012.03.001

was used to detect molecular ion mass ([M]$^-$) and fragmentation was obtained by collision energy of 5–20 eV and mass spectrum was recorded from 50 to 1000 Da. Chirality of the compound was determined by CD spectroscopy on JASCO J-810 spectropolarimeter.

2.3. Extraction and purification

The supernatant of L-phenylalanine added *R. benzoatilyticus* JA2 culture was acidified with 5 N HCl and then extracted with ethylacetate. The ethyl acetate extract was evaporated to dryness under vaccum at 30 °C using rotary flash evaporator (Heidolph, Germany). The dried extract was finally dissolved in 1 ml of HPLC grade methanol. Purification of the compound was done with HPLC method. The method used for purification was similar to the HPLC method used for the L-phenyllactic acid analysis.

2.4. Enzyme assays

2.4.1. Aminotransferase/transaminase activity and dehydrogenase activity

Aminotransferase/transaminase and dehydrogenase activities were done with L-phenylalanine added culture pellets. The L-phenylalanine added culture was centrifuged at 10,000 rpm, 4 °C, for 8 min and the pellet was washed and suspended in 4 ml of 50 mM Tris buffer (pH 7.5). Cells were lysed by sonication (BANDELIN, 8 cycles, 43% amplitude) and the lysate was centrifuged at 16,000 rpm, 4 °C for 20 min. The cell free extract was taken for the assay as enzyme source. Aminotransferase activity was carried in a final volume of 3 ml, containing L-phenylalanine (1 mM), α-ketoglutarate (1 mM) and pyridoxal phosphate (PLP; 50 μM). Dehydrogenase enzyme activity was carried out with the substrates phenylpyruvic acid (2 mM) and NADH (0.5 mM). Reaction was started with the addition of substrates to appropriate amount of cell free extract, incubated for 1 h and then stopped by adding 5 N HCl, the reaction mixture was centrifuged and the clear supernatant was extracted thrice with equal volume of ethyl acetate. Ethylacatate fractions were pooled and concentrated to dryness using Rotary Flash evaporator. The dried extract was dissolved in 100 μl of HPLC grade methanol. Production of L-phenylpyruvic acid and L-phenyllactic acid was measured by HPLC (Mujahid et al. 2010). 1 unit (U) of enzyme activity was expressed as the amount of enzyme required for the formation 1 μmol of product and the results are expressed per unit protein, which was measured by Bradford method (1976).

3. Results and discussion

3.1. Growth and utilization of L-phenylalanine

Growth and utilization of L-phenylalanine was observed with *R. benzoatilyticus* JA2 when the substrate was used as sole source of nitrogen (Fig. 1) but not as carbon source. L-Phenylalanine utilization as sole source of nitrogen by *R. benzoatilyticus* JA2 was observed under both light-anaerobic and dark-aerobic conditions. L-Phenylalanine utilization was less (0.2 mM) in the presence of ammonium chloride compared to that of in its absence (0.85 mM) as also observed earlier with other bacteria (Sáez et al. 1999; Andreotti et al. 1994; Kumavath et al. 2010). During growth and utilization of L-phenylalanine, formation of free ammonia into the media was not observed which, indicates the L-phenylalanine metabolism in *R. benzoatilyticus* JA2 occurs through a transamination process.

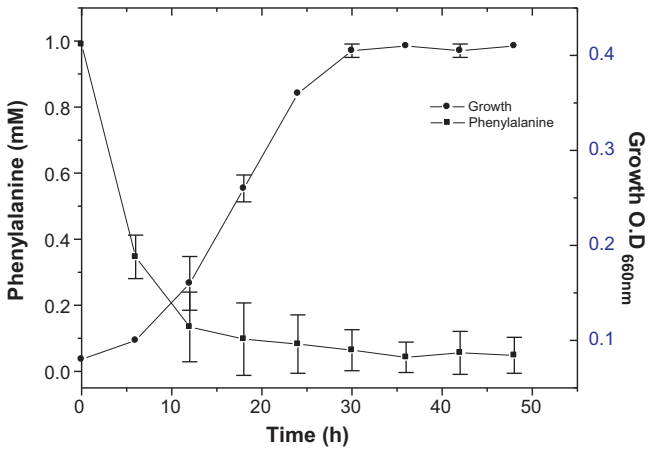

Fig. 1. Growth dependent L-phenylalanine utilization as nitrogen source by *R. benzoatilyticus* JA2.

3.2. Identification of metabolites

HPLC analysis of ethyl acetate extract of L-phenylalanine grown culture supernatant of *R. benzoatilyticus* JA2 indicated a few metabolites whose absorption maxima ranged between 240 and 290 nm depicting them as phenol derivatives (Gómez-Romero et al. 2010) and the same were absent in control condition (without supplementation of L-phenylalanine in the medium). Metabolites with retention times (R_t) 15.5, 23.8 were observed only in L-phenylalanine added culture supernatants (Fig. 2A and B). These two metabolites were identified as L-phenyllactic acid (UVmax 248, 254, 257, 263) and phenylpyruvic acid (UVmax 230, 287) based on their absorption spectra and retention times identical to that of authentic standards. The mass spectral analysis of the metabolites with R_t 15.5 and 23.8 indicated molecular ion peaks at 165[M$^-$] and 163[M$^-$], respectively (Fig. 2C and D) which confirms the metabolites as L-phenyllactic acid and phenylpyruvic acid. Phenylacetic acid (PAA), an intermediate of the L-phenylalanine catabolism was also identified based on the retention time (R_t 18.6 min) and absorbtion spectrum (UVmax 254, 257, 263; Fig. 3) identical to that of authentic standard. However, phenylethanol formation was not observed under anaerobic/microaerophilic conditions in *R. benzoatilyticus* JA2 rather PAA and PLA formation was seen. With the near complete utilization of the L-phenylalanine (0.9 mM), 0.33–0.38 mM of phenylpyruvic acid, 0.31–0.4 mM of L-phenyllactic acid and 0.09–0.1 mM of phenylacetic acid production was observed. CD spectroscopic analysis indicated that compound to be L-phenyllactic acid. Many bacteria utilize L-phenylalanine as nitrogen source and the catabolism leads to the production of phenyl derivates (Somers et al. 2005; Kumavath et al. 2010).

Production of L-phenylpyruvic acid during L-phenylalanine catabolism via transamination reaction was reported earlier in bacteria (Helinck et al. 2004). L-Phenylalanine catabolism by *R. benzoatilyticus* JA2 has lead to the formation of PAA/PLA and neither of the two metabolites was catabolized further. Genome insights also revealed that *R. benzoatilyticus* JA2 lacks PAA catabolic operon (genes) and L-phenylalanine could not support the growth of the organism as sole sources of carbon. These results suggest that L-phenylalanine catabolism occurs by Ehrlich pathway (Hazelwood et al. 2008) leading to the formation of PAA and not complete mineralization of L-phenylalanine in *R. benzoatilyticus* JA2. Production of L-phenyllactic acid is a restricted metabolic potential among bacteria and so far reported with a few lactic acid bacteria (Li et al. 2007; Mu et al. 2009), *Geotrichum candidum* (Dieuleveux

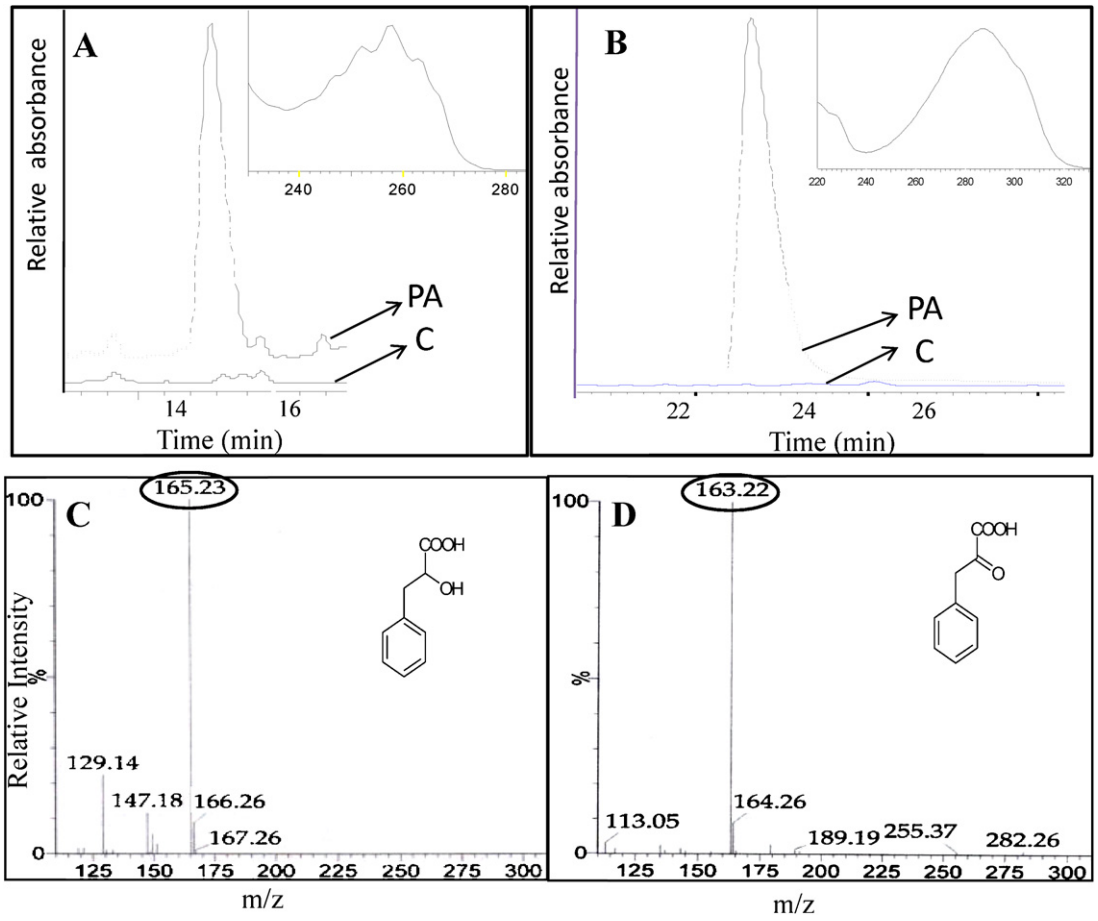

Fig. 2. HPLC chromatograms of ethyl acetate extract obtained from culture supernatants of *R. benzoatiltyicus* JA2. HPLC chromatograms of L-phenyllactic acid (A), phenylpyruvic acid (B), and their corresponding mass spectra (C and D). Chromatogram with solid line indicates control (without L-phenylalanine), dotted one for L-phenylalanine supplemented. Insert shows UV absorption spectra.

et al. 1998), *Bravibacterium* (Kamata et al. 1986) and *Propionibacteria* (Thierry and Maillard 2002). This is the first report of L-phenyllactic acid production by a purple bacterium, which also happens to be the major catabolite of L-phenayalanine. Production of L-phenylpyruvic acid in L-phenylalanine added cultures without ammonia release into the supernatant indicted an aminotransfarase dependent L-phenylalanine metabolism in *R. benzoatilyticus* JA2.

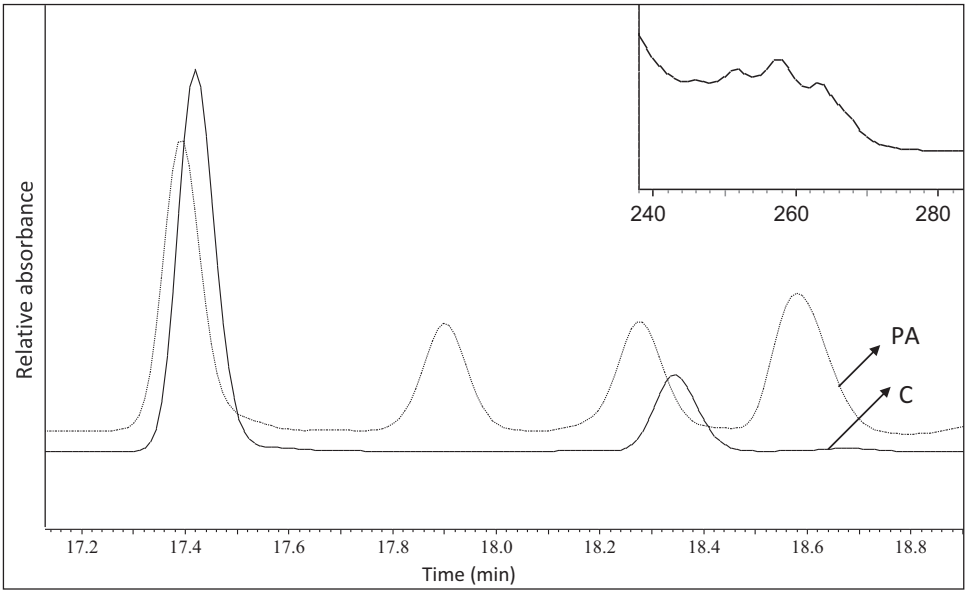

Fig. 3. HPLC chromatograms of L-phenylacetic acid with R_t 18.6 min (chromatogram with solid line indicates control (without L-phenylalanine), dotted one for L-phenylalanine supplemented). Insert shows UV absorption spectrum.

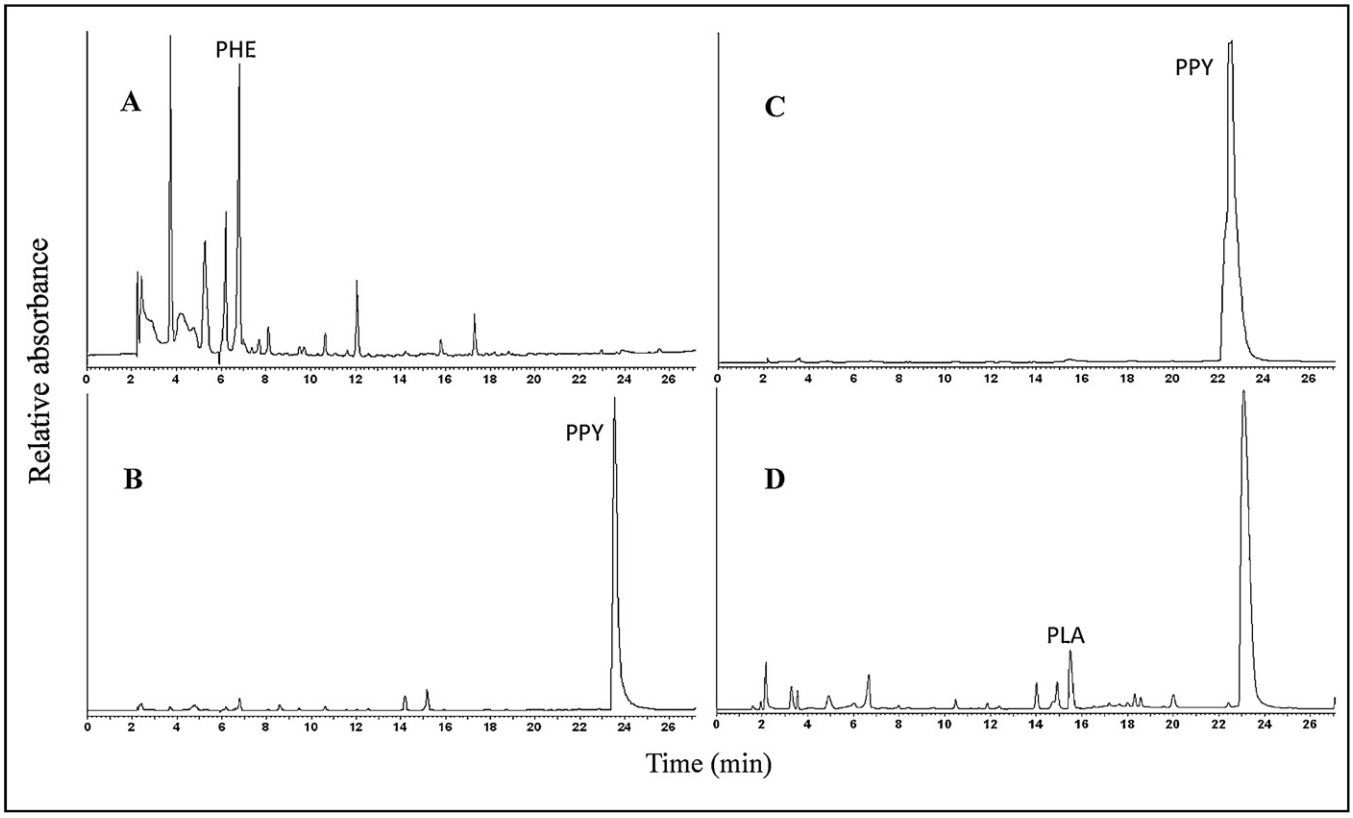

Fig. 4. Aminotransferase activity with pre-denatured sample (A) and reaction after 1 h of incubation (B) with cell free extracts of *R. benzoatilyticus* JA2. Dehydrogenase activity with pre-denatured sample (C) and reaction after 1 h of incubation (D) with cell free extracts of *R. benzoatilyticus* JA2.

3.3. Enzyme activities

Aminotransferase and dehydrogenase are the key enzymes involved in the conversion of L-phenylalanine to L-phenylpyruvic acid and L-phenyllactic acid (Li et al. 2008). Aminotransferase activity was demonstrated with cell free extracts of *R. benzoatilyticus* JA2, when L-phenylalanine acted as an amino donor, α-ketoglutarate as an acceptor in the presence of PLP. L-Phenylpyruvic acid was not observed in the pre-denatured sample (Fig. 4A) while its presence in 1 h incubated sample (Fig. 4B) indicates the presence of an aminotransferase (0.2 U mg^{-1}) in *R. benzoatilyticus* JA2. Dehydrogenase activity (0.7 U mg^{-1}) was also observed (Fig. 4C and D) in *R. benzoatilyticus* JA2 with the formation of L-phenyllactic acid from L-phenylpyruvic acid and the reaction was NADH dependent. Production of L-phenylpyruvic acid and L-phenyllactic acid and their corresponding enzyme activities confirms the L-phenylalanine catabolism via L-phenylpyruvic acid in *R. benzoatilyticus* JA2.

Identification of intermediates like L-phenylpyruvic acid, L-phenyllactic acid, L-phenylacetic acid indicates the L-phenylalanine catabolism via Ehrlich pathway (Fig. 5; Hazelwood et al. 2008). Genome analysis of *R. benzoatilyticus* JA2 revealed the presence of two aromatic aminotransferase genes and one lactate dehydrogenase gene possibly involved in L-phenylalanine catabolism. L-Phenylalanine/L-tryptophan grown cultures could show the transaminase activity for both the substrates L-phenylalanine and L-tryptophan this suggests that aromatic aminotransferase may be non-specific in *R. benzoatilyticus* JA2 (data not shown). Lactate dehydrogenase activity was also reported to be involved in L-phenylpyruvic acid to L-phenyllactic acid production by a *Lactobacillus* sp. (Li et al. 2008). L-Tryptophan catabolism in *R.*

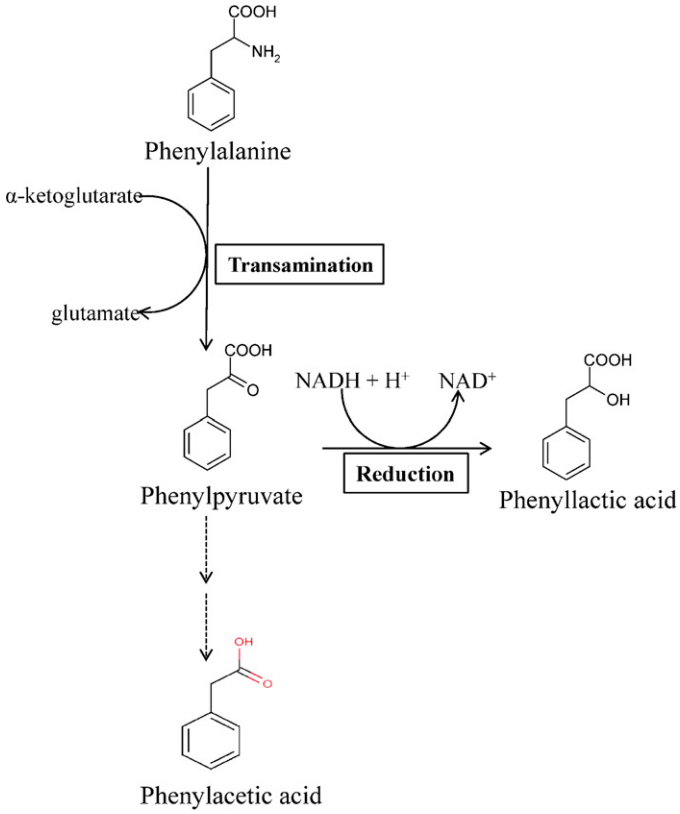

Fig. 5. Proposed pathway of L-phenylalanine metabolism in *R. benzoatilyticus* JA2.

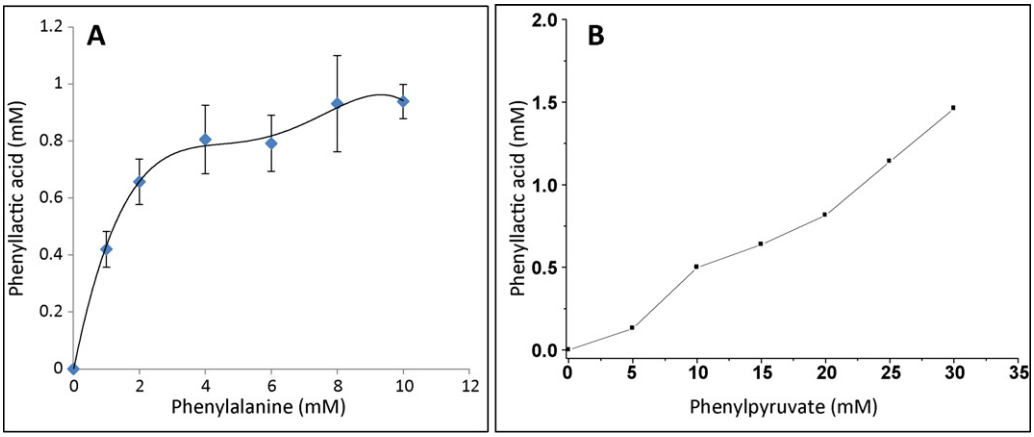

Fig. 6. Effect of L-phenylalanine (A) and phenylpyruvic acid (B) on L-phenyllactic acid production in *R. benzoatilyticus* JA2.

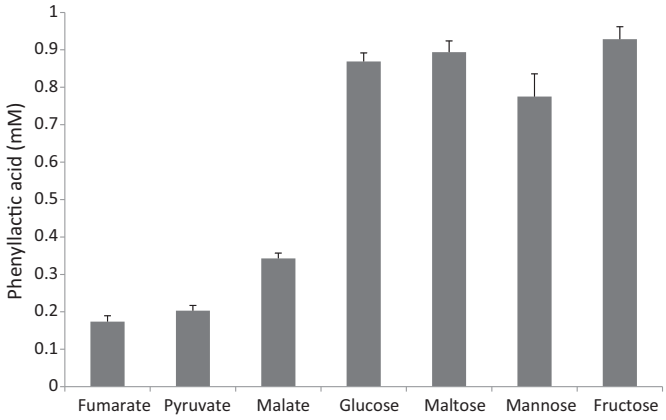

Fig. 7. Effect of carbon sources on L-phenyllactic acid production from L-phenylalanine in *R. benzoatilyticus* JA2. Malate (22 mM) was replaced with same concentration of other carbon sources.

benzoatilyticus JA2 via indole-3-pyruvate pathway was recently reported (Ranjith et al. 2010).

3.4. Production of L-phenyllactic acid

L-Phenyllactic acid was used as an antimicrobial compound (Dieuleveux and Gueguen 1998; Lavermicocca et al. 2003) and is of importance to pharmaceutical industries (Mu et al. 2009), hence its production by *R. benzoatilyticus* JA2 was monitored under different growth conditions. After 24 h of growth, 0.8–0.9 mM of L-phenylalanine was consumed with the production of 0.4 mM of L-phenyllactic acid, accounting to 45% conversion efficiency. The conversion efficiency could be increased to about 70%, when L-phenylalanine was supplemented to the 24 h grown (mid log phase) cultures of *R. benzoatilyticus* JA2.

Concentration of L-phenylalanine and growth conditions further influenced L-phenyllactic acid production by *R. benzoatilyticus* JA2. L-Phenyllactic acid production increases in a dose dependent manner up to 4 mM of L-phenylalanine and remains static at higher concentrations (Fig. 6A). In contrast, production of L-phenyllactic acid increased with increasing L-phenylpyruvic acid (Fig. 6B), an intermediate in the production of L-phenyllactic acid from L-phenylalanine (Li et al. 2007; Mu et al. 2009). L-Phenyllactic acid production was high (0.45–0.7 mM) when L-phenylalanine was used as sole source of nitrogen compared to that used as an additional source (0.15 mM). The yield of L-phenyllactic acid was high (0.45–0.7 mM) under phototrophic conditions (light anaerobic) than under chemotrophic (dark aerobic; 0.02 mM) conditions. Presence of carbon sources influenced L-phenyllactic acid yield in *R. benzoatilyticus* JA2 (Fig. 7). L-Phenyllactic acid yields were high (0.8–0.92 mM) in the presence of sugars. Genome sequence of *R. benzoatilyticus* JA2 indicated the presence of genes encoding decarboxylase and dehydrogenase enzymes which may have involved in the conversion of L-phenylpyruvic acid to L-phenylacetaldehyde and L-phenylacetaldehyde to L-phenylacetic acid (fusel acid).

Our study is the first report of L-phenyllactic acid production by a photosynthetic bacterium, particularly with 70% conversion efficiency of L-phenylalanine to L-phenyllactic acid which is the maximum known (to the best of our knowledge) from bacterial systems till now. We also report L-phenylalanine catabolism via Ehrlich pathway coupled to the production of L-phenyllactic acid in *R. benzoatilyticus* JA2.

Acknowledgements

LP and MM thanks for the CSIR, New Delhi for the award of Senior Research Fellowships.

References

Andreotti G, Cubellis MV, Nitti G, Sannia G, Mai X, Marino G, et al. Characterization of aromatic aminotransferases from the hyperthermophilic archaeon *Thermococcus litoralis*. Eur J Biochem 1994;220:543–9.

Bradford MM. A rapid and sensitive method for the quantitation of microgram quantities of protein utilizing the principle of protein-dye binding. Anal Biochem 1976;72:248–54.

Dieuleveux, Gueguen M. Antimicrobial effects of D-3-phenyllactic acid on *Listeria monocytogenes* in TSB-YE medium, milk, and cheese. J Food Prot 1998;61:1281–5.

Dieuleveux V, Van Der Pyl D, Chataud J, Gueguen M. Purification and characterization of anti-Listeria compounds produced by *Geotrichum candidum*. Appl Environ Microbiol 1998;64:800–3.

Gómez-Romero M, Segura-Carretero A, Fernández-Gutiérrez A. Metabolite profiling and quantification of phenolic compounds in methanol extracts of tomato fruit. Phytochemistry 2010;71:1848–64.

Hazelwood LA, Daran JM, van Maris AJ, Pronk JT, Dickinson JR. The Ehrlich pathway for fusel alcohol production: a century of research on *Saccharomyces cerevisiae* metabolism. Appl Environ Microbiol 2008;74:2259–66.

Helinck S, Le Bars D, Moreau D, Yvon M. Ability of thermophilic lactic acid bacteria to produce aroma compounds from amino acids. Appl Environ Microbiol 2004;70:3855–61.

Kalyan Chakravarthy S, Srinivas TNR, Anil Kumar P, Sasikala Ch, Ramana ChV. *Roseospira visakhapatnamensis* sp. nov. and *Roseospira goensis* sp. nov. Int J Syst Evol Microbiol 2007;57:2453–7.

Kamata M, Toyomasu R, Suzuki D, Tanaka T. D-Phenyllactic acid production by Brevibacterium or Corynebacterium; Brevet Ajinomoto Co Inc., Japan Patent JP 86,108,396; 1986.

Kumavath RN, Ramana ChV, Sasikala Ch. Production of phenols and alkyl gallate esters by *Rhodobacter sphaeroides* OU5. Curr Microbiol 2010;60:107–11.

Lavermicocca P, Valerio F, Visconti A. Antifungal activity of phenyllactic acid against molds isolated from bakery products. Appl Environ Microbiol 2003;69:634–40.

Li X, Jiang B, Pan B. Biotransformation of phenylpyruvic acid to phenyllactic acid by growing and resting cells of a *Lactobacillus* sp. Biotechnol Lett 2007;29: 593–7.

Li X, Jiang B, Pan B, Mu W, Zhang T. Purification and partial characterization of Lactobacillus species SK007 lactate dehydrogenase (LDH) catalyzing phenylpyruvic acid (PPA) conversion into phenyllactic acid (PLA). J Agric Food Chem 2008;56:2392–9.

Mohammed M, Isukapatla A, Mekala LP, Eedara Veera Venkata RP, Chintalapati S, Chintalapati VR. Genome sequence of the phototrophic betaproteobacterium *Rubrivivax benzoatilyticus* strain JA2^T. J Bacteriol 2011;193(11):2898–9.

Mu W, Chen C, Li X, Zhang T, Jiang B. Optimization of culture medium for the production of phenyllactic acid by *Lactobacillus* sp SK007. Bioresour Technol 2009;100:1366–70.

Mujahid M, Sasikala Ch., Ramana ChV. Aniline-induced tryptophan production and identification of indole derivatives from three purple bacteria. Curr Microbiol 2010;61:285–90.

Mujahid Md, Sasikala Ch, Ramana ChV. Production of indole-3-acetic acid and related indole derivatives from L-tryptophan by *Rubrivivax benzoatilyticus* JA2. Appl Microbiol Biotechnol 2011;89:1001–8.

Narayanan TK, Ramananda Rao G. Production of 2-phenethyl alcohol and 2-phenyllactic aid in *Candida* species. Biochem Biophys Res Commun 1974;58:728–35.

Ranjith NK, Ramana ChV, Sasikala Ch. Rubrivivaxin, a new cytotoxic and cyclooxygenase-I inhibitory metabolite from *Rubrivivax benzoatilyticus* JA2. World J Microbiol Biotechnol 2011;27:11–6.

Ranjith NK, Ramana ChV, Sasikala Ch. L-Tryptophan catabolism by *Rubrivivax benzoatilyticus* JA2 occurs through indole 3-pyruvic acid pathway. Biodegradation 2010;21:825–32.

Sáez LP, Castillo F, Caballero FJ. Metabolism of L-phenylalanine and L-tyrosine by the phototrophic bacterium *Rhodobacter capsulatus*. Curr Microbiol 1999;38:51–6.

Sasikala Ch, Ramana ChV. Biodegradation and metabolism of unusual carbon compounds by anoxygenic phototrophic bacteria. Adv Microbial Physiol 1998;39:339–77.

Somers E, Ptacek D, Gysegom P, Srinivasan M, Vanderleyden J. *Azospirillum brasilense* produces the auxin-like phenylacetic acid by using the key enzyme for indole-3-acetic acid biosynthesis. Appl Environ Microbiol 2005;71:1803–10.

Thierry A, Maillard MB. Production of cheese flavour compounds derived from amino acid catabolism by *Propionibacterium freudenreichii*. Lait 2002;82:17–32.